**Republic of Iraq**
**Ministry of Higher Education**
 **and Scientific Research**
**AL-Nahrain University**
**College of Science**
**Department of Physics**

# Construction
# of Mathematical-Statistical Model of Wind Energy in Iraq Using Different Weibull Distribution Functions

## A Dissertation

Submitted to the College of Science/AL-Nahrain University in a Partial Fulfillment of the Requirements for the Degree of Doctor of Philosophy in Physics

## By
## Firas Abdulrazzaq Hadi

B.Sc. Physics / College of Science / University of Baghdad (1998)
M.Sc. Astronomy (Image Processing) / College of Science / University of Baghdad (2001)

## Supervised by

**Dr. Ayad Abdul Aziz Al-Ani**          **Dr. Mohammed Ahmed Salih**
(Professor)                              (Chief of Researchers)

Jul. 2014                                Ramadan1435

بِسْمِ اللهِ الرَّحْمَنِ الرَّحِيمِ

أَمَّنْ يَهْدِيكُمْ فِي ظُلُمَاتِ الْبَرِّ وَالْبَحْرِ وَمَنْ يُرْسِلُ الرِّيَاحَ بُشْرًا بَيْنَ يَدَيْ رَحْمَتِهِ ۗ أَإِلَٰهٌ مَعَ اللَّهِ ۚ تَعَالَى اللَّهُ عَمَّا يُشْرِكُونَ

صــدق الله العلي العظيـم

النمل 63

I

# Supervisor (s) Certification

We, certify that this dissertation entitled "Construction A Mathematical-Statistical Model of Wind Energy in Iraq Using Different Weibull Distribution Functions" was prepared by "Firas Abdulrazzaq Hadi" under our supervision at College of Science/Al-Nahrain University in a partial fulfillment of the requirements for the Degree of Doctor of Philosophy in Physics.

.

Signature:                                          Signature:

Name: ***Dr. Ayad A. Al-Ani***              Name: ***Dr. Mohammed A. Salih***
Title: Professor                                   Title: Chief of Researchers
Address: College of Science, Al-Nahrain   Address: Ministry of Electricity
University
Date:      /     / 2014                           Date:      /     / 2014
**(Supervisor)**                                  **(Supervisor)**

---

In view of the available recommendations, I forward this dissertation for debate by the examining committee.

Signature:

Name: ***Dr. Thamir Abdul-Jabbar Jumah***
Title: Asst. Professor
Address: Head of Department of Physics, Al-Nahrain University
Date:      /     / 2014

# Committee Certification

We examination committee certify that we have read the dissertation entitled "*Construction a Mathematical-Statistical Model of Wind Energy in Iraq Using Different Weibull Distribution Functions*", and examined the student "*Firas Abdulrazzaq Hadi*" in its contents and that in our opinion; it is accepted for the Degree of Doctor of Philosophy in Physics.

Signature:
Name: *Dr. Saad Naji Abood*
Title: Professor
Address: College of Science, Al-Nahrain University
Date:   /   /2014
     **(Chairman)**

Signature:
Name: *Dr. Kais J. Latif*
Title: Professor
Address: College of Science, Al-Mustansiriya University
Date:   /   /2014
    **(Member)**

Signature:
Name: *Dr. Kamal H. Lateef*
Title: Chief of Researchers
Address: Ministry of Science and Technology
Date:   /   /2014
    **(Member)**

Signature:
Name: *Dr. Izzat M. AL-Essa*
Title: Professor
Address: College of Science, University of Baghdad
Date:   /   /2014
    **(Member)**

Signature:
Name: *Dr. Naseer Kareem Kasim*
Title: Chief of Researchers
Address: Ministry of Electricity
Date:   /   /2014
    **(Member)**

Signature:
Name: *Dr. Ayad A. Al-Ani*
Title: Professor
Address: College of Science, Al-Nahrain University
Date:   /   /2014
    **(Member/Supervisor)**

Signature:
Name: *Dr. Mohammed A. Salih*
Title: Chief of Researchers
Address: Ministry of Electricity
Date:   /   /2014
    **(Member/Supervisor)**

---

**I, hereby certify upon the decision of the examining committee.**

Signature:
Name: *Dr. Hadi M. A. Abood*
Title: Asst. Professor
Address: Dean of College of Science, Al-Nahrain University
Date:   /   /2014

Dedicated to

The pure spirit of my father

My mother

Love and Loyalty


To

My wife

My daughters: Hawra'a, Mryam, Farah

Gratitude and respect


Firas

# Acknowledgement

# *Summary*

In the past few years, the world has witnessed a rush towards the use of clean renewable energy sources in order to reduce environmental pollution, energy cost, fuel consuming. Therefore, this work focused toward an important sector in renewable energy, which is wind energy, where the work was divided into four objectives namely;

- *Wind statistics:* This item presents a statistical analysis of the wind resources at five selected sites (Ali Al-karbee, Baghdad, Basrah, Nasiriya, Kerbala) conducted on annual and monthly basis. The statistical of wind data sets were analyzed using Weibull distribution functions, thus, nine analytical methods were considered to estimate Weibull parameters. The results show that the new presented method equivalent energy method (EEM) gives the best power density estimation. The SUZLON S64-950 is our virtual chosen wind turbine whose capacity factor is the criterion used for pairing between each site and wind turbine, where it is equal to 0.12, 0.03, 0.05, 0.08, 0.09 for Ali Al-karbee, Baghdad, Basrah, Nasiriya, and Kerbala sites respectively.

- *Turbulence intensity (TI):* It is very important factor in determining the performance and productivity of the wind turbines. This means, an appropriate turbine class must be known before setting a turbine in a wind farm. In this work we calculate mean *TI* ($50^{th}$ quantile) and representative *TI* ($90^{th}$ quantile) at the provinces of Nasiriya and Kerbala, in addition to determine the wind turbine category after comparison with the normal turbulence model which belongs to IEC standards. The results confirm that category C is suitable for wind turbine installation at the selected sites.

- *Wake effect:* The effects of upstream wind turbines on the performance of the downstream (reference) wind turbine are calculated through effective turbulence intensity ($I_{eff}$) factor at Nasiriya site. Frandsen model for SUZLON S64-950 wind turbine with 71m rotor diameter is used. These effects include the number of upstream wind turbines and the distance of separation between them. In addition, $I_{eff}$ also is estimated for 8 sectors at the selected site. The study shows how the $I_{eff}$ could be increased by increasing the number turbines surrounding the reference one, or decreased by installing an upstream turbine at far distance from the reference one.

- *Financial analysis:* Three methods have been used for economics, namely
  - Cost of energy which depends on kWh of electricity generated.
  - The ratio of the total returns from electricity to the total costs of the turbine.
  - The payback period.

# Table of Contents

# List of Figures

# List of Tables

# Abbreviations

| | |
|---|---|
| $RC_F$ | Rough capacity factor |
| ABL | Atmospheric boundary layer |
| BRICS | Brazil, Russia, India, China, and South Africa |
| C.V. | Coefficient of variation |
| CDF | Cumulative distribution function |
| COD or $R^2$ | Coefficient of determination |
| COE | Cost of energy |
| CRV | Continuous random variable |
| DRV | Discrete random variables |
| EEM | Equivalent energy method |
| EPFM | Energy pattern factor method |
| EU-28 | European Union |
| EWTS | European wind turbine standard II |
| GFRP | Glass Fiber Reinforced Polymers |
| GW | Gamma–Weibull function |
| GWh | Gigawatt-hour |
| H | High pressure |
| Hg | Inches of Mercury |
| $I$ | Expected turbulence intensity under NTM |
| IEC | International electrotechnical commission |
| IL | Internal layer |
| KE | Kinetic energy |
| kWh | kilowatt-hour |
| L | Low Pressure |
| LLSM | Linear least square method |
| LWT | Large wind turbine |
| mb | Millibars |
| M | Meter |
| MENA | Middle East and North Africa |
| MEP | Maximum entropy principle |
| ML | Mixed layer |
| MLE | Maximum likelihood estimation method |

| | |
|---|---|
| MLE-FDM | Modified frequency dependent method |
| MLE-IM | Iterative method |
| MLE-NRM | Newton Raphson Method |
| MLE-MIM | Modified iterative method |
| MLLSM | Modified linear least square method |
| NREL | National renewable energy laboratory |
| NN | Truncated normal function |
| NTM | Normal turbulence model |
| NW | Normal Weibull function |
| PBL | Planetary boundary layer |
| Pd | Probability distribution |
| Pdf | Probability density function |
| PMF | Probability mass function |
| PV | Photovoltaic |
| P.D. | Power density |
| R | Correlation coefficient test |
| R.F. | Relative frequency |
| RC | Roughness class |
| RMSE | Root mean square error |
| RV | Random values |
| SDM | Standard deviation method |
| SL | Surface layer |
| SWT | Small wind turbine |
| $TI$ | Turbulence intensity |
| $TI_v$ | Turbulence intensity as a function of wind speed |
| UBL | Urban boundary layer |
| U. S. Std. | United States Standards |
| WAsP | Wind atlas analysis and application program |
| WIS | Wind energy information system |
| WPD | Wind power density |
| WTG | Wind turbine generator |
| WW | Bimodal Weibull function |

# List of Symbols

| | | |
|---|---|---|
| $a$ | Slope | |
| $A$ | Rotor area | m$^2$ |
| $c$ | Scale parameter | m/sec |
| $C_A$ | Cost per rotor area | \$ |
| $C_F$ | Capacity factor | |
| $c_p$ | Power coefficient | |
| $C_{Pr}$ | Cost per rated power | \$ |
| $C_T$ | Thrust coefficient | |
| $C_t$ | Cost of the turbine | \$ |
| CLC | The European Commission program Corine Land Cover | |
| D | Rotor diameter | m |
| di | The distance to i neighbouring wind turbine | m |
| $E_D$ | Energy density | kWh |
| $E_{out}$ | Energy output | kWh |
| $E_{An}$ | Annual energy | kWh |
| $E_{IR}$ | Energy from cut-in to rated wind speed | kWh |
| $E_{PF}$ | Energy Pattern Factor Method | kWh |
| $E_{RO}$ | Energy from rated to cut-out wind speed | kWh |
| $E_T$ | Energy actually produced by the system | kWh |
| f$_{-s}$ | Frequency of wind speed at a sector | |
| $F(V)$ | Cumulative distribution function | |
| $f(v)$ | Probability density function | |
| G | Gravitational constant | $6.6 \times 10^{11}$ m$^3$ kg$^{-1}$ s$^{-2}$ |
| $I_{char}$ | Characteristic turbulence intensity | |
| $I_{eff}$ | Effective turbulence intensity | |

| | | |
|---|---|---|
| $I_{\text{eff\_s}}$ | Effective turbulence intensity of the combined ambient and wake flows from certain sector | |
| $I_{\text{ref}}$ | Reference turbulence intensity | |
| $I_{\text{ref\_s}}$ | Reference turbulence intensity from certain sector | |
| $I_{\text{rep}}$ | Representative turbulence intensity | |
| $I_{\text{rep\_s}}$ | Representative turbulence intensity for certain sector | |
| $I_{\text{T}}(d_{\text{i}})$ | The maximum center-wake at hub height | |
| $I_{\circ}$ | Ambient turbulence intensity | |
| $I_T$ | Free flow turbulence | |
| $I_T^*$ | Turbulence intensity with increment | |
| $j$ | No. samples size | |
| $k$ | Shape parameter | |
| $l$ | Length of wind blades | m |
| $m$ | Mass | kg |
| $m_i$ | No. observations of a specific wind speed | |
| $\dot{m}$ | Wholer parameter | |
| $n$ | Total number of data | |
| $\acute{n}$ | No. bins | |
| $\dot{n}$ | Velocity power proportionality | |
| N | No. sectors | |
| $\dot{N}$ | No. neighbouring wind turbine | |
| $N_s$ | No. sectors | |
| P | Pressure | N/m$^2$ |
| $P(v)$ | probability function | |
| $P_{ave}$ | Average power | kW |
| $PD_A$ | Actual Power Density | W/m$^2$ |
| $PD_w$ | Weibull based power density | W/m$^2$ |

| | | |
|---|---|---|
| $P_{\bar{v}}$ | Power corresponding to average wind speed | kW |
| $p(v_i)$ | Probability of the discrete wind speed $v_i$ | |
| $P(v_i)$ | Power curve value at each wind speed $v_i$ | kW |
| $\bar{P}$ | Average power | kW |
| $PD_v$ | Average power density | W/m$^2$ |
| $PD_{w-s}$ | Sectorial power density | W/m$^2$ |
| $P_{e,ave}$ | Average output power | Watt |
| $P_o$ | Sea pressure | N/m$^2$ |
| $P_r$ | Rated power | kW |
| $P_T$ | Turbine output power | kW |
| $P_w$ | Wind potential power | kW |
| $\dot{P}_w$ | Probability density function | |
| $r$ | Radius of the wind turbine hub | m |
| $R_{gas}$ | Gas constant | J kg$^{-1}$ Kelvin$^{-1}$ |
| $RC_F$ | Rough capacity factor | |
| $R_f$ | Relative frequency | |
| $T$ | Time period | Days or hours |
| $T_{ref}$ | Reference price per kWh | \$/kWh |
| $V_{ave}$ | annual average wind speed at hub height | m/sec |
| $V_{ref}$ | Basic parameter for wind speed | m/sec |
| $V_{hub}$ | Wind speed at hub height | m/sec |
| $V_{in}$ | Cut-in wind speed | m/sec |
| $V_{out}$ | Cut-out wind speed | m/sec |
| $V_r$ | Rated wind speed | m/sec |
| $w$ | No. different values of wind speed | |
| $WPD_T$ | Turbine output power density | W/m$^2$ |
| $WPD_w$ | Wind potential power density | W/m$^2$ |

| | | |
|---|---|---|
| $X_A$ | Actual variable | |
| $X_e$ | Estimated variable | |
| $x_f$ | Distance between rows | m |
| $x_r$ | Distance within a row | m |
| $Z_o$ | Roughness length | m |
| $Z_l$ | Elevation 1 | m |
| $Z_2$ | Elevation 2 | m |
| $z_{\circ 1}$ | Roughness length at reference location | m |
| $z_{\circ 2}$ | Roughness length at destination location | m |
| $z_{hub}$ | Hub height | m |
| $TI_{90}$ | 90th percentile turbulence intensity | |
| $\overline{TI_v}$ | Average of turbulence intensity in certain bin | |
| $TI_{mea}$ | Average turbulence intensity | |
| $TI_{meas}$ | Measured turbulence intensity | |
| $TI_{pred}$ | Predicted turbulence intensity | |
| $g$ | Location parameter | m/sec |

# Greek Symbols

| | | |
|---|---|---|
| $\alpha$ | Hellmann (friction or wind shear) exponent | |
| $\kappa$ | Von Karman parameter | |
| $\rho$ | Air density | Kg/m$^3$ |
| $\sigma$ | Standard deviation | |
| $\hat{\sigma}$ | Ambient estimated turbulence standard deviation in a farm | |
| $\sigma_{10}$ | Standard deviation of the wind speed over the 10 minutes | m/sec |
| $\sigma^2$ | Variance of wind speed | (m/sec)$^2$ |
| $\sigma_v$ | Standard deviation of wind speeds | m/sec |
| $\sigma_1$ | Standard deviation of NTM for wind speeds at hub height | m/sec |
| $\sigma_{90}$ | 90$^{th}$ percentile standard deviation | m/sec |
| $\sigma_{TI}$ | Standard deviation of turbulence intensity | |
| $\bar{\sigma}$ | Average of standard deviation in certain bin | |
| $v$ | Wind speed | m/sec |
| $v_{10}$ | 10-minutes mean wind speed | m/sec |
| $v_i$ | Set of measured wind speeds | m/sec |
| $v_{me}$ | Wind speed which produces more energy than any others | m/sec |
| $v_{rmc}$ | Root mean cube average wind speed | m/sec |
| $v_f$ | Most probable wind speed | m/sec |
| $v_{pred}$ | Predicted wind speed | m/sec |
| $v_{meas}$ | Measured wind speed | m/sec |
| $v_{me}$ | Wind speed contribute to maximum energy | m/sec |
| $\acute{v}$ | Specific wind speed | m/sec |
| $\bar{v}$ | Mean wind speed | m/sec |
| $\bar{v}_{-s}$ | Mean wind speed at a given sector | m/sec |
| $\bar{v}_a$ | Actual mean wind speed | m/sec |
| $\acute{v}_i$ | Midpoints of frequency intervals | m/sec |
| $\chi^2$ | Chi-square test | |

# Chapter One

# CHAPTER ONE

## *Introduction and Literature Review*

### 1.1 Introduction

Energy is a requirement of any house, building, and city. Nation without energy, the world would cease to exist since almost everything in developed countries relies on power for its existence (either directly or indirectly). As a result, society is faced with the challenge of meeting this unceasing demand for energy and must determine how to generate enough power to meet the immediate demands, but also to plan for the supply of energy into the future, **[Sha12]**.

Energy comes from different sources and is produced in large enough quantities to meet the increasing demand. This is achieved through the development of large scale power plants, towards the end of the nineteenth and early twentieth century, designed to produce energy in one location and send it over electrical power lines to the source of the demand. Originally, many power plants used water or coal to generated power, both of which were resources that were available in abundance. Most recently, in the later half of the twentieth century, development was focused on nuclear power, **[And07]**.

Anyway, it is known that coal and oil reserves are being depleted as a result of huge consumption demands, but it has also been seen that burning coal or oil to generate power produces harmful pollutant that add into the atmosphere. Furthermore, the world consumption of these types of resources is occurring faster than they can naturally be replenished and, as a result, is not a sustainable behavior, **[Sha12]**.

With the two preceding issues of environmental impact and sustainable fuel supply, different types of energy production technologies have been developed. Recently, there has been a shift towards green energy; the most common forms of green energy generation are hydro, wind, and solar photovoltaic (PV), while there are others, such as tidal and biomass. These forms of renewable energy use energy resources that renew at a faster rate, or at least at pace, with our demand as long as the consumption of the resources are managed appropriately, **[Sha12]**.

## 1.2 Energy Sources

Energy can take a wide variety of forms, heat (thermal), light (radiant), mechanical, electrical, chemical, and nuclear energy. The forms of energy can be classified in two general categories: potential and kinetic. Potential energy is energy stored in an object; chemical, mechanical, nuclear, gravitational, and electrical are all stored energy. Kinetic energy does work like motion and sound. The process of changing energy from one form into another is called energy transformation and systems do it in different efficiencies.

Primary energy sources (meaning energy is created directly from the actual resource) can be classified in two groups: nonrenewable and renewable, **[Alk07]**:

- *Non-Renewable Energy Sources* – Energy from the ground that has limited supplies, either in the form of gas, liquid or solid is called nonrenewable resources. They cannot be replenished, or made again, in a short period of time. Examples include: oil (petroleum), natural gas, coal and uranium (nuclear). Oil, natural gas and coal are called "fossil fuels" because they have been formed from the organic remains of prehistoric plants and animals.

- *Renewable Energy Sources* – Energy that comes from a source that's constantly renewed, such as the sun and wind, can be replenished naturally in a short period of time. Because of this we do not have to worry about them running out. Examples include: solar, wind, biomass and hydropower.

On the other hand, energy that is converted from primary sources is secondary sources of energy. Secondary sources of energy are used to store, move, and deliver energy in an easily usable form. Examples include electricity and hydrogen.

## 1.3 Renewable Energy and Global Status

Around the world, policy support and investment in renewable energy have continued to focus primarily on the electricity sector. Consequently, renewables have accounted for a growth rating share of electric generation capacity added globally each year. In 2013 only, renewables made up more than

56% of net additions to global power capacity and represented far higher shares of capacity added in several countries around the world, **[REN14]**.

At the end of the previous year (2013), renewables estimated by 26.4% of the world's power generating capacity. This was enough to supply an estimated 22.1% of global electricity, with wind power providing about 2.9% (see **Fig. 1.1**). While renewable capacity continues to rise at a rapid rate from year to year, renewable electricity's share of global generation is increasing more slowly. This is in large part because overall demand keeps rising rapidly and also because much of the renewable capacity being added is variable, **[REN14]**.
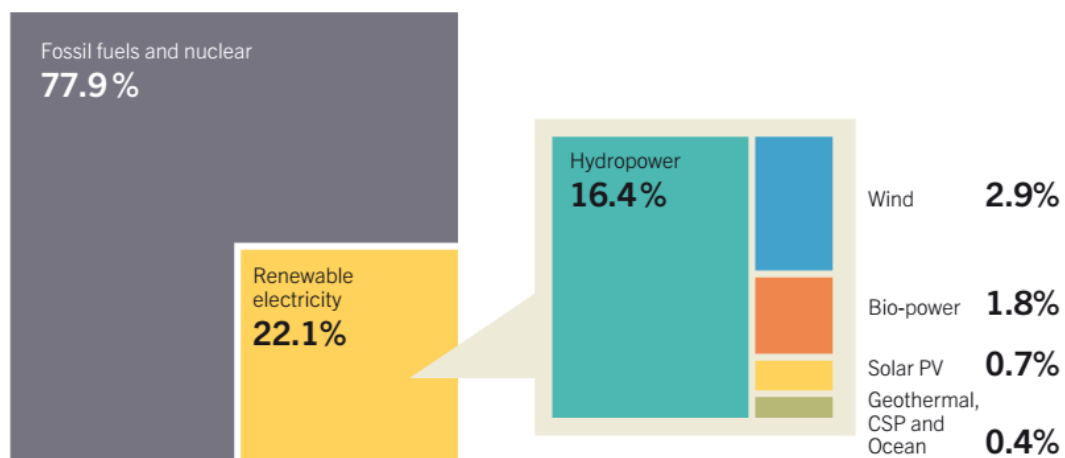


**Fig. 1.1 Estimated renewable energy share of global electricity production, end-2013, [REN14].**

China, United States, Brazil, Canada, and Germany remained the top countries for total installed renewable electric capacity in the end of the year 2013. China was home about 24% of the world's renewable power capacity, including an estimated 260 GW of hydropower. The top countries for non-hydro capacity are again China, United States, and Germany, followed by Spain, Italy, and India. (see **Fig. 1.2**).

The wind industry continued to be challenged by downward pressure on prices, increased competition among turbine manufacturers, competition with low-cost gas in some markets, and declines in key markets. At the same time, falling capital costs and technological advances increased capacity factors, improving the cost-competitiveness of wind-generated electricity relative to fossil fuels.
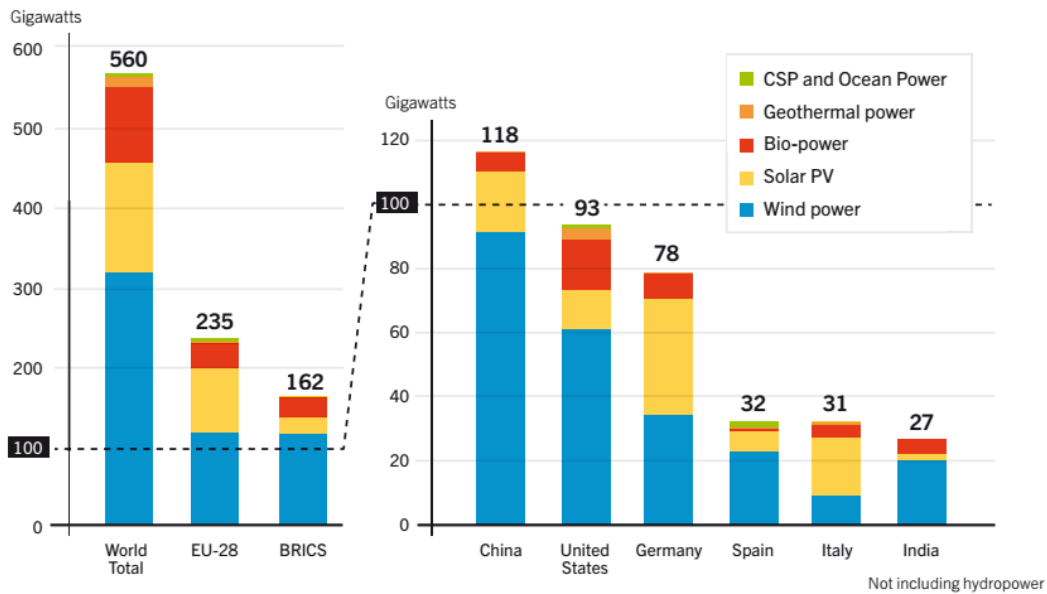
**Fig. 1.2 Renewable power capacities in the world, EU-28, BRICS, and top six countries, 2013, [REN14].**

Thus, more than 35 GW of wind power capacity was added in 2013, bringing the global total above 318 GW (see **Fig. 1.3**). Following several record years, the wind power market declined nearly 10 GW compared to 2012, at the end of 2013, at least 85 countries had seen commercial wind activity, while at least 71 had more than 10 MW of reported capacity by year's end, and 24 had more than 1 GW in operation. Annual growth rates of cumulative wind power capacity have averaged 21.4% since the end of 2008, and global capacity has increased eightfold over the past decade, **[REN14]**.
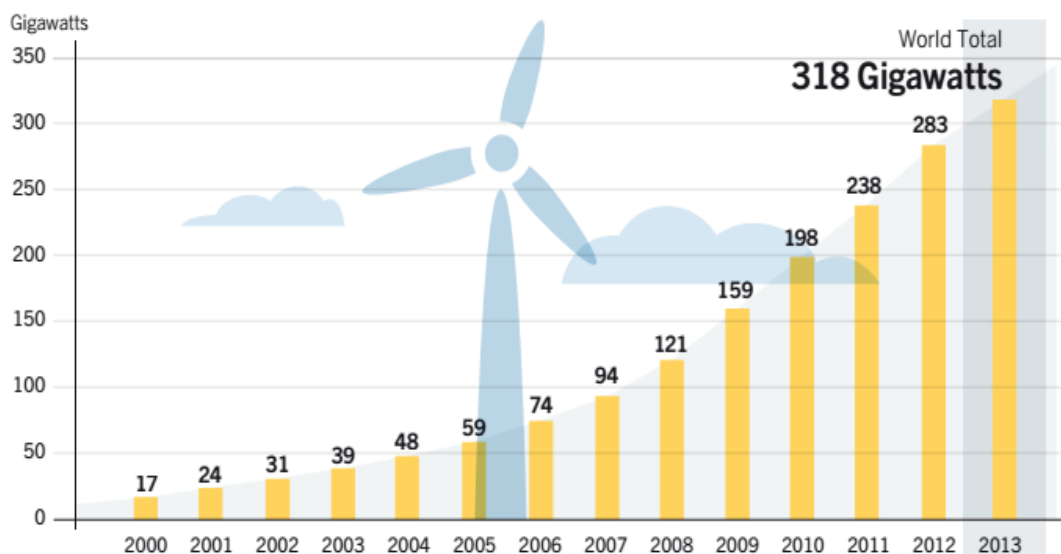


**Fig. 1.3 Wind power total world capacity, 2000-2013, [REN14].**

## 1.4 Facts on Wind Energy

In fact, there is no practical upper limit to the percentage of wind that can be integrated into the electricity system. It has been estimated that the total solar power received by the earth is approximately $1.8 \times 10^{11}$ MW. Of this solar input, only 2% (i.e. $3.6 \times 10^9$ MW) is converted into wind energy and about 35% of wind energy is dissipated within 1000m of the earth's surface. Therefore, the available wind power that can be converted into other forms of energy is approximately $1.26 \times 10^9$ MW. Because this value represents 20 times the rate of the present global energy consumption, wind energy in principle could meet entire energy needs of the world, **[Ton10]**.

Compared with traditional energy sources, wind energy has a number of benefits and advantages, unlike fossil fuels that emit harmful gases and nuclear power that generates radioactive wastes, wind power is a clean and environmentally friendly energy source. As an inexhaustible and free energy source, it is available and plentiful in most regions of the earth. In addition, more extensive use of wind power would help reduce the demands for fossil fuels, which may run out in this century, according to their present consumptions. Thus, as the most promising energy source, wind energy is believed to play a critical role in global power supply in the 21$^{st}$ century, **[Ton10]**.

Wind energy converts kinetic energy that is present in the wind into more useful forms of energy such as mechanical energy or electricity. The amount of potential energy depends mainly on wind speed, but is also affected slightly by the density of air, which is determined by the air temperature, pressure and altitude, **[Sha13]**.

Wind energy is the least cost type of renewable energy technology, yet it is a huge source and according to the reports from United Nations, the total potential for wind energy alone can satisfy the electricity world demand by 20 times. In the past few years, the economics of wind energy has improved dramatically in many developed countries, such that it is now the least expensive option among all energy technologies, **[Alk07]**.

**Table 1.1: Wind energy potential in MENA countries**, [Alk07].

| Country | Full load hours per year (h/y) |
|---|---|
| Egypt | 3,015 |
| Morocco | 2,708 |
| Oman | 2,463 |
| Libya | 1,912 |
| Iraq | 1,789 |
| Saudi Arabia | 1,789 |
| Syria | 1,789 |
| Algeria | 1,789 |
| Tunisia | 1,789 |
| Kuwait | 1,605 |
| Jordan | 1,483 |
| Yemen | 1,483 |
| Qatar | 1,421 |
| Bahrain | 1,360 |
| Lebanon | 1,176 |
| UAE | 1,176 |

It is important to know that areas with annual full load hours over 1,400 h/year were considered as economic potential. Accordingly, Middle East and North Africa countries (MENA) have good wind energy resources. The full load hours per year for these countries is shown in **Table 1.1**, it is obvious that all MENA countries have good wind energy potential especially Egypt, Morocco and Oman, **[Sha13]**.

## 1.5 Wind Energy in Iraq

Iraq does suffer from a growing shortage of electrical energy because of an increasing rise in demand especially after 2003. Electrical power generation stations fail to comply with the demand for power because of limited production capabilities and numerous defects due to corruption.

This prompts the Iraqis to look for alternatives such as generators, large or small, which in turn constitute consuming extra money, fuel, and the harm caused to human life and the lives of future generations. Green sources like wind, solar and biomass energies are not being utilized sufficiently at present, but these energies could play an important role in the future of Iraq's renewable energy. Additionally, the potential of offshore-wind energy in the Gulf (near Basrah in the southern part of Iraq) needs to be investigated, **[Kaz12]**.
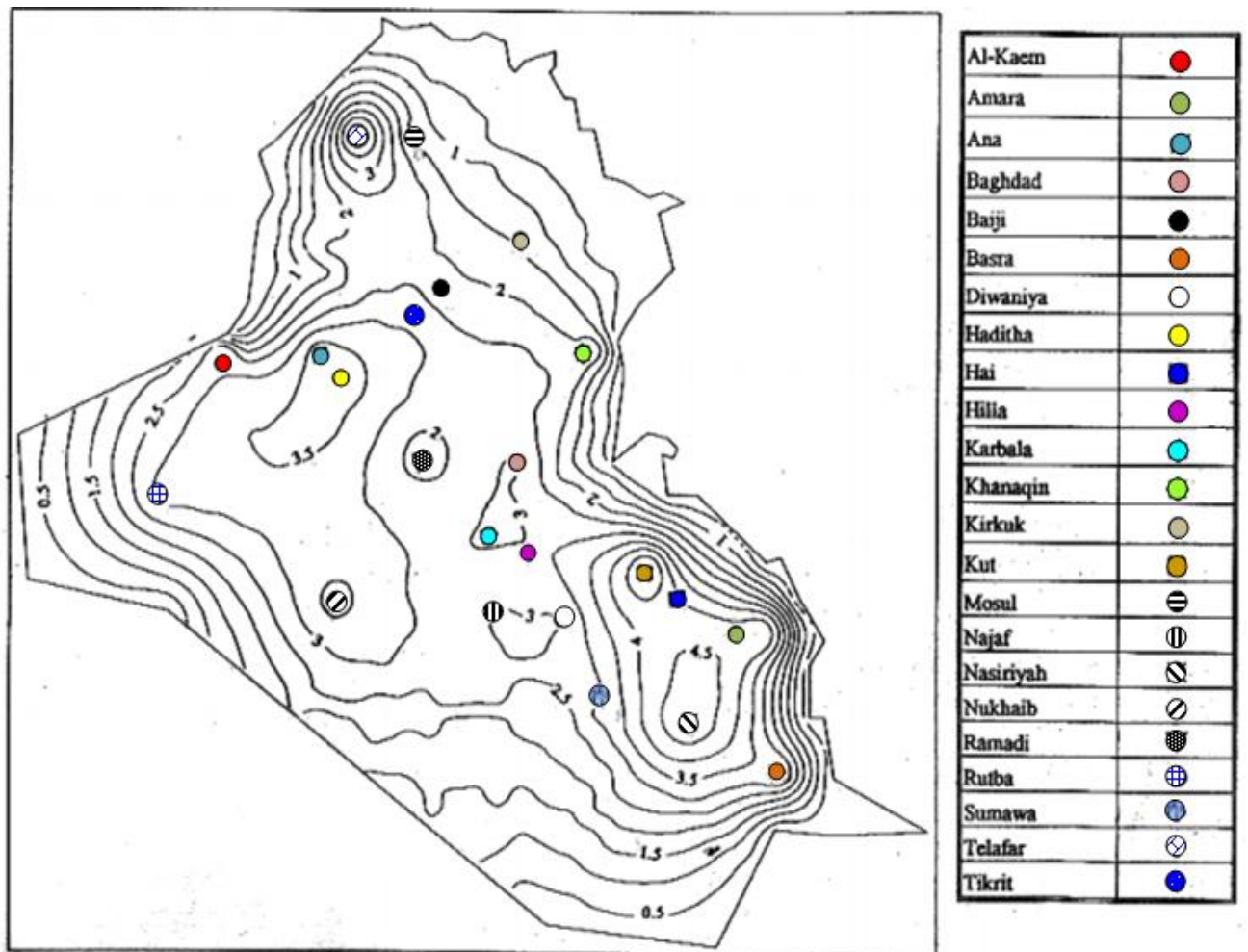


**Fig. 1.4 Mean wind speed in Iraq at 10m above ground, [Ahm10].**

Wind energy in Iraq can be divided into three zones, 48% of Iraq has low annual wind speed, 35% has annual wind speed 3.1-4.9 m/sec, 8% has relatively high annual wind speed and the residual has calm values. The diurnal pattern of wind

speed in Iraq has peak values at mid-day and early hours of the morning, the peak values of wind speed varies in range 5-10 m/sec (**Fig. 1.4**), [**Ahm10**].

The approximate power densities for wind territories are as follows:

174 W/m$^2$ in Al-Emarra, 194 W/m$^2$ in Al-Nekhaib, 337 W/m$^2$ in AlKout, 353 W/m$^2$ in Ana, and 378 W/m$^2$ in Nasiriya. From these results, an average energy of approximately 287.2 W/m$^2$ can be obtained, [**Ahm10**].

## 1.6 Aim of Study

The aim of research is to study the basic elements that important in constructing an integrated wind energy project. These elements include statistical methods based on Weibull distribution function for the purpose of obtaining accurate results. In addition to know the effects that the turbine is experienced at its location and the effects between turbine and another in a wind farm.

## 1.7 Study Importance

The search for alternatives to traditional fuel such as wind power must give satisfactory results and success in life, to achieve this purpose, it is essential to build a scientific basis for wind energy work. Therefore, the importance of this research is laying in draw scientific bases to the following issues:

1- Building a program able to deal with wind data in various time-date series.
2- Find out wind speed time variation charts, by which it is possible to locate the zeros values, missing values, and errors in the data.
3- Determining the direction of wind blow in addition to the direction that gives most energy, which can be used for taking the appropriate wind farm layout.
4- Determining the best technique for Weibull parameters estimation.
5- This study clarifies how Weibull parameters could be used for wind power calculations.
6- By calculating capacity factor the suitability of the turbine with the site could be found out.
7- Estimating the output energy from wind turbine by noting the reducing in wind potential energy.
8- Calculating the hours of power generation.

9- Declaring how fatigue load could be reduced.

10- Declaring how wake effect could be reduced.

11- Defining the finance option in graphical format.

12- Using short term wind data for estimating wind energy potential of prospective sites, since most preceding studies made long term data for energy estimation.

## 1.8 Literature Survey

The energies of wind, sun and water have been used for thousands of years for several purposes, but in the past century, especially the last three decades, a lot of studies were intensified for the use of these energies in electricity generation. Globally, the interest is increased in wind energy (the fastest growing) for electric power generation surpassing other alternatives such as solar and tidal energy.

The following are some of the studies and researches divided according to main topics of the thesis, most of which come as university theses, as well as research in magazines and scientific journals, which are:

- **Studies on probability distribution**

**Corotis R.B. et al., 1978, [Cor78]:** employed the Weibull pdf in various regions of the world in the evaluation of wind energy potential; or to be more precise, in the statistical analyses of wind characteristics and wind power density.

**Koeppl G.W., 1982, [Koe82]:** prospected for large wind turbine generators, suggested his probabilistic models, a number of significant models have been proposed to represent wind speed probability density functions.

**Oliva R.B., 1997, [Oli97]:** pointed that the characteristics of the two parameter Weibull distribution have given rise to it becoming the most widely used and accepted probability distribution in the specialized literature on wind energy and other renewable energy sources

**Chadee J.C. and Sharma C., 2001, [Cha01]:** pointed out that the added location parameter introduces difficulties in the estimation, and a positive value

for it gives rise to an unrealistic condition of zero probability of wind speeds less than the parameter value.

**Sinan A. and Ebru K.A., 2009, [Sin09]:** represent a theoretical approach of wind speed frequency distributions observed in the region of study through applications of two component mixture Weibull distributions and offer less relative errors in determining the annual mean wind power density. The parameters of the distributions are estimated using the least squares method and Statistica software.

**Chang T.P., 2011, [Cha11]:** compared the MEP and mixture pdf's such as the WW and NW with other two mixture functions proposed for the first time to wind energy field, i.e. the GW and NN.

The results show that for wind speed distributions, the proposed GW pdf describes best according to the Kolmogorov–Smirnov test followed by the NW and WW pdf's, while the NN pdf performs worst. As for wind power density, the MEP and GW pdf's perform best followed by the WW and NW pdf's. The GW pdf could be a useful alternative to the conventional Weibull function in estimating wind energy potential.

**Wu J. et al., 2013, [Wuj13]:** employed three probability density functions, i.e., two-parameter Weibull, Logistic and Lognormal to wind speed distribution modeling using data measured at a typical site in Inner Mongolia, China, from 2009 to 2011. The performance of the Weibull function is worse than the Logistic function. The Logistic function provides a more adequate result in wind speed distribution modeling. Therefore, the Logistic function is applied to the consequent wind energy assessment through the availability factor, capacity factor, and turbine efficiency of a wind turbine.

- **Studies on wind energy**

**Pelka D.G. et al., 1978, [Pel78]:** discussed the large-scale generation of electrical power by wind turbine fields. It is shown that the maximum power which can be extracted by a wind turbine is 16/27 or 59.3% of the power available in the wind.

**Richardson R.D. and McNerney G.M., 1993, [Ric93]:** presented a brief discussion of wind energy development, and the operating and design principles

are discussed. Development of a wind energy system and the impacts on the utility network including frequency stability, voltage stability, and power quality are discussed.

**Ahmed M.A. and Ahmed F., 2004, [Ahm04]:** published a study to evaluate wind power in coastal areas in Pakistan depending on the distribution of Weibull and the use of different diameters of the blades; they found that promising areas are Jivani and Pasni.

**Sovacool B.K., 2013, [Sov13]:** assesses the number of birds killed per kWh generated for wind electricity, fossil fuel, and nuclear power systems. The study estimates that wind farms and nuclear power stations are responsible each for between 0.3 and 0.4 fatalities per GWh of electricity while fossil fueled power stations are responsible for about 5.2 fatalities per GWh. Within the uncertainties of the data used, the estimate means that wind farms killed approximately 20,000 birds in the United States in 2009 but nuclear plants killed about 330,000 and fossil fueled power plants more than 14 million.

- **Researches on Turbulence**

**Scruton C. and Rogers E.W.E., 1971, [Scr71]:** discuss the relevant characteristics of turbulence and their dependence on the local terrain. For designing based on unsteady loadings due to turbulence are assessed through the concept of aerodynamic.

**Elliot D. L. and Cadogan J. B, 1990, [Ell90]:** discover the importance of other variables in an analysis of power curves for three 2.5 MW wind turbines. When the power curves were stratified by turbulence intensity, the observed output power for a given hub-height wind speed increased substantially with turbulence intensity.

**Park M. and Park S., 2006, [Par06]:** examined the effects of the topographical slope angle and atmospheric stratification on turbulence intensity of surface-layer. It is found that both the friction velocity and the variance for each component of wind normalized by the mean wind speed decrease with increase in the topographical slope angle.

**Rodrigues C.V. et al., 2010, [Rod10]:** present an alternative criterion for determining the wind speed at which the turbulence intensity must be referred

to, this is also extended and successfully tested in the case of the wind shear factor.

**Ernst B. and Seume J.R., 2012, [Ern12]:** investigated the turbulence intensity and the wind shear exponent using data from the FINO 1 research platform, the results are analyzed and compared with the IEC standard 61400-3. Based on this analysis, simulations are performed to determine the effect of wind field on the fatigue and the extreme loads on the rotor blades.

- **Studies on wake effect**

**Elliott D.L. 1991, [Ell91]:** examined the status of current knowledge about wake effects and array losses and suggests future research.

**Huang H.S. and Chiang C.T. 2006, [Hua06]:** evaluated the reliability worth of a distribution system with large wind farm and the wake effect between wind turbines is considered. According to reliability worth indices, the proper wind farm capacity, layout, engineering parameters and connection point with distribution feeders are chosen.

**Yongxing L. and Feng X., 2010, [Yon10]:** analyzed wake flow factors, which are important for establishing wake flow model, and then discuss several models used presently.

**Husiena W. et al., 2013, [Hus13]:** studied the modeling of the wake effect on the energy extracted from the wind farms. It covers the wake effect of the interaction of the upstream wind rotor with/without the upstream right and/or upstream left wind rotor. A mathematical model representing a single wake model based on the linear description of the wake is developed in order to predict the wind speed inside the wake region at any downstream distance within the wind farm.

- **Studies in Iraq and other Arab countries**

**Al-Azzawi S.I. and Zeki N.A., 1986, [Ala86]:** published research to evaluate the wind energy potential in Iraq using monthly and annual average wind speed for some meteorological stations in Iraq.

**Radwan A., 1987, [Rad87]:** assesses wind power using Weibull distribution, also have found that shape parameter ranging from (7.1 to 7.2) and between (3.0-6.0) for scale parameter.

**Darwish A. S. and Sayigh A. A., 1988, [Dar88]:** studied the potential of wind energy in Iraq. Nine selected metrological stations were used to draw the regional distribution of mean wind speed in Iraq. The study shows that Annah and Najaf districts have very good average wind speed (about 5m/s). A full statistical analysis has been carried out for each station which involved monthly average speed, annual values of shape and scale parameters of Weibull distribution. An important result of the study is that one sixth of the country enjoys annual wind speed is greater than 5.0 m/sec, which is suitable to establishing wind farms.

**Pallabazzer R . and Gabow A., 1991, [Pal91]:** studied the possibility of generating energy in the surrounding areas of the Red Sea and the Gulf of Aden, where they found that the coastal areas are promising locations.

**Abboud B. A., 2000, [Abb00]:** exploited renewable energies in the human settlements serving in remote areas, dealing with the definition of renewable energy, including wind power and the justifications for use in remote areas and exploited in Anbar province.

**Hirat I.A., 2006, [Hir06]:** addressed the possibility of using wind to generate electrical power through the study of types of surface winds for different regions in Iraq.

**Mohammed G. K. and Aboelyazied M. K., 2007, [Moh07]:** described the annual wind speed variability in Hurghada city for the period 1973–2001. The wind speed and direction were measured at the latitude of masts as 10, 24.5, and 31m. The research concluded that if the annual mean wind speed varies by ±10% around a long-term value the corresponding natural variability of the available wind energy is about ±25%.

**Mohammed A. I., 2007, [Mod07]:** analyzed the average month speed for the period from 1970 to 2000 for 19 stations in Iraq. Data were subjected to different analyses foremost of them Weibull distribution. The energy density, roughness length and the class where also calculated in terms of this distribution, also calculating the persistence of the speed in terms of elements with continuous and discontinuous nature. The study also deals with the feasibility of wind speed at 40 m height for (V47-660 kW) turbine. She is found that each of Telafar, Kut & Al-Hai are most promising area.

**Shaban A. H., 2013, [Sha13]:** used Geographical information systems to produce maps for wind speed monitoring; also many image processing and remote sensing techniques were applied to perform the project's task.

**Joudah H. G., 2014, [Jou14]:**The study investigates the variation in speed and direction of wind in the area south latitude 33o in Iraq to explore the possibility of generating electricity from wind, nine climate stations located in this area were selected for this purpose. The probability of seasonal and annual wind speed density was calculated using Weibull distribution by applying the Wind Power Density equation. It appears that Ali Al-Gharbi, Nasiriya and Basra stations were ideal areas in which a high density is available that is suitable to generate electricity at the seasonal and annual level.

## 1.9 Dissertation Layout

Dissertation is divided into four chapters.

*Chapter one:* presents introduction to renewable energy share of global electricity, facts on wind energy, and a literature review of relevant publications.

*Chapter two:* produces a strong mathematical foundation for equations which will be used in chapter three.

*Chapter three:* describes regions of interest and available data in addition to the experimental results with their discussion are involved.

*Chapter four:* summarizes and concludes the main results in this work. Future direction is also discussed.

# Chapter Two

# CHAPTER TWO

## *Wind Energy Assessment Methodology and Siting Preliminaries*

## 2.1 Introduction

Wind energy is the most promising energy source which is believed to play an important role in global power supply in the 21$^{st}$ century. Compared with traditional energy sources, wind energy has a number of benefits and advantages. Unlike fossil fuels that emit harmful gases and nuclear power that generates radioactive wastes, wind power is a clean and environmentally friendly energy source. As an inexhaustible and free energy source, it is available and plentiful in most regions of the earth. In addition, more extensive use of wind power would help reduce the demands for fossil fuels, which may run out sometime in this century, according to their present consumptions, **[Ali07]**.

## 2.2 The Wind

Wind results from the movement of air due to change in temperature by san radiation which cause a difference in atmospheric pressure. Wind flows from regions of higher to lower pressure in an attempt to equalize imbalance in air pressure. The weight of the air above different regions varies and, hence, so does the atmospheric pressure. If the pressure gradient force were the only force acting upon air, we would always find wind blowing directly from higher toward lower pressure regions, and the air will move in response to equalize the differences in pressure (see **Fig. 2.1**). The letter L in the map indicates a region of low atmospheric pressure while the letter H in the map represents regions of high atmospheric pressure, **[Aza10, Ahr01]**.

The solar radiation received by the earth heats up the atmospheric air. The intensity of sun radiation will be more at the equator region (0$^{o}$ latitude) as the sun is directly overhead. Air around the poles region gets less warm, as the angle at which the radiation reaches the surface is less. Thus, differences in pressure

between the equator and poles (result from the differential heating of the surface of the earth) will produce general circulation of the atmosphere.
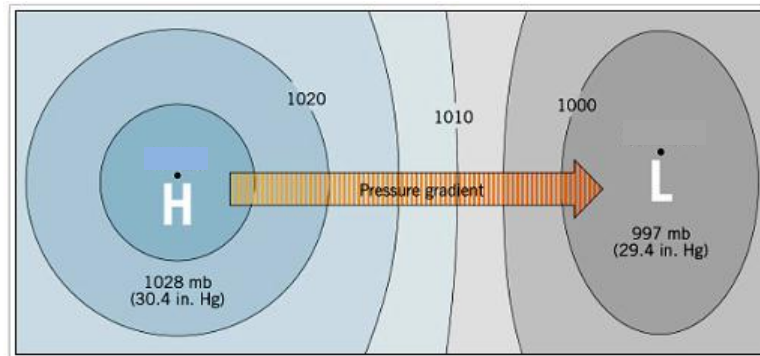


**Fig. 2.1 Pressure difference causes air flow, [Ahr01].**

With the assumption of ***single cell model*** the general circulation of the atmosphere would look much like the representation in **Fig. 2.2**, **[Ahr01, Mat06]**.
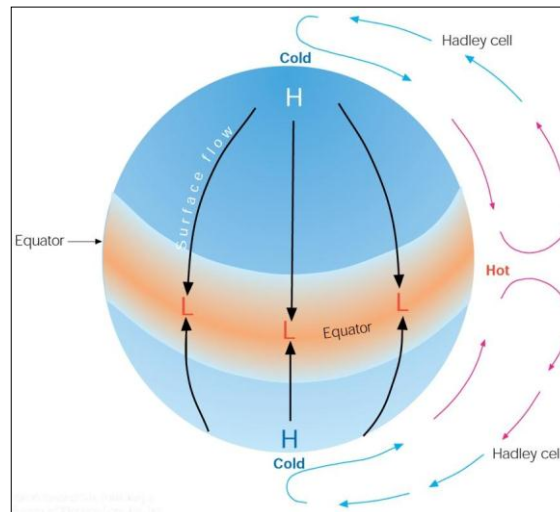


**Fig. 2.2 Wind motion affected by earth temperature difference, [Ahr01].**

In general, the pressure gradient force is the force that causes the wind to blow. But, if the pressure gradient force were the only force acting upon air, then we would always find wind blowing directly from higher toward lower pressure. Actually, the wind does not always blows directly from high to low pressure,

because the movement of air is controlled not only by pressure differences but also by other forces as well, such as Coriolis force, **[Ahr01, Dan10]**.

The Coriolis force is an apparent force because the rotation of the earth causes the wind to deflect to the right of its intended path in the northern hemisphere and to the left of its intended path in the southern hemisphere, see **Fig. 2.3**.
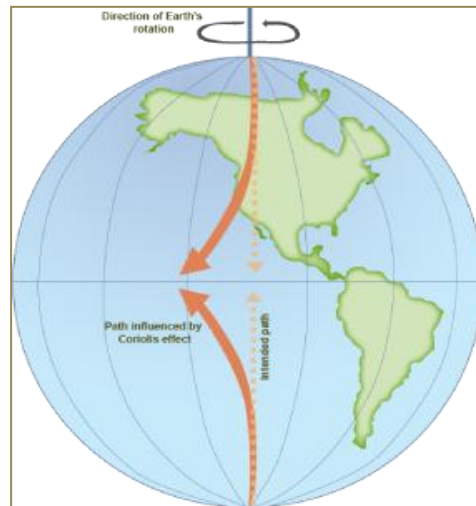


**Fig. 2.3 The inclination of wind direction due to Coriolis force [Ahr01]**

As the wind speed increases, the Coriolis force increases; hence, the stronger the wind, the greater the deflection. Additionally, the Coriolis force increases for all wind speeds from a value of zero at the equator to a maximum at the poles.

On the other hand, surface of the earth is subject to unequal solar radiation on each part of the world, producing different types of wind. The closed circulation of air between the equator and the poles as shown in **Fig. 2.3** is not the proper model for a rotating earth. Thus, to describe air movement, meteorologists have divided the earth in six zones as shown in **Fig. 2.4**, **[Ahr01]**.

In large-scale atmospheric movements, the combination of the pressure gradient due to the uneven solar radiation and the Coriolis force due to the earth's self-rotation causes the *single* cell to break up into three convectional cells in each hemisphere: the Hadley cell, the Mid-latitude cell, and the Polar cell (**Fig. 2.4**). Each cell has its own characteristic circulation and the pattern is called ***three cell model***, **[Aza10, Ahr01]**.
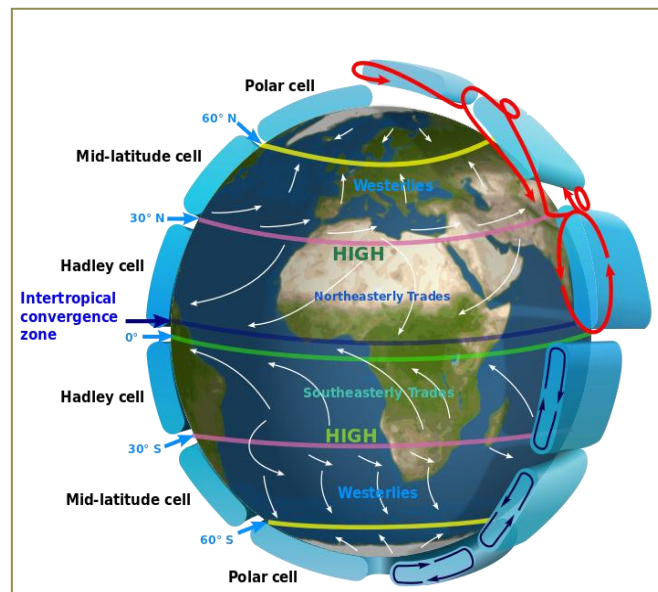
**Fig. 2.4 Idealized atmospheric circulations, [Lif].**

## 2.3 Wind Structure

Wind structure can be classified in terms of basic cause into, **[Sha13]**:

- **Geotropic wind**: wind at altitudes greater than 1km, the pressure and Coriolis force are equal and independent of surface topography.

- **Earth's surface wind**: The surface of the Earth exerts a frictional drag on the air blowing just above it and results in a no slip condition such that wind speed is zero.

- **Boundary layer:** it is exists between geotropic and earth's surface wind, in which wind speed increases from zero to its geotropic value at the top of the boundary layer. Surface roughness determines the thickness of the boundary layer, such that over rough terrain this layer is thicker then that over flat terrain.

## 2.4 Wind Direction

Direction of wind is an important factor in the siting of a wind energy conversion system. It is reported by the direction from which it originates. For example, a northerly wind blows from the north to the south. Wind direction is usually reported in cardinal directions or in azimuth degrees. For example, a wind coming from the south is given as 180 degrees; one from the east is 90 degrees. If we receive the major share of energy available in the wind from a

certain direction, it is important to avoid any obstructions to the wind flow from this side. Fluctuation in the wind direction with time is shown below **(Fig. 2.5)**. Recently, anemometers are used to identify the wind direction. However, most of the anemometers used today have provisions to record the direction of wind along with its speed, **[Ahr01, Mat01]**.
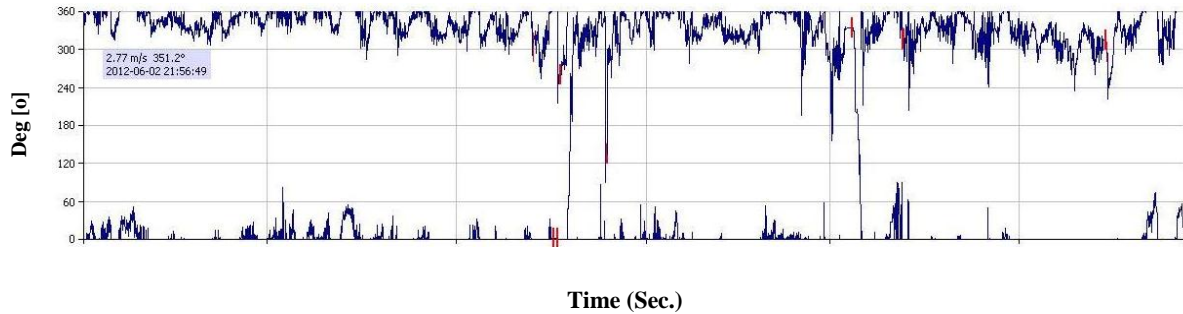


**Time (Sec.)**
**Fig. 2.5 Fluctuations in the wind direction, [Was].**

## 2.5 The Wind Rose

Information on the speed and direction of wind, in a combined form, can be presented in the wind roses. The wind rose is a chart which indicates the distribution of wind in different directions. The chart may be divided into 8, 12 or even 16 equally spaced sectors representing different directions. If wind rose presents the percentage of time for which we receive wind from a particular direction, then it is called frequency rose. Wind direction frequency information is important because, **[Bro12]**:

- it shows us the direction from which we get most of our wind.
- it optimizes the layout of wind turbines within a wind farm
- it is used for carrying out wake modeling.

The product of above percentage and the average wind speed in this direction will give us the average strength of the wind spectra. Typical wind rose for a location is shown in **Fig. 2.6**, **[Mat06]**. Radial lines lengths are proportional to the frequency of the wind from the compass point, with the circles forming a scale. The frequency of calm conditions is indicated sometimes in the center. The longest lines identify the prevailing wind directions. Wind roses generally are used to represent annual, seasonal, or monthly data, **[Man02]**.
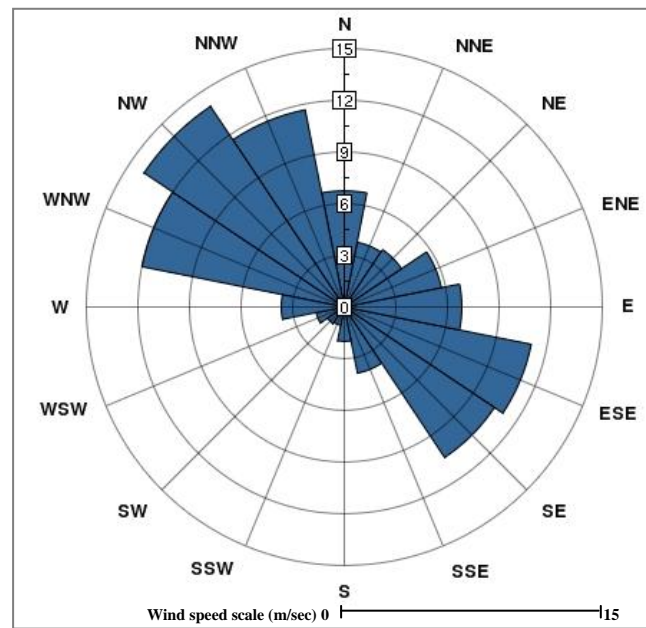
**Fig. 2.6 Wind rose showing the distribution of frequency or speed
in different directions, [Mat06].**

## 2.6 Wind Speed

Wind speed is one of the most critical characteristics in wind power generation. In fact, wind speed varies in both time and space, determined by many factors such as geographic and weather conditions. **Table 2.1** relates wind speed to observed conditions at land; its full name is the Beaufort wind scale.

**Table 2.1: Beaufort wind scale and state of the land, [Ahr01].**

| Beaufort Scale | Wind speed at 10 m height m/s | Description | Land conditions |
|---|---|---|---|
| 0 | 0.0-0.4 | Calm | Calm. Smoke rises vertically. |
| 1 | 0.4-1.8 | Light air | Smoke drift indicates wind direction. Leaves and wind vanes are stationary. |
| 2 | 1.8-3.6 | Light breeze | Wind felt on exposed skin. Leaves rustle. Wind vanes begin to move. |
| 3 | 3.6-5.8 | Gentle breeze | Leaves and small twigs constantly moving, light flags extended. |
| 4 | 5.8-8.5 | Moderate breeze | Dust and loose paper raised. Small branches begin to move. |
| 5 | 8.5-11 | Fresh breeze | Branches of a moderate size move. Small trees begin to sway. |

| | | | |
|---|---|---|---|
| 6 | 11-14 | Strong breeze | Large branches in motion. Whistling heard in overhead wires. Umbrella use becomes difficult. |
| 7 | 14-17 | Moderate gale | Whole trees in motion. Effort needed to walk against the wind. |
| 8 | 17-21 | Fresh gale | Some twigs broken from trees. Cars veer on road. Progress on foot is seriously impeded. |
| 9 | 21-25 | Strong gale | Some branches break off, and some small trees blow over. |
| 10 | 25-29 | Storm | Structural damage. |
| 11 | 29-34 | Violent | Widespread vegetation and structural damage. |
| 12 | >34 | Hurricane | Severe widespread damage to vegetation and structures. |

Because wind speed is a random parameter, measuring wind speed data are usually used statistical methods.

## 2.7 Statistical Analysis of Wind Data

For estimating the wind energy potential of a site, the wind data collected from the location should be properly analyzed and interpreted. The data are grouped over time spans in which we are interested in. For example, if we want to estimate the energy available at different hours, then the data should be grouped in an hourly basis. The data may also be categorized on daily, monthly or yearly bases, **[Gar06]**.

Long term wind data from the meteorological stations near to the candidate site can be used for making preliminary estimates. This data, which may be available for long periods, should be carefully extrapolated to represent the wind profile at the site. One year wind data recorded at the site is sufficient to represent the long term variations in the wind profile.

One worthwhile statistical quantity that will be studied first is the average or arithmetic mean**.**

## 2.7.1 Mean wind speed

Modern wind measurement systems give the mean wind speed at the site averaged over a pre-fixed time period. Ten minutes average is very common as most of the standard wind analysis softwares which tuned to handle data over ten minutes. This short term wind data are further grouped and analyzed with the help of models and softwares to make precise estimates on the energy available in the wind.

If we have a set of numbers, such as a set of measured wind speeds $v_i$, the mean of the set is defined as **[Mat06]**:

$$\bar{v} = \frac{1}{n} \sum_{i=1}^{n} v_i \qquad (2.1)$$

where *n* is the number of wind data.

However, for wind power calculations, averaging the speed using **Eq. 2.1** is a misleading. For example, 1 hour wind data from a site collected at 10 minutes interval are shown in **Table 2.2**. As per **Eq. 2.1**, the average wind speed is 6.45 m/sec, taking the air density as 1.24 kg/m$^3$, the corresponding average power is 166.37 W/m$^2$. If we calculate the power density corresponding to individual velocities and then take the average, the result would be 207 W/m$^2$. This means that, by calculating the average using **Eq. 2.1** is under estimating the wind power density by 20%, **[Mat06]**.

**Table 2.2: Wind speed at 10 minutes interval**

| No | $v$ (m/sec) | $v^3$ (m/sec)$^3$ | P.D. W/m$^2$ |
|----|----|----|----|
| 1 | 4.3 | 79.51 | 49.29 |
| 2 | 4.7 | 103.82 | 64.37 |
| 3 | 8.3 | 571.79 | 354.51 |
| 4 | 6.2 | 238.33 | 147.76 |
| 5 | 5.9 | 205.38 | 127.33 |
| 6 | 9.3 | 804.36 | 498.70 |

Thus, for wind energy calculations, the speed should be weighed for its power content while computing the average. The average wind speed represented by the root mean cube is, **[Mat06]**:

$$v_{rmc} = \left( \frac{1}{n} \sum_{i=1}^{n} v_i^3 \right)^{1/3} \tag{2.2}$$

If we use **Eq. 2.2**, the average speed in the previous example is 6.94 m/sec and the corresponding power is 207 W/m². This shows that due to the cubic speed power relationship, the weighted average expressed in **Eq. 2.2** should be used in wind energy analysis.

Wind speeds are observed many times during a year of observations. The numbers of observations of a specific wind speed $v_i$ will be defined as $m_i$, then the mean is **[Pat06]**:

$$\bar{v} = \frac{1}{n} \sum_{i=1}^{w} m_i v_i \tag{2.3}$$

where $w$ is the number of different values of wind speed observed and $n$ is still the total number of observations. In general we use **Eq. 2.3** when we deal with the histogram intervals.

### 2.7.2 Mod and median speed

We now define the following terms applicable to wind speed, **[Wuj13]**:

- *Mod speed:* is defined as the speed corresponding to the hump in the distribution function. This is the speed of the wind most of the time.
- *Median wind speed:* if $n$ is odd, the median is the middle number after all the numbers have been arranged in order of size. If $n$ is even the median is halfway between the two middle numbers when we rank the numbers.

### 2.7.3 Variance of wind speed

Arithmetic mean to set of numbers does not tell us the deviation from the mean. The Variance $\sigma^2$ to that set of data describes this variability by square each deviation to get all positive quantities as, **[Pat06]**:

$$\sigma^2 = \frac{1}{n-1} \sum_{i=1}^{n} (v_i - \bar{v})^2 \tag{2.4}$$

In term of frequency intervals the variance $\sigma^2$ is represented by, **[Pat06]**:

$$\sigma^2 = \frac{1}{n-1} \left[ \sum_{i=1}^{w} m_i \acute{v}_i^2 - \frac{1}{n} \left( \sum_{i=1}^{w} m_i \acute{v}_i \right)^2 \right] \tag{2.5}$$

The two terms inside the brackets are nearly equal to each other so full precision needs to be maintained during the computation.

### 2.7.4 Standard deviation of wind speed data

The standard deviation $\sigma$ is then defined as the square root of the variance **[Pat06]**:

$$\sigma = \sqrt{variance} \tag{2.6}$$

### 2.7.5 Skewness and kurtosis

To grasp the characteristics of the data better, the distributional pattern of the data were surveyed and researched by two statistics: Skewness and Kurtosis, the expression of these two statistics are shown in the following equations, **[Nan04]**:

$$Skewness = \frac{1}{n-1} \sum_{i=1}^{n} (v_i - \bar{v})^3 / \sigma^3 \tag{2.7}$$

$$Kurtosis = [\frac{1}{n-1} \sum_{i=1}^{n} (v_i - \bar{v})^4 / \sigma^4] - 3 \tag{2.8}$$

where $\bar{v}$ and $\sigma$ are defined by **Eqs'. 2.1 and 2.6**, respectively.
Skewness is a description of the symmetrical characteristic of the data, where Skewness=0 means the distributions of the data is symmetric, or else, it is not symmetric, Positive skewness indicates a distribution with an asymmetric tail extending toward more positive values. Negative skewness indicates a

distribution with an asymmetric tail extending toward more negative values. Kurtosis is a measure of the relative peakedness of its frequency curve, where Kurtosis=0 means the data is the same as the standard normal distribution, positive kurtosis indicates a peaked distribution and negative kurtosis indicates a flat distribution.

## 2.8 Wind Speed Frequency Distribution

Apart from the distribution of the wind speeds over a day or a year it is important to know the number of times per month or per year during which the given wind speeds occurred, i.e. the frequency distribution of the wind speeds. To arrive at this frequency distribution we must divide the wind speed domain into a number of intervals, mostly of equal width of 1 m/sec or 0.5 m/sec. Then starting at the first interval of say 0-1 m/sec, the number of times is counted in the period concerned that the wind speed was in this interval. When the number of hours in each interval (or distribution) is plotted against the wind speed, the frequency distribution emerges as a histogram (see **Fig. 2.7-a**), **[Qam09]**.

The sorting of the data into narrow wind speed bands is called binning of the data. In our case a bin width of 1m/sec has been used. The central value of each bin i.e. 0.5 m/sec, 1.5 m/sec etc. The histogram provides information about how often the wind is blowing for each wind speed bin, **[Aza10, Aza11]**.

Cumulative histogram is constructed by plotting the cumulative time for which the wind speed is below the upper limit of the wind class interval. The cumulative histogram of the above data (**Fig. 2.7-a**) is shown in **Fig. 2.7-b**, **[Ahr01]**.

If we join the midpoints of the frequency and cumulative histograms in **Fig. 2.7** we get smooth curves with a well-defined pattern represent probability density (or distribution function) as shown in **Figs. 2.7-a** and **2.7-b respectively** (blue curves). This shows that it is logical to represent the wind speed distributions by standard statistical functions. Various probability functions were fitted with the field data to identify suitable statistical distributions for representing wind regimes. It is found that the Weibull and Rayleigh distributions can be used to describe the wind variations in a regime with an acceptable accuracy level,

**[Mat06]**. To obtain wind speed frequency distribution the following two procedures are necessary, **[Qam09]**.



**(a) Ordinary histogram**                    **(b) Cumulative histogram**
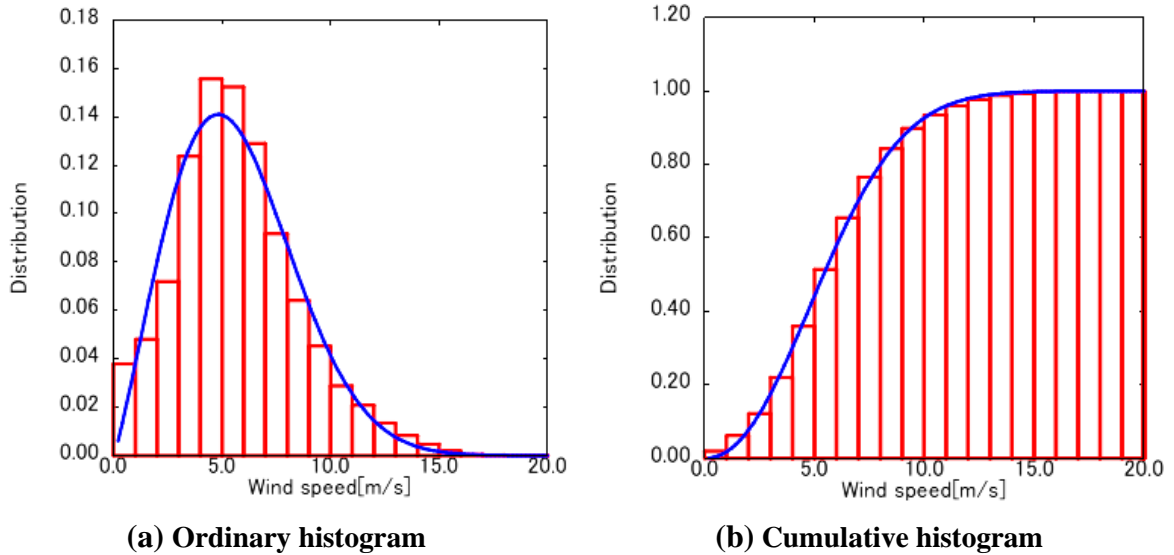
**Fig. 2.7 An ordinary and cumulative histograms of the same data, [Tak].**

- *Binning of data:* explained above.
- *Finding relative frequency:* It is proportional to wind speed recurrence in each bin. It can be viewed as the estimate of probability of a given wind speed in each bin. Relative frequency is defined as in **Eq. 2.9** below, **[Aza11]**:

$$R_f = \frac{\text{Frequency of given wind speed}}{\text{Total period}} \tag{2.9}$$

## 2.9 Weibull Distribution

When the percentage frequency distribution is plotted against the wind speed, the frequency distribution emerges as a curve. The top of this curve is the most frequent wind speed. This frequency distribution is used also to identify the most suitable wind turbine for the site. The Weibull distribution (named after the Swedish physicist W. Weibull, who applied it when studying material strength in tension and fatigue in 1930s) provides a close approximation to the probability laws of many natural phenomena. For more than half a century the Weibull's distribution has attracted the attention of statisticians working

on theory and methods as well as various fields of statistics. Hundreds or even thousands of papers have been written on this distribution and the research is ongoing. Together with the normal, exponential distributions, the Weibull's distribution is without any doubt, the most popular model in statistics. It is of utmost interest to theory orientated statisticians because of its great number of special features which enable to fit, in addition to its ability to fit data from various fields such as life data, weather data, economics, business administration, health, physical, social sciences, hydrology, biology, and engineering sciences, **[Aza12, Sun12]**.

For wind data analysis, prior studies have also shown that statistical methods such as the Weibull and Rayleigh (a special case of Weibull) distribution models can equally be used, but Weibull is a *two parameter*s distribution while the Rayleigh has only *one parameter*. This makes the Weibull somewhat more versatile and the Rayleigh somewhat simpler to use. The two-parameter Weibull probability distribution function is the most appropriate, accepted and recommended distribution function for wind speed data analysis, and it forms the basis for commercial wind energy applications and software, such as the Wind Atlas Analysis and Application Program (WAsP) and the recently developed Nigerian Wind Energy Information System (WIS) software. This is because it gives a better fit for measured probability density distributions than other statistical functions.

In Weibull distribution, the variation in wind speed is characterized by two functions; The *probability density function* and the *cumulative distribution function,* which are plotted as blue curves in **Figs. 2.7-a** and **2.7-b**, respectively, **[Mat06, Mod07]**.

## 2.9.1 Two parameters probability density function (pdf)

The two-parameter Weibull distribution is given by,

$$f(v) = \frac{k}{c} \left(\frac{v}{c}\right)^{k-1} exp\left(- \left(\frac{v}{c}\right)^{k}\right) \qquad (2.10)$$

where, $f(v) \geq 0 , v \geq 0 ; \; k > 0 , c > 0$

And:

$f(v)$ = the probability of observing wind speed $v$.

$k$ = the dimensionless Weibull shape parameter (or factor).

$c$ = the  scale parameter in the units of wind speed (m/sec).

There is also a special case of the Weibull distribution known as Rayleigh distribution (one-parameter Weibull distribution). This in fact takes the same form as the two-parameter Weibull pdf, the only difference being that the value of $k$ is assumed to be 2.0, **[Ulg02, Bry06]**.


## 2.9.2 Three parameter probability density function (pdf)

Here, the location parameter is added, and it can take positive or negative values. When location parameter is equal to zero, the pdf equation reduces to two parameter Weibull function. The variation in wind speed at a particular site can be best described using the Weibull distribution density function, which illustrates the probability of different wind speeds occurring at the site during a period of time. Three-parameters Weibull distribution expression can be expressed as, **[Ulg02]**:

$$f(v) = \frac{k}{c} \left(\frac{v-g}{c}\right)^{k-1} exp\left(-\left(\frac{v-g}{c}\right)^{k}\right) \qquad (2.11)$$

where,  $g$ = the location parameter, and $g \leq v$.

## 2.10 Weibill Parameters

The most general expression of the Weibull pdf is given by the three-parameters. An important aspect of the Weibull pdf is how each of

- the shape parameter $k$,
- the scale parameter $c$,
- the location parameter $g$,
- and the wind speed variable $v$.

affects the pdf curve. These effects will be shown below.

## 2.10.1 Weibull shape parameter, *k*

Shape factor is a measurement of the width of the distribution. Different values of the shape parameter can have effects on the behavior of the distribution. This is demonstrated in **Fig. 2.8**. In fact, some values of the shape parameter will cause the distribution equations to reduce to those of other distributions. For example, **[Lys83]**: if

| | |
|---|---|
| $k = 1$ | The Weibull distribution is equivalent to the exponential distribution. |
| $k = 2$ | The Weibull distribution is equivalent to the Rayleigh distribution. |
| k is between 3 and 4 | The Weibull distribution which approximates the normal distribution provides the best estimation. |
| $k = 5$ | The Weibull distribution approximates the peaked normal distribution. |
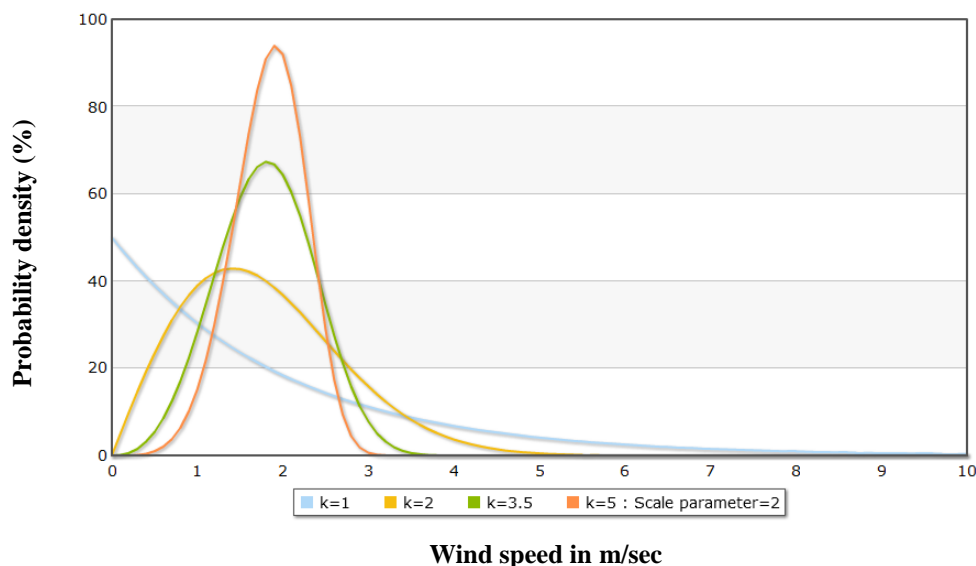


**Wind speed in m/sec**

**Fig. 2.8 Effect of Weibull shape parameter on probability plot, [work of researcher].**

## 2.10.2 Weibull scale parameter, *c*

Scale factor is closely related to the mean wind speed. Increasing the value of scale parameter while holding shape parameter constant has the effect

of stretching out the pdf. Since the area under a pdf curve is a constant value equal one, the peak of the pdf curve will decrease with the increase in $c$, as indicated in **Fig. 2.9**.
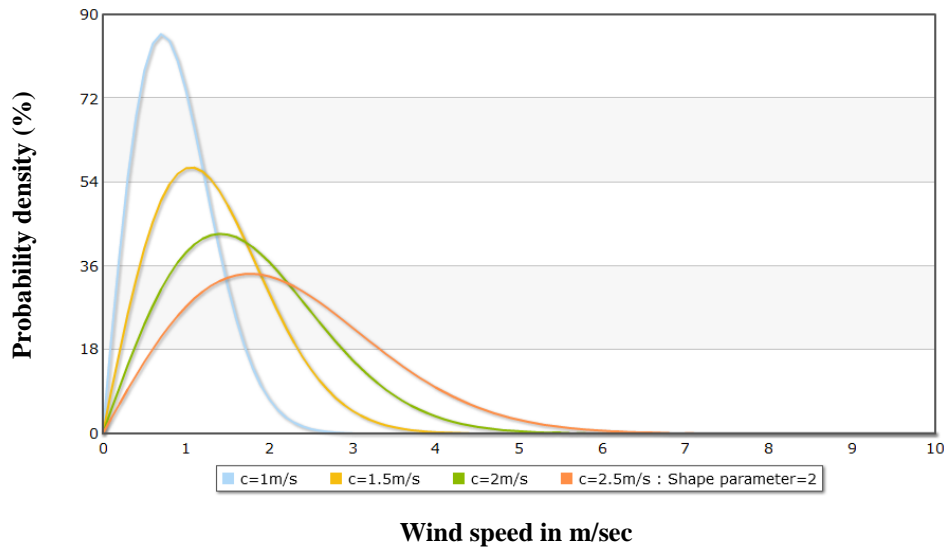


**Fig. 2.9 Effect of Weibull scale parameter on probability plot, [work of researcher].**

Scale parameter has the folloeing properties**, [Ulg02]**:

- If $c$ is increased, while $k$ and $g$ are kept the same, the distribution gets stretched out to the right and its height decreases.
- If $c$ is decreased, while $k$ and $g$ are kept the same, the distribution gets pushed in towards the left (i.e. towards its beginning or towards 0), and its height increases.
- $c$ has the same unit as wind speed.

## 2.10.3 Weibull locatin parameter, $g$

The location parameter $g$, as the name implies, locates the distribution along the wind speed axis. Changing the value of $g$ has the effect of sliding the distribution and its associated function either to the right (if $g > 0$) or to the left (if $g < 0$).
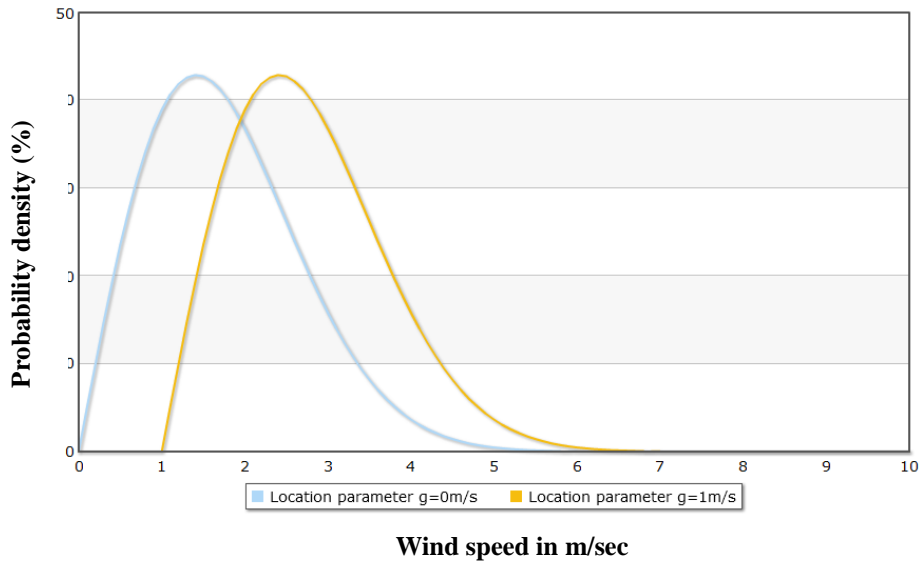
**Fig. 2.10 Effect of Weibull location parameter on probability plot, [work of researcher].**

Location parameter has the following properties, **[Ulg02]**:

- if $g = 0$ the distribution starts at $v = 0$ or at the origin.
- If $g > 0$ the distribution starts at the location $g$ to the right of the origin (see **Fig. 2.10**).
- If $g < 0$ the distribution starts at the location $g$ to the left of the origin.
- The parameter $g$ may assume all values.
- $g$ has the same units as $v$.

## 2.11 Cumulative Distribution Function

The cumulative distribution function $F(v)$ (for $v \geq 0$), indicating the time fraction or probability that the wind speed $v$ is smaller than or equal to a given wind speed $\grave{v}$, **[Qam09]**:

$$F(v) = P\ (v\ \leq\ \grave{v}) \qquad (2.12)$$

Cumulative distribution function is the integration of Weibull density function (pdf). It is the cumulative of relative frequency of each speed interval. The equation of cumulative Weibull Function is given by, **[Rei11]**:

$$F(v) = \int_{0}^{v} f(v)\,dv \qquad (2.13)$$

or,

$$F(v) = 1 - e^{-\left(\frac{v}{c}\right)^k} \tag{2.14}$$

Average wind speed of a regime which following the Weibull distribution is given as first raw moment by, **[Mat06]**:

$$v_m = \int_0^\infty v\, f(v)\, dv \tag{2.15}$$

By substituting **Eq. 2.10**, we get

$$v_m = \int_0^\infty v\, \frac{k}{c} \left(\frac{v}{c}\right)^{k-1} e^{-(v/c)^k}\, dv \tag{2.16}$$

In another form,

$$v_m = k \int_0^\infty \left(\frac{v}{c}\right)^k e^{-(v/c)^k}\, dv \tag{2.17}$$

Taking following representations,

$$x = \left(\frac{v}{c}\right)^k, \qquad dv = \frac{c}{k}\, x^{\left(\frac{1}{k}-1\right)}\, dx \tag{2.18}$$

Substituting (2.18) in **Eq. 2.17** we get,

$$v_m = c \int_0^\infty e^{-x}\, x^{1/k}\, dx \tag{2.19}$$

The form of standard gamma function is given by,

$$\Gamma n = \int_0^\infty e^{-x} x^{n-1}\, dx \tag{2.20}$$

Hence, from **Eq. 2.19**, the average wind speed can be expressed as

$$\bar{v} = c\, \Gamma\left(1 + \frac{1}{k}\right) \tag{2.21}$$

Now, the second raw moment is represented by

$$\mu_2 = \int_0^\infty v^2\, f(v)\, dv \tag{2.22}$$

The standard deviation of wind speed following the Weibull distribution is:

$$\sigma_v = (\mu_2 - \bar{v}^2)^{1/2} \tag{2.23}$$

Substituting the two-parameter pdf in **Eq. 2.22** and solve the result, we will get

$$\mu_2 = c^2 \int_0^\infty e^{-x}\, x^{2/k}\, dx \tag{2.24}$$

Thus, the $2^{nd}$ raw moment can be expressed as a gamma function in the form

$$\mu_2 = c^2\, \Gamma\!\left(1 + \frac{2}{k}\right) \tag{2.25}$$

By the same method the $3^{rd}$ and the $4^{th}$ raw moment can be expressed in the following two forms

$$\mu_3 = c^3\, \Gamma\!\left(1 + \frac{3}{k}\right) \tag{2.26}$$

$$\mu_4 = c^4\, \Gamma\!\left(1 + \frac{4}{k}\right) \tag{2.27}$$

It is important to know that $1^{st}$ raw moment is equal to the conventional mean and also useful for measure distribution location, while $2^{nd}$, 3rd, and $4^{th}$ raw moments have useful measures for spread, skewness, and Kurtosis (Peakedness) respectively, **[Rei11]**.

The cumulative distribution function can be used for estimating the time for which wind is within a certain speed interval. Probability of wind speed being between $v_1$ and $v_2$ is given by the difference of cumulative probabilities corresponding to $v_2$ and $v_1$. Thus

$$P\,(\,v_1 < v < v_2\,) = F\,(\,v_2\,) - F\,(\,v_1\,) \tag{2.28}$$

That is

$$P\left(v_1 < v < v_2\right) = e^{-\left(v1/c\right)^k} - e^{-\left(v2/c\right)^k} \tag{2.29}$$

We may be interested to know the possibilities of extreme wind at a potential location, so that the system can be designed to sustain the maximum probable loads. The probability for wind speed $v$ being equal to or greater than $v_x$ is

$$P(v \geq v_x) = 1 - \left(1 - e^{-\left(v_x/c\right)^k}\right) = e^{-\left(v_x/c\right)^k} \tag{2.30}$$

After multiplying **Eq. 2.29** by (8760.25 hour), it's possible to estimate the number of hours per year that the wind speed will be between $v_1$ and $v_2$. By the same way, it is also possible to estimate the number of hours per year that the wind speed is greater than or equal to $v_x$ using **Eq. 2.30**.

## 2.12 Common Weibull Statistics

The formulas below represent common Weibull statistical properties with the shape, scale and location parameters equal to $k$, $c$ and zero respectively. The mean, median and mod of the wind data can be calculated as follows **[Pat06 , Ulg02]**:

$$Mean; \;\; \text{defined in Eq.} \, 2.21$$

$$Median = c \cdot \ln(2) \tag{2.31}$$

$$\text{Mod} = 0 \text{ for k=1} \tag{2.32}$$

The wind speed $v_{me}$ is the speed which produces more energy than any other wind speed, which is given by:

$$v_{me} = c \left(\frac{k+2}{k}\right)^{1/k} \tag{2.33}$$

Therefore, the maximum energy obtained from $v_{me}$ wind speed is:

$$E_{max} = \frac{1}{2}\rho \, \text{Area} \, v_{me}^3 \, f(v_{me})(8760) \tag{2.34}$$

Finally, the most probable wind speed can be given by, **[Odo12]**:

$$v_F = \text{Mod} = c \left(\frac{k-1}{k}\right)^{1/k} \text{ for k} > 1 \qquad (2.35)$$

The most probable wind speed (modal speed) corresponds to the hump in the distribution function. This is the speed of the wind most of the time, while the wind speed carrying maximum energy can be used to estimate the wind turbine design or rated wind speed, **[Wuj13]**.

Once the $v_F$ and the $v_{me}$ wind speeds are known, the wind turbine operating range can be estimated and is given by, **[Ayo12]**.

$$v_{me} \leq V_O \leq (2 \text{ to } 4)\, v_{me}$$

$$(1.5 \text{ to } 3)\, v_F \leq V_r \leq V_O \qquad (2.36)$$

$$0.3\, v_F \leq V_I \leq 0.8\, v_F$$

where $V_O$ is the wind speed at which the wind turbine shuts down (cutout wind speed), $V_I$ is the wind speed at which the wind turbine starts to produce power known as cutin wind speed and $V_r$ is the wind speed at which the wind turbine operates at full rating.

Prior studies have shown that wind turbine system operates most efficiently at its rated wind speed. Therefore, it is required that the rated wind speed and the wind speed carrying maximum energy should be as close as possible, **[Mod07]**. The standard deviation of the Weibull density function can be shown to be:

$$\sigma \,(\textit{Standard Deviation}) = c \cdot \sqrt{\Gamma\left(1 + \frac{2}{k}\right) - \left(\Gamma\left(1 + \frac{1}{k}\right)\right)^2} \qquad (2.37)$$

using **Eq.** above and **Eq. (2.21)** we get,

$$\frac{\sigma}{\bar{v}} = \frac{\sqrt{\Gamma\left(1 + \frac{2}{k}\right) - \left(\Gamma\left(1 + \frac{1}{k}\right)\right)^2}}{\Gamma\left(1 + \frac{1}{k}\right)} \qquad (2.38)$$

The relation between $\dfrac{\sigma}{\bar{v}}$ and $k$ is shown in **Fig. 2.11**, **[Scr71]**:
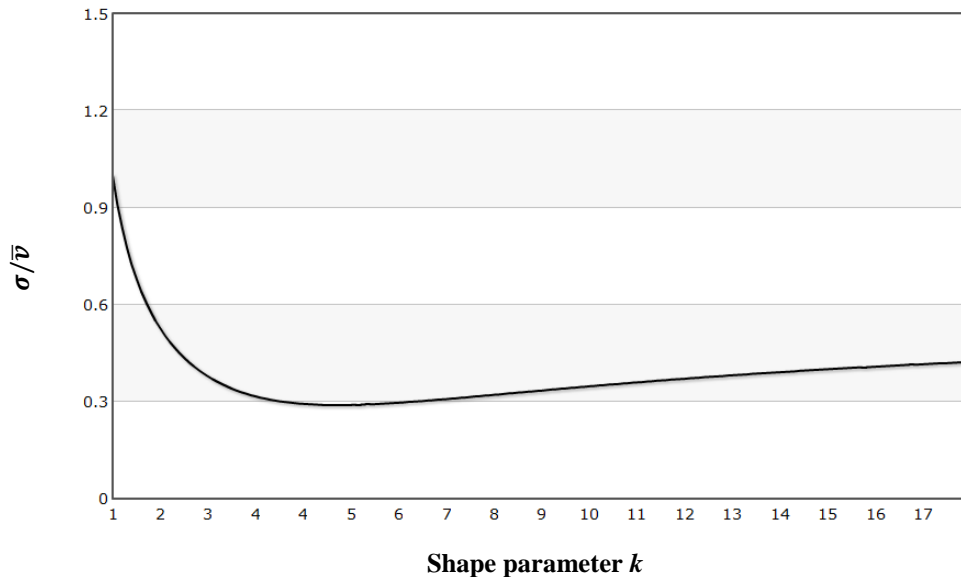
**Fig. 2.11: The relative standard deviation of a Weibull distributionas
a function of the Weibull shape factor *k*, [work of researcher].**

If the mean wind speed and standard deviation of the distribution is calculated then the corresponding *k*-value can be found from **Fig. 2.11**.

The relation in **Eq. 2.38** also called coefficient of variation, one should use the coefficient of variation instead of the standard deviation for comparison between data sets with different units or widely different means.

## 2.13 Methods for Estimating Weibull Parameters

Weibull parameters regulate the wind speed distribution to optimize the performance of a wind conversion system. It is therefore, very essential to accurately estimate the parameters for any candidate site for installation of wind energy conversion systems. Various methods have been proposed for estimating the parameters and the suitability of each method varies with sample data, which in turn, varies from location to location, **[Sal13]**.

Our adopted methods for estimating *k* and *c* are:

1. Standard deviation method (SDM)
2. Energy pattern factor method (EPFM)
3. Maximum likelihood estimation (MLE) using Newton-Raphson method (MLE-NRM)
4. MLE using iterative method (MLE-IM)

5. MLE using frequency dependent iterative method (MLE-FDM)
6. MLE using modified iterative method (MLE-MIM)
7. Linear least square method (LLSM)
8. Modified linear least square method (MLLSM)
9. Equivalent energy method (EEM)

### 2.13.1 Standard deviation method (SDM)

This method is useful where only the mean wind speed and standard deviation are available. In addition, it has relatively simple expressions when compared with other methods. Moreover, it is unlike most of the other methods that may require more detailed wind data (which, in some cases, are not readily available) for the determination of the Weibull distribution shape and scale parameters. The shape and scale factors are thus computed from the mean and standard deviation of wind data as an acceptable approximation in forms, **[Mod07, Ibr13]**:

$$k = \left(\frac{\sigma}{\bar{v}}\right)^{-1.086} \tag{2.39}$$

$$c = \frac{\bar{v}}{\Gamma\left(1 + \frac{1}{k}\right)} \tag{2.40}$$

To be more accurate, scale factor can be determined from the following expressions given by, **[Odo12]**:

$$c = \frac{\bar{v}\, k^{2.6674}}{0.184 + 0.816\, k^{2.73855}} \tag{2.41}$$

**Eq. 2.41** is used in this study to estimate the monthly and annual scale factor.

### 2.13.2 Energy pattern factor method (EPFM)

Energy pattern factor (EPF) or Cube Factor is the ratio between the total power available in the wind and the power corresponding to the cube of the mean wind speed, **[Ibr13]**:

$$E_{PF} = \frac{\text{Total amount of power available in the wind}}{\text{Power calclated by mean cube speed}} \qquad (2.42)$$

In terms of wind speed we have:

$$E_{PF} = \frac{1}{n}\sum_{i=1}^{n} v_i^3 \Big/ \left(\frac{1}{n}\sum_{i=1}^{n} v_i\right)^3 \qquad (2.43)$$

Once the energy pattern factor for a regime is found from the wind data, an approximate solution for $k$ is:

$$k = 3.957\, E_{PF}^{-0.898} \qquad (2.44)$$

### 2.13.3 MLE using Newton-Raphson method (MLE-NRM)

Let $v_1,\ v_2,\ v_3,\ldots\ldots,\ v_n$ be a random sample of size $n$ drawn from a probability density function $f(v,\theta)$ where $\theta$ is an unknown parameter. The likelihood function of this random sample is the joint of the $n$ random variables and is a function of the unknown parameter, thus **[Myu03]**:

$$L = \prod_{i=1}^{n} f(v_i,\theta) \qquad (2.45)$$

is the likelihood function. The MLE is the value of $\theta$ that maximizes $L$ or, equivalently, the logarithm of $L$.

$$\frac{d\log L}{d\theta} = 0 \qquad (2.46)$$

Now, we apply the MLE to estimate the Weibull parameters, namely the shape parameter and the scale parameters. Consider the Weibull probability density function (pdf) given in **Eq. (2.10)**, then likelihood function will be:

$$L(v_1, v_2, \ldots, v_n, k, c) = \prod_{i=1}^{n} \frac{k}{c}\left(\frac{v}{c}\right)^{k-1} exp\left(-\left(\frac{v}{c}\right)^k\right) \qquad (2.47)$$

Taking the logarithms of **Eq. (2.47)**, differentiating with respect to $k$ and $c$ in turn and equating to zero, we obtain the estimating equations:

$$\frac{\partial \ln L}{\partial k} = \frac{n}{k} + \sum_{i=1}^{n} \ln v_i - \frac{1}{c} \sum_{i=1}^{n} v_i^k \ln v_i = 0 \tag{2.48}$$

$$\frac{\partial \ln L}{\partial c} = \frac{-n}{c} + \frac{1}{c^2} \sum_{i=1}^{n} v_i^k = 0 \tag{2.49}$$

Eliminating $c$ between these two above equations and simplifying the results, yields

$$\frac{\sum_{i=1}^{n} v_i^k \ln v_i}{\sum_{i=1}^{n} v_i^k} - \frac{1}{k} - \frac{1}{n} \sum_{i=1}^{n} \ln v_i = 0 \tag{2.50}$$

which may be solved to estimate $k$. This can be accomplished by the use of standard iterative procedures (that is, Newton-Raphson method), which can be written in the form, **[Ibr13, Par10]**:

$$(\textit{Newton-Raphson}) \qquad k_{m+1} = k_m - \frac{f(k_m)}{f'(k_m)} \tag{2.51}$$

where,

$$f(k) = \frac{\sum_{i=1}^{n} v_i^k \ln v_i}{\sum_{i=1}^{n} v_i^k} - \frac{1}{k} - \frac{1}{n} \sum_{i=1}^{n} \ln v_i \tag{2.52}$$

and,

$$f'(k) = \sum_{i=1}^{n} v_i^k (\ln v_i)^2$$

$$-\frac{1}{k^2} \sum_{i=1}^{n} v_i^k (k \ln v_i - 1) - \left(\frac{1}{n} \sum_{i=1}^{n} \ln v_i\right) \left(\sum_{i=1}^{n} v_i^k \ln v_i\right) \tag{2.53}$$

Once $k$ is determined, $c$ can be estimated as:

$$c = \left(\frac{\sum_{i=1}^{n} v_i^k}{n}\right)^{1/k} \tag{2.54}$$

Here, $v_i$ is the wind speed in time step $i$ and $n$ the number of nonzero wind speed data points, **[Par10, Vey05]**.

## 2.13.4 MLE using iterative method (MLE-IM)

After rearranging **Eq. 2.50**, it is possible to estimate the shape factor as follows, **[Vey05, Ahm09]**:

$$k = \left( \frac{\sum_{i=1}^{n} v_i^k \ln(v_i)}{\sum_{i=1}^{n} v_i^k} - \frac{\sum_{i=1}^{n} \ln(v_i)}{n} \right)^{-1} \tag{2.55}$$

The above equation must be solved using iterative procedure, after which **Eq. 2.54** is applied in order to estimate scale parameter. Care must be taken to apply **Eq. 2.55** only to the nonzero wind speed data points.

## 2.13.5 MLE using frequency dependent iterative method (MLE-FDM)

It is applied by converting the wind speed time series in frequency distribution format. The shape parameter $k$ and the scale parameter $c$ are estimated using the following relationship, **[Rin09]**:

$$k = \left( \frac{\sum_{i=1}^{\acute{n}} \acute{v}_i^k \ln(\acute{v}_i)\, P(\acute{v}_i)}{\sum_{i=1}^{\acute{n}} \acute{v}_i^k\, P(\acute{v}_i)} - \frac{\sum_{i=1}^{\acute{n}} \ln(\acute{v}_i)}{\acute{n}} \right)^{-1} \tag{2.56}$$

$$c = \left( \frac{1}{\acute{n} * P(\acute{v}_i)} \sum_{i=1}^{\acute{n}} \acute{v}_i^k \right)^{1/k} \tag{2.57}$$

where $\acute{v}$ is the wind speed central to the bin $i$, $\acute{n}$ is the number of bins, $P(\acute{v} \geq 0)$ is the probability for wind speed equal to or exceeding zero. **Eq. 2.57** is solved using iterative procedure by guessing a suitable initial value of $k$ **Eq. 2.57** is then solved explicitly to estimate $c$.

## 2.13.6 MLE using modified iterative method (MLE-MIM)

It is another modification to the MLE method, which considers a new way for parameters finding. This modification is based on estimation of the best three Weibull parameters for pdf representation; accordingly, it is possible to have a very good fitting between pdf and histogram (wind speed distribution) of the site.

From a three–parameter Weibull distribution $(c, k, g)$ given by **Eq. 2.11**, **[Rin09]**:

$$-\frac{nk}{c} + \frac{k}{c} \sum_{i=1}^{n} \left(\frac{v_i - g}{c}\right)^k = 0 \tag{2.58}$$

By simplifying above gives:

$$c = \left[\frac{1}{n} \sum_{i=1}^{n} (v_i - g)^k\right]^{1/k} \tag{2.59}$$

After some substitutions and arrangements available in reference **[Rin09]**, shape parameter is given by:

$$k = \left(\frac{\sum_{i=1}^{n}(v_i - g)^k \, ln(v_i - g)}{\sum_{i=1}^{j}(v_i - g)^k} - \frac{\sum_{i=1}^{n} ln(v_i - g)}{n}\right)^{-1} \tag{2.60}$$

As mentioned before, - ve. of $g$ will slide the curve to the left direction, while +ve. of $g$ will slide the curve to the right direction.

## 2.13.7 Linear least square method (LLSM)

This method is also called *Graphical Method*. With the help of this method the parameters are estimated with the regression line equation by using cumulative density function. The cumulative density function of Weibull distribution with two parameters is given by **Eq. 2.14**, **[Ahm09]**:

$$F(v) = 1 - e^{-\left(\frac{v}{c}\right)^k} \tag{2.14}$$

Then, it could perform the necessary mathematical operations on **Eq. 2.14** to linearize it in order to minimize the least squared error between the linearized ideal curve and the actual data points. The process is somewhat of an art and there may be more than one procedure which will yield a satisfactory result. Whether the result is satisfactory or not has to be judged by the agreement between the Weibull curve and the actual data, **[Pat06]**.

Rearranging **Eq. 2.14** in terms of wind speed $i$ yields:

$$1 - F(v_i) = e^{-\left(\frac{v_i}{c}\right)^k} \tag{2.61}$$

Now taking the logarithm of **Eq. 2.61** twice, **[Gar06, Vey05]**:

$$ln[-ln(1 - F(v_i))] = k \ln v_i - k \ln c \tag{2.62}$$

This is in the form of an equation of a straight line

$$y_i = ax_i + b \tag{2.63}$$

where $x_i$ and $y_i$ are variables, $a$ is the slope, and $b$ is the intercept of the line on the $y$ axis, such that:

$$
\begin{aligned}
y_i &= ln\big[-ln\big(1 - F(v_i)\big)\big] \\
a &= k \\
x_i &= ln\, v_i \\
b &= -k \ln c
\end{aligned}
\tag{2.64}
$$

The idea is to find the values of $a$ and $b$ in **Eq. 2.63** such that a straight line drawn through the $(x_i, y_i)$ points has the best possible fit. Parameters $k$ and $c$ are given by, **[Gar06, Vey05]**:

$$k = \frac{n \sum_{i=1}^{n} x_i y_i - \sum_{i=1}^{n} x_i \sum_{i=1}^{n} y_i}{n \sum_{i=1}^{n} x_i^2 - \left(\sum_{i=1}^{n} x_i\right)^2} \tag{2.65}$$

$$c = \exp\left(\frac{k \sum_{i=1}^{n} x_i - \sum_{i=1}^{n} y_i}{nk}\right) \tag{2.66}$$

## 2.13.8 Modified linear least square method (MLLSM)

The linear least square method could be modified by limiting the upper and lower data points of $y_i$ values in **Eq. 2.64**. This process may work to isolate the anomalous points which may give adequate results. Then, it is possible to follow chart and verify the best straight line passing through the points.

## 2.13.9 Equivalent energy method (EEM)

A new method for the estimation of Weibull parameters, called the Equivalent Energy Method, is based on the energy content of the distribution and it has been developed to improve the accuracy of the parameters. This new method uses optimized procedure to determine the Weibull parameters which

best fit the measured wind speed frequency distribution and equals the cube of the wind speed, i.e. the energy content of the wind, **[Sil05]**.

According to the Weibull distribution, the probability of wind speed occurrences is greater than or equal to a specific value, *v*, is defined by:

$$P(v) = e^{-(\frac{v}{c})^k} \tag{2.67}$$

Now the probability of having wind speeds greater than or equal to *v-1* and lower than *v* ($v-1 \leq v < v$) is, **[Sil05]**:

$$P(\mathrm{v}) = P(v-1) - P(v) \tag{2.68}$$

$$P(\mathrm{v}) = e^{-(\frac{v-1}{c})^k} - e^{-(\frac{v}{c})^k} \tag{2.69}$$

Statistically a stochastic variable $P_v$ represented by the probability function $P$ can be defined as:

$$P_{\mathrm{v}} = P(\mathrm{v}) + \varepsilon = \left( e^{-(\frac{v-1}{c})^k} - e^{-(\frac{v}{c})^k} \right) + \varepsilon \tag{2.70}$$

where $\varepsilon$ corresponds to the stochastic term.

Using the condition of energy content equivalence between the observed wind speeds and the Weibull distribution, the scale factor, *c*, can be written from the mean cube expression as, **[Sil05]**:

$$c = \left( \frac{\bar{v}^3}{\Gamma(1 + \frac{3}{k})} \right)^{\frac{1}{3}} \tag{2.71}$$

Substituting **Eq. 2.71** in **Eq. 2.70** yields:

$$P_{\mathrm{v}} = e^{-\left( \frac{(v-1)\left(\Gamma(1+\frac{3}{k})\right)^{\frac{1}{3}}}{\bar{v}} \right)^k} - e^{-\left( \frac{v\left(\Gamma(1+\frac{3}{k})\right)^{\frac{1}{3}}}{\bar{v}} \right)^k} + \varepsilon \tag{2.72}$$

The Weibull shape factor, k, can be estimated by applying the least squares technique to the following expression:

$$\sum_{i=1}^{\acute{n}} [P_{v_i} - e^{-\left(\frac{(v_i-1)\left(\Gamma\left(1+\frac{3}{k}\right)\right)^{\frac{1}{3}}}{\bar{v}}\right)^k} + e^{-\left(\frac{v_i\left(\Gamma\left(1+\frac{3}{k}\right)\right)^{\frac{1}{3}}}{\bar{v}}\right)^k}]^2 \qquad (2.73)$$

$$= \sum_{i=1}^{\acute{n}} (\varepsilon_i)^2$$

$P_{v_i}$ = the probability of having wind speeds for $i^{th}$ bin,

$\acute{n}$ = the number of bins of the wind speed histogram,

$v_i$ = the highest wind speed value of the $i^{th}$ bin,

$\bar{v}^3$ = the mean cube (observed).

After $k$ is compute, the scale factor is calculated from **Eq. 2.71**.

## 2.14 Goodness of Fit

To examine whether a theoretical probability density function is suitable to describe the wind speed data or not, several tests are used for validating the accuracy of the predicted wind speed distribution obtained from Weibull probability density function; such as the *root mean square error* test **(RMSE)**, *Chi-square* test ($\chi^2$), *correlation coefficient* test **(R)**, and Coefficient of Determination **(COD)**. Using multiple statistics tests helps to avoid biased results.

### 2.14.1 Root mean square error (RMSE)

The **RMSE** has been used for measuring the difference between the predicted and the actual (measured) values. The root mean square error value is defined as, **[Lao12, Alb06]**:

$$RMSE = \left[\frac{1}{\acute{n}} \sum_{i=1}^{\acute{n}} (y_i - x_i)^2\right]^{1/2} \qquad (2.74)$$

where,

$y_i$ = is the $i^{th}$ actual wind distribution (measured data).

$x_i$ = is the predicted wind distribution from the Weibull.

$\acute{n}$ = is the number of wind speed dataset (bins).

## 2.14.2 Chi-square test ($\chi^2$)

Also, the Chi-Square method is used for testing the predicted wind distribution with respect to the actual wind distribution. The mathematical expression for the Chi-square test "$\chi^2$" is defined as, **[Lao12, Alb06]**:

$$\chi^2 = \sum_{i=1}^{\acute{n}} \frac{(y_i - x_i)^2}{x_i} \tag{2.75}$$

Where $x_i$, $y_i$ and $\acute{n}$ are defined in Eq. (2.74).

## 2.14.3 Correlation coefficient (R)

The correlation coefficient is a statistical technique that is used to determine the linear relationship between two datasets. The mathematical equation for R is defined as, **[Lao12, Kol12]**:

$$R = \frac{\acute{n} \sum_{i=1}^{\acute{n}}(y_i \cdot x_i) - \sum_{i=1}^{\acute{n}} y_i \cdot \sum_{i=1}^{\acute{n}} x_i}{\sqrt{\acute{n} \sum_{i=1}^{\acute{n}} y_i^2 - \left(\sum_{i=1}^{\acute{n}} y_i\right)^2} \cdot \sqrt{\acute{n} \sum_{i=1}^{\acute{n}} x_i^2 - \left(\sum_{i=1}^{\acute{n}} x_i\right)^2}} \tag{2.76}$$

where $x_i$, $y_i$ and $\acute{n}$ are defined in **Eq. 2.74**. The values of **R** always lie between -1 and 1.

## 2.14.4 Coefficient of determination (COD or $R^2$)

The square of **R** is defined as the coefficient of determination **COD** or $\mathbf{R^2}$. The value of $\mathbf{R^2}$ measures the strength of the linear relationship between the estimated and actual frequencies of the bins; $\mathbf{R^2}$ is smaller than the values of **R**. In general, the more distribution function can be selected according to the lowest values of **RMSE** and $\mathbf{\chi^2}$ and highest values of **R** and **COD, [Lao12]**.

## 2.14.5 Percentage error

The percentage error (%) of a variable *X* is defined as, **[Kol12]**:

$$\text{Error}(\%) = \frac{|X_e - X_A|}{X_A} \cdot 100\% \qquad (2.77)$$

Where,

$X_e$ = estimated variable

$X_A$ = actual variable evaluated from measured data.

On the other hand, the annual error (%) in calculating variable *X* is calculated by the following equation, **[Kol12]**:

$$\text{Error}(\%) = \frac{1}{12}\sum_{i=1}^{12}\frac{|X_e - X_A|}{X_A} \cdot 100\% \qquad (2.78)$$

## 2.15 Planetary Boundary Layer

The Planetary Boundary Layer is the lowest layer of the troposphere. In this layer, wind is influenced by friction. The wind is more gusty and turbulent within this layer because of friction against vegetation and surface topography, from which turbulent eddies and a chaotic flow develop in the wind flow pattern. Above the PBL, the wind speed is much stronger and uniform because of the significant decrease in friction, **[Hos11, Car11]**.

The wind speed profile in the PBL has a logarithmic form due to the friction at the surface. All surfaces have some degree of roughness exerting a frictional force on the air above it.

Friction acts to resist the wind flow and forces it to move at the same speed as the surface that it is in contact with. This force is called **shearing stress** and it is responsible for the deceleration near the surface so that the mean wind speed reaches zero near the ground, which gives rise to a large wind speed gradient, **[Yan06]**.
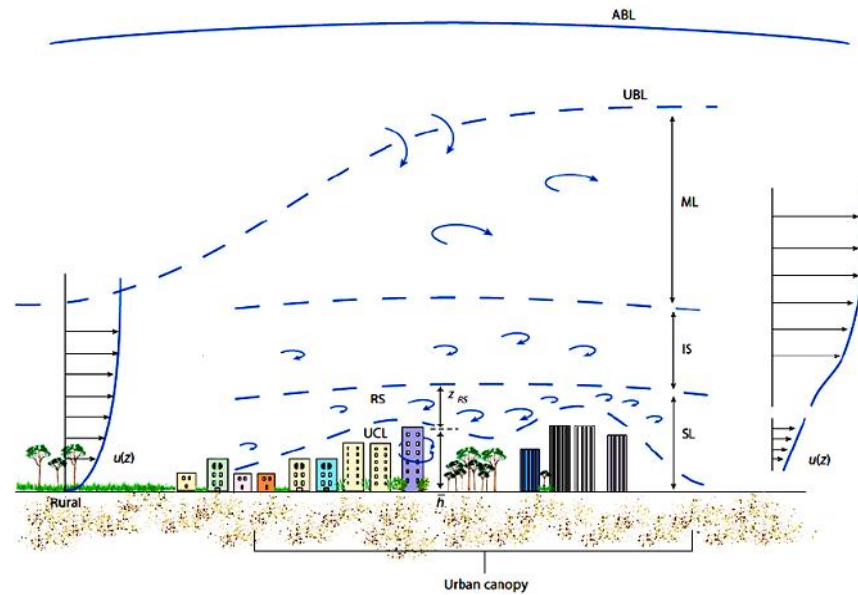
**Fig. 2.12 The PBL above an urban area, [Car11].**

**Fig. 2.12** shows the PBL above an urban area. Wind turbines have to operate within this atmospheric boundary layer. The properties and intensity of this air flow determine the amount of extractable energy and also the loads on the wind turbines, **[Gas12]**.

## 2.16 Roughness Length and Classes

The roughness of a surface depends on the sizes and distribution of the so called roughness elements. The roughness elements can have the size of gravel to the size of trees or houses and be distributed far away from each other or very dense. In this layer, the vertical wind profile takes an exponential form but it is completely dependent on the geometry of the roughness elements and cannot be generally described, **[Yan06]**.

Roughness length and roughness classes are characteristic of the landscape used to evaluate wind conditions at a wind turbine site. Where, roughness length describes the roughness characterization of a terrain, it represents the height above the surface at which the mean logarithmic wind profile theoretically reaches zero, thus it uses length scale to characterize the roughness of a terrain. Also, it affects wind speed, wind direction, friction speed and atmospheric stability, **[Ern12]**.

It is possible to determine the roughness length, as shown below:

$$ln\, z_\circ = \frac{v_1\, ln\, z_2 - v_2\, ln\, z_1}{v_1 - v_2} \tag{2.79}$$

The roughness class (RC) is defined in term of the roughness length in meters, according to**, [Ulg02, Sil06]**:

$$RC = 1.699823015 + \frac{ln\, z_\circ}{ln\, 150} \qquad for\, z_\circ \le 0.03$$

$$RC = 3.912489289 + \frac{ln\, z_\circ}{ln\, 3.333} \qquad for\, z_\circ > 0.03 \tag{2.80}$$

The relationship between roughness class and roughness length is illustrated in **Table 2.3**, in addition to photos and descriptions of the landscape for each roughness class; this procedure will help the reader to get a clear idea of these classes.

**Table 2.3: Roughness classes and the associated roughness lengths, [Mod07, Sil06].**

| RC | Zo (m) | Images | Landscape |
|---|---|---|---|
| 0 | 0.0002 |  | Water surface |
| 0.5 | 0.0024 |  | Completely open terrain with a smooth surface, i.e. concrete runways in airports, grass, etc. |
| 1 | 0.03 |  | Open agricultural area without fences and very scattered buildings. Only softly rounded hills |
| 1.5 | 0.055 |  | Agricultural land with some houses and 8 metre tall sheltering hedgerows with a distance of approx. 1250 metres |
| 2 | 0.1 |  | Non-irrigated land; Permanently irrigated land |

| 2.5 | 0.2 |  | Annual crops associated with permanent crops; Fruit trees |
|-----|-----|------|------|
| 3 | 0.4 |  | Villages, small towns, agricultural land with many or tall sheltering hedgerows, forests and very rough and uneven terrain |
| 3.5 | 0.8 |  | Broad-leaved forest; Mixed forest |
| 4 | 1.6 |  | Continues urban fabric |

## 2.17 Extrapolation of Wind Speed at Different Hub Heights

The reduced speed at lower elevations also reduces the overall mass flow through the turbine, reducing the total output power and increasing the fatigue over the life of the turbine. This makes turbine tower height important because wind speed gradients can change substantially in the ABL.

The standard height of meteorological towers for wind speed observations is 10 meters. Since wind turbine hub heights are typically more than 20 meters, extrapolation of wind speeds to the planned hub height is usually required, the most elementary models for predicting the adjusted wind speed are the power law and the logarithmic law, **[Ros98]**.

*The power law* states, **[Dav12]**:

$$v_2(z_2) = v_1(z_1) \left(\frac{z_2}{z_1}\right)^\alpha \qquad (2.81)$$

where $v_1$ and $v_2$ are simultaneous steady wind speeds at elevations $z_1$ and $z_2$, respectively. $\alpha$ is the Hellmann (friction or wind shear) exponent. The IEC standards recommend a wind shear exponent of 0.2 for onshore and 0.14 for offshore conditions, respectively. But, for most data sets, the wind shear exponent is not known and, even if published, may not be accurate. Wind shear

exponent is depending on surface roughness and stability stats of the atmosphere. **Table 2.4** presents the relationship between surface roughness length and wind shear exponent in different terrain types.

**Table 2.4: Surface roughness length and wind shear exponent, [Gip04].**

| Terrain type | Surface roughness length $z_o$ (m) | Wind shear exponent |
|---|---|---|
| Ice | 0.00001 | 0.07 |
| Snow on flat ground | 0.0001 | 0.09 |
| Calm open sea | 0.0001 | 0.09 |
| Coast with onshore wind | 0.001 | 0.11 |
| Snow-covered crop stubble | 0.002 | 0.12 |
| Cut grass | 0.007 | 0.14 |
| Short-grass prairie | 0.02 | 0.16 |
| Crops, tall grass prairie | 0.05 | 0.19 |
| Hedges | 0.085 | 0.21 |
| Scattered trees and hedges | 0.15 | 0.24 |
| Trees, hedges, a few buildings | 0.3 | 0.29 |
| Suburbs | 0.4 | 0.31 |
| Woodlands | 1 | 0.43 |

Two empirical methods for determining power law exponent are given below, **[IEC05, Man02]**:

**1-** The power law exponent as a function of wind speed and height:

$$\alpha = [0.37 - 0.088 \ ln(v_1)]/\left[1 - 0.088 \ ln\left(\frac{z_1}{10}\right)\right] \qquad (2.82)$$

**2-** The power law exponent dependent on surface roughness:

$$\alpha = 0.096 \ log_{10} \ z_\circ + 0.016 \ (log_{10} \ z_\circ)^2 + 0.24 \qquad (2.83)$$

for 0.001 m $< z_\circ <$ 10m

The relation between Hellmann exponent with each of diurnal profile of wind speed and surface roughness is shown in the following **Figs. 2.13-a** and **2.13-b**, respectively.
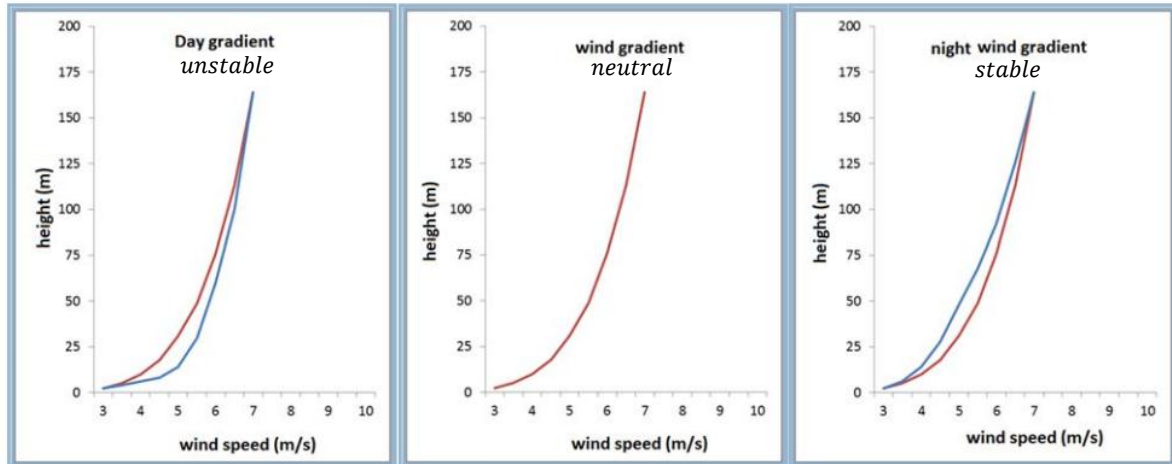


**(a)**
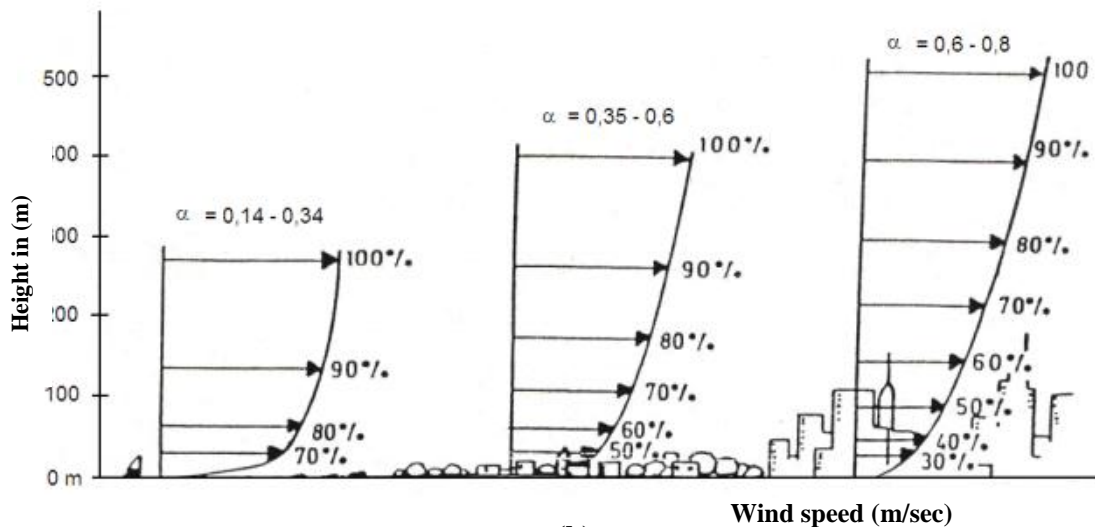


**(b)**

**Fig. 2.13 The relation between Hellmann exponent and (a) diurnal profile (b) surface roughness, [Cir13].**

The other elementary model is *the logarithmic law*, **[Bro12, Dav12]**:

$$v_2(z_2)/v_1(z_1) = \left(\frac{ln(z_2/z_\circ)}{ln(z_1/z_\circ)}\right) \qquad (2.84)$$

Both the power and logarithmic laws are only valid for flat terrain. The wind velocities at different heights relative to that at 10m affected by the roughness heights using **Eq. 2.84**, are shown in **Fig. 2.14**.

Logarithmic extrapolation is mathematically derived from theoretical understanding of how the wind moves across the surface of the earth. In contrast, the power law is derived empirically from actual measurements. The power law equation may be less scientific, but it works well and is more conservative than the logarithmic method. Anyway, power law is equal to logarithmic law between 40 and 110 meters, **[Gip04]**.
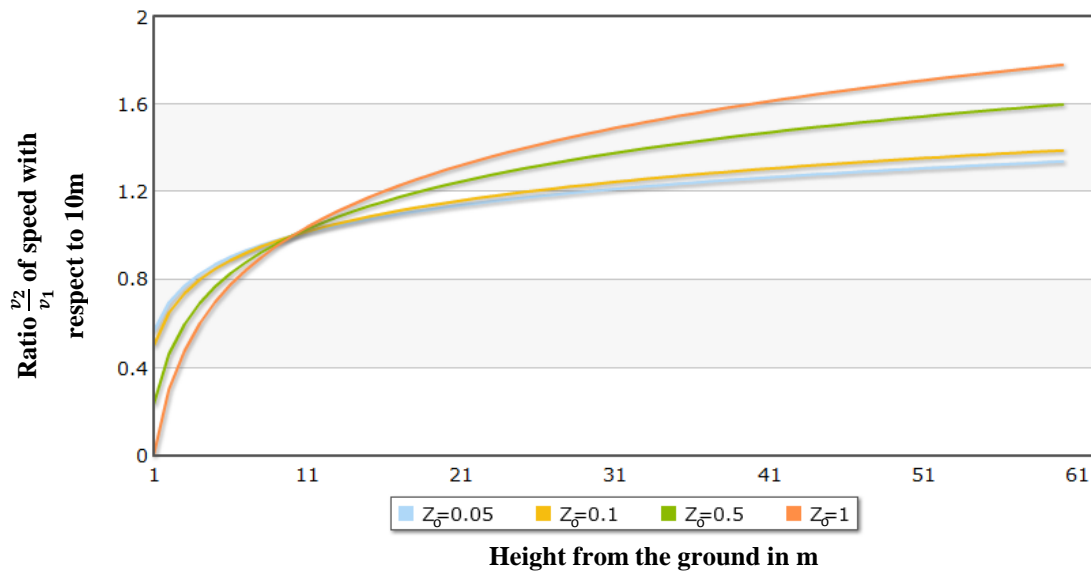


**Fig. 2.14 Speed ratio with respect to 10m for different roughness heights, [Mat06].**

Note that **Eqs 2.81** and **2.84** give estimation on the speed at one location. In case one wants to compare two locations (for example, meteorological station and wind turbine site), each with its own roughness length with similar wind profile, then Wieringa's assumption that the wind speed at 60m height is unaffected by the roughness, leads to the formula, **[Mat06, Rei11]**:

$$\frac{v_2(z_2)}{v_1(z_1)} = \left( \frac{ln\left(\frac{60}{z_{\circ 1}}\right) \, ln(z_2/z_{\circ 2})}{ln\left(\frac{60}{z_{\circ 2}}\right) \, ln(z_1/z_{\circ 1})} \right) \tag{2.85}$$

where, $z\circ_1, z\circ_2$ is the roughness length at the reference and destination locations; for example, a meteorological station, where the wind speed is being measured at height $z_1$, and $z\circ_2$ the roughness length at the site location such as a wind turbine location with the wind speed is estimated at a height $z_2$.

## 2.18 Extrapolation of Weibull Parameters

Since the boundary layer development and the effect of the ground are non-linear with respect to wind speed, the scale factor *c* and shape factor *k* of the Weibull distribution will change as a function of height. Thus, if the wind distribution is desired at some height over than the anemometer level, then it is possible to extrapolate this distribution through Weibull parameters extrapolation by, **[Sun12, Jus78, Dor78]**:

$$c(z_2) = c(z_1) \left(\frac{z_2}{z_1}\right)^{\alpha} \tag{2.86}$$

$$k(z_2) = k(z_1) \left[1 - 0.088 \, ln\left(\frac{z_1}{10}\right)\right] / \left[1 - 0.088 \, ln\left(\frac{z_2}{10}\right)\right] \tag{2.87}$$

where $c(z_1)$ and $k(z_1)$ are the scale and shape factors at the measurement height $z_1$, $c(z_2)$ and $k(z_2)$ are the scale and shape factors at destination height $z_2$. The exponent $\alpha$ is defined as, **[Sun12, Dor78, Ola12]**:

$$\alpha = [0.37 - 0.088 \, ln(c_1)] / \left[1 - 0.088 \, ln\left(\frac{z_1}{10}\right)\right] \tag{2.88}$$

## 2.19 Wind Turbine Site Selection

A wind turbine needs air that moves uniformly in a linear direction. Eddies and swirls, "turbulence", do not make good current for a wind turbine. When considering a location to mount a wind turbine, it is necessary to consider turbulence-generating obstacles such as silos, trees, houses and other wind turbines. Proper location is the key to avoiding the damaging effects of turbulence; these effects can also be minimized by mounting a wind turbine on a tall tower, **[Dan10].**

As shown in **Fig. 2.15**, all obstacles create a downstream zone of turbulent air. It typically extends vertically about twice the height of the obstruction and extends

downwind approximately 15 to 20 times the height of the obstruction, **[Dan10, Tem12]**.
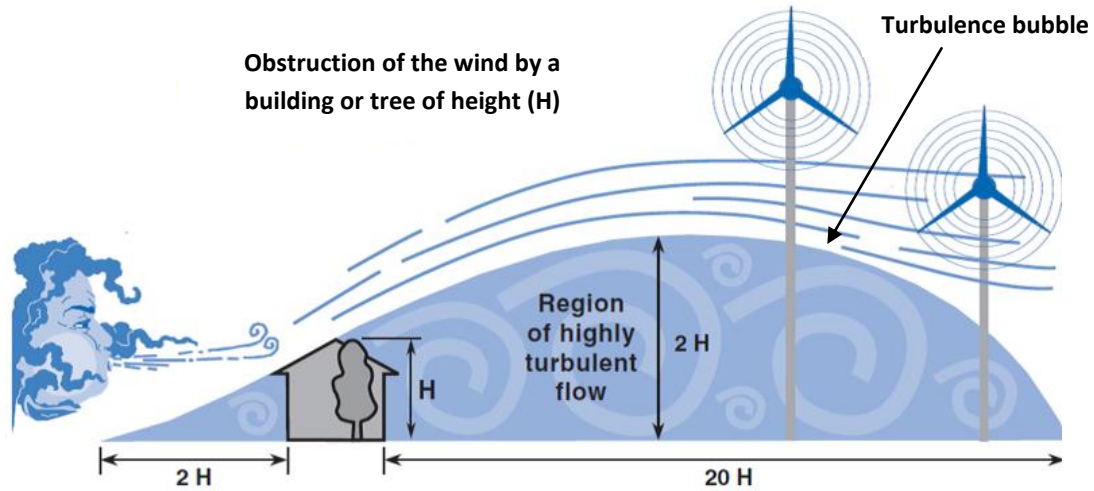


**Fig. 2.15 Obstruction effects on wind follow, [Enc].**

## 2.20 Wind Power

Calculations of wind power are derived from the equation of kinetic energy (*KE*); kinetic energy exists whenever an object of a given mass is in motion with a translational or rotational speed.

When a parcel of air is in motion, the kinetic energy in moving air can be determined as, **[Ton10, Ros98]**:

$$KE = \frac{1}{2}mv^2 = \frac{1}{2}(\rho A x)v^2 \tag{2.89}$$

where *KE* in Joules, *m* is the air mass in *kg*, *v* is the wind speed, $\rho$ is the air density in $kg/m^3$, *x* is the thickness of the parcel in m and *A* is the swept (rotor) area of blades, as shown in **Fig. 2.16**. The wind power can be obtained by differentiating the kinetic energy in wind with respect to time, i.e., **[Gar06]**:

$$P_w = \frac{dKE}{dt} = \frac{1}{2}\rho A v^2 \frac{dx}{dt} = \frac{1}{2}\rho A v^3 \tag{2.90}$$

This gives the amount of power in the area swept by the wind turbine rotor, $P_w$ measured in watt.

From **Eq. 2.90** the following conclusions can be drawn, **[Ton10]**:

- Higher wind power requires a higher wind speed.
- A longer length in blades will increase the power gain. Finally,
- A higher air density yields higher wind power.

Because wind output power is proportional to the cubic power of the mean wind speed, a small variation in wind speed can result in a large change in wind power, on the other hand the power of the wind is not converted into mechanical form completely, since this would decelerate the air mass flow to zero, it would block the rotor area for following air masses. So, we need to include some additional terms to get a practical equation for a wind turbine power (wind turbine mechanical power) as follows, **[Par95]**.

$$P_T = \frac{1}{2}\rho A c_p v^3 \qquad (2.91)$$

where $c_p$ is power coefficients (will explain in another paragraph).
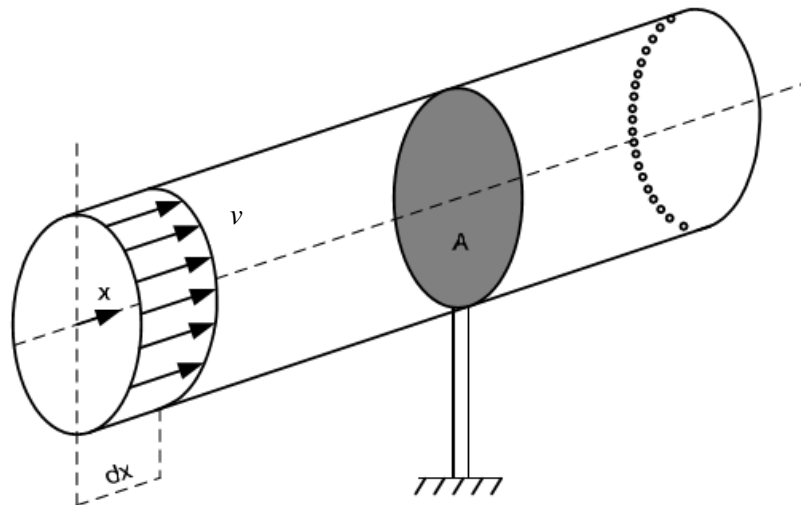


**Fig. 2.16 Wind mass flow through the wind turbine cross sectional area $A$,
[Gas12].**

## 2.21 Wind Turbine

For any wind turbine, the power and energy output increases dramatically as the wind speed increases. Therefore, the most cost effective wind turbines are located in the windiest area. Wind speed is affected by local terrain and

increases with height above the ground, so wind turbines are usually mounted in tall towers.

In general there are three size ranges of wind turbines used today in the market, **[Alk07, Sha13, Min09]**:

- Large scale, corresponds to large turbines (more than 1MW). They are typically installed in large arrays, but can also be installed in small quantities on distribution lines.
- Medium scale, corresponds to medium sized turbines (100 kW - 1MW) intended for remote grid production, often in conjunction with diesel generation or load-side generation to reduce consumption of higher cost grid power and possibly to even reduce peak loads.
- Small scale, corresponds to micro and small scale turbines (several kWs - 100 kW) intended for remote power, battery charging, or net metering type generation. The small turbines can be used in conjunction with solar photovoltaic, batteries, and inverters to provide constant power at remote locations where installation of a distribution line is not possible or is more expensive.

## 2.21.1 Types of main wind turbines

Wind turbines are classified into two categories, according to the direction of their rotational axis, **[Par09]**:

- Horizontal-Axis Wind Turbines (HAWT)
- Vertical-Axis Wind Turbines (VAWT)

## 2.21.1.1 Horizontal-axis wind turbines (HAWT)

Horizontal-axis wind turbines capture kinetic wind energy with a propeller type rotor and their rotational axis is parallel to the direction of the wind (see **Fig. 2.17**), **[Par09]**.

**Fig. 2.17 Horizontal axis wind turbine (HAWT), [Min09].**

## 2.21.1.2 Vertical-axis wind turbines (VAWT)

The axis of rotor is vertical, wind stream is perpendicular to axis of rotor rotation; axis of rotor rotation is perpendicular to surface of the earth. VAWT use straight or curved bladed (Darrieus type) rotors with rotating axes perpendicular to the wind stream (see **Fig. 2.18**), **[Par09]**.



**Fig. 2.18 Vertical axis wind turbine (VAWT), [Min09].**

## 2.21.2 Advantages and disadvantages of wind turbines

*Disadvantages,* **[Alk07, Min09]**:

- Storage device in some cases is always necessary; because no wind means no energy production.
- Without communication with an electric power system the wind power station cannot work, and in wind-diesel stations the special control systems providing parallel work of the wind turbine and diesel-generators.
- Wind turbines have small capacity factor.

*Advantages,* **[Min09]**:

- No fuel required.
- Zero $Co_2$ and other harmful gaseous emissions.
- No water consuming.
- Alienation the fertile earth is much less, than on hydroelectric power station and thermal power station.
- Possibility of full automation of work, absence of the personnel on duty.
- Short term of a construction, such that it is possible to construct for 18 months a 50 MW power station and further expansion is possible.
- Simple technology of work of station.

## 2.21.3 Wind turbine characteristics

Apart from the wind distribution prevailing at the site and its availability to the turbine, the characteristics of a wind machine should match well with the prevailing wind spectra to ensure maximum energy exploitation.

Hence, this section will define the major characteristics affecting the performance of a wind energy conversion system which has significant influence on any wind power project performance, **[Mat06]**.

## 2.21.3.1 Power curve

Power curve is graphical representation of the power production of a wind turbine at different wind speeds (**Fig. 2.19**). The power curve of the machine reflects the aerodynamic, transmission and generation efficiencies of the system in an integrated form. The output power increases continuously with the increase

in the wind speed until reaching a saturated point, to which the output power reaches its maximum value, defined as the rated output power.

This curve has four variables explained below, **[Mat06]**:
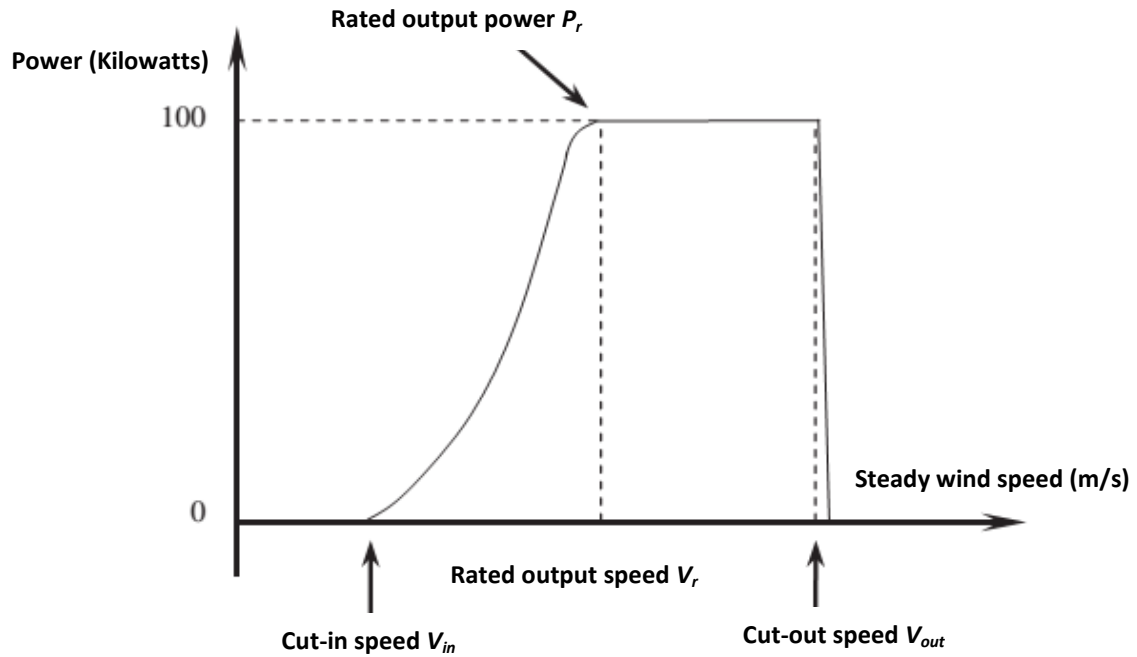


**Fig. 2.19 Typical wind turbine power curve, [Ton10].**

### 1. Cut-in speed, $V_{in}$

At very low wind speeds, there is insufficient torque exerted by the wind on the turbine blades to make them rotate. However, as the speed increases, the wind turbine will begin to rotate and generate electrical power. The speed at which the turbine first starts to rotate and generate power is called the cut-in speed. Some manufacturers recommend installing a turbine with the lowest cut-in speed possible in areas of low wind to make better use of the wind resource, **[Pow, Doe05]**.

### 2. Rated wind speed, $V_r$

Rated speed is the lowest wind speed at which the rated output power of a wind turbine is produced. At the rated speed, more increase in the wind speed will not increase the output power due to the activation of the power control, **[Dan10, IEC05]**.

### 3. Cut-out speed, $V_{out}$

As the speed increases above the rate output wind speed, the forces on the turbine structure continue to rise and, at some point, there is a risk of damage to the rotor. As a result, a braking system is employed to bring the rotor to a standstill. This is called the cut-out speed and is usually around 25 meters per second, **[Dan10, IEC05]**.

### 4. Rated output power, $P_r$

Typically somewhere the output power reaches the limit that the generator isn't capable of generate more than it. This limit to the generator output is called the rated output power, **[Dan10, IEC05]**.

In brief, the wind speed conditions from the area and the characteristics of the wind turbine generator itself (particularly the cut-in, rated and cut-off wind speed parameters), represent the main factors that affect energy production from a wind turbine. It is therefore desirable to select a wind turbine which is best suited for a particular location in order to obtain a maximum output power. The suitability of wind turbine to a specific location is given by the capacity factor and efficiency values (power coefficient), **[Fro10]**.

### 2.21.3.2 Capacity factor, $C_F$

Capacity factor is an indicator of how much a particular wind turbine makes energy in a particular place. It is given by the ratio of the energy actually produced by the system ($E_T$) to the energy that could have been produced by it - as if the machine would have operated at its rated power throughout the time period. Thus, **[Mat06]**:

$$C_F = \frac{E_T}{T\, P_r} \tag{2.92}$$

where, $T$ is the time period.

Also, $C_F$ of a wind turbine can be estimated using the following expressions based on Weibull distribution function, **[Sun12]**:

$$C_F = \frac{e^{-(\frac{V_{in}}{c})^k} - e^{-(\frac{V_r}{c})^k}}{(\frac{V_r}{c})^k - (\frac{V_{in}}{c})^k} - e^{-(\frac{V_{out}}{c})^k} \tag{2.93}$$

Hence, $C_F$ is a function of the turbine as well as the wind regime characteristics. All wind turbines have capacity factors, and they vary depending on resource, technology and purpose. Typical wind power capacity factors are 20-40%. $C_F$ can be computed for a single turbine, a wind farm consisting of dozens of turbines or an entire country consisting of hundreds of farms, **[Mat06, Nem11]**. Information on the capacity factor of the turbine at a given site may not readily available during project identification. Under such situations, it is advisable to calculate the rough capacity factor ($RC_F$).

$$RC_F = \frac{P_{\bar{v}}}{P_r} \tag{2.94}$$

Where, $P_{\bar{v}}$ is the power corresponding to the average wind speed.

### 2.21.3.3 Power coefficient, $c_p$

The capacity factor is not an indicator of efficiency. A measure of turbine efficiency is the power coefficient. This coefficient indicates how efficiently a turbine converts the wind energy into electricity, thus it varies with the wind speed. Power coefficient ($c_p$) is defined as the ratio of power extracted by the turbine ($P_T$) to the total contained in the wind resource ($P_w$) as follows, **[Nem11, Win08]**:

$$c_p = P_T/P_w \tag{2.95}$$

$c_p = 0.59$ (Betz limit for the maximum value), large modern megawatt turbines have peak of between 40% and 50% whereas, for smaller turbines producing a few kilowatts, $c_p$ lies between 20% to 30%, [Par95].

### 2.21.3.4 Average output power, $P_{e,ave}$

The average output power of a turbine is a very important parameter of a wind energy system since it determines the total power production and the total income. The average output power from a wind turbine is the power produced at

each wind speed times the fraction of the time that wind speed is frequented, integrated over all possible wind speeds, such that, **[Gar06]**:

$$P_{e,ave} = \int_0^\infty P(v) f(v)dv \qquad (2.96)$$

where $P(v)$ is the power curve value at wind speed $v$, $f(v)$ is the Weibull pdf of wind speeds. After substitution and mathematical calculation we find that, **[Mat06, Gar06]**:

$$P_{e,ave} = C_F \cdot P_r \qquad (2.97)$$

This means that $P_{e,ave}$ determines the performance of a wind turbine installed at a given site using the amount of capacity factor and $P_r$.

## 2.22 Blade Swept Area

If $l$ is the length of wind blades and $r$ is the radius of the wind turbine hub, then in such a case, the cross sectional area $A$ (or rotor area) can be calculated from, **[Ton10]**:

$$A \approx \pi l^2 \qquad (2.98)$$

where $l \gg r$ such that the hub radius length could be neglected.

From **Eq. 2.98** we can infer that by doubling the length of wind blades, the swept area (consequently, the output power) can be increased by the factor up to 4, the figure below illustrates this fact.
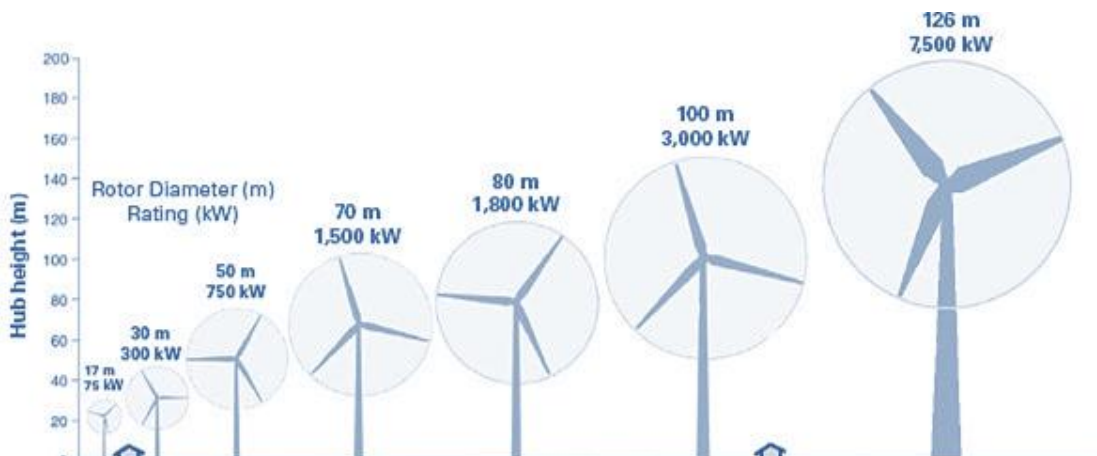


**Fig. 2.20 The power of wind generator is directly proportional to rotor area, [Ewe09].**

## 2.23 Air Density

Air density can be determined to varying degrees of accuracy with the following methods, **[Ton10, Hug]**:

1- For constant value of air density based on U.S.Std. Atmosphere, at sea level; we have

$$\rho = 1.225 \text{ kg/m}^3 \tag{2.99}$$

2- If we have the location's elevation z above sea level (in meters):

$$\rho = 1.225 - (1.194 * 10^{-4}) * z \tag{2.100}$$

where z = the region's elevation above sea level (in meters)

3- If we have pressure and temperature data; air density can be given by:

$$\rho = P / R_{gas}T \text{ (kg/m}^3) \tag{2.101}$$

where,       P = air pressure (in units of Pascal or Newton/m$^2$)

$R_{gas}$ = the specific gas constant (287 J kg-1Kelvin-1)

T = air temperature in Kelvin (deg. C + 273.15)

4- If we have only temperature data then,

$$\rho = (Po/ RT) * \exp(-G*z/RT) \text{ (kg/m}^3) \tag{2.102}$$

where       $P_o$= std. sea level atmospheric pressure (101,325 Pascals)

G = gravitational constant (6.67384 × 10$^{-11}$ m$^3$ kg$^{-1}$ s$^{-2}$)

## 2.24 Wind Power Density Assessment

Wind power density is a comprehensive index used to estimate the potential electrical output of a wind farm once the area swept by wind turbine rotors and the power system efficiency are known. It is defined as the available wind power in airflow through a perpendicular cross-sectional area. The equations for wind power density (WPD) is simply as that **Eq. 2.90 and Eq. 2.91** divided by rotor area as, **[Ton10, Ros98]**:

$$WPD_w = \frac{1}{2}\rho v^3$$

$$WPD_T = \frac{1}{2}\rho c_p v^3$$

(2.103)

## 2.24.1 Wind power density classes

The classes of wind power density at two standard wind measurement heights are listed in **Table 2.5** (created by NREL). This table gives the wind classes as a function of wind power density and wind speed measured at the heights of 10m and 50m above the ground, where wind classes between 1 and 7 are used – a wind class of 7 indicates the highest potential, **[Qam09, Eri12]**.

**Table 2.5: Wind class, power density, and wind speed, [Ahm12].**

| Wind Class | WPD at 10 m (W/m²) | $\bar{v}$ at 10 m (m/s) | WPD at 50 m (W/m²) | $\bar{v}$ at 50 m (m/s) | Description |
|---|---|---|---|---|---|
| 1 | 0 - 100 | 0.0 - 4.4 | 0 - 200 | 0.0 - 5.6 | Poor |
| 2 | 100 - 150 | 4.4 - 5.1 | 200 - 300 | 5.6 - 6.4 | Marginal |
| 3 | 150 - 200 | 5.1 - 5.6 | 300 - 400 | 6.4 – 7.0 | Satisfactory |
| 4 | 200 - 250 | 5.6 - 6.0 | 400 - 500 | 7.0 - 7.5 | Good |
| 5 | 250 - 300 | 6.0 - 6.4 | 500 - 600 | 7.5 - 8.0 | Excellent |
| 6 | 300 - 400 | 6.4 - 7.0 | 600 - 800 | 8.0 - 8.8 | Prominent |
| 7 | 400 - 1000 | 7.0 - 9.4 | 800 - 2000 | 8.8 - 11.9 | Splendid |

## 2.24.2 Wind power density-Weibull based $PD_w$

The expected monthly or annual wind power density per unit area of a site based on a Weibull probability density function can be expressed as follows, **[Ahm12, Yan13]**:

$$PD_w = \frac{1}{2}\rho c^3 \Gamma\left(1 + \frac{3}{k}\right)$$

(2.104)

Substituting the scale factor in above equation by the formula presented in **Eq. 2.21**, yields, **[Sad12]**:

$$\overline{PD}_w = \frac{\rho \bar{v}^3 \Gamma(1 + \frac{3}{k})}{2[\Gamma\left(1 + \frac{1}{k}\right)]^3} \qquad (2.105)$$

This equation gives the mean wind power density based on the Weibull pdf which depends on cube mean wind speed $\bar{v}$.

### 2.24.3 Actual power density $PD_A$

From **Eq. 2.103**, the speed is obtained using the actual wind distribution, to give actual wind power density, i.e., **[Lao12]**:

$$PD_A = \frac{1}{2}\rho \int_0^\infty v^3\, p(v)dv \qquad (2.106)$$

where $p(v)$ are the probabilities determined from the actual wind speed data. The discrete form of **Eq. 2.106** is formulated as, **[Gar06]**:

$$PD_A = \frac{1}{2}\rho \sum_{i=1}^{w} p(v_i)v_i^3 \qquad (2.107)$$

where $w$ is the number of different values of wind speed observed, here $p(v_i)$ represents the probability of the discrete wind speed $v_i$ being observed which is given by following equation:

$$p(v_i) = \frac{m_i}{n} \qquad (2.108)$$

the numbers of observations of a specific wind speed $v_i$ will be defined as $m_i$, the letter $n$ represents the total number of observations.

If the Weibull density function fits the actual wind data exactly, then $\overline{PD}_w$ in the wind predicted by **Eq. 2.105** will be the same as $PD_A$ predicted by **Eq. 2.107**. The greater the difference between the values obtained from these two equations, the poorer is the fit of the Weibull density function to the actual data.

### 2.25 Energy Assessment

Energy output from wind project depends on (1) the distribution of wind speed within the regime and (2) power response of the turbine to different wind

speeds. The following subsections will express different mathematical terms for output energy calculations, **[Mat06]**.

### 2.25.1 Wind potential energy in a selected site

One of the most important steps in wind energy projects is the energy estimation for a selected site. Wind energy available in the regime over a period is usually taken as the yardstick for evaluating the site energy potential, **[Sad12, Far12]**. Once each of the preceding $PD_w$ and $PD_A$ is given, the wind energy density ($E_D$) for a desired duration, $T$, can be calculated as:

$$E_D = PD_w \ or \ PD_A \ \times T \tag{2.109}$$

### 2.25.2 Energy production from wind turbine using capacity factor

The yearly energy production of the turbine can be estimated using the following equation, **[Far12]**:

$$E_{out} = P_{e,ave} \times T = C_F \times P_r \times 8760 \tag{2.110}$$

where, 8760 represents the number of hours in one complete year, $C_F$ capacity factor as defined before.

If $C_F$ is unknown, one could use $RC_F$ to find energy output from a wind turbine by following equation:

$$\bar{E}_{wind} = RC_F \times P_r \times 8760 \tag{2.111}$$

Since the turbine doesn't working all 8760 hours, thus for realistic calculations it should replace it by the number of working hours of the turbine.

### 2.25.3 Annual output energy

The annual wind speed distribution $f(v)$ is combined with the power curve of the turbine $P(v_i)$ to give the energy generated at each wind speed $v_i$ and hence the total energy generated throughout the year. It is usual to perform the calculation using 1m/s wind speed bins as this gives acceptable accuracy. The annual energy for a wind turbine could be generated in typical year expressed mathematically as, **[Elm09]**:

$$E_{An} = \left[\sum_{i=1}^{n} f(v_i)P(v_i)\right] \times T \tag{2.112}$$

**Fig. 2.21** shows the graphical representation of the above equation, "a" represents the power curve of a commercial 1MW turbine with 3.5 m/sec cut-in, 15m/s rated and 25m/s cut-out velocities. Curve "b" represents the probability density function at a site with 8m/s mean wind speed, assuming the Weibull distribution with $k=2$. The energy corresponding to different wind velocities are plotted in curve "c". In **Fig. 2.21**, $E_{An}$ at 10m/s is given from multiplying $f$ and $P$ at the same wind speed (10 m/sec) in curves "a" and "b" respectively. The energy corresponding to this speed is indicated in the curve "c". Total energy available from this turbine at this site, over a period, can be estimated by integrating curve "c" within the limits of the cut-in and cut-out velocities and multiplying it with the time factor, **[Mat06]**.
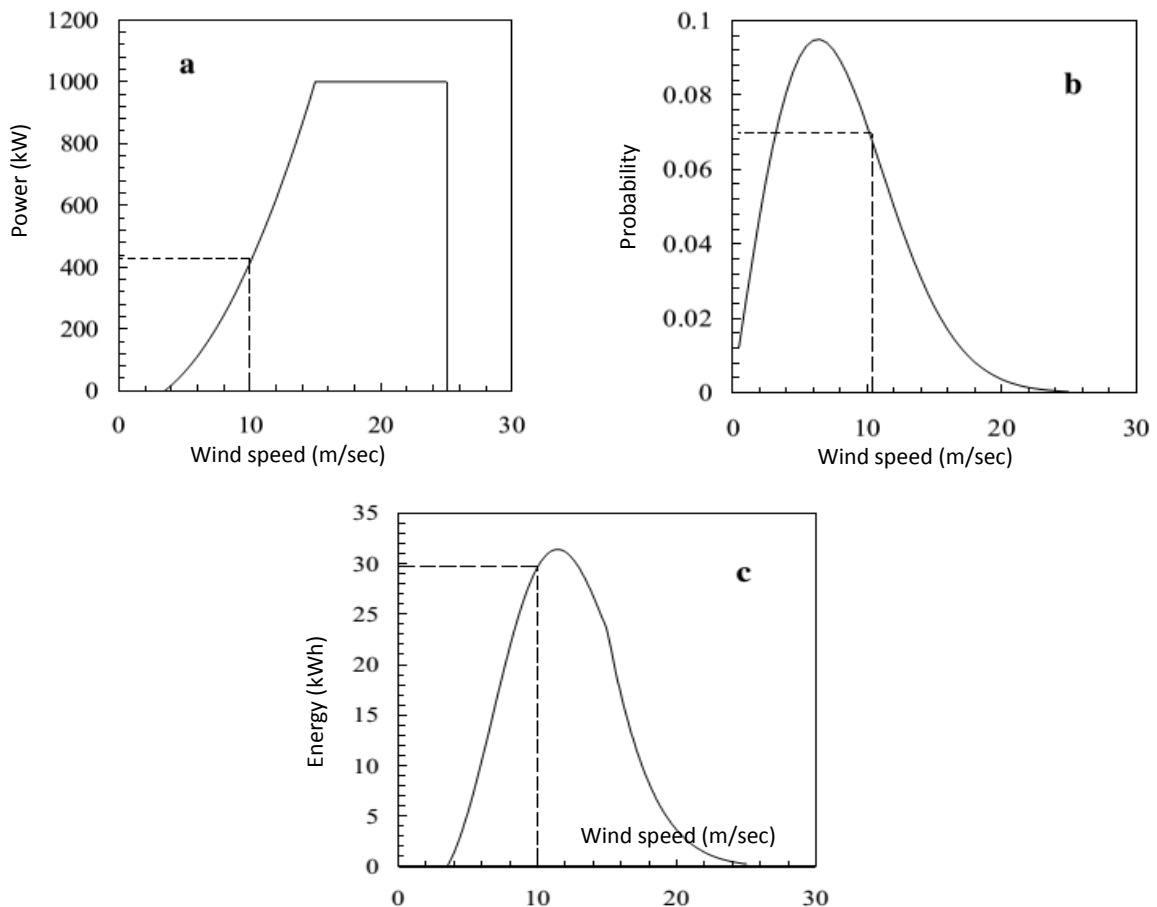


**Fig. 2.21 Expected output energy-graphical representation, [Mat06].**

The total energy generated by the turbine $E_{An}$, over a period can also be estimated by, **[Mat06]**:

$$E_{An} = E_{IR} + E_{RO} \qquad (2.113)$$

where, $E_{IR}$ and $E_{RO}$ are the two energy distinct regions of the power curve such that $E_{IR}$ from cut-in to rated wind speed, and $E_{RO}$ from rated to cut-out wind speed. $E_{IR}$ can be expressed as:

$$
\begin{aligned}
E_{IR} = {}& \frac{P_R T c^{\dot{n}}}{\left(V_r^{\dot{n}} - V_{in}^{\dot{n}}\right)} \int_{X_{in}}^{X_r} X^{\frac{\dot{n}}{k}} e^{-X} dX \\
& - \frac{P_R T V_{in}^{\dot{n}}}{\left(V_r^{\dot{n}} - V_{in}^{\dot{n}}\right)} \left[e^{-X_{in}} - e^{-X_r}\right]
\end{aligned}
\qquad (2.114)
$$

$$E_{ro} = T P_r \left(e^{-X_r} - e^{X_o}\right) \qquad (2.115)$$

where $\dot{n}$ is speed power proportionality and for ideal case $\dot{n} = 3$,

We have $\quad X_{in} = \left(\frac{V_{in}}{c}\right)^k , X_r = \left(\frac{V_r}{c}\right)^k \ and \ X_o = \left(\frac{V_{out}}{c}\right)^k \qquad (2.116)$

## 2.26 Site Assessment

Wind turbines are subjected to environmental and electrical conditions that may affect their loading, durability and operation.

The International Electrotechnical Commission provides standards for all methods relating to wind turbines; one of these standards that in our concern is IEC 61400-1, **[IEC05, Nie09]**.

Turbine classification is the responsibility of manufactures and site assessment is the responsibility of project developers. To achieve a turbine type certificate the turbine must be proofed safe for wind conditions. Wind conditions for this purpose are specified by simple models, reference wind speed, and reference turbulence intensity. For site assessment the following criteria apply, **[Nie09]**:

- The 50-year extreme wind must be lower than the reference wind for the turbine type

- Flow-line inclination at hub height must be within $\pm 8$ for all wind direction.

- The wind-speed distribution must be lower than that assumed in the turbine certificate in a range from 0.2 to 0.4 times the reference wind. More exposure in this wind-speed range would enhance fatigue damage.

- The effective turbulence intensity ($I_{\text{eff}}$), must be lower than the applicable IEC model in a range from 0.6 times the rated speed to the cut-out speed. The applicable model is either characteristic turbulence intensity ($I_{\text{char}}$) or representative turbulence intensity ($I_{\text{rep}}$) depending on whether the turbine type certificate is issued according to IEC 61400 2 or 3.

## 2.27 Turbulence

Turbulence can be thought of as random wind speed fluctuations imposed on the mean wind speed (**Fig. 2.22**). These fluctuations occur in all three directions, **[Man02]**.
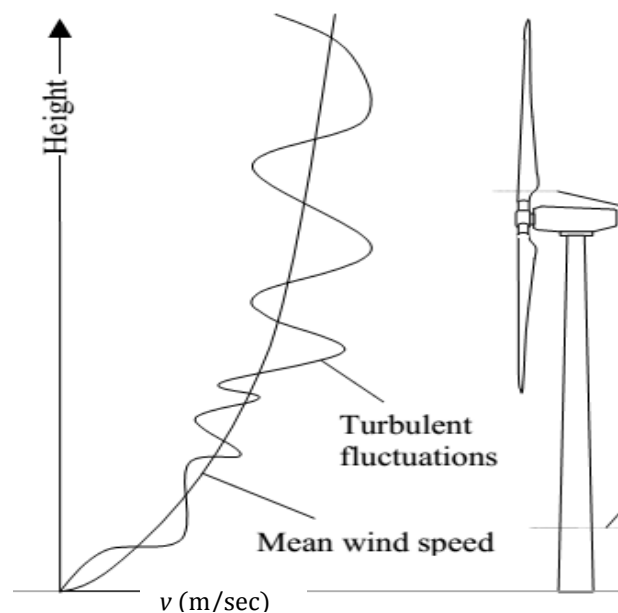


**Fig. 2.22 Wind fluctuations around the mean, [Fra07].**

Turbulence reduces the harnessable energy of the wind, and causes vibration and unequal forces on the wind turbine, especially the blades that may weaken and

damage the machine. Turbulence, therefore, increases wear and tear on wind turbine and, over time, can destroy it.

Proper location is the key to avoiding the damaging effects of turbulence, such that, when considering a location to mount a wind turbine, be sure to consider turbulence-generating obstacles. Turbulence can also be minimized by mounting a wind turbine on a tall tower, **[Dan10]**.

## 2.27.1 Ambient turbulence intensity

Is defined as the ratio of the wind speed standard deviation to the mean wind speed which they are determined from the same set of sampling data over a specific period of time, **[IEC05, IEC06]**.

In wind resource analysis, turbulence is measured by turbulence intensity, which is a dimensionless quantity. It is usually calculated for short time periods, minutes to an hour, given as **[Man02, Bur01, Nel09, Pet98]**:

$$TI_v = {\sigma_v}/{\bar{v}} \qquad\qquad (2.117)$$

where $\sigma_v$ is the standard deviation of wind speed variations about the mean wind speed $\bar{v}$. Due to this definition $TI_v$ can become infinitely large when the wind speed reaches zero.

Wind turbulence intensity is critical parameter and limits the operational life of the wind turbine. It is site dependent and should be well understood before any real installation. High turbulence intensity is associated with increased wind turbine system wear and increased operation and maintenance costs, **[Mah11, Ro10]**.

The turbulence intensity at a site is defined by the International Electrotechnical Commission (IEC) by IEC 61400, which is defined as a set of design requirements made to ensure that wind turbines are appropriately engineered against damage from hazards within the planned lifetime, **[Mad08, Mor11]**. Since we will examine the turbulence intensity at a site in terms of its impact on the small and large wind turbines, thus it is necessary to have knowledge about the IEC 61400 suitability conditions which belongs to each type of wind turbine.

## 2.27.2 Small and large wind turbines safety standards and classes

There is a standard for small wind turbines (SWT), which is numbered IEC61400-2, this standard describes the normal turbulence model (NTM), which contains four standard classes. The basic parameters defining these classes are listed in **Table 2.6**, **[Hos11, IEC06].**

**Table 2.6: Basic parameters for SWT classes (IEC 61400-2), [IEC06].**

| SWT Class | I | II | III | IV | S |
|---|---|---|---|---|---|
| $V_{ave}$ (m/s) | 10 | 8.5 | 7.5 | 6.0 | |
| $V_{ref}$ (m/s) | 50 | 42.5 | 37.5 | 30.0 | manufacturer |
| $I_{15}$ | 0.18 | 0.18 | 0.18 | 0.18 | |
| a | 2 | 2 | 2 | 2 | |

IEC6400-2 defines the basic parameters as follows:

- $V_{ave}$ is annual average wind speed at hub height.
- $V_{ref}$ is basic parameter for wind speed used for defining wind turbine classes. A turbine designed for a reference wind speed $V_{ref}$, is designed to withstand climates for which the extreme 10 min average wind speed with a recurrence period of 50 years at turbine hub height is lower than or equal to $V_{ref}$, **[Hos11]**.
- $I_{15}$ is the dimensionless characteristic value of the turbulence intensity at 15 m/sec, **[IEC06]**.
- a is a slope parameter for turbulence standard deviation model, **[Car11]**.

On the other hand, there is a standard for Large wind turbines (LWT), which is numbered IEC61400-1. Actually, the IEC61400-1 turbulence model has edition 2 and 3. The difference between them is summarized below;

- IEC61400-1 edition 2 defines the characteristic turbulence intensity $I_{char}$ as the mean plus standard deviation of measurements. Load cases are defined by the $I_{char}$ at 15m/s, called $I_{15}$ (**Eq. 2.18**).
- IEC61400-1 edition 3 defines the representative turbulence intensity $I_{rep}$ as the mean + 1.28 times standard deviation of measurements. Load cases are defined by the reference turbulence intensity $I_{ref}$ which is equal to the mean turbulence intensity at 15m/s (**Eq. 2.19**).

The 84th-quantile characteristic value of hub height turbulence intensity at 10min average wind speed in edition 2 is defined as:

$$I_{char} = I_{15} + \sigma_{I_{15}} \tag{2.118}$$

where $I_{15}$ ambient turbulence intensity characteristic value at 15m/sec

Little extreme turbulence may cause most of the fatigue damage. Therefore, the IEC standard applies representative turbulence intensity for turbine classification, which is defined as a high percentile of the expected natural variation, and this variation will generally decrease with wind speed, **[Mor11]**. Consequently, the 90th-quantile representative value of hub height turbulence intensity at 10min average wind speed in edition 3 is defined as:

$$I_{rep} = I_{ref} + 1.28\sigma_{I_{ref}} \tag{2.119}$$

where $I_{ref}$ represents reference turbulence intensity at 15m/s.

In addition to specify other basic parameters which define the wind turbine classes and subclasses given in the two editions, **[IEC05]**.

**Table 2.7: Basic parameters for LWT classes for IEC 61400-1 edition 2, [IEC05]**

| LWT Class | | I | II | III | IV | S |
|---|---|---|---|---|---|---|
| $V_{ave}$ (m/s) | | 10 | 8.5 | 7.5 | 6.0 | |
| $V_{ref}$ (m/s) | | 50 | 42.5 | 37.5 | 30.0 | manufacturer |
| $I_{15}$ | A | 0.18 | | | | |
| | B | 0.16 | | | | |

**Table 2.8: Basic parameters for LWT classes for IEC 61400-1 edition 3, [IEC05]**

| LWT Class | | I | II | III | S |
|---|---|---|---|---|---|
| $V_{ave}$ (m/s) | | 10 | 8.5 | 7.5 | |
| $V_{ref}$ (m/s) | | 50 | 42.5 | 37.5 | |
| $I_{ref}$ | A | 0.16 | | | manufacturer |
| | B | 0.14 | | | |
| | C | 0.12 | | | |

According to IEC6400-1, the basic parameters are defined as follows, **[Hos11]**:

- $V_{ave}$ and $V_{ref}$ were defined before.
- A refers to a higher turbulence category
- B refers to a medium turbulence category
- C refers to a lower turbulence category

However, since site assessment should follow of either edition, therefore our results will be restricted to edition three only.

### 2.27.3 NTM and *TI*s percentile values for SWT and LWT

The classification of LWTs and SWTs comes under the standard IEC 61400-1 and IEC 61400-2 respectively, this is done by comparing the measured turbulence intensity (*TI*) of our site to standard NTM described by IEC 61400-1 edition 3 (2005 for LWT) or to NTM described by IEC 61400-2 (2006 for SWT). In other words, site assessment rule is that turbulence intensity must not exceed the NTM model corresponding to the selected wind turbine class in a specified wind speed range, **[Ves11, Moh14]**. To be able to compare the computed $\sigma_v$ and *TI* with the NTM, the values of $\sigma_v$ and *TI* must be first created. This is done by assuming that **[Rob12, Moh14]**:

- the 50th percentiles of $\sigma_v$ and *TI* represents the average values of $\sigma_v$ and *TI* at each bin are given by

$$\sigma_{50} = \bar{\sigma}_v \qquad (2.120a)$$

$$TI_{50} = \overline{TI}_v \qquad (2.120b)$$

- while, the 90th percentiles of standard deviation and *TI* is given by

$$\sigma_{90} = \bar{\sigma}_v + 1.28\sigma_\sigma \tag{2.121a}$$

$$TI_{90} = \overline{TI}_v + 1.28\sigma_{TI} \tag{2.121b}$$

The 50th and 90th percentiles can be understood from **Fig. 2.23**.
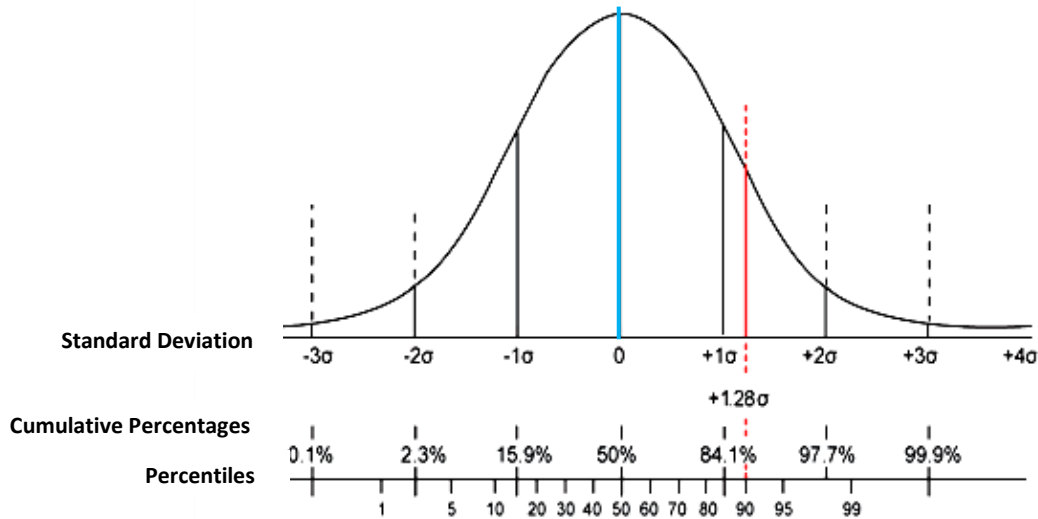


**Fig. 2.23 Normal distribution curve of standard deviation and the cumulative percentage together with percentiles. Red and blue lines represent the 90th and 50th percentiles respectively, [Hos11].**

For IEC 61400-2 (SWT), the values of NTM standard deviation for wind speed, $\sigma_1$, shall be given by the 90th or 50th percentile value of wind speed at hub height. These values can be given as, **[IEC05, Moh14]**:

$$\sigma_1 = \frac{I_{15}(15 + a\,V_{hub})}{(a+1)} + 2(p_r - 1)I_{15} \tag{2.122}$$

Using the values of '$a$' and '$I_{15}$' for SWTs from **Table 2.9**, the 2nd term is a modification which let the model correspond to different percentile values, such that, $p_r = 0$ for the 50th percentile, and $p_r = 1.28$ for the 90th percentile. The NTM of standard deviation, $\sigma_1$, is shown in **Fig. 2.24-a**. While NTM for the turbulence intensity is calculated by **Eq. 2.123** is shown in **Fig. 2.24-b**, **[Hos11, Car11, IEC05]**.

$$TI = \sigma_1 / V_{hub} \tag{2.123}$$

**Table 2.9: Basic parameters for LWT and SWT turbines classes, [DTU11].**

| IEC 61400-2 (SWT) | | | | | |
|---|---|---|---|---|---|
| **Class** | I | II | III | IV | S |
| $I_{15}$ | 0.18 | 0.18 | 0.18 | 0.18 | Manufacture |
| **a** | 2 | 2 | 2 | 2 | |
| **IEC 61400-1 edition 3 (LWT)** | | | | | |
| **Class** | I | II | III | S | |
| **a** | 3 | 3 | 3 | | |
| **Category** | A | B | C | Manufacture | |
| $I_{ref}$ | 0.16 | 0.14 | 0.12 | | |

$I_{15}$   Represents characteristic value of turbulence intensity at wind speed 15m/s.

$I_{ref}$   Represents the value of the turbulence intensity at 15m/s.

A    Refers to a higher turbulence category

B    Refers to a medium turbulence category

C    Refers to a lower turbulence category
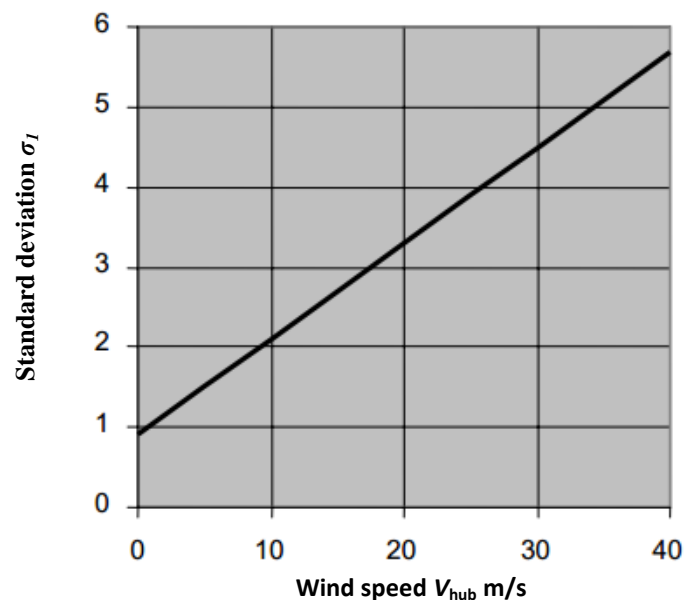


**a- Standard deviation of turbulence for NTM belongs to SWT**
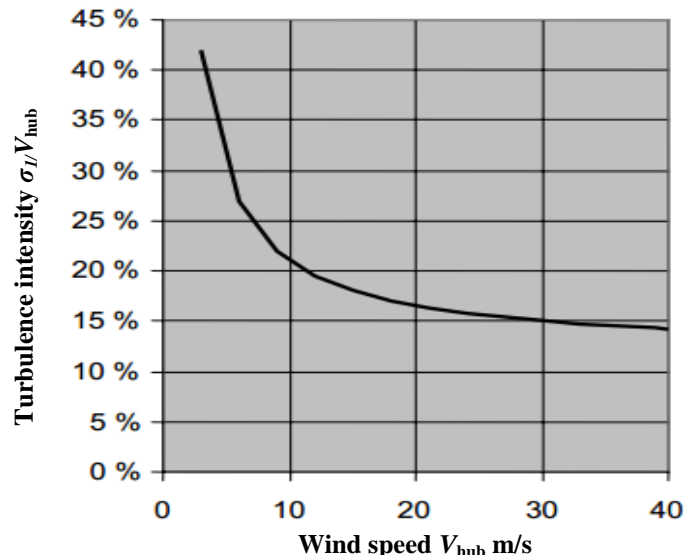
**b – Turbulence intensity for NTM belongs to SWT**

**Fig. 2.24 Characteristic wind turbulence, [Hos11].**

NTM in IEC 61400-1 edition 3 (LWT), the expected standard deviation, $\sigma_1$, is given in **Eq. 2.124,** such that $p_r = 0$ for the 50th percentile, and $p_r = 1.28$ for the 90th percentile. Variables of '$a$' and '$I_{ref}$  for LWTs are listed in **Table 2.9**, **[IEC06, Car11]**:

$$\sigma_1 = I_{ref}\left[\frac{(15 + a\, V_{hub})}{(a + 1)} + 1.44 p_r\right] \qquad (2.124)$$

Values for the turbulence standard deviation, $\sigma_1$, and the turbulence intensity $\sigma_1/V_{hub}$ are shown in **Figs 2.25-a** and **2.25-b**, respectively, **[IEC05, Hos11]**.
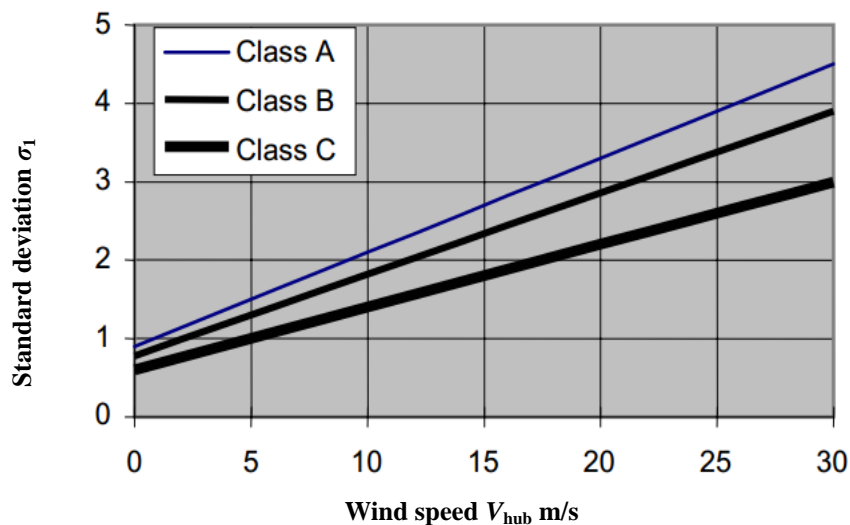


**a – The 90th percentile standard deviation of turbulence for the NTM**

b – The 90<sup>th</sup> percentile turbulence intensity for the NTM
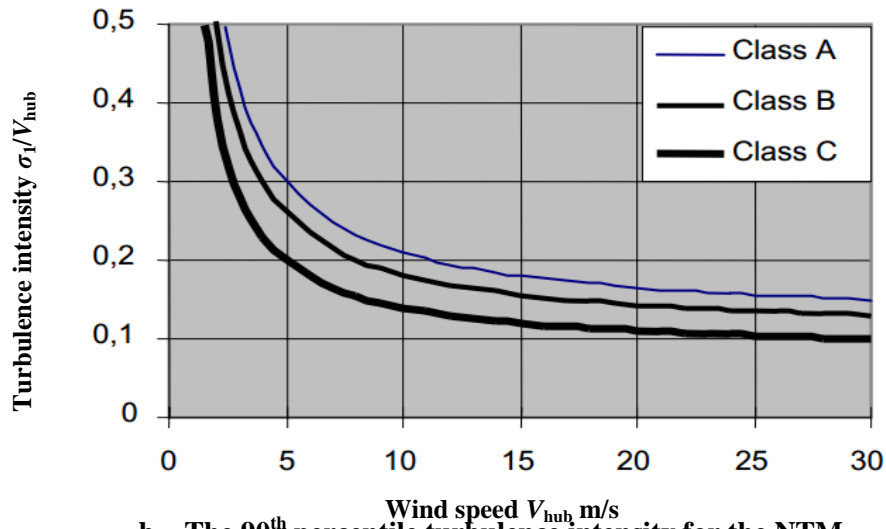
**Fig. 2.25 NTM under IEC 61400-1 3$^{rd}$ edition for LWT, [IEC05].**

## 2.28 $I_{ref}$ and $I_{rep}$ Calculations

Reference turbulence intensity is the expected value of hub height turbulence intensity at a 10min average wind speed 15m/sec (see **Fig. 2.26**). It could be estimated using following formula, **[IEC05, Tan, Gia08]**.

$$I_{ref}^{WTG} = I_{15}^{mast} \frac{\bar{v}_{mast}}{\bar{v}_{WTG}}$$                    (2.125)

where, $I_{15}^{mast}$ is calculated at the met mast from recorded measurements.

$\bar{v}_{mast}$ is the mean wind speed at the met mast**.**

$\bar{v}_{WTG}$ is the mean wind speed at turbine hub height.
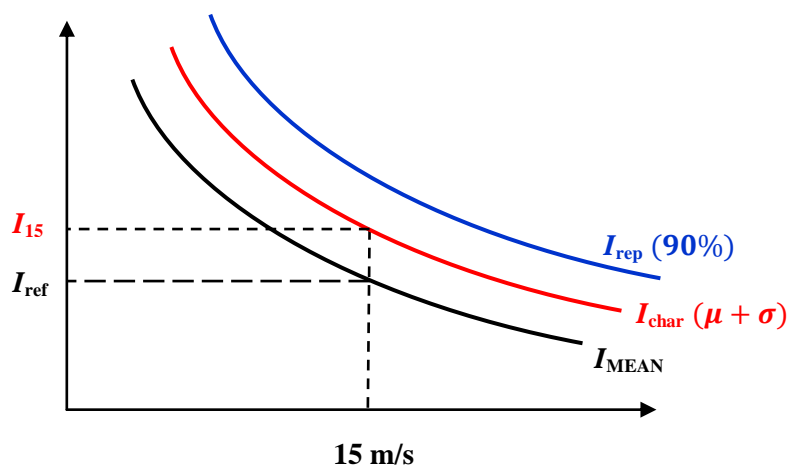


**Fig. 2.26 $I_{ref}$ under definition of IEC 61400, [DTU11].**

After computing $I_{ref}$, it is possible now to find the 90$^{th}$ percentile of the representative turbulence intensity $I_{rep}$. IEC 61400-1 3$^{rd}$ edition doesn't explain how to calculate $I_{rep}$, either as an average value independent of wind sectors (using **Eq. 2.119**), or as a weighted $I_{rep}$ values in different wind sectors at any bin (often 15m/sec) could be found using equation below;

$$I_{rep} = \sum_{i=1}^{N} f_s\, I_{rep\_s} \tag{2.126}$$

$$I_{rep\_s} = I_{ref\_s} + 1.28\, \sigma_{ref\_s} \tag{2.127}$$

where, $N$ is number of sectors, and $f_i$ is frequency of wind speed at a sector

## 2.29 Extrapolation of Turbulence

It is necessary to know that **Eq. 2.125** could be used to extrapolate the ambient turbulence intensity (*TI*) from the position of the measurement to the turbine hub height. Thus the measured turbulence intensity is simply corrected with the ratio between the measured wind speed $v_{meas}$ and the predicted wind speed $v_{pred}$ as follows, **[Lan11]**:

$$TI_{pred} = TI_{meas}\, \frac{v_{meas}}{v_{pred}} \tag{2.128}$$

where $TI_{pred}$ and $TI_{meas}$ represent the predicted and measured *TI*. Furthermore, the simple formula used for a logarithmic wind profile over flat terrain is given by, **[Pet98]**:

$$TI = 1/\ln\left(\frac{z}{z_\circ}\right) \tag{2.129}$$

where $z_o$ is the roughness length, and $z$ is new height

## 2.30 Effects of Turbulence on Power Curve

A simple method exists for estimating an upper bound of the increase in power due to turbulence effects, which can be estimated by, **[Ell90]**:

$$\bar{P} = P_{\bar{v}}\left[1 + 3\left(\frac{\sigma}{\bar{v}}\right)^2\right] \tag{2.130}$$

where, $\bar{P}$, $P_{\bar{v}}$, and $\frac{\sigma}{\bar{v}}$ represent the average output power, the power at mean wind speed $\bar{v}$, and the turbulence intensity, respectively.

The term $3(\sigma/\bar{v})^2$ represents an estimate of the upper bound of the fractional increase in power due to turbulence effects.

## 2.31 Wake and Wind Farm Turbulence

The rising demand for wind power together with environmental and economic constraints currently leads to a continuous increase in the size of wind turbines and wind farms. A drawback from installing wind turbines in large arrays is the wake penalty that arises when a wind turbine operates in the lee of a previous one, such that, a wake evolves downstream of the turbine when the turbine extracts power from the wind (see **Fig. 2.27**), **[Gau]**.

If another nearby turbine is operating within this wake, the output power for this downstream turbine is reduced when compared to the turbine operating in the free wind. This reduction of output power is depending on the wind distribution, the wind turbine characteristics and the wind farm geometry, **[Gau]**.



**Fig. 2.27 Wake effects from neighbouring wind turbines, [Gau].**

Wind turbine wakes within an array can result in energy losses and increased structural fatigue loading. The severity of wake conditions is affected by

ambient turbulence intensity, atmospheric stability conditions, and prevailing wind directions. Wake characteristics are also strongly influenced by the physical parameters including the number of turbines in operation, their spacing, and neighbouring wind turbine geometry, **[Mus13]**.

## 2.31.1 Wake modeling

Wind turbines and wind farms are very costly, thus grouping of huge turbines into large wind farms will maximize their production and reduce maintenance needs. But wind farms introduce two major issues: reduced power production from a wind turbine working in the wake of another and the shortening of the lifespan of the rotors due to increased turbulence intensity in the wake, **[Lon13]**.

In some studies, any wake models used are: straightforward, dependent on relatively few wake measurements and simplicity in terms of computing power.

One of the empirical formulas for the turbulence intensity in the wake of a wind turbine was derived by Frandsen, who developed a model for the design turbulence, which includes the characteristics of the material of the wind turbine in the calculation of turbulence intensity. The model is used in the IEC guidelines and allows a fast calculation of turbulence intensity in the wind farm, **[Lon13]**.

The model states the following: if the smallest separation distance between two wind turbines in a wind farm is more than 10 rotor diameters, wake effects do not have to be accounted for. However, if the minimum separation is less than 10 rotor diameter, the wake effects have to be calculated in terms of the turbulence intensity as follows, **[Ren07]**.

## 2.31.2 Effective turbulence intensity $I_{eff}$

Wake effects from neighbouring wind turbines may be taken into account during normal operation for fatigue calculation by effective turbulence intensity ($I_{eff}$) using Frandsen model. The effective turbulence intensity model (Frandsen model) integrates load situations with ambient turbulence and load situations under wake conditions to give the total effective turbulence as, **[IEC05, Ren07]**:

If minimum $d_i \geq 10\,D$ then, **[IEC05, Cir13]**:

$$I_{\text{eff}} = \frac{\sigma_v}{V_{hub}}$$

(2.131)

If minimum $d_i < 10\,D$ then:

Basic Frandsen formula

$$I_{\text{eff}} = \left[ (1 - \dot{N} \cdot \dot{P}_w) I_0^{\dot{m}} + \dot{P}_w \sum_{i=1}^{\dot{N}} I_T^{\dot{m}}(d_i) \right]^{1/\dot{m}}$$

(2.132)

where $I_T(d_i)$ is the maximum center-wake which is given by

$$I_T(d_i) = \sqrt{\frac{0.9}{\left(1.5 + 0.3\dfrac{d_i}{\sqrt{C_T}}\right)^2} + I_0^2}$$

(2.133)

Where,

$I_{\text{eff}}$ : the effective turbulence intensity.

$\sigma_v$: The ambient estimated turbulence standard deviation in a farm.

$d_i$ : The distance (normalized by rotor diameter) to neighbouring wind turbine no. i.

$\dot{m}$ : Wohler parameter. It depends on the material of the structural component.

$\dot{N}$ : The number of neighbouring wind turbines.

$\dot{P}_w$ : Probability density function (equal to 0.06).

$I_0$ : Ambient turbulence intensity (previously estimated).

$C_T$: the characteristic wind turbine thrust coefficient for the corresponding hub  height wind speed. If the thrust coefficient for the neighbouring wind turbines is not known, a general value given below can be used, **[Fro10]**:

$$C_T \approx \frac{7\ (m/s)}{V_{hub}}$$

(2.134)

Applying the formulas, no reduction in mean wind speed inside the wind farm can be assumed. Effective *TI* could be given in sector model as follows

$$I_{\text{eff}=} \left[ \sum_{s=1}^{N_s} f_{\_s} \cdot I_{\text{eff}\_s}^{\dot{m}} \right]^{\frac{1}{\dot{m}}} \tag{2.135}$$

where $I_{\text{eff}\_s}$ = effective turbulence intensity of the combined ambient and wake flows from certain sector.

$N_s$ = number of sectors

$f_{\_s}$ = frequency of wind speed at a sector

Wake effects from wind turbines "hidden" behind other machines need not be considered, e.g. in a row only wakes from the two units closest to the machine in question are to be taken into account. The number of closest neighbouring wind turbines $\dot{N}$ is given in table below, **[Ver02]**:

**Table 2.10: The relation between $\dot{N}$ and turbine arrangement in a wind farm, [Ver02].**

| Wind farm configuration | $\dot{N}$ |
|---|---|
| 2 wind turbine | 1 |
| 1 row | 2 |
| 2 row | 5 |
| Inside a wind farm with more than 2 rows | 8 |

The wind farm configurations are illustrated in **Fig. 2.28** for the case "Inside a wind farm with more than 2 rows".
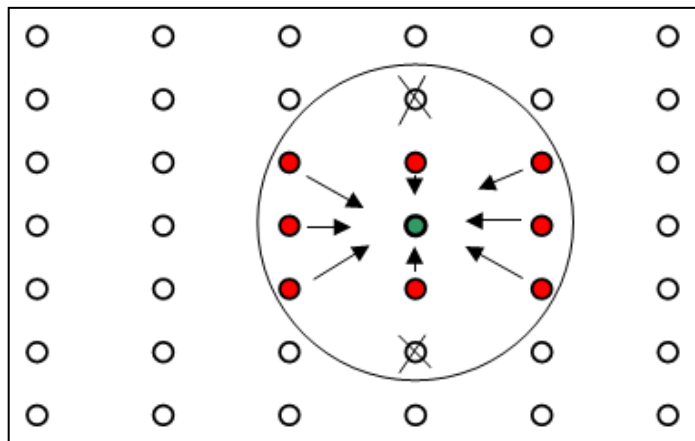


**Fig. 2.28 Example of determination of neighbouring wind turbines, [Ver02].**

## 2.32 Wind Turbine Economics

The economic aspect of energy generation also plays a key role in the wind project decision making. Thus, along with issues like "how efficient is the system" and "how much energy it will produce", the question "at what cost can we generate energy" is also relevant in choosing a source from the available options. This means that the project is to be optimized for the lowest possible cost per kWh generation.

Following subsections are essential factors in determining whether a particular installation is worthwhile or not. The information that is necessary to make an assessment of the economic viability of a wind turbine installation is, **[Mat06, Wpr, Bla09]**:

- Turbine and installation costs: which comprises the production, blades, transformer, tower, transportation to the site, erection, foundation, grid connection, road construction and buildings.

- Annual maintenance costs: The usual guideline is 1% to 3% of the turbine cost and one might expect maintenance costs to be higher towards the end of the turbine life.

### 2.32.1 Cost of energy methods

They can be applied to wind energy systems, assuming that one has a reliable estimate for the capital costs and operation-maintenance costs. Thus, cost of energy COE is defined as the unit cost to produce energy from the wind generation system and it can be expressed by the cost per kilowatt-hour, **[Wan09, Bla09]**.

The cost per kilowatt-hour of wind turbine is an important factor for electricity generation. Also, this ratio may be interest to some wishing to compare the economics of different sources of renewable energy.

The expression used for the cost of the electricity per kilowatt-hour is, **[Wpr]**:

$$cost\ per\ kWh$$
$$= \frac{Turbine\ and\ other\ costs + (Annual\ recurrent\ costs \times lifetiem)}{No.hrs \times lifetime\ (years) \times P_{e,ave}} \quad (2.136)$$

Where $No.\,hrs$ is the number of wind turbine generation hours, and the *lifetime* default value is 20 years.

This represents the total cost of installing and running the turbine divided by the number of kilowatt-hours generated over the turbine lifetime.

## 2.32.2 Total returns on total cost ratio (the return on investment)

This ratio can be expressed as, **[Wpr]**:

$$\frac{Total\ return}{Total\ cost}$$
$$= \frac{8760 \times lifetime\ (years) \times P_{e,ave}(\bar{v}) \times T_{ref}}{Turbine\ and\ other\ costs + (Annual\ recurrent\ costs \times lifetiem)} \qquad (2.137)$$

where $T_{ref}$ is the reference price per kilowatt-hour in the units of the installation and maintenance costs. $8760 = 365 \times 24$ the lifetime in hours.

The numerator represents the total payments received for the electricity generated by the turbine over its lifetime, while the denominator is the cost of the turbine and its installation and all the annual recurrent costs.

## 2.32.3 Calculating the payback period

The time it takes to recover the cost of a wind turbine installation. The payback period can be expressed as follows
 (if turbine cost and installation are known first), **[Wpr]**:

$$Payback\ period\ (years) = \frac{Turbine\ and\ other\ costs}{8760 \times P_{e,ave} \times T_{ref} - recurrent\ costs} \qquad (2.138)$$

# Chapter Three

# CHAPTER THREE

## *Results and Discussion*

### 3.1 Introduction

Generally, this chapter will examine five sites located in Iraq state in the light of topics and methodology adopted in chapter two, starting from the characteristics of the site, finding the suitable Weibull probability density function at that area, calculating the wind potential energy and how the power will be produced after a virtual turbine is located there, measuring the site turbulence intensity, as well as determining the wake effect of a single or multiple turbines to the another one located at a wind farm, finally, studying the financial analysis to determine the feasibility of wind conversion systems.

### 3.2 Areas of Study

The feasibility and applicability of wind energy development depend on the physical characteristics of the study area and the wind resource. The study areas are located south of latitude 34° south of Iraq, and they include the following sites Baghdad, Basrah, Kerbala, Nasiriya, and Ali Al-karbee. We will begin to study the last one because it is a promising area depending on the previous studies**, [Mod07].** Ali Al-karbee is the placed in the north of Maysan - Iraq, and is considered the province key. It is located in the area between Maysan and Wasit, and between Baghdad and Basra approximately in the same distance. It is 100 km from Maysan, 90 km from Wasit, and around 260 km from Baghdad and Basra. **Fig. 3.1** shows the location of chosen site in eastern region near the border between Iraq and Iran.

The following sections describe the wind data recorded from this site as well as the analysis performed on them.
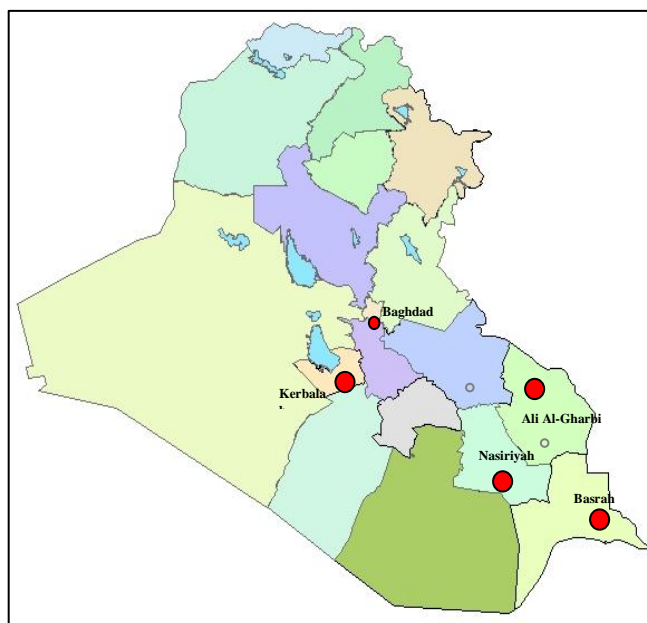
**Fig. 3.1 Iraq map, indicating the areas of study.**

## 3.3 Description of Wind Data Measurements

The wind data used in Ali Al-karbee were recorded in the year 2010 at 10m above ground level related to the selected site and were collected in a period of one year from Ali Al-karbee Meteorological station, a department of Iraqi Metrological Organization and Seismology. **Table 3.1** gives information about this station.

**Table 3.1: Information on the meteorological station, [Hus13].**

| Name of station | Code | Longitude | Latitude | Altitude (meter) | Station height (meter) |
|---|---|---|---|---|---|
| Ali Al-karbee | 666 | 46°.25′.47″ | 32°.16′.48″ | 14 | 10 |

The analysis of the winds has been carried out from the recorded series of daily values of speed and direction recorded every 3 hours. The consideration of these analysis shows a 20% zeros values from 2920 data records, which as a result will intensively reduce wind speed spectrum. **Table 3.2** clarifies these facts in addition to some important statistics like minimum-maximum values, mean wind speed (this value is located within Beaufort gentle breeze scale), in addition to standard deviation and variance data.

**Table 3.2: Wind characteristics of Ali Al-karbee site.**

| Data attribute | Value |
|---|---|
| Date of records | 2010 |
| No. of data | 2920 |
| No. of zeros | 589 (20.17%) |
| Calms ( Speed 0-0.51m/sec) | 589 (20.17%) |
| Maximum (m/sec) | 18 |
| Minimum  (m/sec) | 0 |
| Mean wind speed | 3.838 |
| Mean wind speed (Cubic root) | 5.63 |
| Std. | 3.00 |
| Variance | 9.03 |
| Time step (hours) | 3 |

## 3.4 Description of the User Program

There are many programs specialized in wind energy field given free on web, but they do not operate at full functions beside a limited time period and lack of reliability. Also, the license software for this kind of applications is very expensive. Thus, a program designated for wind energy analysis has been built using Visual Basic 6 environment. The program is used for solving expressions mentioned in chapter two numerically since these equations cannot be resolved analytically. The procedure of program has been tested with the results published in books, researchs, and softwares dedicated for this purpose.

The block diagram is shown in **Fig. 3.2.** The input data rows include wind speed, wind direction, date and time of records; the program could deal with them all, or which one available. After reading wind data the program will estimate Weibull parameters ($c$, $k$) using nine methods. The criteria for choosing the best parameters are goodness of fit tests besides pdf graphical plots. Present program has four models dedicated for wind characteristics, the output power from wind turbine, site assessment, and economics. In general the program is written to become suitable with the nature of data available in Iraq, and the results compensate the lack in information in such field of study.

START

Read wind speed, wind direction, Date and time of record
If exist

Calculation

| Plot wind speed-time variation graph | | Plot wind rose graph |

Estimate Weibull parameters (c, k) at 10m height numerically and graphically using 9 methods

Determine best Weibull parameters (c, k) using different criterion methods

**Wind characteristics**

| c, k extrapolation | Air density extrapolation | | speed extrapolation freq. | |
|---|---|---|---|---|
| Prob. of Max freq. | Roughness length | Mod | Skewness | Kurtosis |
| Max speed | Min speed | Mean speed | Median speed | speed Std. | No. of data |
| Max frequency | Speed of Max frequency | Variance | Coeff. of variation | CDF |

**Turbine output power**

| Power density for each speed | Max power density |
|---|---|
| Mean power density (weibull based) | Mean power density |
| Total power density | Mean power output |
| | Turbine max power |

**Site Assessment**

| 8 sector wind roses | 4 wind rose for TI |
|---|---|
| Ambient turbulence intensity | Graphical lines for TI |
| Average TI | One of each 8 sectors TI |
| 90%Ti | Effect of TI on power curve |
| Std of average TI | Wake effects independent |
| Std of 90 TI | Wake effect of each 8 sectors |
| Depends of TI on wind speed | Freq. of TI for each wind |

**Economics**

| Total return | Cost of system per unit rotor size |
|---|---|
| Cost per kilowatt | Cost per rated power |
| | Payback period |

END

**Fig. 3.2 The flowchart of the program.**

## 3.5 General Wind Conditions

They include two following items; wind rose and wind speed characteristics

## 3.5.1 Wind rose

**Fig. 3.3** shows the annual wind rose at Ali Al-karbee site for the year 2010. Wind rose clarifies the dominant wind direction which is an important parameter in the installation and arrangement of wind turbines and construction fields. Also, the analysis indicates that the main prevailing wind in the Ali Al-karbee region is northwestern, such that about 64% of the annual wind data is blowing from that direction, 14% of the wind direction is southeastern, while about 20% of wind speeds have calm values, and the residual percentages are distributed amongst other directions with speeds more than calm value. Here, about 80% of data have values more than calm value which is a positive feature of this site (**Table 3.3**).
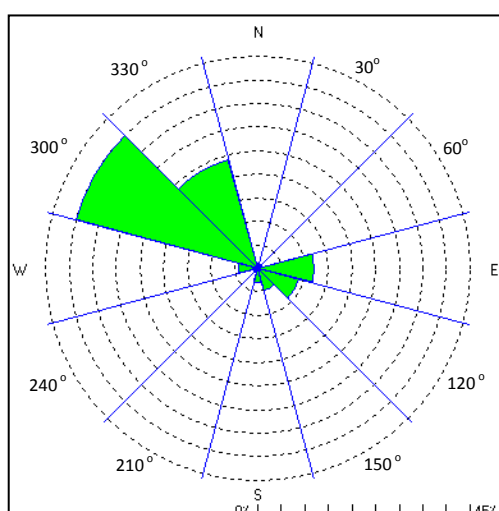


**Fig. 3.3 Wind rose diagram for Ali Al-karbee 2010, 10m height.**

**Table 3.3: Frequency of data percentages in each sector**

| Sector center (deqree) | 0 | 30 | 60 | 90 | 120 | 150 | 180 | 210 | 240 | 270 | 300 | 330 |
|---|---|---|---|---|---|---|---|---|---|---|---|---|
| Freq.% (zeros not in count) | 0.7 | 0.1 | 1.3 | 11.8 | 9.2 | 5.1 | 2.7 | 1.1 | 0.7 | 3.6 | 40.1 | 23.6 |

However, **Table 3.3** doesn't tell us how much the percentage of speed value in each sector. **Table 3.4** gives the percentage of different wind speed intervals in each sector from 0-330 (centered). Now, by multiplying the percentages in

89

**Table 3.4** with the total number of data in its particular sector we will get **Fig. 3.4**. This **Fig.** shows graphical representation of the **Table 3.4**, in addition, by which you could compare the percentages of wind speed interval values that contributes to a total number of data in a certain sector and this is done using vertical bars. Thus, in a most frequent direction (sector 300) the wind speeds over 10 m/sec occur by 6% and 8-10 m/sec occur by 7% and so on, while in the secondary predominant direction (sector 330) the wind speed over 10 m/sec occurs 12% and 8-10 m/sec occurs by 11% and so on.

**Table 3.4: Frequency of data intervals percentages in each sector**

| Speed interval | Sector center | | | | | | | | | | | |
|---|---|---|---|---|---|---|---|---|---|---|---|---|
| | 0° | 30° | 60° | 90° | 120° | 150° | 180° | 210° | 240° | 270° | 300° | 330° |
| No. data | 16 | 2 | 30 | 277 | 215 | 119 | 62 | 26 | 17 | 83 | 934 | 550 |
| 0.5-2 m/s | 18 | 0 | 16 | 8 | 6 | 12 | 12 | 19 | 11 | 9 | 7 | 4 |
| 2-4 m/s | 12 | 0 | 26 | 24 | 25 | 36 | 32 | 34 | 41 | 30 | 24 | 11 |
| 4-6 m/s | 43 | 0 | 23 | 39 | 44 | 36 | 41 | 30 | 35 | 46 | 44 | 41 |
| 6-8 m/s | 0 | 50 | 23 | 14 | 13 | 6.7 | 9.6 | 7.6 | 11 | 8.4 | 9.5 | 18 |
| 8-10 m/s | 6.2 | 0 | 0 | 9.0 | 6.0 | 6.7 | 3.2 | 7.6 | 0 | 4.8 | 7.7 | 11 |
| >10 m/s | 18 | 50 | 1 | 3.9 | 3.7 | 1.6 | 0 | 0 | 0 | 0 | 6.2 | 12 |
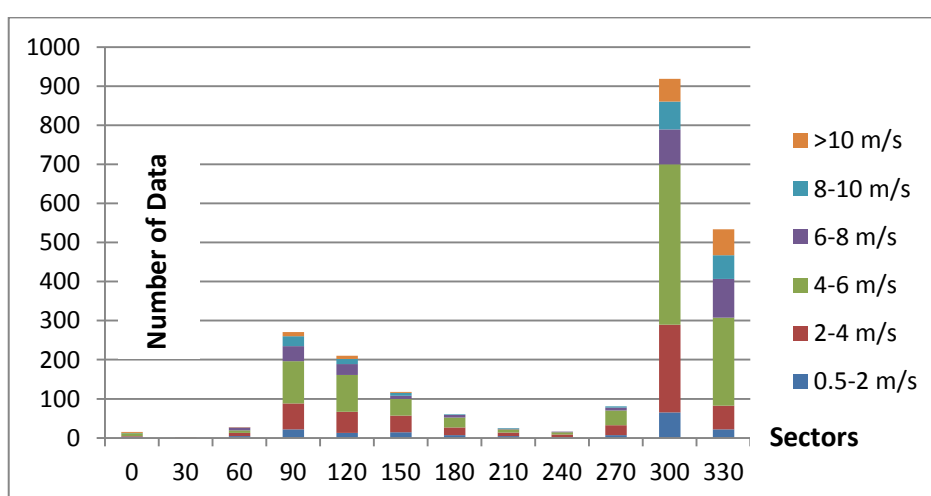


**Fig. 3.4 Wind speed intervals percentages at each sector.**

**Fig. 3.5** shows monthly based wind rose for 10m height, it helps in understanding the variability in the wind direction every month. Simply, it could be inferred that the main prevailing wind direction at the study area is north-western, while the dominant wind directions in the months Jan., Feb., Mar., Apr., and Dec. range between northwestern (300 -330 sectors) and southeastern (90-120 sectors). In more details, winds mostly bear from 300 and 330 sectors, has occurrences of 60-65% (in Sep.) and 40-43% (in May), respectively. While winds which mostly bear from 90 and 120 sectors have occurrences of 25-27% (in Feb.) and 25-28% (in Jan.), respectively. Other months point out the occurrence of sector 300 is the most dominant one, and it reaches its maximum value at approximately 61% from total records in September.



|  Jan  |  Feb  |  Mar  |
|-------|-------|-------|
|  Apr  |  May  |  Jun  |
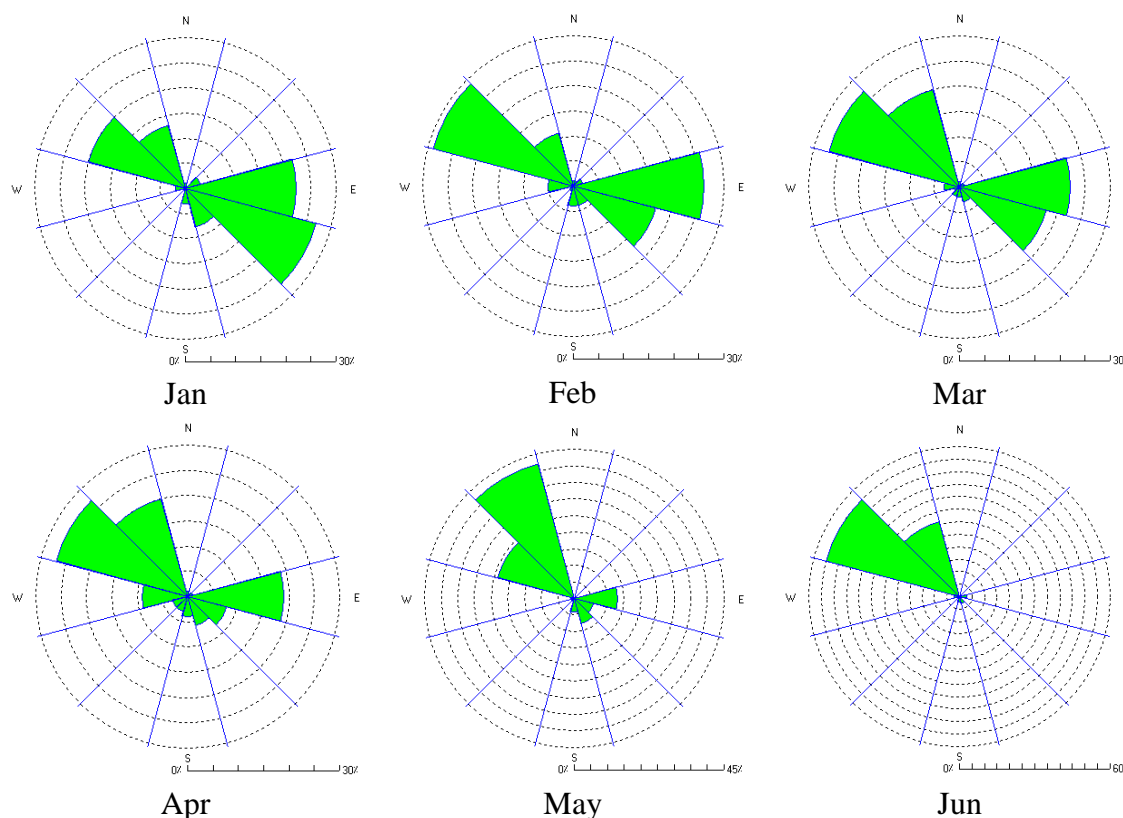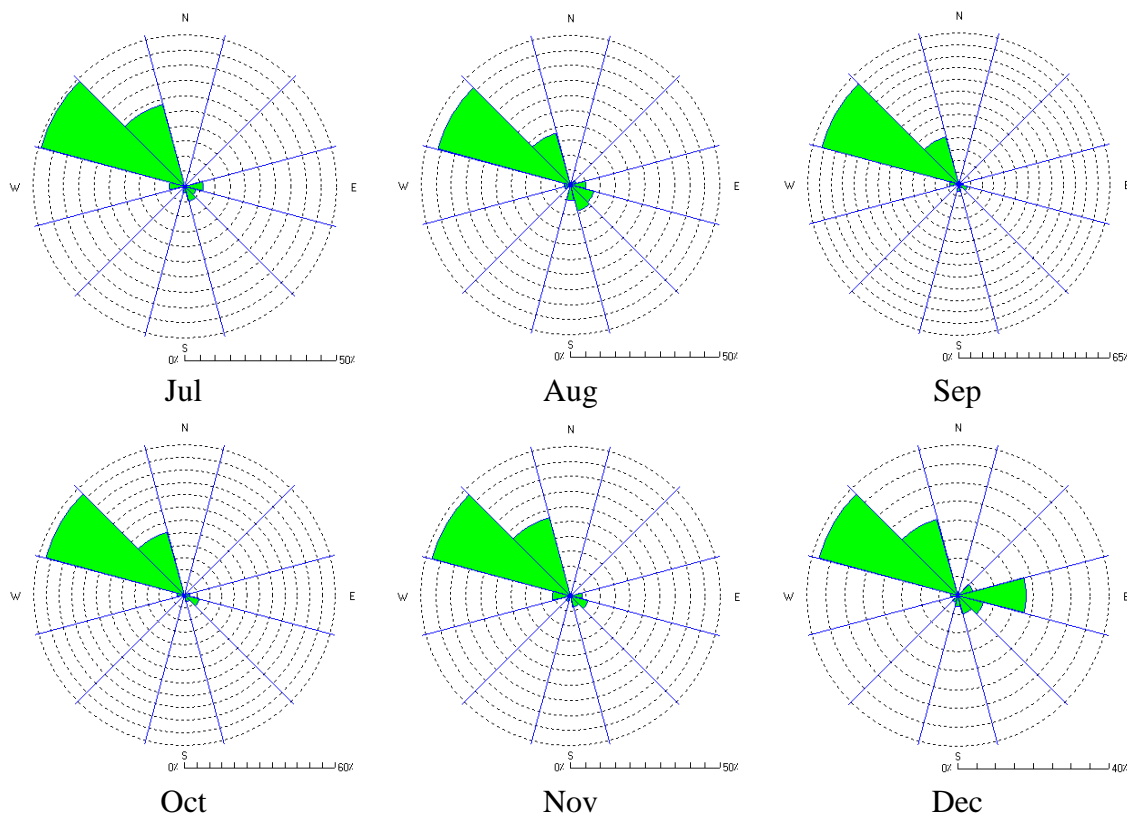
**Fig. 3.5 Monthly wind roses at Ali Al-karbee 2010.**

## 3.5.2 Wind speed characteristics

The wind speed data at the selected station are statistically analyzed. **Fig.3.6** shows the mean daily wind speed values at Ali Al-karbee for the year 2010.
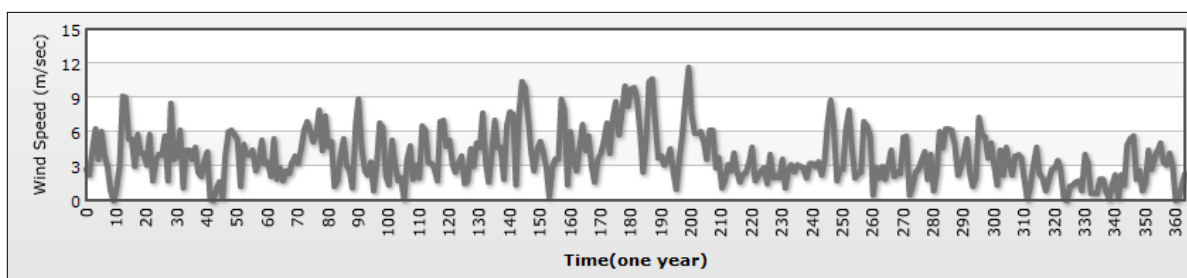


**Fig. 3.6 Mean daily wind speed values at Ali Al-karbee throughout the year 2010.**

The mean is taken here by averaging the records during one day. It could be inferred from the diagram that wind data has not a clearly seasonal effect; but instead of that there is a little increment in the wind speed in the mid of year. This increment seems to be somewhat clear in the period between the days 140-

92

200, which are almost from mid-April to mid-June and the maximum mean wind speed throughout the year is about 11.6 m/sec.

**Fig. 3.7** illustrates the monthly mean wind speed variation. This shows how changing mean wind speed helps to understand the behavior at each month.

The mean monthly wind speed is higher in June and July and it varies from 5.1 and 5.4 m/sec, while the minimum values in November and December vary from 2.2 and 2.5 m/sec, where this increase and decrease in the data values are due to the seasonal effect. Furthermore, **Fig. 3.7** gives an idea about the days when the wind speeds is higher than rest of days.
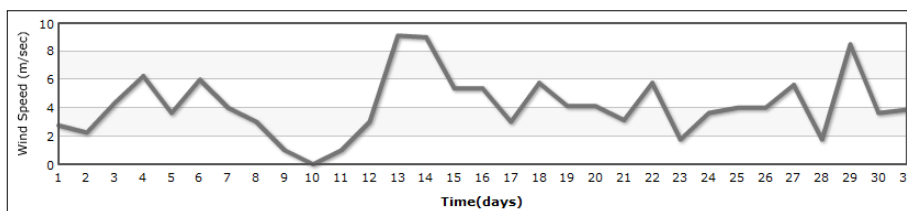


**Jan (mean 4.1m/s)**
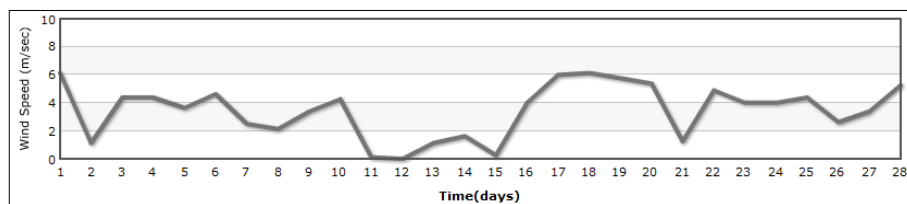


**Feb (mean 3.4m/s)**
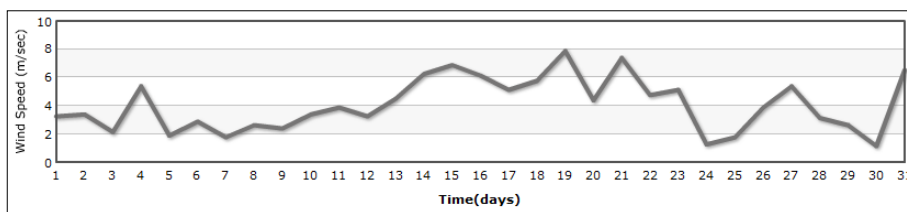


**Mar (mean 4m/s)**
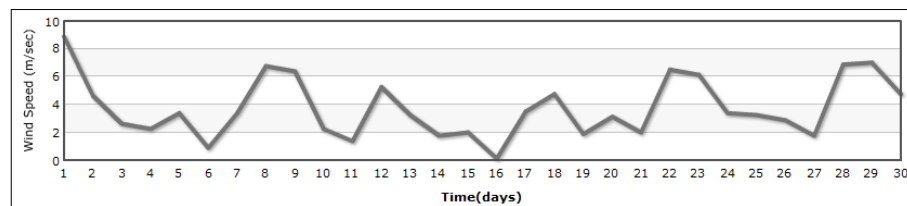


**Apr (mean 3.7m/s)**
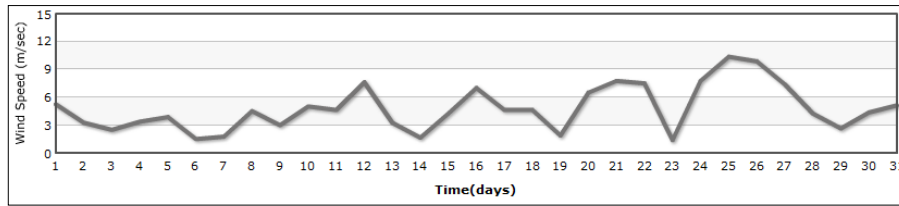
**May (mean 4.7m/s)**
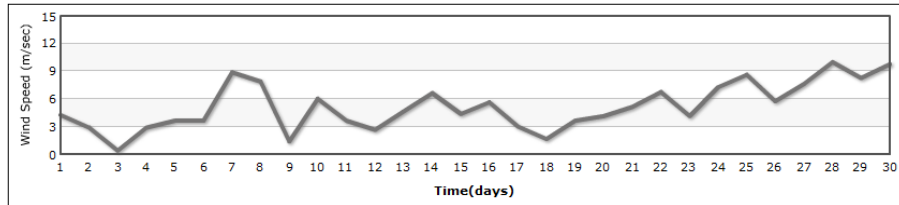


**Jun (mean 5.1m/s)**
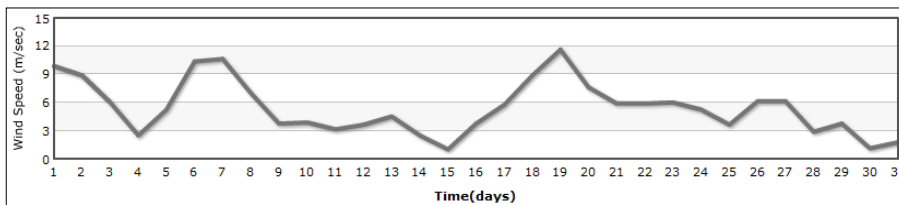


**Jul (mean 5.4m/s)**
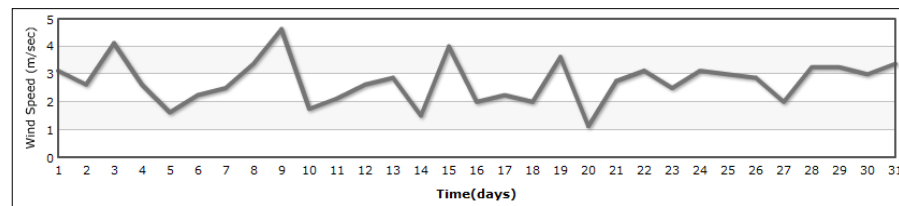


**Aug (mean 2.7m/s)**
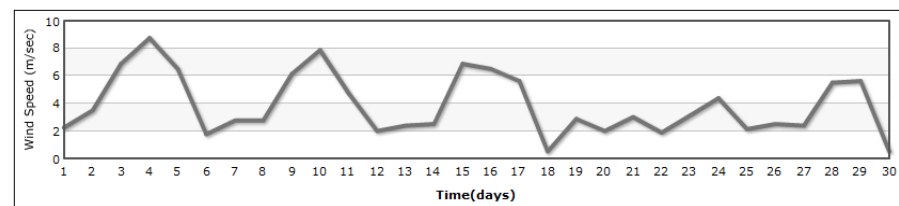


**Sep (mean 3.8m/s)**



**Oct (mean 3.7m/s)**

94
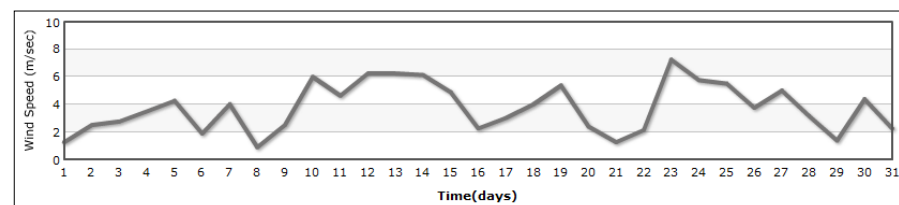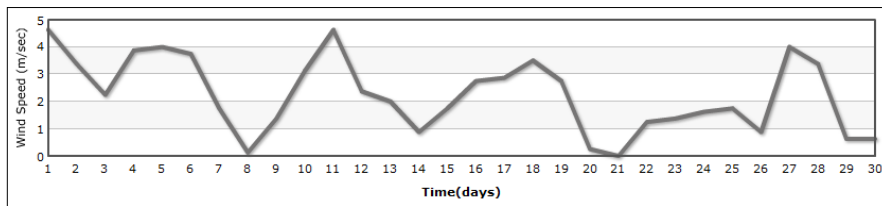
**Nov (mean 2.2m/s)**
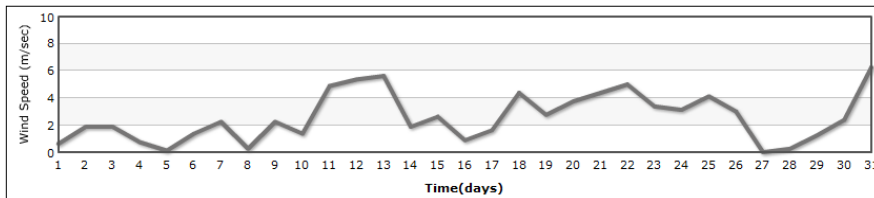


**Dec (mean 2.5m/s)**

**Fig. 3.7 Monthly wind variation at Ali Al-karbee site 2010.**

Sometimes we need to know the frequency of certain wind datum in a series such as zeros, thus it is useful to represent all recorded points in a specific diagram. Accordingly, the time variation of all individual wind speed in each month (as shown in **Fig. 3.8)** is a good representation for that purpose. This diagram highlights an interesting characteristic of the wind speed. The number of zeros in the months of February, April, August, and December are much more than the rest of months. As a result, Weibull representation will deviate from high wind speed to low wind speed (toward y-axis) in these months.



**Jan**



**Feb**

95
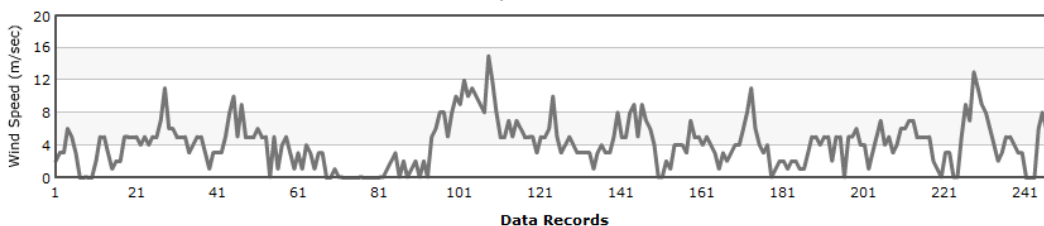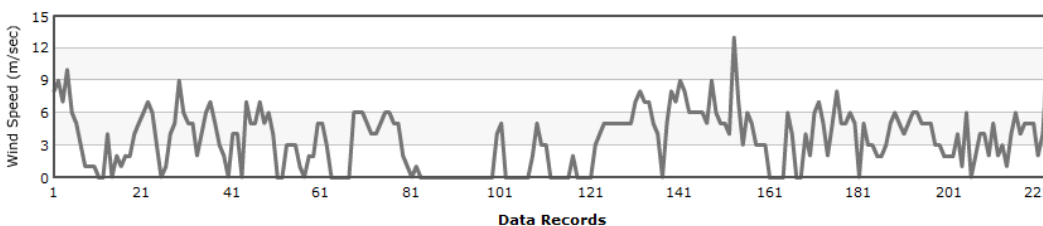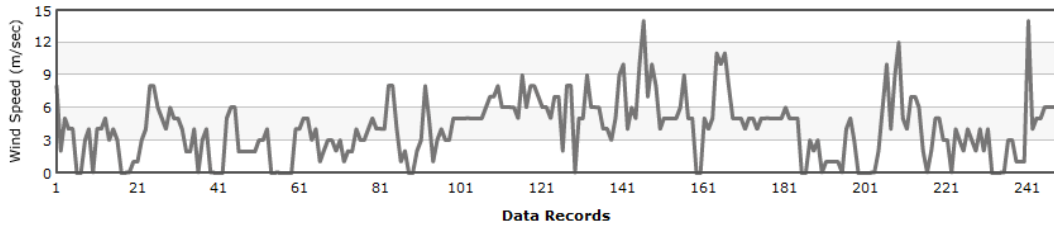
**Mar**



**Apr**



**May**



**Jun**



**Jul**



**Aug**

**Sep**



**Oct**



**Nov**



**Dec**
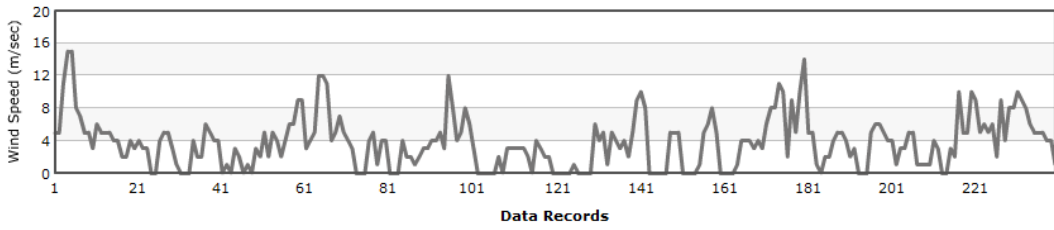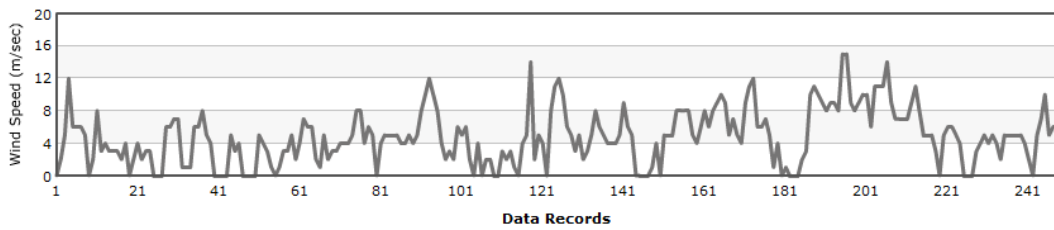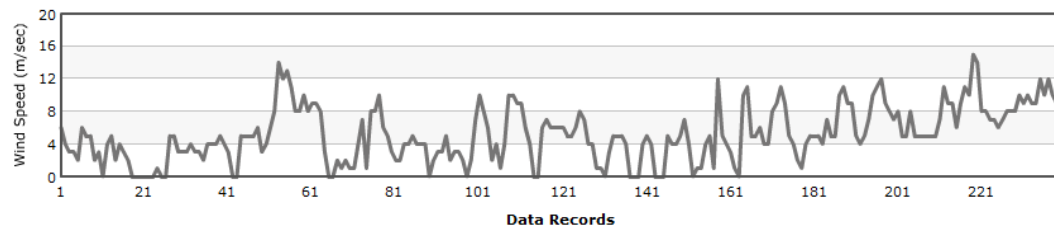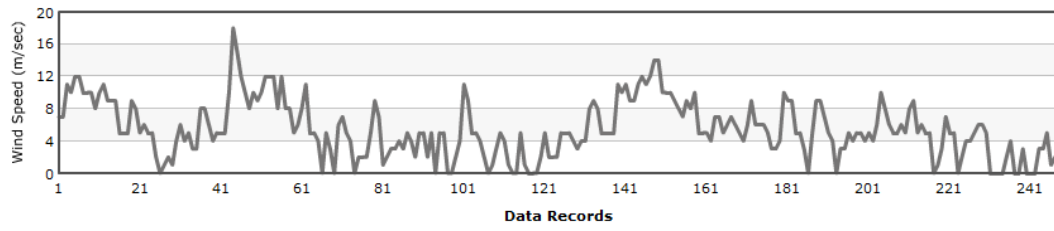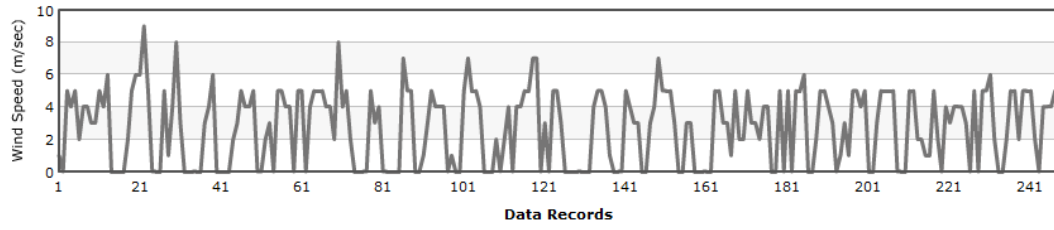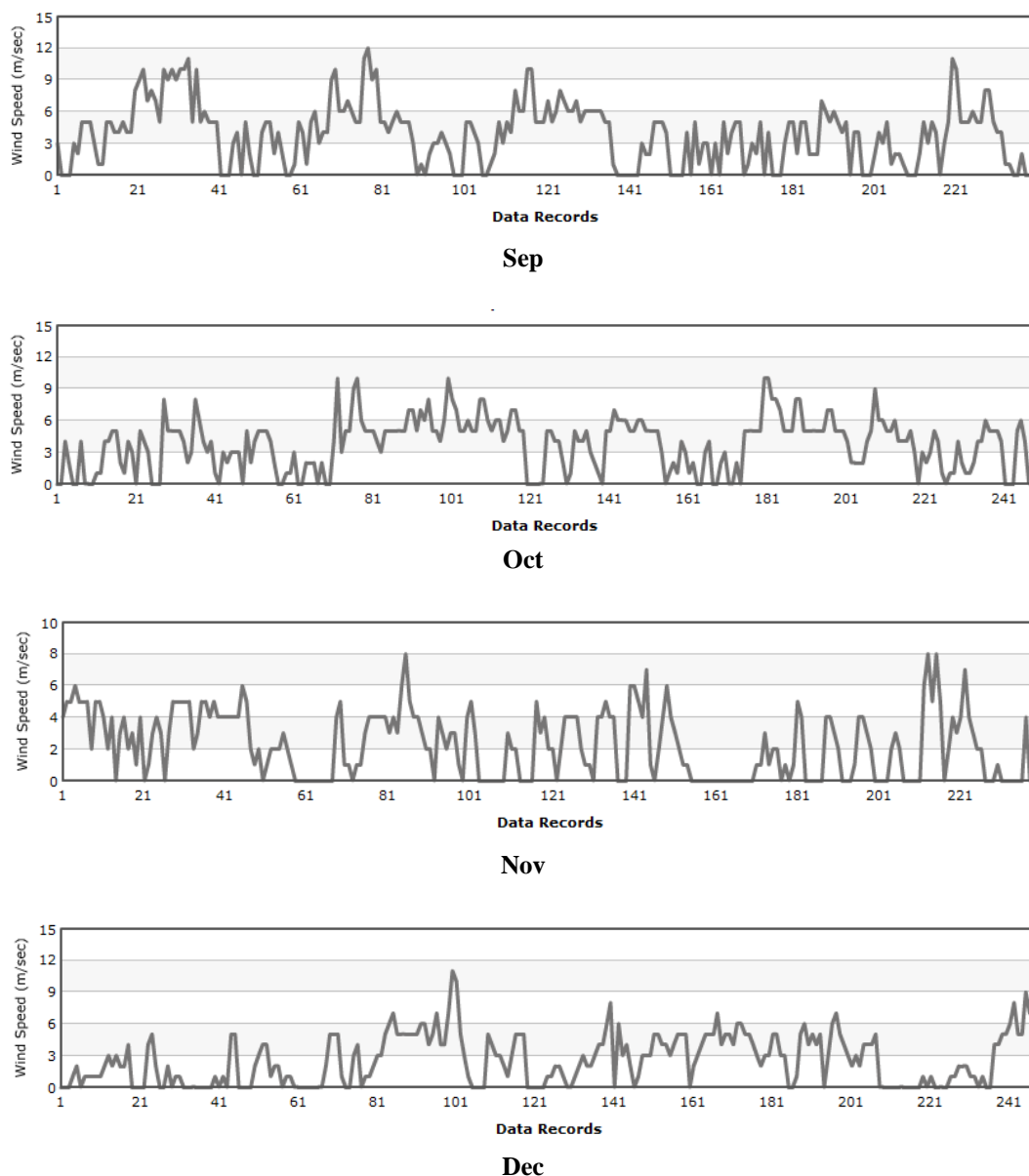
**Fig. 3.8 Monthly wind speed variation for all individual data .**

## 3.6 Performance Comparison of Nine Methods in Estimating Weibull Parameters – Annual Based

An accurate test of probability distribution for wind speed values is very important in evaluating wind energy potential of a region. In this section, we try to determine appropriate theoretical pdf (probability density function) by comparing nine methods for estimating Weibull parameters for one year data of Ali Al-karbee in 2010. Below an approach consisting of three tests has been used.

### 3.6.1 Graphical test

The nine methods used for estimating Weibull parameters (briefly shown in chapter two) are Standard deviation method (SDM), Energy pattern factor method (EPFM), Maximum likelihood estimation - Newton Raphson method (MLE-NRM), Maximum likelihood estimation - iterative method (MLE-IM), Maximum likelihood estimation - frequency dependent iterative method (MLE-FDM), Maximum Likelihood Estimation - modified Iterative Method (MLE-MIM), Linear least square method (LLSM), Modified linear least square method (MLLSM), and Equivalent energy method (EEM). Weibull scale and shape parameters estimated by these nine methods for Ali Al-karbee site at 10m above ground surface are listed in **Table 3.5**.

**Table 3.5: Estimated shape and scale parameters at 10m heigh
for Ali Al-karbee 2010**

| Mechanism | $c$ (m/sec) | $k$ |
|---|---|---|
| SDM | 4.16 | 1.30 |
| EPFM | 4.21 | 1.40 |
| MLE-NRM | 5.13 | 1.50 |
| MLE-IM | 5.44 | 1.97 |
| MLE-FDM | 8.40 | 1.90 |
| MLE-MIM Location parameter =1.98 | 4.05 | 1.26 |
| LLSM | 3.56 | 1.22 |
| MLLSM | 3.71 | 1.15 |
| EEM | 3.75 | 1.19 |

All these methods are depicted as a curve fitting line (red line) made by Weibull probability density function shown in **Fig. 3.9a-i**.

At the same plots of the pdfs, there are also histograms of the wind speed binning at 1m/sec plotted in blue bars which will make an easy way for comparison between measurement values and estimated distributions. In other

words **Fig. 3.9a-i** shows how the calculated Weibull distribution function matches with the observed wind speed histogram for Ali Al-karbee Location.



a- SDM

b-  EPFM

c- MLE-NRM

d- MLE-IM

e-  MLE-FDM

f- MLE-MIM

g-  LLSM

h- MLLSM

i- EEM
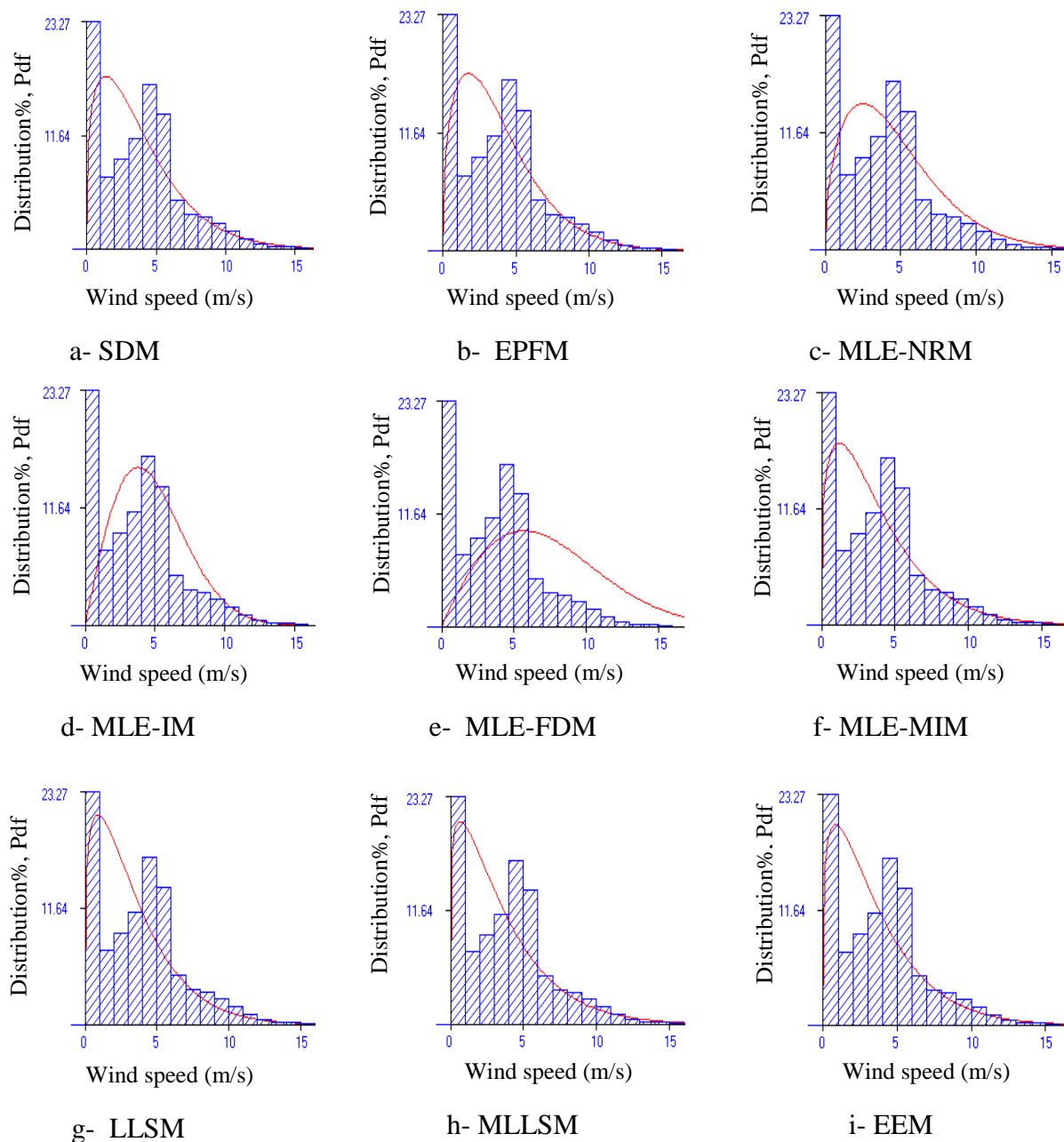
**Fig. 3.9 Weibull parameters Estimation by nine methods for Ali Al-karbee 2010.**

It could be inferred that the shape and scale parameter values estimated with all preceding methods (except MLE-FDM) give reasonable fit to measured data set. But, in order to make the comparison easier, the performance of the pdfs relative to the histogram of the measured data is plotted in one diagram excluding MLE-

FDM (see **Fig. 3.10**). The diagram presents more insight of the distributions fitting to wind speed data.

From the figure it could be concluded that:

   i.   except for MLE-NRM and MLE-IM, all methods exhibit reasonable fit to wind data.

   ii.  there is a similar behavior between theoretical distributions starting from 2 m/sec, except for MLE-NRM and MLE-IM.

   iii. there is a clear difference in the peaks of pdfs located within first bin 0-1 m/sec.

Despite this, it must be noted that the suitability of each model varies with sample data distribution, which, consequently, varies from location to location, **[Sey09]**.
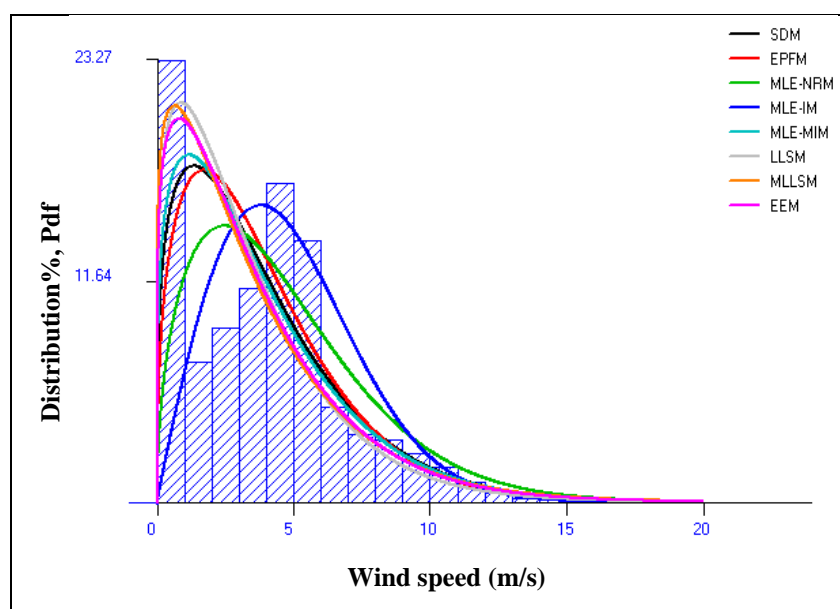


**Fig. 3.10 Comparison between theoretical pdfs and measured wind speed histogram for Ali Al-karbee 2010.**

Another graphical test is studied by plotting the cumulative distribution functions (cdfs) and the histogram for one year measured data (Ali Al-karbee 2010) in **Fig. 3.11**. The blue bars represent histogram of the measured data at bin size 1m/sec, while the black lines represent cdfs curves having shape and scale parameters aforementioned in **Table 3.5**.

a- SDM



b- EPFM



c- MLE-NRM



d- MLE-IM



e- MLE-FDM



f- MLE-MIM



g- LLSM



h- MLLSM



i- EEM
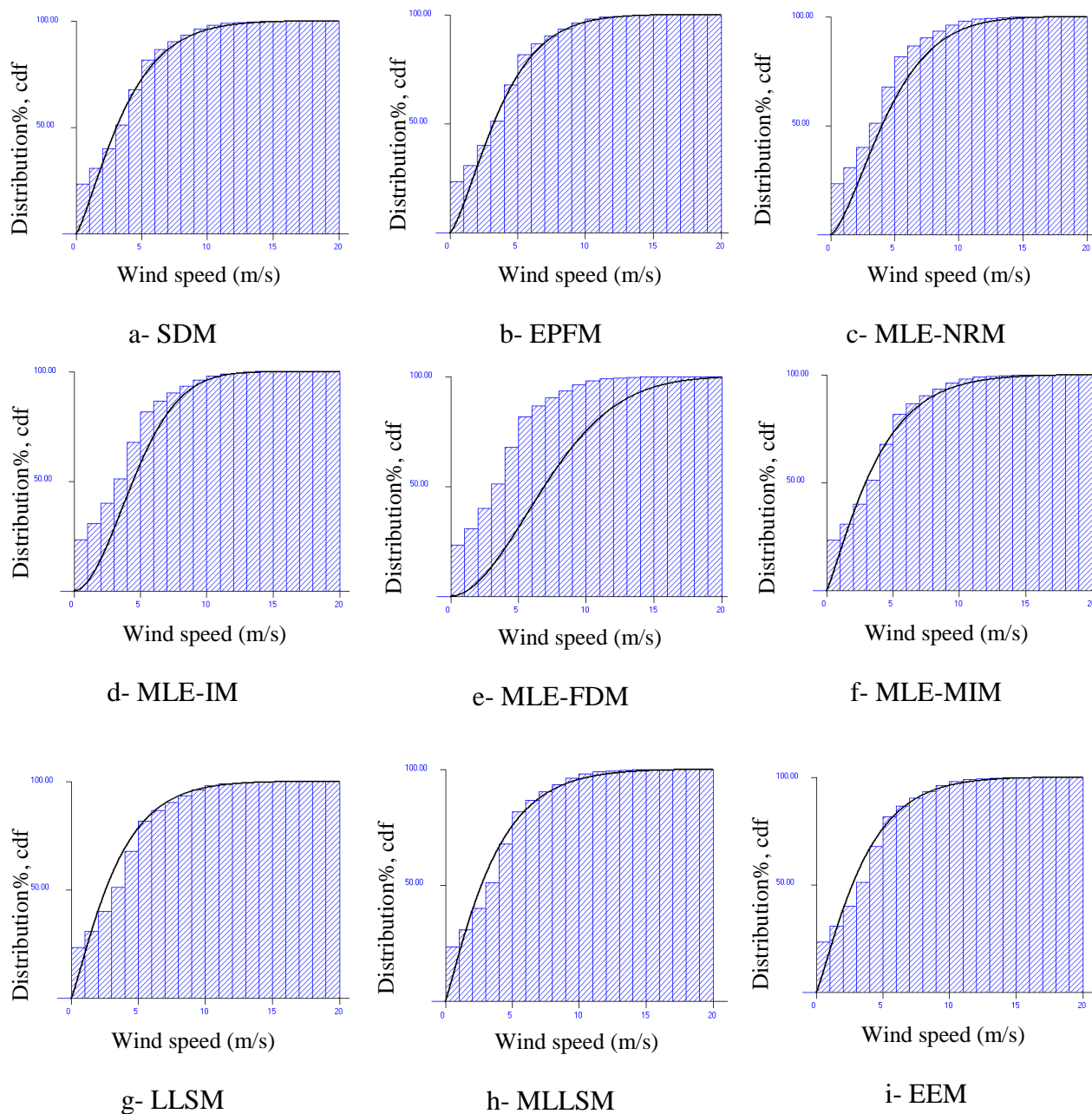
**Fig. 3.11 Estimated cdfs for each method and observed wind speed histogram for Ali Al-karbee 2010.**

**Fig. 3.11** shows a well match between cdfs curves and histograms except for three methods (i.e. MLE-NRM, MLE-IM, and MLE-FDM). This **Fig.** illustrates how fit estimation curves with the measured histogram are, while the three methods exhibit significantly anomalous representation to wind data.

To simplify the comparison, the results that have been obtained from **Fig. 3.11,** is plotted in one graph (Fig. 3.12), and it is easily to show the abnormal behavior of these three methods beside a good closeness of the other methods.
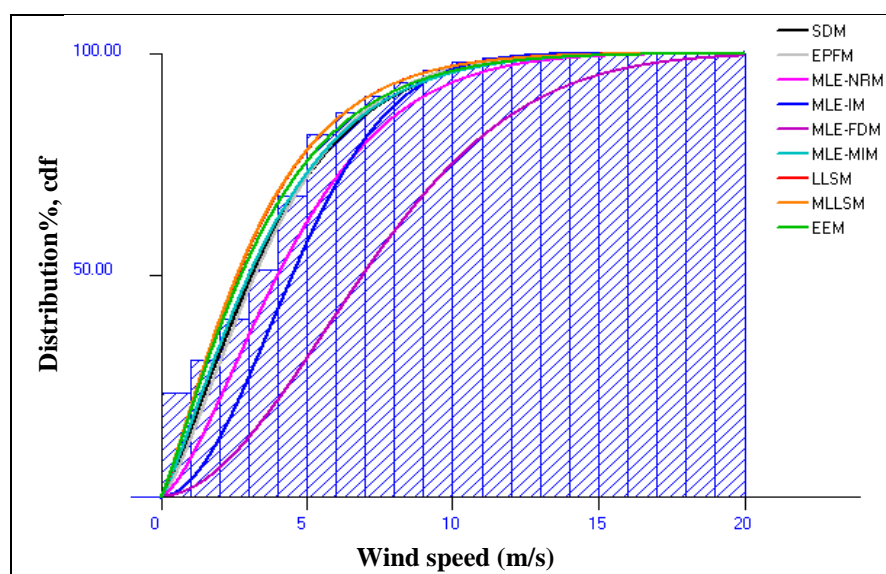
**Fig. 3.12 Comparison between theoretical cdfs
and observed wind speed histogram for Ali Al-karbee 2010.**

### 3.6.2 Analytical test- goodness of fit test

In the previous section we tested the nine methods in graphical ways, and the results show that there are three method which yield worst graphical fit; these methods are MLE-NRM, MLE-IM, and MLE-FDM. But this does not give enough impression about the best way for Weibull parameters estimation. Thus, in order to evaluate the suitability of the estimated distributions for wind speed data, various analytical criteria have been made. Four criteria (explained in chapter 2) are presented to get more insight into the wind data fitting techniques; these are RMSE, Chi-Square ($\chi^2$), correlation coefficient (R), and coefficient of determination (COD).

The best distributional model can be determined according to the lowest values of RMSE and $\chi^2$ and highest values of R and COD. **Table 3.6** summarize statistical errors resulting from computing the goodness of fit between estimated probability distribution functions and histogram of the measured data. It is shown that MLE-MIM gives the best distributional model according to the lowest values of RMSE and $\chi^2$, besides the highest values of R and COD.

Aforementioned Judgment criteria are also applied to find the relative errors between theoretical cumulative distribution functions and observation data. **Table 3.7** illustrates the results of these criteria and they clarify that the best goodness of fit is observed with EEM.

102

**Table 3.6:  Comparison of the accuracy test results using the
Weibull pdf at 10m height for Ali Al-karbee 2010**

| Mechanism | RMSE | $\chi^2$ | R | COD |
|-----------|------|----------|-----|-----|
| SDM | 0.04 | 0.21 | 0.62 | 0.39 |
| EPFM | 0.04 | 0.23 | 0.58 | 0.34 |
| MLE-NRM | 0.04 | 0.35 | 0.57 | 0.32 |
| MLE-IM | 0.05 | 1.21 | 0.37 | 0.14 |
| MLE-FDM | 0.06 | 3.04 | 0.09 | 0.00 |
| MLE-MIM | 0.03 | 0.21 | 0.63 | 0.40 |
| LLSM | 0.04 | 0.26 | 0.57 | 0.33 |
| MLLSM | 0.04 | 0.24 | 0.62 | 0.39 |
| EEM | 0.04 | 0.23 | 0.62 | 0.38 |

**Table 3.7:  Comparison of the accuracy test results using the
cdf at 10m height for Ali Al-karbee 2010**

| Mechanism | RMSE | $\chi^2$ | R | COD |
|-----------|------|----------|-----|-----|
| SDM | 0.05 | 0.50 | 0.96 | 0.93 |
| EPFM | 0.05 | 0.73 | 0.95 | 0.92 |
| MLE-NRM | 0.08 | 1.68 | 0.87 | 0.77 |
| MLE-IM | 0.12 | 6.66 | 0.78 | 0.61 |
| MLE-FDM | 0.26 | 16.81 | 0.03 | 0.01 |
| MLE-MIM | 0.05 | 0.41 | 0.96 | 0.93 |
| LLSM | 0.05 | 0.28 | 0.96 | 0.92 |
| MLLSM | 0.04 | 0.23 | 0.96 | 0.93 |
| EEM | 0.04 | 0.27 | 0.97 | 0.94 |

## 3.6.3 Evaluation of mean wind speed and power density

The summary of mean wind speeds ($\bar{v}$) and wind power densities ($PD_w$) calculated for this site are shown in **Tables 3.8**, and they are calculated using estimated Weibull parameters by nine mentioned methods. Then the estimated parameters are substituted into **Eqs 2.21** and **2.104** to determine $\bar{v}$ and $PD_w$, column 2 and 4, respectively (at standard air density). Also, the percentage error

in evaluating mean wind speed and wind power density (using **Eq. 2.77**) is listed in **Table 3.8**, column 3 and 5, where actual mean wind speed ($\bar{v}_a$) is 3.83 m/sec and actual power density ($PD_A$) is equal to 109.5 W/m$^2$. The percentage of error in column 3 for evaluating mean wind speed is shown as a graphical representation in **Fig. 3.13**.

**Table 3.8: Comparison of methods in estimating mean speed and power density**

| Method | $\bar{v}$ (m/sec) | Error (%) | $PD_w$ (w/m$^2$) | Error (%) |
|--------|------------------|-----------|------------------|-----------|
| SDM | 3.84 | 0.26 | 118.5 | 8.24 |
| EPFM | 3.83 | 0 | 104.2 | 4.85 |
| MLE-NRM | 4.64 | 21.1 | 166.0 | 51.5 |
| MLE-IM | 4.80 | 25.3 | 132.8 | 21.2 |
| MLE-FDM | 7.40 | 93.21 | 509 | 364 |
| MLE-MIM | 3.76 | 1.82 | 118.1 | 7.90 |
| LLSM | 3.30 | 13.8 | 86.5 | 21 |
| MLLSM | 3.53 | 7.83 | 116.5 | 6.39 |
| EEM | 3.53 | 7.83 | 109.5 | 0 |
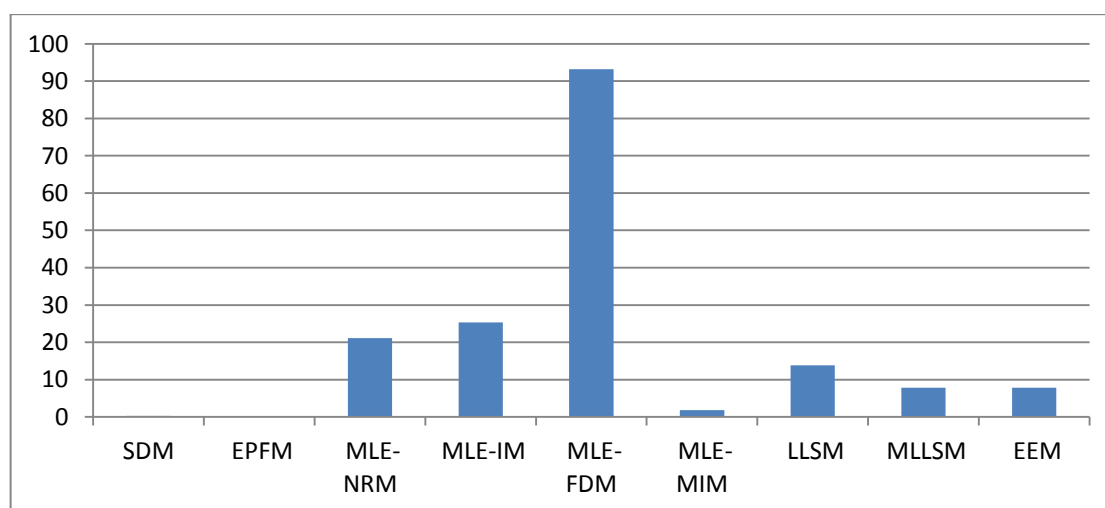


**Fig. 3.13 Error values obtained in calculating the mean wind speed by different methods.**

In the same way, the graphical representation of errors in **Table 3.8** column 5 is given in **Fig. 3.14**.
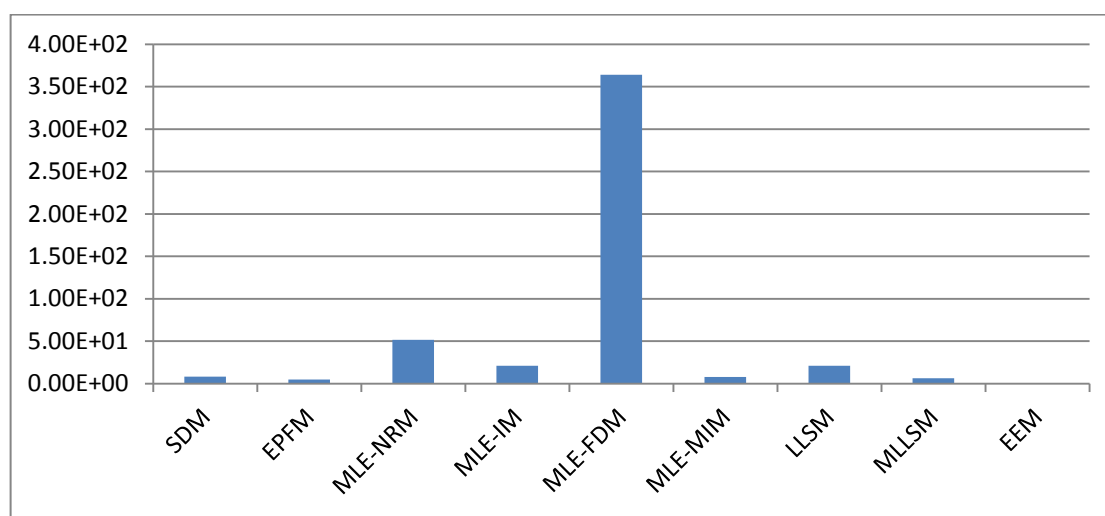
**Fig. 3.14 Error values obtained in calculating the power density by different methods.**

However, the results show that the error percentage test has its lowest value when we estimate mean wind speed using EPFM, while the error percentage test has its lowest value when we estimate power density using EEM.

Finally, the summary of best methods for Weibull parameters estimation (*c, k*) for Ali-Al-Gharbi site (2010) at 10m height is given in the table below (**Table 3.9**). From this table it is possible to conclude that the EEM is a distinct technique for wind energy applications at this region.

**Table 3.9: Summary of the previous results**

| Method | Graphical Test | | Numerical test | | Error percentage | |
|---|---|---|---|---|---|---|
|  | pdf | cdf | pdf | cdf | $v_m$ | P.D. |
| EPFM | ✓ | ✓ | ✗ | ✗ | ✓ | ✗ |
| MLE-MIM | ✗ | ✗ | ✓ | ✗ | ✗ | ✗ |
| EEM | ✓ | ✓ | ✗ | ✓ | ✗ | ✓ |

## 3.7 Performance Comparison of Nine Methods in Estimating Weibull Parameters - Monthly Based

In this section, we will test methods mentioned before for Weibull parameters estimation in the same way we tested methods for one year, but now for monthly based data. Since the monthly calculations will give huge results,

thus it is sufficient to take one month (January) instead of 12 and see the results. This way will give a general understanding of how methods will behave with monthly based data. Like the previous section, an approach consisting of three tests has been used to judge the suitability of these methods for parameters estimation.

## 3.7.1 Graphical test

The estimated scale and shape parameters produced by the nine mechanisms for January month are listed in **Table 3.10**. The extreme value of scale parameter is for MLE-FDM and explains the anomaly behavior of this method in pdf representation. The highest value in scale parameter estimated by MLE-FDM makes the distribution stretch out to the right with a decrease in height (as explained in chapter two), see **Fig. 3.15e**.

**Table 3.10: Estimated shape and scale parameters at 10m height for Ali Al-karbee, January**

| Mechanism | $c$ (m/sec) | $k$ |
|---|---|---|
| SDM | 4.59 | 1.48 |
| EPFM | 4.64 | 1.63 |
| MLE-NRM | 5.11 | 1.50 |
| MLE-IM | 5.41 | 1.98 |
| MLE-FDM | 8.27 | 1.73 |
| MLE-MIM, $g$ =1.98 | 4.65 | 1.68 |
| LLSM | 4.00 | 1.35 |
| MLLSM | 4.37 | 1.55 |
| EEM | 4.67 | 1.56 |

An accurate determination of Weibull distribution for monthly based data (only January of 2010) is illustrated in **Fig. 3.15**. This test has shown how much the fit of Weibull distribution to wind speed is. Thus, when the graphics are reviewed it can easily be seen that MLE-FDM method gives the worst fitness.
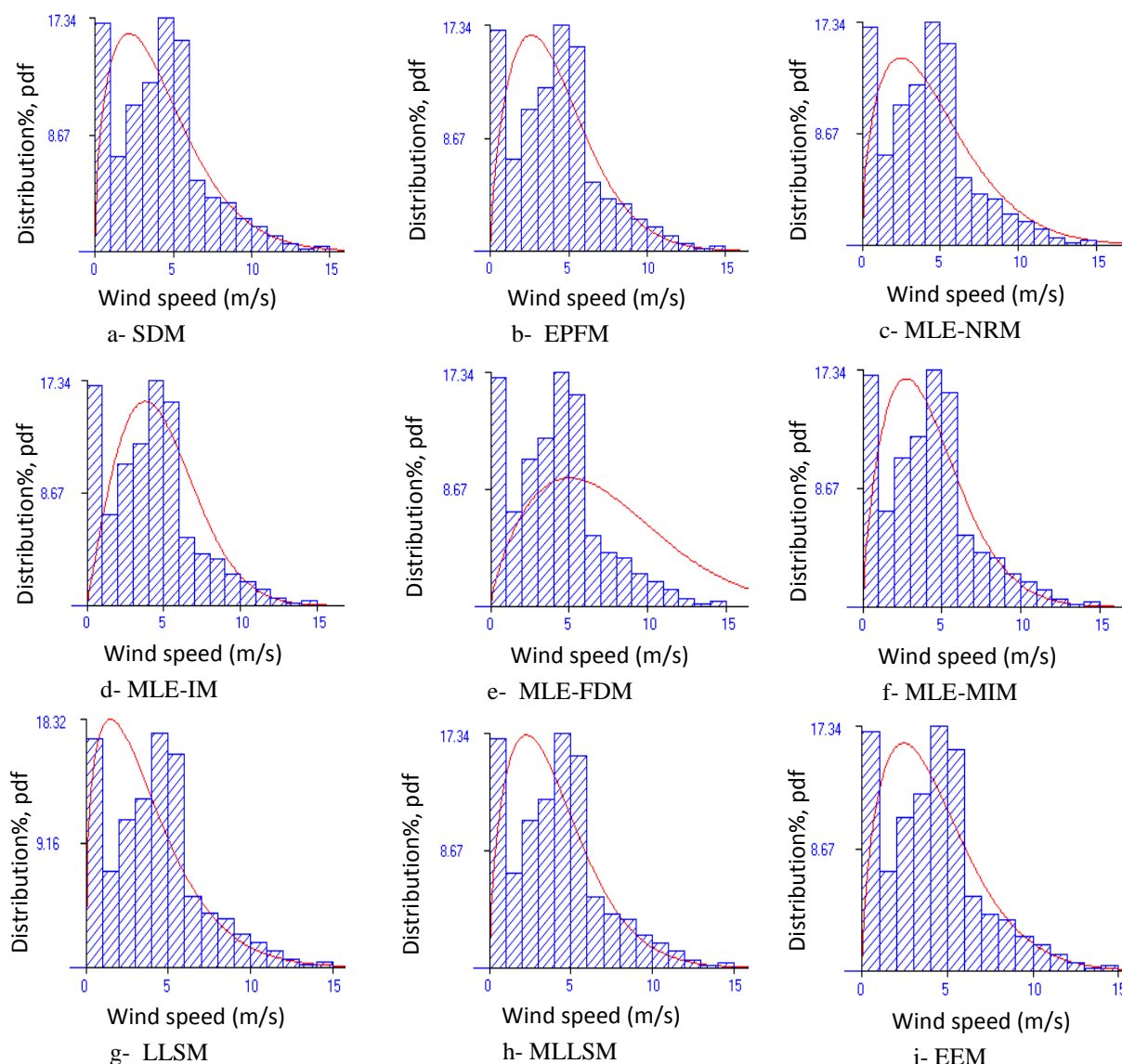
**Fig. 3.15 Estimates of the Weibull parameters by nine methods for Ali Al-karbee, January month-2010.**

The plot of measured histogram and the estimated Weibull distribution functions in one graph (**Fig. 3.16**) excepting for MLE-FDM, reveals the slightly different distribution plots between these techniques.

The curves of cumulative distribution functions having shape and scale parameters aforementioned in **Table 3.10** are plotted in **Fig. 3.17**, in addition to the histogram of the measured data for Ali Al-karbee in January-2010. The theoretical curve of cdfs calculated by MLE-FDM has the lowest graphical fit followed by cdfs calculated using MLE-NRM and MLE-IM; that is because these three methods produce more scale parameter values as shown in **Table 3.10**. As a result, the curves will deviate from the real measurements toward high wind speed values; consequently, the peaks of the curves will decrease.
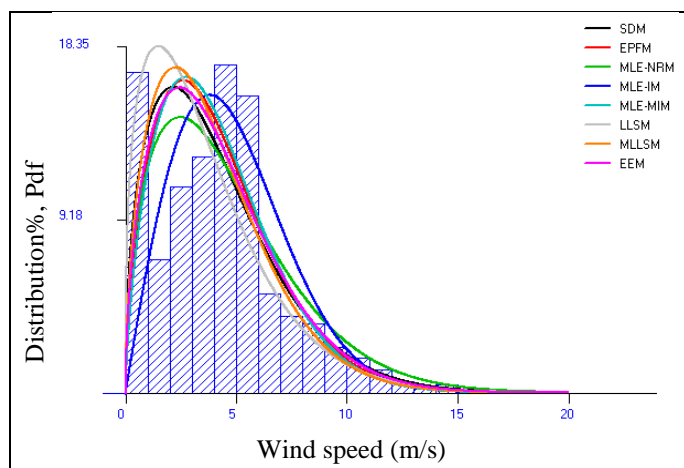
**Fig. 3.16 Comparison between theoretical pdfs and measured wind speed histogram for Ali Al- karbee, January month-2010.**
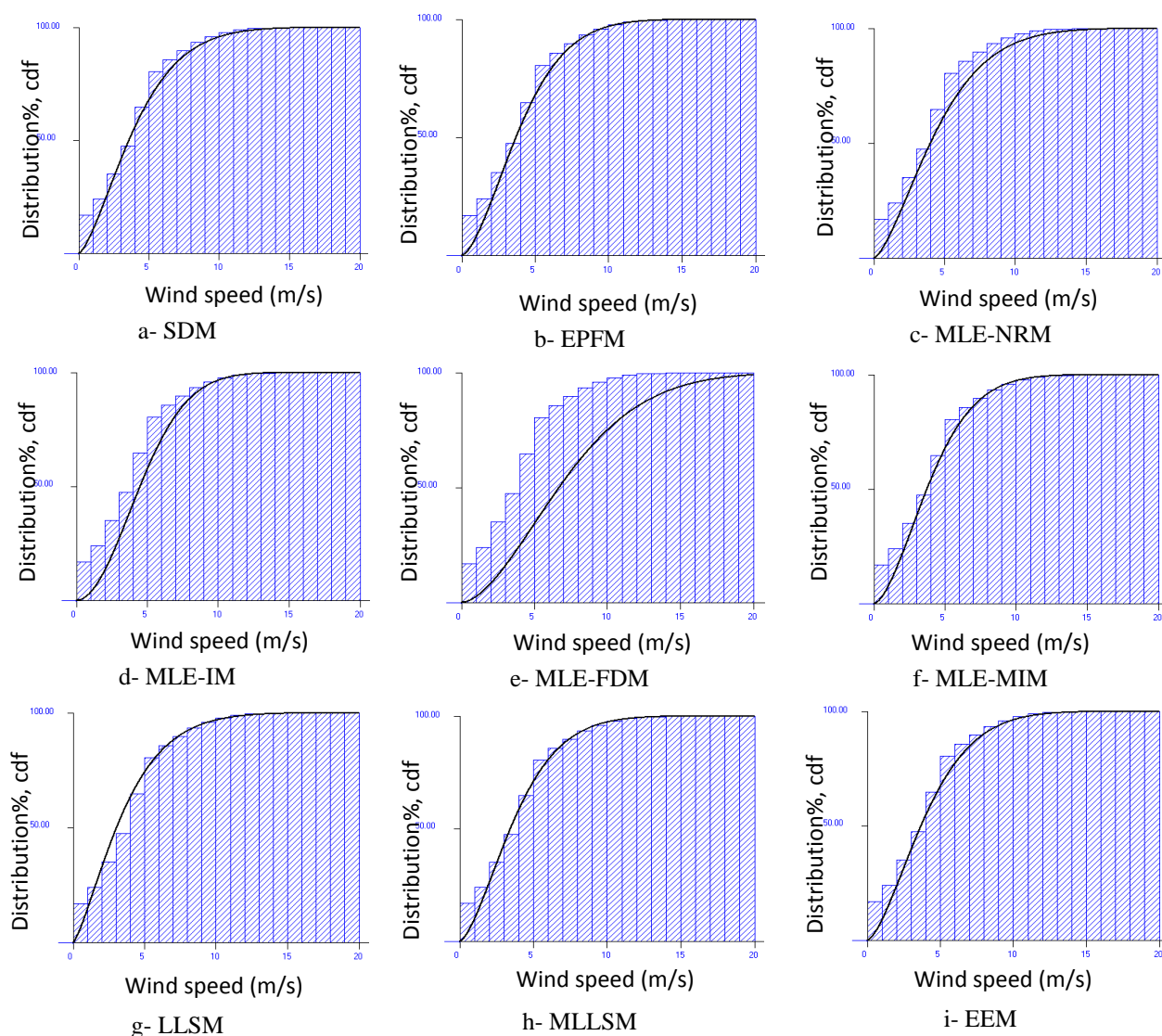


**Fig. 3.17 Estimated cdfs for each method and measured wind speed histogram for Ali Al-karbee, January month-2010.**

For simple comparison between the methods we plot all of them in one figure (**Fig. 3.18**), which illustrates how fit estimation curves having shape and scale parameters listed in **Table 3.10** with the measured wind speed data. Closely fitting of the curves means the more potential of wind power and energy density in the wave of the wind there, **[Sey09]**. Thus, except for MLE-NRM, MLE-IM, and MLE-FDM methods, the rest techniques show good match with the measured wind speed data (histogram).
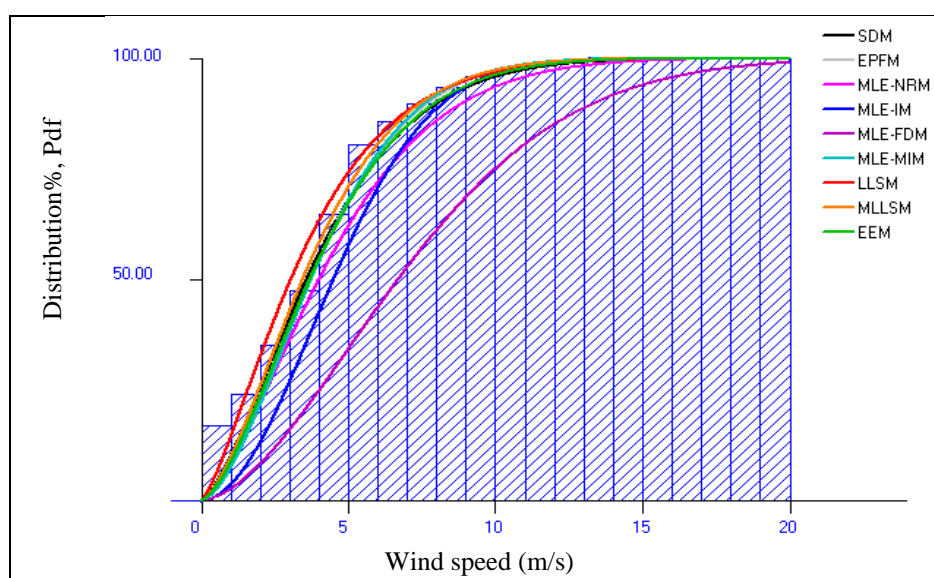


**Fig. 3.18 Comparison between theoretical cdfs and observed wind speed histogram for Ali Al-karbee, January month-2010.**

## 3.7.2 Analytical test- goodness of fit test

As mentioned before, to determine proper theoretical pdf distribution, an approach consisting of four goodness of fit tests (RMSE, $\chi^2$, R, and COD) which have been used in addition to the above graphical test, the results of the analysis are given in **Table 3.11**. The MLE-NRM shows lowest RMSE value and near to the lowest of $\chi^2$, besides highest values of R and COD. As a result, the MLE-NRM is found to be the most accurate one for parameters estimation in term of goodness of fit.

Goodness of fit between the measured and the cdf (estimated by nine methods) values for the January month are listed in **Table 3.12**. Comparing the accuracy test results at 10m height; the LLSM proves to be the best mechanism for estimating cdf's parameters according to the lowest value of RMSE and $\chi^2$; the highest COD and R values.

**Table 3.11:  Comparison of the accuracy test results using the
Weibull pdf at 10m height for Ali Al-karbee January month-2010**

| Method | RMSE | $\chi^2$ | R | COD |
|---|---|---|---|---|
| SDM | 0.038 | 0.17 | 0.62 | 0.38 |
| EPFM | 0.039 | 0.21 | 0.59 | 0.35 |
| MLE-NRM | 0.036 | 0.19 | 0.65 | 0.42 |
| MLE-IM | 0.041 | 0.60 | 0.54 | 0.29 |
| MLE-FDM | 0.054 | 1.09 | 0.21 | 0.04 |
| MLE-MIM | 0.039 | 0.24 | 0.58 | 0.34 |
| LLSM | 0.042 | 0.21 | 0.52 | 0.27 |
| MLLSM | 0.039 | 0.20 | 0.57 | 0.32 |
| EEM | 0.037 | 0.18 | 0.61 | 0.38 |

**Table 3.12:  Comparison of the accuracy test results using the
cdf at 10m height for Ali Al-karbee January month-2010**

| Mechanism | RMSE | $\chi^2$ | R | COD |
|---|---|---|---|---|
| SDM | 0.04 | 0.51 | 0.97 | 0.94 |
| EPFM | 0.05 | 0.86 | 0.96 | 0.93 |
| MLE-NRM | 0.07 | 0.77 | 0.93 | 0.88 |
| MLE-IM | 0.10 | 3.50 | 0.87 | 0.77 |
| MLE-FDM | 0.25 | 6.53 | 0.22 | 0.05 |
| MLE-MIM | 0.05 | 1.00 | 0.96 | 0.93 |
| LLSM | 0.04 | 0.24 | 0.98 | 0.96 |
| MLLSM | 0.04 | 0.56 | 0.97 | 0.95 |
| EEM | 0.05 | 0.70 | 0.97 | 0.94 |

### 3.7.3 Evaluation of mean wind speed and power density

In **Table 3.13** the mean wind speeds ($\bar{v}$) and wind power densities ($PD_w$) are estimated at 10m height for January month, where they are calculated by substituting the estimated Weibull parameters by nine mentioned methods into Weibull based equations **2.21** and **2.104**, respectively (at standard air density). Furthermore, the percentile error of the nine methods in estimating $\bar{v}$ and $PD_w$ are shown in **Table 3.13** (columns 3 and 5) using **Eq. 2.77**, where actual mean wind speed ($\bar{v}_a$) is 4.15 m/sec and actual power density ($PD_A$) is 116.6 W/m$^2$. It could infer that EPFM gives better result for mean wind speed estimation; While EEM gives better result for wind power density calculation.

Errors in calculating the mean wind speeds and power densities using the estimated Weibull distributions in comparison to those using the measured wind speed data are presented in **Fig.s 3.19** and **3.20**, respectively.

**Table 3.13: Comparison of different methods according to the power density and mean speed for January month at 10m height**

| Method | $\bar{v}$ (m/sec) | Error (%) | $PD_w$ (w/m$^2$) | Error (%) |
|--------|--------|--------|--------|--------|
| SDM | 4.16 | 0.24 | 121.26 | 3.99 |
| EPFM | 4.15 | 0 | 105.4 | -9.60 |
| MLE-NRM | 4.62 | 11.3 | 163.4 | 40.1 |
| MLE-IM | 4.79 | 15.4 | 130.6 | 12.0 |
| MLE-FDM | 7.36 | 77.3 | 550.5 | 371 |
| MLE-MIM | 4.16 | 0.24 | 101.7 | -12.7 |
| LLSM | 3.66 | -11.8 | 96.4 | -17.3 |
| MLLSM | 3.93 | -5.3 | 96.1 | -17.5 |
| EEM | 4.20 | 1.20 | 116.6 | 0 |
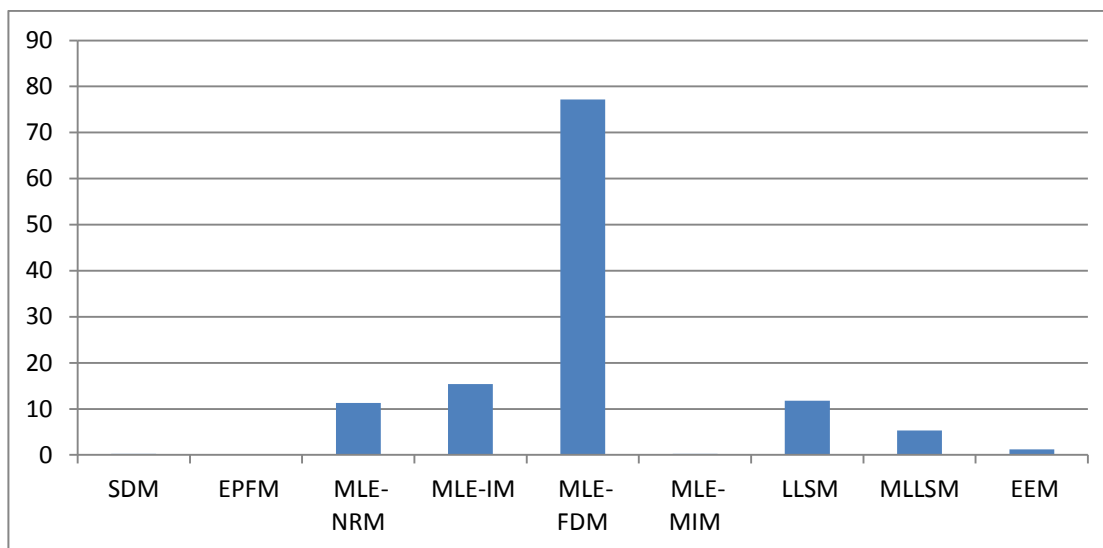
**Fig. 3.19 Error values obtained from calculating the mean speed by different methods**
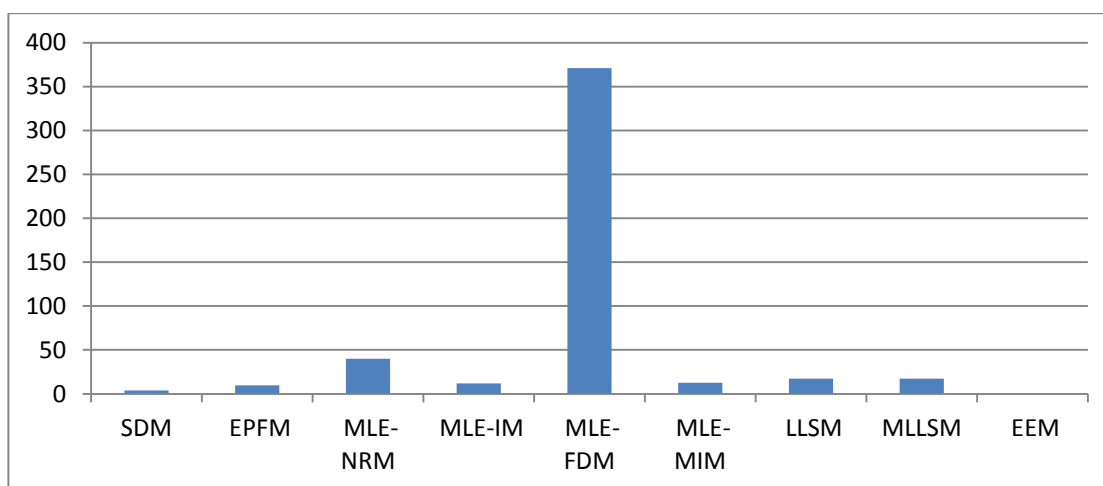


**Fig. 3.20 Error values obtained from calculating the power density by different methods**

Finally, the summary results of Ali Al-karbee for January month are presented in **Table 3.14**. Four superior methods are listed in this table to compare their performance simply. It is obvious that each of EPFM, MLE-NRM, LLSM, and EEM shows reasonable fit with the measured data. Almost they equal in graphical test. On the other hand, the EEM is found to be the most accurate method according to power density estimation, therefore you could say that EEM gives best result for parameters estimation at Ali Al-karbee location.

**Table 3.14: Summary of the previous results**

| | Graphical Test | | Numerical test | | Error percentage | |
|---|---|---|---|---|---|---|
| Method | pdf | cdf | pdf | cdf | $v_m$ | P.D. |
| EPFM | ✓ | ✓ | ✗ | ✗ | ✓ | ✗ |
| MLE-NRM | ✗ | ✗ | ✓ | ✗ | ✗ | ✗ |
| LLSM | ✓ | ✓ | ✗ | ✓ | ✗ | ✗ |
| EEM | ✓ | ✓ | ✗ | ✗ | ✗ | ✓ |

## 3.8 Wind Site Characteristics - Weibull Based

Previously, we analyzed the performance of nine methods in estimating Weibull parameters for wind energy application. The results prove that EEM is the most efficient technique for parameters estimation; therefore its results will be used in all subsequent calculations.

This section is dedicated for studying wind characteristics at Ali Al-karbee site for one year (2010) and 10m high.

### 3.8.1 Analysis of results of the wind speed

**Tables 3.15** shows the results of applying different statistics (mentioned in **sections 2.11** and **2.12**) related to wind speed for one complete year (2010). The characteristics of the wind speed at 10m height above the surface are described based on Weibull parameters. The parameters are concluded from measured data after applying the EEM.

Following points are observed:

- The annual mean wind speed recorded shows the suitability of the wind resources at this site for micro and small wind energy systems.
- The mean and the median are unequal, then distribution appears to be asymmetric
- Since the mean wind speed is bigger than the median, the distribution is skewed to the right. This thing could also be inferred from the positive sign of $3^{rd}$ raw moment.
- The skewness of the wind speed data is positive, indicating that the distribution is asymmetric with tail extending toward positive values.
- Kurtosis has positive value which indicates that we have peaked distribution.

- The maximum frequency is 0.20 at wind speed of 0.8 m/sec.
- Conventional and Weibull based mean wind speeds are matched.

**Table 3.15: Descriptive statistics of wind data measured
at Ali Al-karbee (2010)**

| Characteristic | Value |
|---|---|
| $c$ (m/sec) | 3.75 |
| $k$ | 1.19 |
| Mean speed (m/sec) | 3.53 |
| Median speed (m/sec) | 2.75 |
| Modal speed (m/sec) | 0.80 |
| Max frequency | 0.20 |
| Variance (m/sec)$^2$ | 8.90 |
| The Std. of wind velocity (m/sec) | 2.98 |
| Coefficient of variation | 3.17 |
| $1^{st}$ raw moment (Mean speed, Weibull based) (m/sec) | 3.53 |
| $2^{nd}$ raw moment (m/sec)$^2$ - measure of Spread | 21.3 |
| $3^{rd}$ raw moment (m/sec)$^3$- measure of Skewness | 179.3 |
| $4^{th}$ raw moment (m/sec)$^4$- measure of Kurtosis (Peakedness) | 1,901.8 |

## 3.8.2 Analysis of results of the wind sectors

Depending on the wind direction, it is possible to distribute data on 12 sectors; then, data in each sector could be made in a histogram form depending on the wind speed values (see **Fig. 3.21**). Each sector has its corresponding histogram graph binning at 1m/sec. Moreover, pdfs estimated by EEM are plotted in red lines for each histogram.

Now, after finding $c$ and $k$ for wind regime in all sectors it is possible to find mean wind speeds and power densities in addition to the frequency of wind speed occurrence for each sector (**Table 3.16**). The total mean wind speed and power production for one year at Ali Al-karbee site are given in the bottom of the table, after summing the multiplication frequency of occurrence percentages with mean wind speed or with power density for each sector. The output result may not be exact the same as the production based on the Weibull $c$ and $k$ parameters of the total wind distribution; however, in most cases the difference should be small.
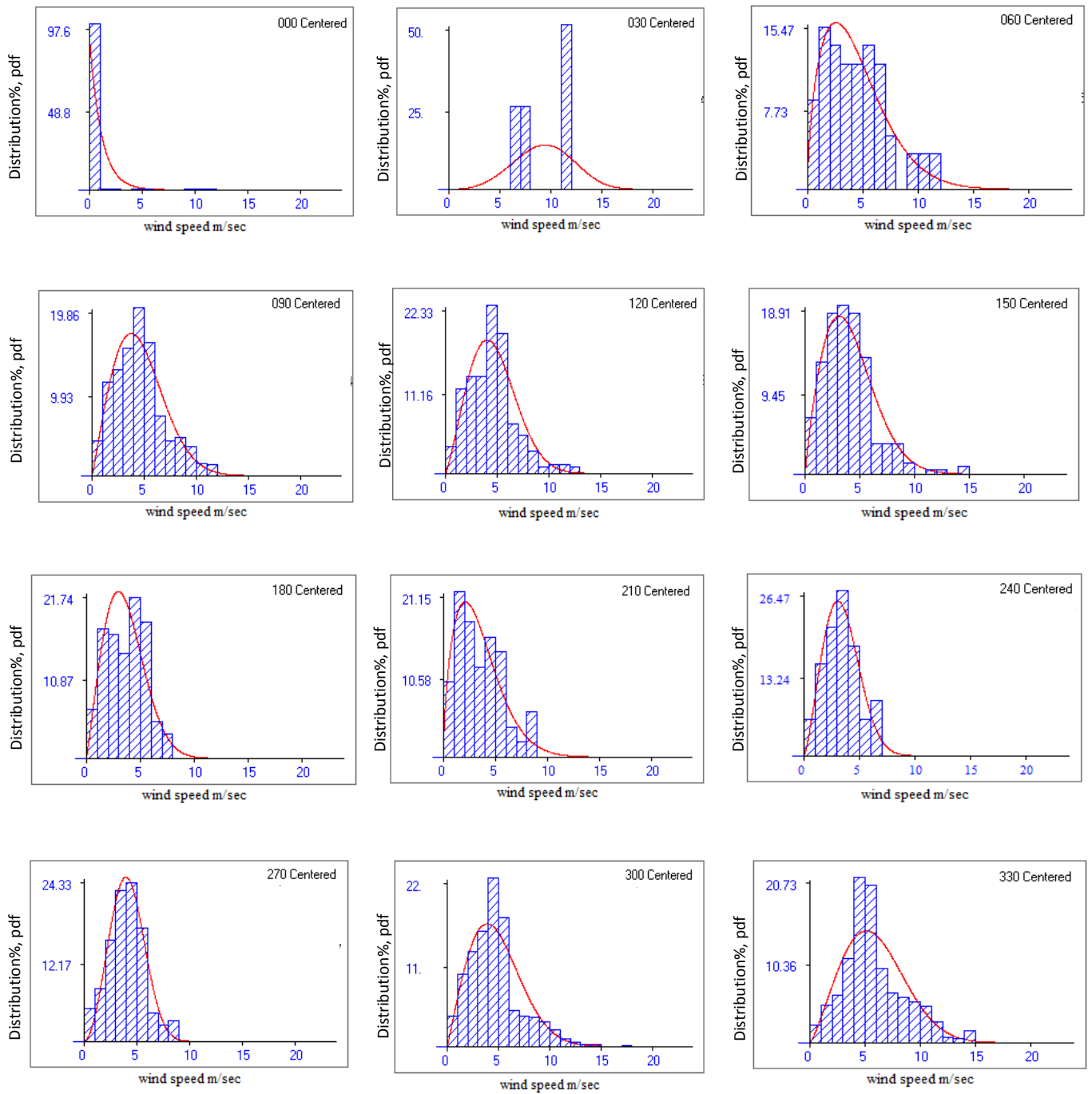
**Fig. 3.21. Probability plot and wind speed histogram for 12 different sectors.**

**Table 3.16:  Frequency percent, Weibull fitting Parameters, predicted mean and power density in 12 sectors**

| Sector (center) | Frequency % | $c$ (m/sec) | $K$ | $\bar{v}$_s | $PD_{w-s}$ (W/m²) | Col.2×Col.6 |
|---|---|---|---|---|---|---|
| 0 | 20.71 | 1.11 | 1.00 | 1.12 | 5.140 | 106.4 |
| 30 | 6.84E-02 | 10.3 | 3.60 | 9.24 | 634.2 | 43.4 |
| 60 | 1.02 | 4.88 | 1.57 | 4.39 | 131.8 | 134.4 |
| 90 | 9.48 | 5.19 | 2.05 | 4.60 | 111.3 | 1055.1 |
| 120 | 7.36 | 5.24 | 2.24 | 4.63 | 105.5 | 776.48 |
| 150 | 4.07 | 4.66 | 1.88 | 4.13 | 88.47 | 360 |
| 180 | 2.12 | 4.04 | 2.08 | 3.58 | 51.97 | 110.1 |
| 210 | 0.89 | 3.83 | 1.60 | 3.44 | 61.82 | 55 |
| 240 | 0.58 | 3.87 | 2.33 | 3.42 | 41.00 | 23.78 |
| 270 | 2.84 | 4.60 | 2.83 | 4.09 | 61.47 | 174.5 |
| 300 | 31.98 | 5.42 | 2.04 | 4.80 | 127.5 | 4077.4 |
| 330 | 18.83 | 6.64 | 2.25 | 5.87 | 213.9 | 4027.7 |
| Total $(PD_w, \bar{v}) = \frac{1}{100}\sum_{s=1}^{12} freq\_s\% \cdot (PD_{w\_s}, \bar{v}\_s)$ | | | | $v_m = 4.1$ m/sec | | $PD_w = 109.4$ W/m² |

## 3.8.3 Analysis of results of the wind potential power

The product of percentage of time we receive wind from a particular direction and Weibull based power density form **Eq. 2.104**, will help in identifying the energy supplied by different directions. **Fig. 3.22** shows the energy rose for Ali Al-karbee site (2010) at 10m height. Wind energy in this site is distributed mainly at northwestern direction, specifically sectors 300 and 330 and sectors 90 and 120. The energy available at the northwestern direction approaches 74% of energy site while southeastern direction provides about 17% of energy site.
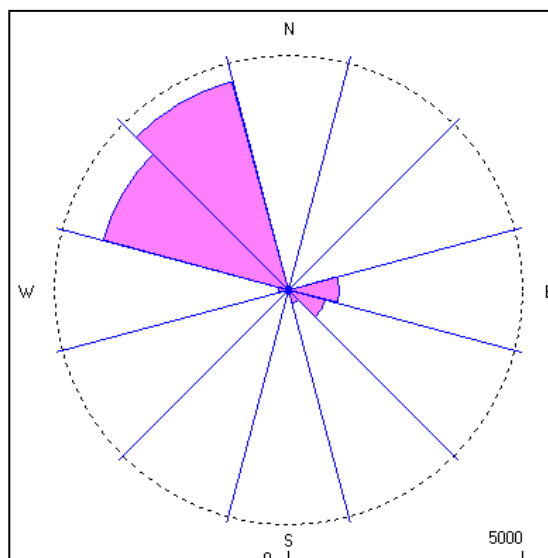
**Fig. 3.22 Annual energy rose for Ali Al-karbee 2010.**

**Table 3.16** column7 gives the contribution of power density percent in each sector. While **Table 3.17** shows how much the estimated Weibull based power density using EEM agrees with one calculated using cube wind speed of measured data (**Eq. 2.103),** and actual power density frequency dependent (**Eq. 2.107)**. The speed which gives maximum power density is equal to 8.5m/sec and plotted at the peak of the pdf (see **Fig. 3.23**), In **Fig. 3.23** the power density is plotted as a function of wind speed using estimated Weibull parameters.

**Table 3.17 Actual power and energy potential for Ali Al-karbee Site.**

| Site properties | Value |
|---|---|
| $WPD_w$ (W/m$^2$) at 10m height (cube measured data) | 109.51 |
| $PD_A$ (W/m$^2$) at 10m height (frequency dependent) | 105.53 |
| $PD_w$ from estimated $c$ & $k$ parameters at 10m height (W/m$^2$) | 109.52 |
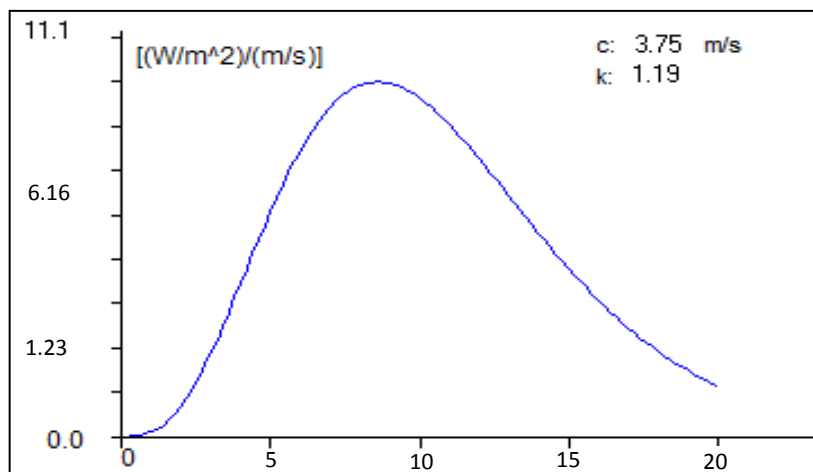
**Fig. 3.23 Power density vs. wind speed, Speed of maximum power density is 8.5 m/s.**

## 3.9 Monthly Wind Site Characteristics - Weibull Based

This section is dedicated for studying monthly wind characteristics at Ali Al-karbee, the calculations using Weibull parameters predicted by EEM.

### 3.9.1 Monthly of analysis of wind speed data

**Table 3.18** shows the descriptive statistics (introduced in **Sections 2.11, and 2.12**) of wind speed, which reveal obvious variation in monthly periods. These statistics could be summarized as follows:

iv.   Positive skewness coefficients mean distributions one with tails extended toward positive values.

v.   More negative kurtosis coefficients mean more flatness distributions.

vi.   The two significant wind speeds for wind energy estimation (the most probable wind speed $v_f$ and the wind speed carrying maximum energy $v_{me}$) are given in this table.

vii.   A median speed has its highest value in the summer season, particularly in July while its lowest value appears in the winter season, particularly in November.

viii.   From standard deviations values one can conclude that the deviation of wind speeds from its mean value is increased in summer and reaches its maximum value in July. Which it is evidence of increasing in wind speed values, that in turn decreases the turbulence at this time

ix.   The coefficients of variation suggest that variability in wind speed data in November and December is more than in other months.

**Table 3.18: Monthly brief analysis of the wind speed characteristics calculated by EEM at 10 meter height.**

| Month | Skewness | Kurtosis | $v_f$ (m/s) | $v_{me}$ (m/sec) | Mean (m/s) | Median (m/s) | Std. (m/sec) | C. V. (%) |
|-------|----------|----------|-------------|------------------|------------|--------------|--------------|-----------|
| Jan | 0.646 | 0.581 | 2.42 | 7.92 | 4.20 | 3.69 | 2.75 | 65.6 |
| Feb | 0.276 | -0.456 | 0.42 | 7.73 | 2.97 | 2.23 | 2.66 | 89.4 |
| Mar | 0.547 | 0.562 | 2.52 | 7.61 | 4.12 | 3.67 | 2.63 | 63.7 |
| Apr | 0.940 | 0.948 | 0.58 | 8.99 | 3.53 | 2.68 | 3.10 | 87.9 |
| May | 0.506 | -0.030 | 2.43 | 9.26 | 4.70 | 4.05 | 3.23 | 68.8 |
| Jun | 0.373 | -0.414 | 3.16 | 9.39 | 5.12 | 4.56 | 3.24 | 63.4 |
| Jul | 0.424 | -0.094 | 3.73 | 9.69 | 5.52 | 5.00 | 3.31 | 60.1 |
| Aug | 0.072 | -1.200 | 0.07 | 6.50 | 2.27 | 1.59 | 2.18 | 97.1 |
| Sep | 0.415 | -0.310 | 0.91 | 8.28 | 3.50 | 2.76 | 2.88 | 82.4 |
| Oct | 0.084 | -0.498 | 2.12 | 6.85 | 3.64 | 3.21 | 2.37 | 65.2 |
| Nov | 0.446 | -0.824 | 0 | 5.82 | 1.93 | 1.34 | 1.94 | 100 |
| Dec | 0.607 | -0.237 | 0 | 6.69 | 2.22 | 1.54 | 2.23 | 100 |

**Fig. 3.24** demonstrates monthly mean wind speed values throughout the year obtained from Weibull probability model at a height of 10 m for Ali Al-karbee station. The mean speed in July is the maximum, while the one in November is the minimum, which gives a meaning that wind in our location is seasonable.
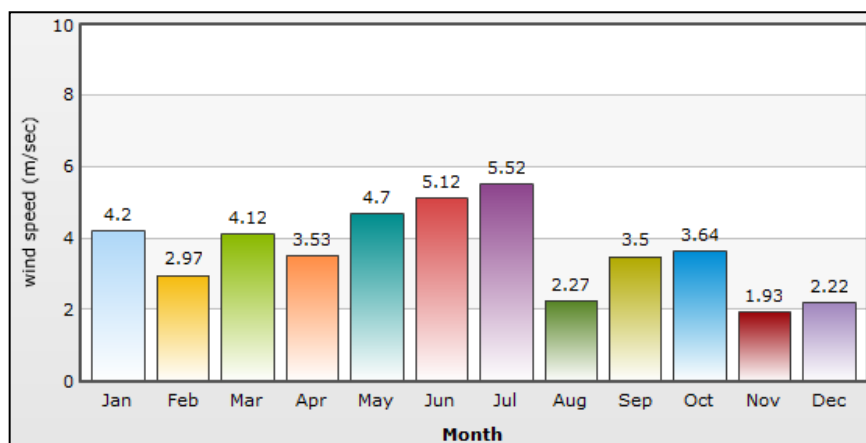


**Fig. 3.24 Monthly mean wind speed variations throughout the year 2010 predicted by Weibull pdf.**

119

The monthly estimated power density for our station is plotted in **Fig. 3.25**. Wind power density is calculated using predicted Weibull parameters (*c* & *k*) by EEM. It is obvious from this **Fig.** that power density is increased in summer months and reaches it highest value in July 232.7 W/m$^2$. While lowest value is shown at November 26.8 W/m$^2$. Thus, this area will have maximum production in summer month (except August), and this is an advantage for the construction site of the wind farm.
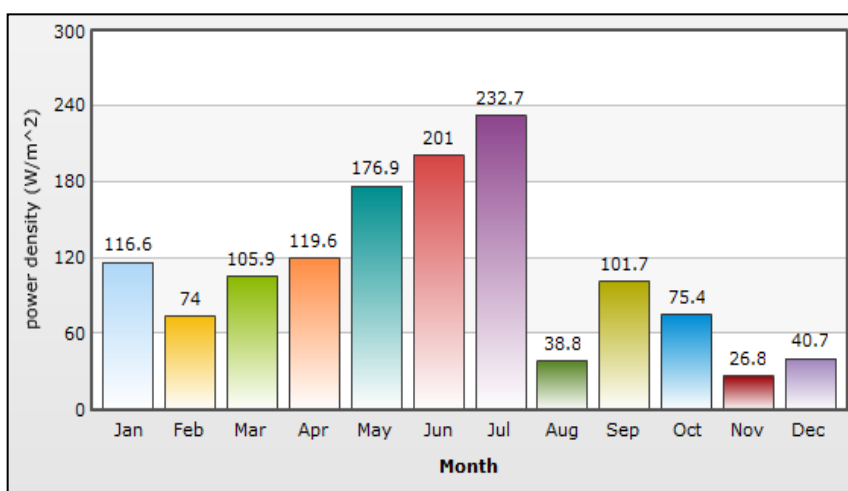


**Fig. 3.25 Comparison between the monthly power density variation for the year 2010 predicted by Weibull pdf.**

### 3.9.2 Monthly analysis of results of pdf and cdf

**Fig. 3.26** shows monthly Weibull pdf plotted against the histogram of wind speed data. It has been found that the estimated curve is trying to keep up the variations in wind data, and crest of pdf is close to crest of measured wind data. The monthly Weibull probability density and cumulative distributions of the measured data for the whole year of the location is shown in **Fig. 3.27** and **Fig. 3.28** respectively. The peak of the density function frequencies of the location skewed towards the higher values of the mean wind speed. From **Fig. 3.27** the most frequents wind speed of the location were found to vary from about 1.93m/s in the month of November with peak frequency of approximately 20% to 5.52m/s expected in the month of July with approximate peak frequency of 11%. Any point at curve in **Fig. 3.28** represents the fraction of time (or probability) that the wind speed is equal to or lower than corresponding wind speed value at x-axis.
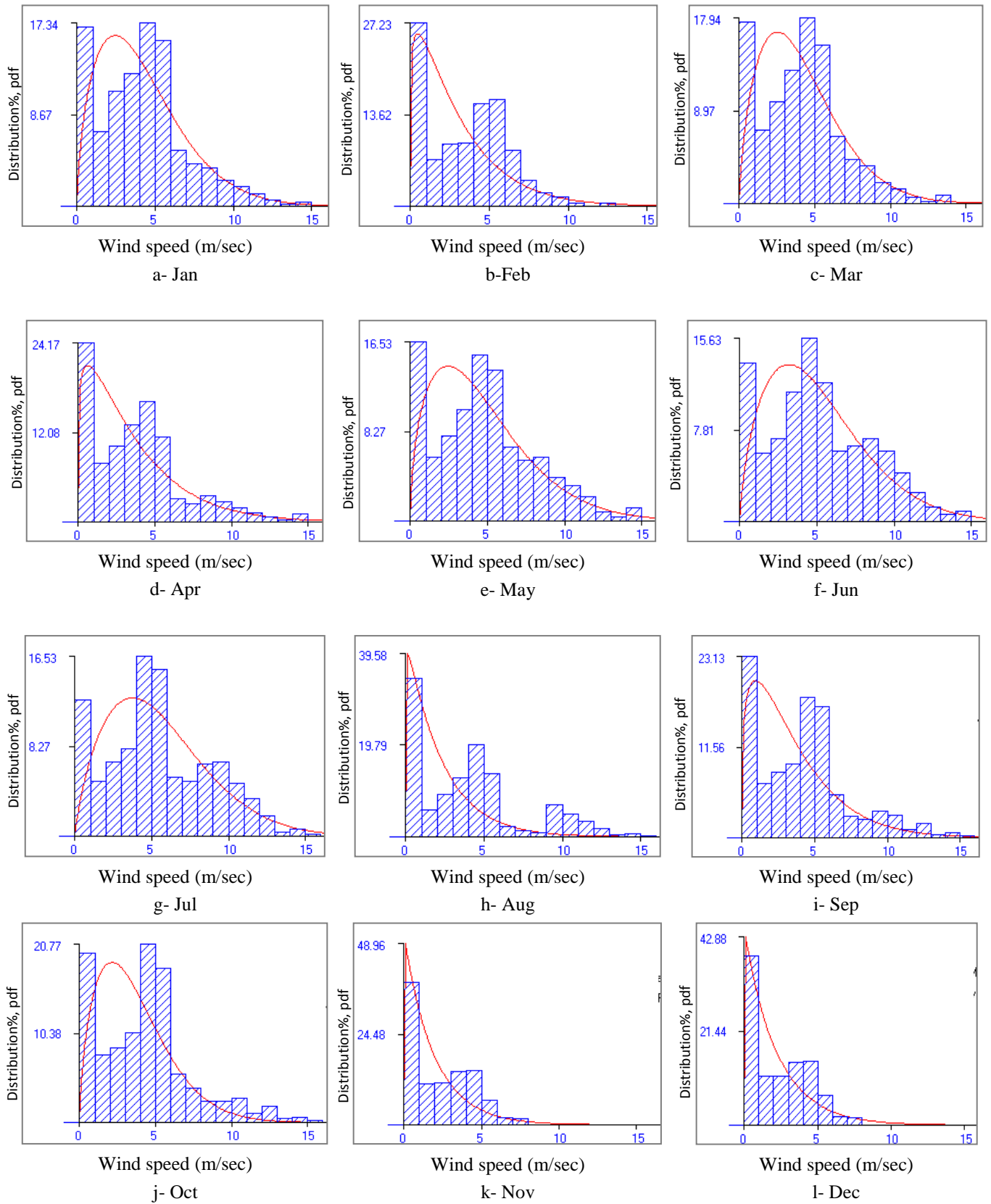
**Fig. 3.26 Monthly pdf and wind speed histogram.**

121
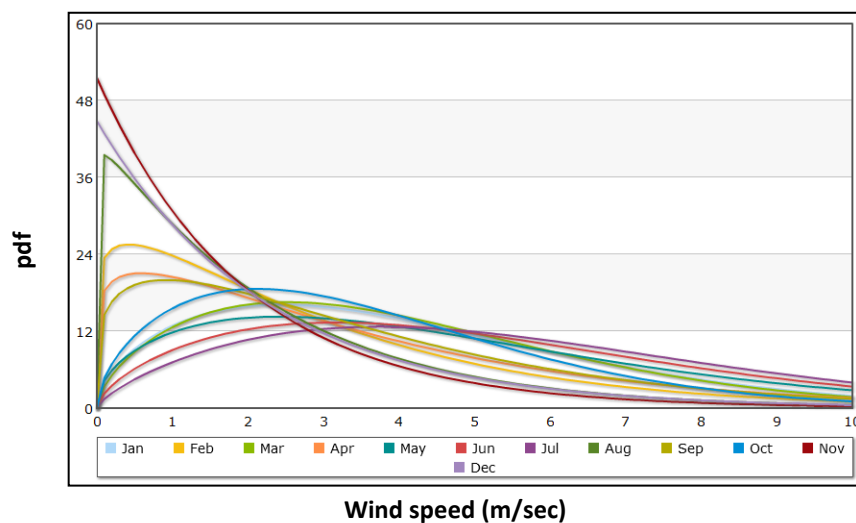
**Fig. 3.27 Monthly pdfs forAli Al-karbee 2010 (*c* & *k* computed by EEM).**
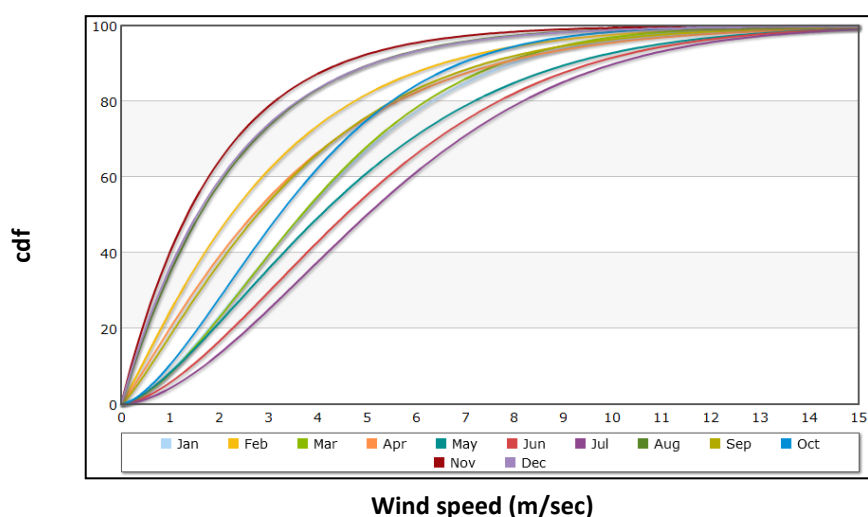


**Fig. 3.28 Monthly cdfs forAli Al-karbee 2010 (*c* & *k* computed by EEM).**

From **Figs. 3.27** and **3.28**, in it is obvious that the increment in Weibull parameters causes shifting in pdf and cdf toward right axis. As a result, both mean and median wind speeds will increase also.

### 3.9.3 Monthly analysis of Weibull parameters

The statistical parameters for fitness evaluation of pdf are presented in **Figs. 3.29** and **3.30**. These **Figs.** show the monthly Weibull shape and scale parameters calculated by using EEM. Since the scale factor directly relates with the average wind speed, it may be concluded from **Fig. 3.29** that mean wind speed is higher in July than in other months.
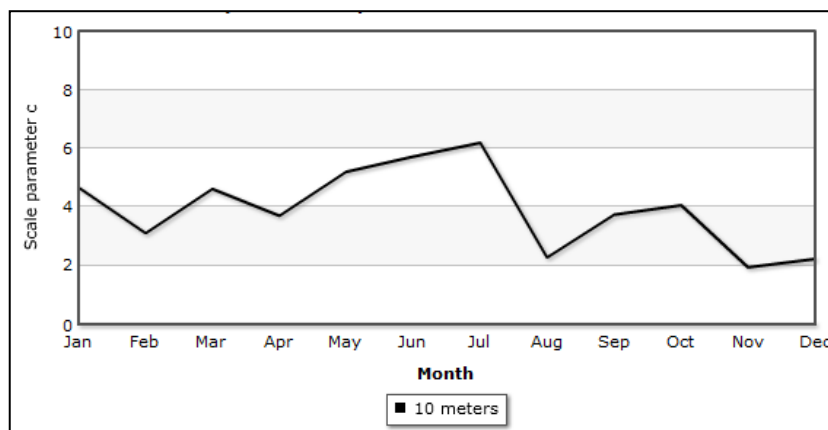
**Fig. 3.29 Monthly variation of parameter *c* of the Weibull distribution.**

**Fig. 3.30** indicate that the monthly variation of parameter *k* is similar to that in parameter *c*.
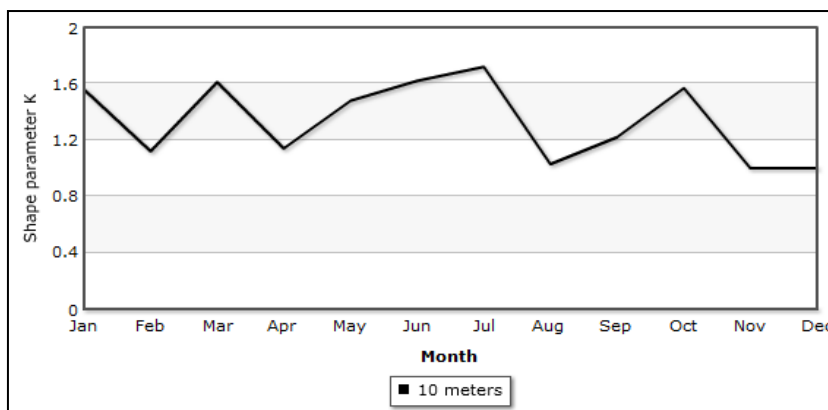


**Fig. 3.30 Monthly variation of parameter *k* of the Weibull distribution.**

Since there an inverse relation between coefficient of variation and *k* according to **Eq. (3.1), [Win08]**:

$$k = (\frac{0.9}{C.V.})^{1.09} \qquad (3.1)$$

thus, any increasing or decreasing in C.V. (**Table 3.18**) will coincide with decrease or increase in value of *k* respectively.

**3.9.4 Analysis of results of the wind potential power (monthly based)**

     **Fig. 3.31** shows the energy roses during the whole year of 2010 at Ali Al-karbee site. It is obvious from this figure that the energy from the northwestern is available throughout the year in spite of decreases in some months, such as the cold months. Also it can be seen that energy comes from southeastern direction is increased in cold months such as Janury, February, and March.
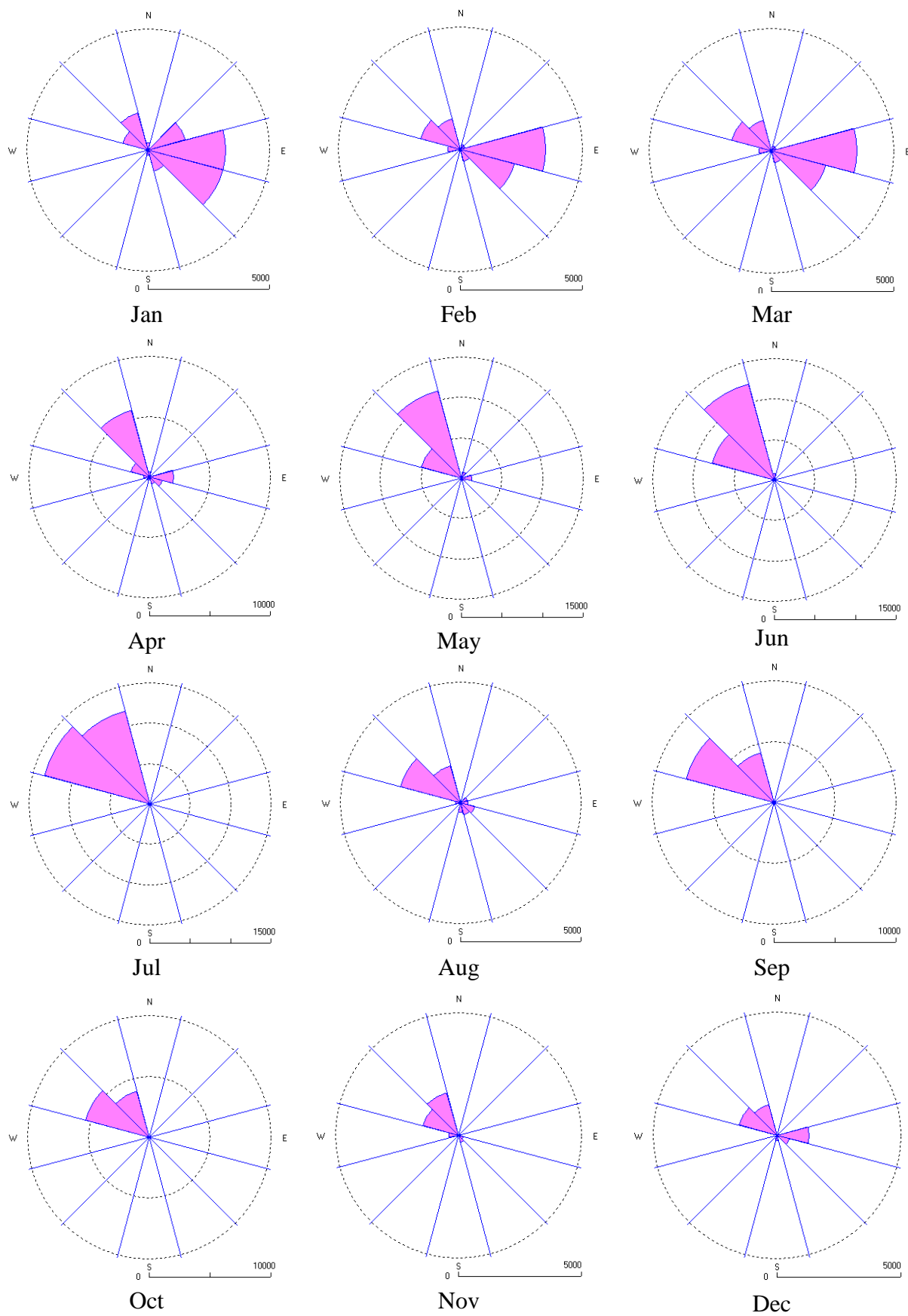
**Fig. 3.31 Monthly energy wind roses for Ali Al-karbee 2010.**

124

## 3.10 Turbine –Weibull Model

The characteristics of the wind speed are different from site to site. Also, wind turbine generator, WTG characteristics are different from one to another. Pairing between the performance parameters of wind speed characteristics of each site and the WTG can increase the wind energy captured and reduce the cost of the generated energy. The main characteristics of wind speed in a certain site are the shape parameter, $k$ and the scale parameter, $c$ that can be obtained from Weibull distribution statistical technique (as we done before). Also, the main performance parameters of the WTG are, cut-in, cut-out and rated wind speeds and rated power of the WTG.

### 3.10.1 Specification of the chosen wind turbine

The SUZLON S64-950 is our chosen wind turbine. The machine produces a nominal output power of 1.25 MW. With a rotor diameter of 71m, it can be operated at wind speeds between 2m/s and 25m/s. **Table 3.19** shows the main specifications of the chosen turbine

**Table 3.19: Wind turbine technical specification**

| SUZLON S64-950 | | |
|---|---|---|
| **Number of blades** | 3 |  |
| **Rotor diameter** | 64 m | |
| **Swept area** | 3218 m$^2$ | |
| **Blade material** | GFRP | |
| **Rotational speed at rated power** | 20.62 rpm | |
| **Cut-in wind speed** | 3 m/sec | |
| **Cut-out wind speed** | 25 m/sec | |
| **Rated wind speed** | 11 m/sec | |
| **Rated power** | 950 KW | |
| **Hub heights** | 57 m | |

### 3.10.2 Wind resource extrapolation

Previously, the Weibull parameters have been estimated at 10m height. Now, since the hub height of the chosen turbine is 57m, thus it is necessary to extrapolate each wind speed to this height.

**Figs. 3.32** and **3.33** show comparisons between Weibull shape and scale parameters (*c, k*) calculated at 10m height and those estimated by EEM after extrapolate all wind speeds to new height 57m, respectively. These factors have been extrapolated to 57m height using power law (**Eq. 2.81)** for each month in the year 2010 (where $\alpha = 0.14$).

The monthly extrapolation of parameters $k$ at new height (57m) remains constant in comparison with the values that measured at 10m (see **Fig. 3.32**). A lower value of $k$ indicates a greater deviation from the mean wind speed while a higher value of $k$ indicates a small variation from the mean wind speed and the probability curve becomes more peaked. That is because $k$ has invers proportionality with standard deviation of the distribution according to **Eq. 3.2, [Win08]**.

$$k = (\frac{0.9}{\frac{\sigma}{\overline{v}}})^{1.09}$$
(3.2)
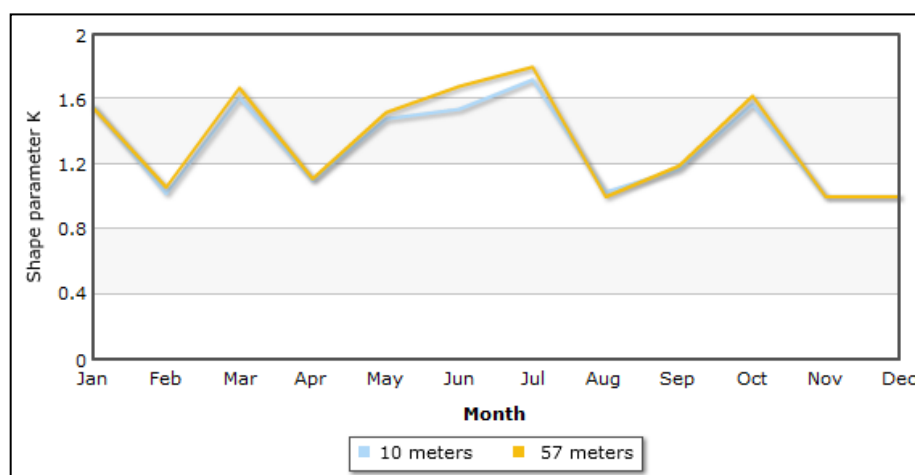


**Fig. 3.32 Comparison between the values of the monthly Weibull shape parameters at 10 and 57m hub heights.**

At a 10m height, the wind site has scale parameter $c$ values ranging between 2.23 to 6.19 using the EEM. While at 57m height, the scale parameter has values ranges between 2.49 to 8.07 at 57m, as shown in **Fig. 3.33** below. Since the

mean wind speed has a direct proportion with *c* value (**Eq. 2.21**), thus the wind speed will increase with heights also. Accordingly, the site  has  gentle wind moving towards  the moderate  wind  range  in  the  month  of  July.
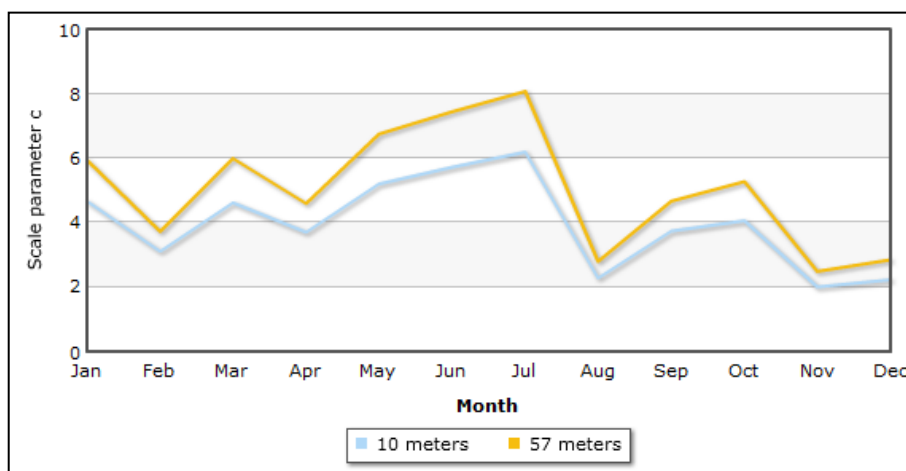


**Fig. 3.33 Comparison between the values of the monthly Weibull scale parameters at 10m and 57m heights.**

After computing *c* and *k* at new height (57m), then we could calculate new wind potential power density at this height using **Eq. 2.104**. **Fig. 3.34** displays the monthly variation in the potential power densities, based on the Weibull function at 10m, as well as extrapolated potential power density at 57m. This figure shows the extent of the increase in the potential power density at the new height compared with the original height.
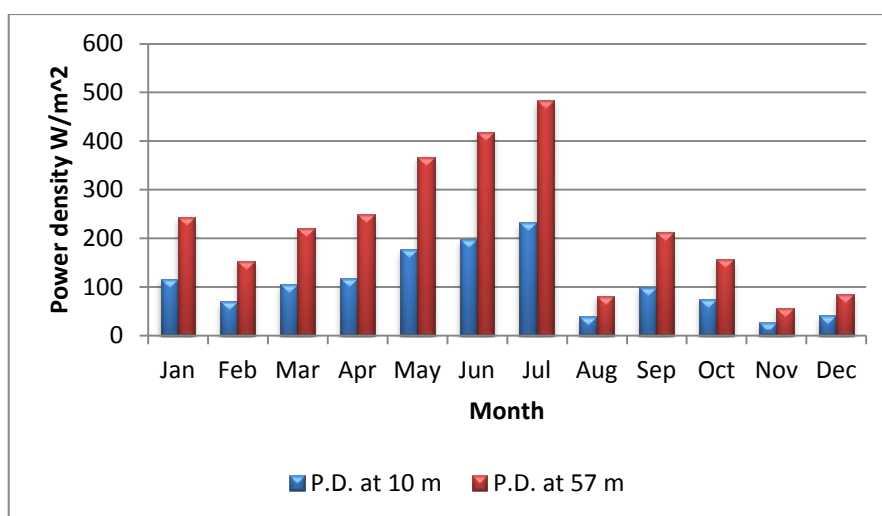


**Fig. 3.34 Extrapolated of monthly *PD_w* from 10m to 57m at Ali Al-karbee site 2010.**

The monthly values of the Weibull parameters (*c* and *k*) at 57m above the ground level are estimated using EEM, after extrapolated all wind speeds in each month to 57m using power law, and the results are listed in **Table 3.20**. In addition to the monthly extrapolated Weibull parameters using **Eqs. 2.86** and **2.87** are also shown in this table.

**Table 3.20: Monthly extrapolated Weibull parameters and power density for Ali Al-karbee station (2010) at 57m.**

| Parameters | Using Power law | | | Extrapolate Weibull parameters | | |
|---|---|---|---|---|---|---|
| | $c$ (m/sec) | $k$ | P.D. (w/m$^2$) | $c$ (m/sec) | $k$ | P.D. (w/m$^2$) |
| January | 5.94 | 1.55 | 242.26 | 7.55 | 1.84 | 386 |
| February | 3.72 | 1.06 | 153.72 | 5.39 | 1.32 | 250 |
| March | 5.99 | 1.67 | 220.04 | 7.46 | 1.9 | 358 |
| April | 4.59 | 1.11 | 248.42 | 6.24 | 1.34 | 375 |
| May | 6.75 | 1.52 | 367.45 | 8.25 | 1.74 | 542 |
| June | 7.44 | 1.68 | 417.51 | 8.92 | 1.91 | 608 |
| July | 8.07 | 1.8 | 483.5 | 9.52 | 2.03 | 692 |
| August | 2.80 | 1.0 | 80.78 | 4.18 | 1.21 | 145 |
| September | 4.66 | 1.19 | 211.41 | 6.28 | 1.44 | 322 |
| October | 5.27 | 1.62 | 156.77 | 6.72 | 1.85 | 270 |
| November | 2.49 | 1 | 56.46 | 4.23 | 1.18 | 161 |
| December | 2.85 | 1 | 85.11 | 4.67 | 1.29 | 172 |
| 1- $PD_w$ (estimated by power law) | | | 226.9 | 4- $PD_w$(after extrapolat $c$ & $k$) | | 356.7 |
| 2- $PD$ (source data) | | | 227.4 | | | |
| 3- $PD_w$ (fitted distribution) | | | 220.0 | | | |

At the end of the table power density is calculated in four ways; first, estimate Weibull parameters (using EEM) after extrapolating the wind speed for each month to 57m height (using power law), then calculating $PD_w$ average value for the year 2010 after calculating it for each month, the result is 226.9 w/m$^2$. Second way depends on raises wind speed data from 10m to 57m, then

calculates the power density for each new wind speed, the average of these values is the source power density equal to 227.4 w/m$^2$. The third way is achieved by fitting the distribution yielding from 2$^{nd}$ way, the estimation process gives $c$=4.61m/sec, $k$=1.16, $\sigma$ =3.83, $\bar{v}$ =4.4 m/sec, $PD_w$ =220 w/m$^2$. The $PD_w$ calculated by the 4$^{th}$ way is achieved by extrapolating $c$ and $k$ using **Eqs 2.86-2.88** (gives 356.7w/m$^2$).

Its obvious that the first three ways give near results, while the 4$^{th}$ one is too much higher than others. This means that **Eqs 2.86-2.88** give an over estimate power density.

## 3.11  Wind Turbine Performance Results

The performance of wind turbine will be studied through output power and capacity factor, as follows:

### 3.11.1 Analysis of output power

**Table 3.21** shows the output properties of the chosen wind turbine if it is installed at Ali Al-karbee site. This table gives the maximum output power or mechanical output power mentioned by **Eq. 2.91**, where $c_p$ (power coefficient) given from manufacture power curve = 0.44, annual mean wind speed at 10m = 5.6336 m/sec (for root mean cube), annual mean wind speed at 57m = 7.188 (for root mean cube), air density =1.225 kg/m$^3$, and rotor diameter = 64m. Also, the number of wind turbine generation power per a day and a year is given in this table, where $c$ and $k$ are found by using EEM for this site. In addition to number of wind turbine generation hours for different wind speeds with the help of cumulative distribution function (see **section 2.11**). Finely, capacity factor at 10m height for our site is computed using **Eq. 2.93** is equal to $C_F = 15\%$.

All outputs are recalculated again at wind turbine hub height. Wind turbine mechanical power is increased about 48% from ground level. While, capacity factor becomes $C_F = 22\%$ after extrapolating wind speed to 57m.

**Fig. 3.35** shows the results of calculating the power curve from SUZLON S64-950 turbine versus a range of mean wind speeds variations after installing the turbine at Ali Al-karbee site. For comparison, **Fig. 3.35** also shows theoretical power curve coming from manufacturer of the turbine at the same graph. It can be seen that the output power in a variable wind can be significantly different

from the steady wind output. At the lower mean wind speeds of around 1 to 6 m/sec, the output power is the same as theoretical power curve whereas at the mean speed of more than 6 m/sec, the output power is less than the theoretical one. These proportions are rather typical of many wind turbines.

**Table 3.21: Turbine output results.**

| Properties | Values 10m | Values 57m |
|---|---|---|
| Scale factor  $c$, (m/sec) | 3.75 | 4.61 |
| Shape factor $k$ | 1.19 | 1.16 |
| $P_{T\_Max}$ (Watt) (turbine mechanical power) | 155061 | 322083 |
| No. of generation hours  per a day | 11 | 13 |
| No. of generation hours  per a year | 4068.4 | 4764.3 |
| Annual energy (kWh) | 63084 | 1534516 |
| prbability of wind speed between cut-in and cut-out | 0.46 | 0.54 |
| The prbability of wind speed that exceeding 5 m/sec | 0.24 | 0.33 |
| The prbability of wind speed that exceeding 7 m/sec | 0.12 | 0.19 |
| Capacity factor  $C_F$ | 0.15 | 0.22 |
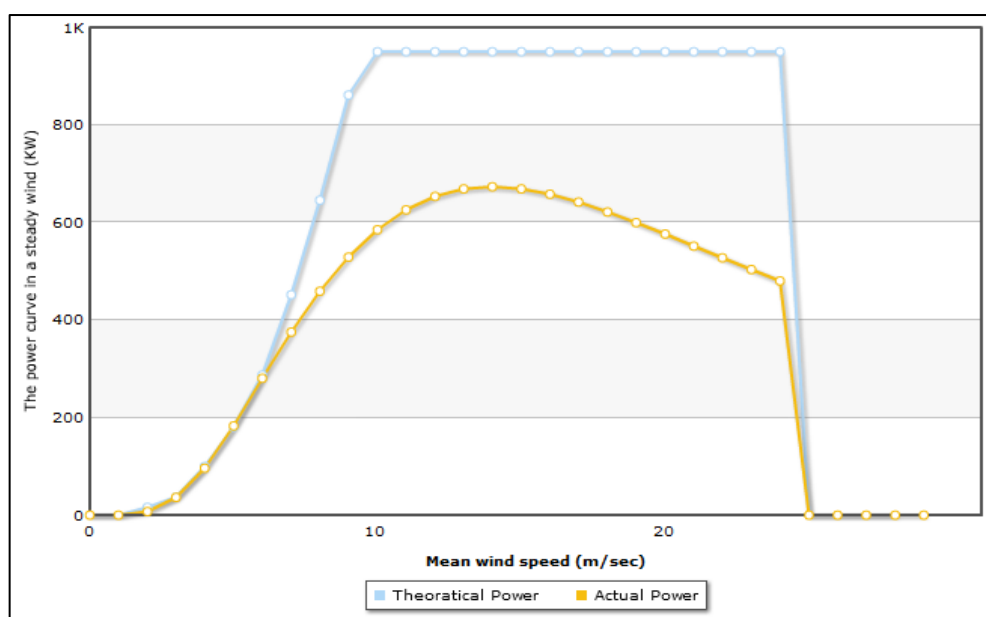


**Fig. 3.35 Mean output power from SUZLON turbine at Ali Al-karbee site.**

### 3.11.2 Analysis of capacity factor

Several wind turbines of different specifications are available in the market. A wind energy project planner can choose a system (best suited for his site) from these available options. Hence, it is important to identify the effect of functional velocities ($V_{in}$, $V_r$ and $V_{out}$) on the turbine performance at the given location. This subsection employs Weibull distribution function through **Eq. 2.93** to perform capacity factor analysis at Ali Al-karbee site. The chosen wind turbine generator has characteristics listed in **Table 3.19**, while the properties of site at 10m and 57m height defined by Weibull parameters are given in **Table 3.21**.

**Fig. 3.36** shows $C_F$ versus different cut-in (a, d), cut-out (b, e), and rated (c, f) wind speed values. The effect of cut-in speed $V_{in}$ is a noticeable decrease in the capacity factor. Whereas the effect of cut-out speed $V_{out}$ on the system performance is prominent up to 18 m/sec at 10m height and 24 m/sec at 57m. With further increase in the cut-out velocity, the capacity factor is not improved considerably.

Now, the effect of cut-in $V_{in}$ on the capacity factor is summarized by decreasing of system performance with increase in $V_{in}$. The reason is evident from turbine power curve, such that the increase in $V_{in}$, area under the power curve reduces, which is finally reflected as the reduction in the capacity factor.

The same thing is true for the effect of rated speed $V_r$ on the capacity factor, such that the increase in $V_r$, area under the power curve reduces, which is finally casing a reduction in the capacity factor.

Cut-out wind speed often ranged between 20-25m/sec, at this range system performance or capacity factor has no considerable improve, and this can be reflected from the stable state of power curve at this region.

Another important fact that could be inferred from **Fig. 3.36** is that; performance of a wind turbine improves (the increment in $C_F$) with its tower height since wind velocity increases with height. Hence, the taller the tower, the higher will be the power available.
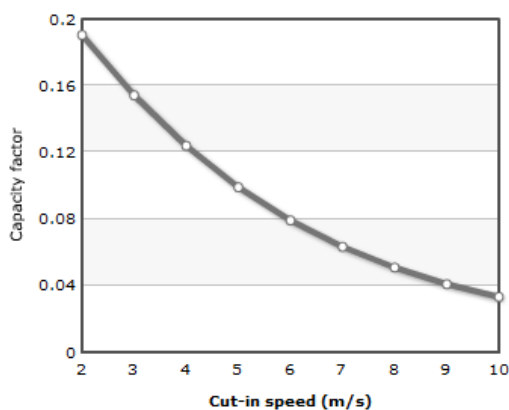
a- Effect of cut-in speed on the system
performance at 10m
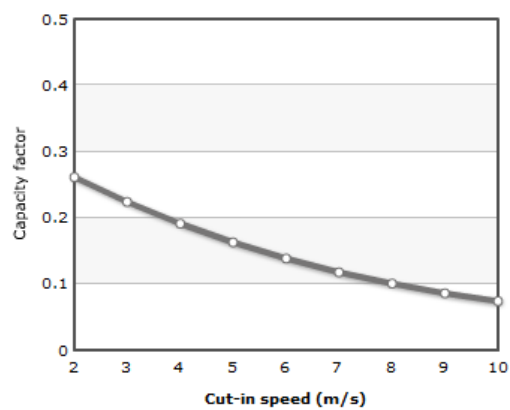
d- Effect of cut-in speed on the system
performance at 57m
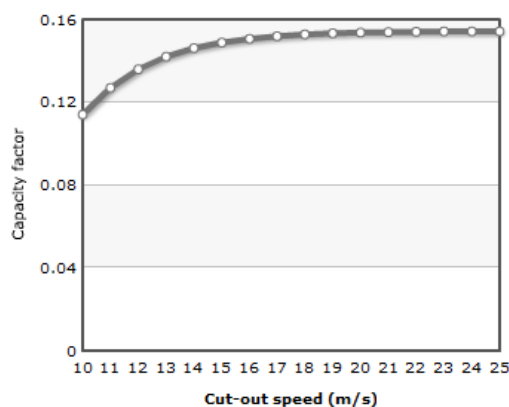
b- Effect of cut-out speed on the system
performance at 10m
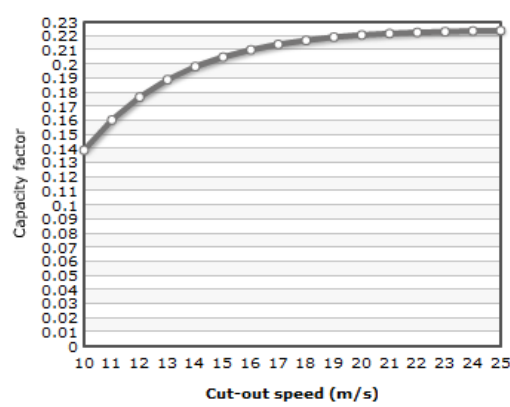
e- Effect of cut-out speed on the system
performance at 57m
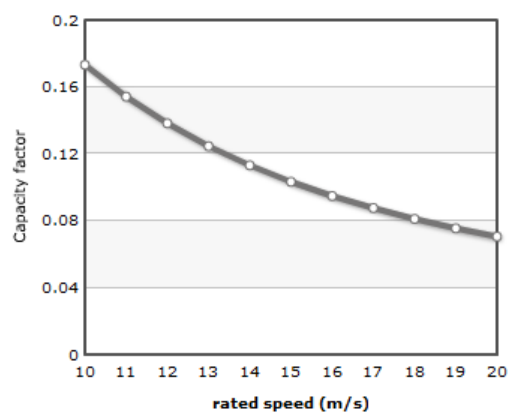
c- Effect of rated speed on the system
performance at 10m
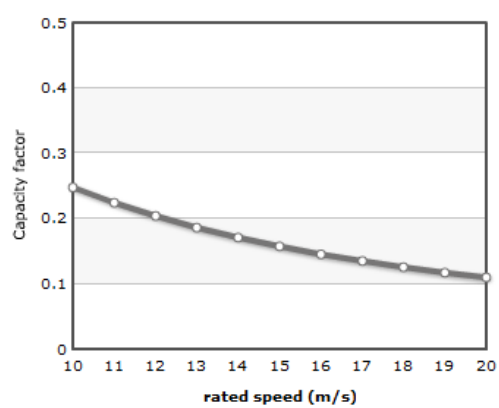
f- Effect of rated speed on the system
performance at 57m

**Fig. 3.36 The effect of turbine velocities on capacity factor
for different heights.**

## 3.12 Roughness Length and Roughness Class

The roughness length of the chosen site can be calculated as follows:
We first must calculate wind speed at hub height (here 57m) using power law **Eq. 2.81**. Then apply **Eq. 2.79** to find roughness length. Now, you could easily find the roughness class by **Eq. 2.80**, see **Table 3.22**.

**Table 3.22: Roughness length and roughness class at Ali Al-karbee 2010.**

| Input variables | | |
|---|---|---|
| **Properties** | value | Methodology |
| **$v_1$ (m/sec)** | 3.53 | EEM |
| **Power exponent** | 0.14 | Given by IEC |
| **Output variables** | | |
| **Properties** | value | Methodology |
| **$v_2$ (m/sec)** | 4.50 | Power law (**Eq. 2.81**) |
| **Roughness length $z_o$ (m)** | 0.0182 | Roughness law (**Eq. 2.79**) |
| **Roughness class RC** | $0.9 \approx 1$ | By Eq. 2.80 |

## 3.13 Summary of Results of Different Locations

Previously, we studied wind zone for Ali Al-karbee from several aspects such as time variation (values and directions), finding the best way for Weibull parameters estimation, calculating energy before and after turbine installation, data extrapolation, number of generation hours, capacity factor and so.
Now we will examine other locations, they are Baghdad, Basrah, Kerbala, and Nasiriya; then give the most important results to those who are interested in wind energy projects.

**Table 3.23: Most important information for different location**

| Properties | Baghdad | Basrah | Nasiriya | Kerbala |
|---|---|---|---|---|
| Longitude | 44˚.13′.47″ | 47˚.46′.48″ | 46˚.13′47″ | 44˚.2′.59″ |
| Latitude (m) | 33˚.15′.35″ | 30˚.31′.11″ | 31˚.1′.11″ | 32˚.34′.12″ |
| Altitude (m) | 35 | 2 | 5 | 29 |
| Date of records | 2010 | 2010 | 2010 | 2012 |
| No. of records | 9280 | 9747 | 8736 | 51622 |
| Zeros percentage | 1.4 % | 25% | 0.7% | 11% |
| Annual prevalent direction | 330˚ | 330˚ | 330˚ | 330˚ |
| Fitting method | MLE-MIM | MLE-MIM | EEM | EEM |
| $c$ (m/sec) at 10m | 3.14 | 4.44 | 4.7 | 4.07 |
| $k$ at 10m | 1.81 | 2.08 | 1.84 | 1.47 |
| Mean speed (m/sec) | 2.79 | 3.92 | 4.17 | 3.67 |
| Median (m/sec) | 2.56 | 3.72 | 3.85 | 3.17 |
| Modal (m/sec) | 2.01 | 3.24 | 3.06 | 1.87 |
| Max frequency | 0.25 | 0.19 | 0.17 | 0.18 |
| Standard deviation (m/sec) | 1.65 | 2.4 | 2.4 | 2.55 |
| Variation coefficient | 57.4% | 50.8% | 56.6% | 69.2% |
| Skewness | 46 | 111 | 151 | 140 |
| Kurtosis | 237 | 724 | 1152 | 1173 |
| Total P.D. w/m$^2$ | 28.53 | 68.4 9 | 93.07 | 85.02 |
| Most energy direction | 330˚ | 330˚ | 330˚ | 330˚ |
| $c$ (m/sec) at 57m height | 3.82 | 5.66 | 6.00 | 5.19 |
| $k$ at 57m height | 1.81 | 2.05 | 1.84 | 1.47 |
| Total P.D. (w/m$^2$) at 57m height | 51 | 144 | 193 | 176 |
| Mean wind speed (m/sec) at 57m | 3.39 | 5.01 | 5.32 | 4.69 |
| Hrs of generation per year at 10m | 3487 | 5616 | 5580 | 4507 |
| Hrs of generation per year at 57m | 4582 | 6496 | 6210 | 5174 |
| Annual energy (kWh) | 751988 | 3010194 | 3856869 | 2930388 |
| $C_F$ at 10m height | 0.04 | 0.10 | 0.14 | 0.14 |
| $C_F$ at 57m height | 0.08 | 0.20 | 0.25 | 0.22 |

### 3.14 Turbulence in Nasiriya

Nasiriya was selected as an open space site to study turbulence intensity effects on small and large wind turbines (SWT & LWT). Nasiriya is the capital of the province of Dhi-qar in Iraqi state on the Euphrates about 225 miles (370 km) southeastern of Baghdad. **Fig. 3.39** shows its position on Iraq map.

Data was collected from Weather Underground website for three years (2008, 2009 and 2010), the results was also compared to the Normal Turbulence Model (NTM), as it is defined for the standard SWT and LWT classes by the IEC (2006) and IEC (2005), respectively.



**Fig. 3.37 Nasiriya location in Iraq**

### 3.14.1 Standard deviation of wind speed calculations

The standard deviation of wind speed is plotted as a function of mean wind speed, $\bar{v}$ in both **Figs. 3.38** and **3.39**. The red dots represent each of calculated $\sigma_v$ value. A linear regression is calculated, with the use of the least square method, and drawn as a pink color line through all of the $\sigma_v$ points. The calculated $50^{th}$ and $90^{th}$ percentile standard deviations ($\sigma_{50} \ and \ \sigma_{90}$) by **Eqs.2.120a** and **2.121a**, respectively, are compared to the NTM for SWT and LWT given by **Eqs. 2.122** and **2.124**, respectively. Where the orange and black lines in **Fig. 3.38** represent the $90^{th}$ and $50^{th}$ NTM percentile, while the orange, black and green lines in **Fig.3.39** represent the three turbine categories A, B and C, respectively, such that the NTM in the three left graph represent the $50^{th}$ percentile, while the NTM in the three right graph represent the $90^{th}$ percentile in this figure.

After substitution of variables values in **Eq.2.122** in case of 90th percentile of the NTM we get $\sigma_1 = 0.12\bar{v} + 1.00$. This means that the 90th percentile of the NTM has an initial magnitude of $\sigma_1 = 1m/s$ for $\bar{v} = 0$ m/sec which is a physical impossibility and should only be seen as a theoretic value. This model is justified in the application of wind turbines since wind speeds below the cut-in wind are irrelevant for the loading calculations.

**Fig. 3.38**, shows the results for January – December 2008, 2009 and 2010 respectively, drawn under NTM that belongs to small wind turbine, while **Fig. 3.39** is drawn under NTM that belongs to large wind turbine. There is a large spreading in the resultant values of $\sigma_v$ at this height and $\sigma_v$ takes both small and large values. For wind speeds lower than 12 m/sec there is a large amount of small scale standard deviations. This indicates that the flow at this height, is characterized by small scale turbulent eddies.

The majority of the $\sigma_v$ lies underneath the NTM 90th percentile for both cases small and large wind turbines for each year of the study, as shown in **Figs. 3.38** and **3.39**. The most extreme value of $\sigma_v$ is measured starting from 5m/s. A comparison with the NTM thus shows that the standard model correctly describes the observed increase in $\sigma_v$ with increasing wind speed at this altitude. The linear regression has a deviates from the NTM which is seen to poorly represent the $\sigma_v$ at 2008 and 2009, while we see a close approximation between this line and NTM at 2010. Since the wind speeds are low, it is difficult to draw any real conclusion about how the pattern will look like for higher wind speeds in such environment but the overall agreement with **Figs. 3.38** and **3.39** can be said to give a hint of what kind of turbulence characteristics might be found there.
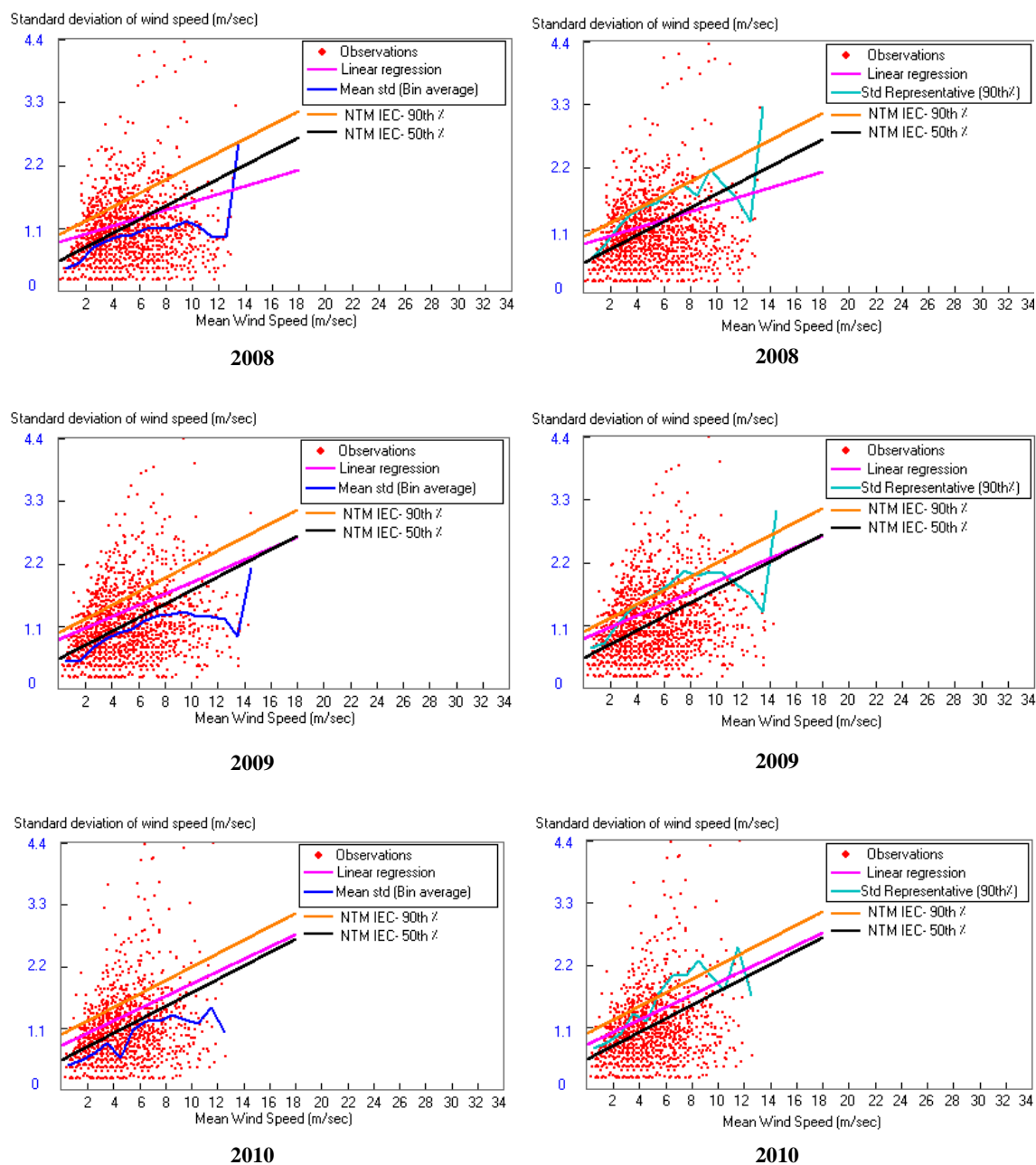
**Fig. 3.38 Standard deviation as a function of $\bar{v}$ which belongs to Nasiriya site for SWT.**
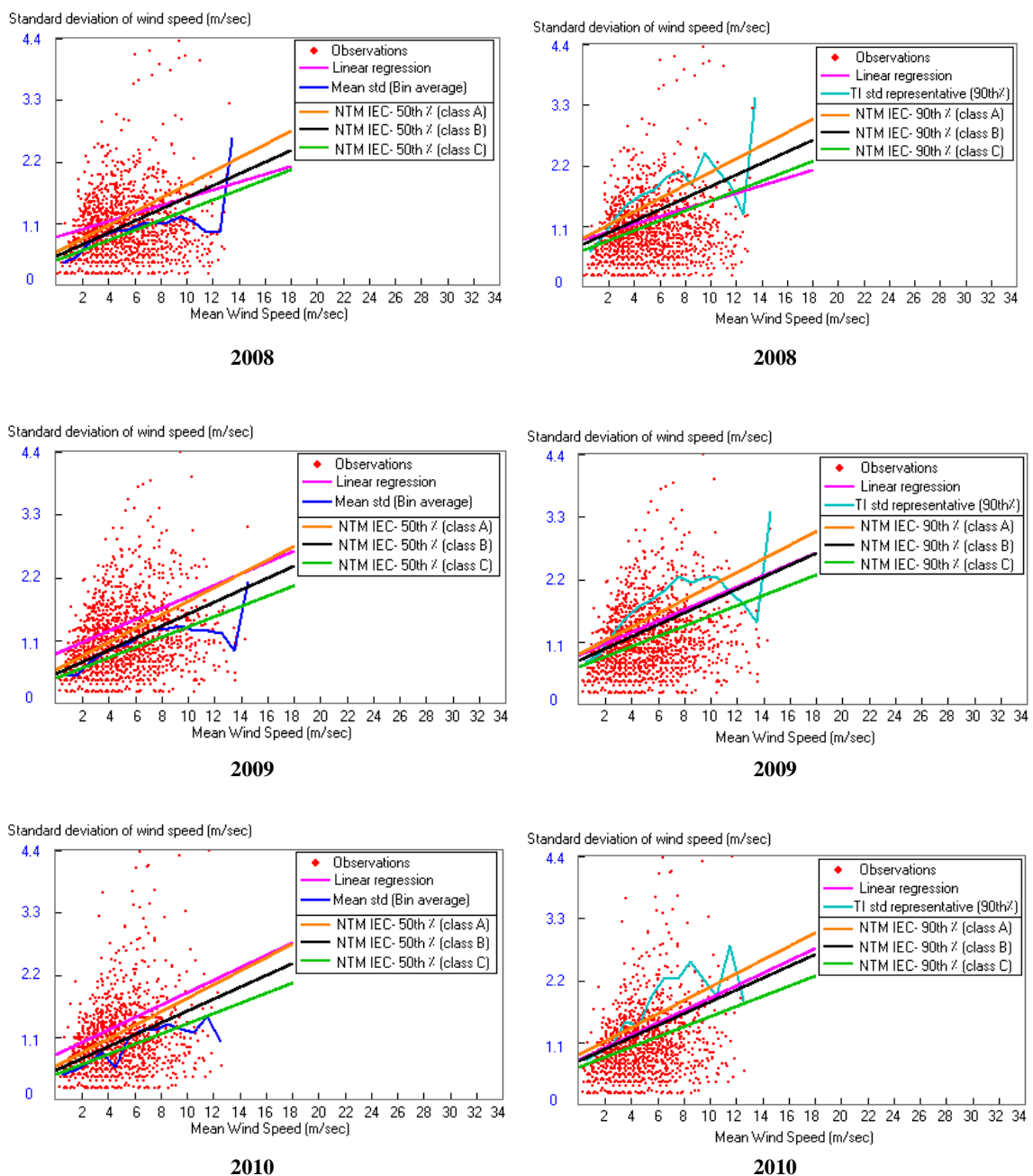
**Fig. 3.39 Standard deviation as a function of $\overline{v}$ which belongs to
Nasiriya site for LWT.**

.

### 3.14.2 Turbulence intensity calculations

Figs. **3.40** and **3.41** show the results of turbulence intensity $TI_v$ given by **Eq. 2.117** in red dots. The calculated mean and representative $TI$ ($TI_{50}$ and $TI_{90}$) by **Eqs.2.120b** and **2.121b** are compared to the NTM for SWT and LWT given by **Eqs. 2.122 and 2.124** divided by mean wind speed $\bar{v}$, where the orange and black lines in **Fig. 3.40** represent the $90^{th}$ and $50^{th}$ NTM percentile, respectively. While the orange, black and green lines in **Fig.3.41** represent the three turbine categories A, B and C, respectively, such that the NTM in the three left graph represent the $50^{th}$ percentile, while the NTM in the three right graph represent the $90^{th}$ percentile in this figure.

The y-axes of the all preceding graphs are cut at 0.6 for convenience, values greater than this are only found for low wind speeds which corresponds to minimal loadings on the wind turbines and are thus irrelevant for the results. It can be seen from these **Figs**. that the large scale turbulence intensity occurs for lower wind speeds, and decreases continually. Also, most of the measured $TI_v$ clusters are under the NTM limits, except some points, where a few of the measurements contain larger values than these estimated by the NTM. It should be noted that all $TI_v$ in **Figs. 3.40** and **3.41** at a wind speed equal to 15 m/sec has average value of $TI_v = 0\%$.

The observations in **Figs. 3.40** and **3.41** show that the pattern of the turbulence intensity at this site differs from the NTM, and $TI_v$ is found to be both lower and higher than the NTM. For the highly turbulent cases, it seems like the observed $TI_v$ values in most cases higher than the model for low wind speeds, as indicated by the dots with high $TI_v$.

Regression is calculated, with the use of the least square method, and is drawn as a pink color curve through all of the data points. In **Figs. 3.40** and **3.41**, the mean turbulence intensity ($TI_{50}$) is calculated using **Eq. 2.120b** is plotted for speed interval of 1m/s in blue line (left column of these **Figs**.). The cyan line (right column of these **Figs**.) represents the $90^{th}$ percentile of the observed turbulence intensity ($TI_{90}$) is calculated using **Eq. 2.121b**. These values can then be compared to the $50^{th}$ and $90^{th}$ percentiles to give a conclusion about turbine category. Since, the point of primary interest is the mean $TI$ at 15 m/sec, which is (0%), this indicates no turbulence and that a category C wind turbine is possible for both wind turbine types (LWT and SWT).
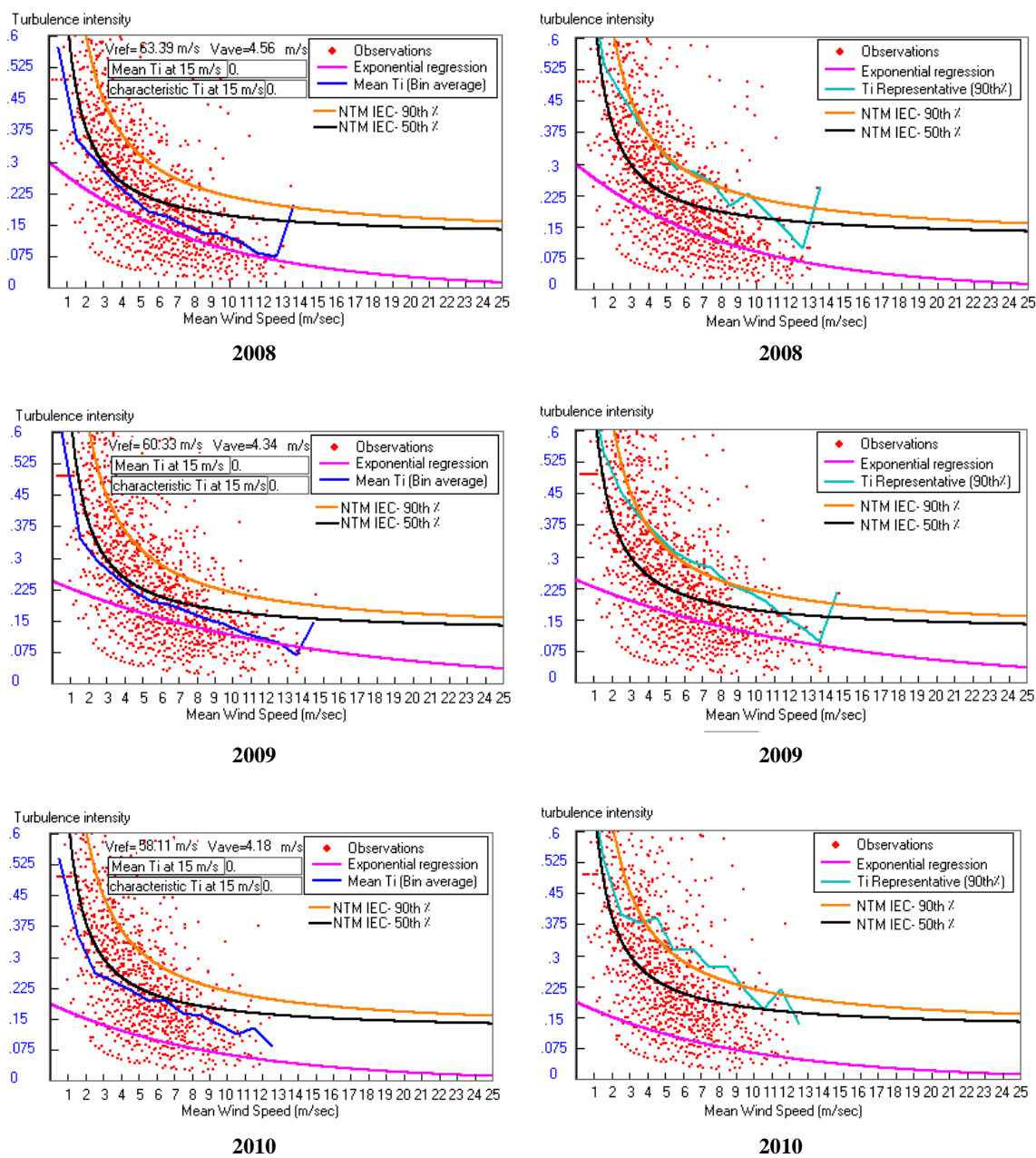
**Fig. 3.40** *TI* as a function of $\bar{v}$ which belongs to Nasiriya
site for SWT.
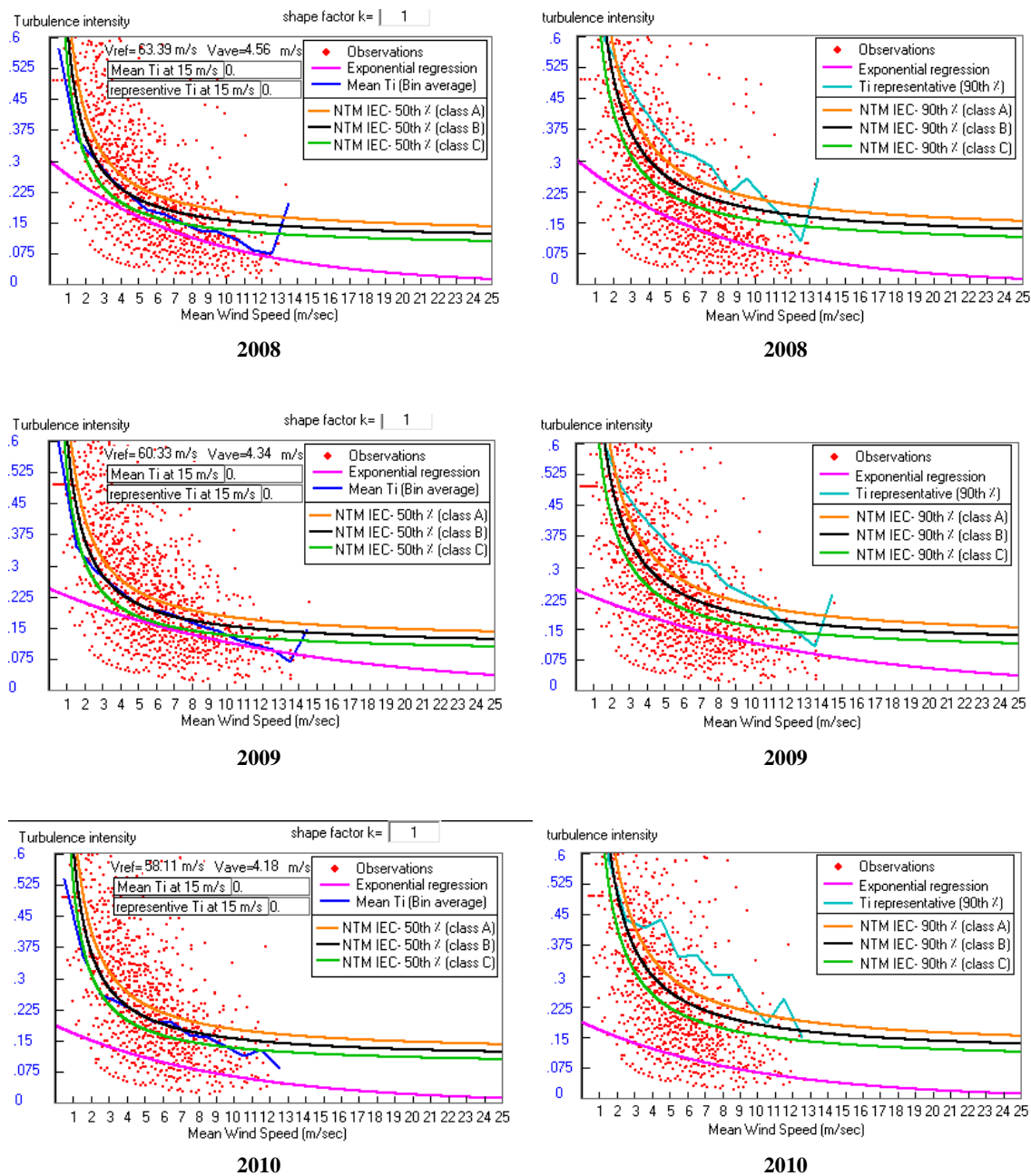
**Fig. 3.41** *TI* as a function of $\overline{v}$ which belongs to Nasiriya site for LWT.

### 3.14.3 Histogram of turbulence intensity

In **Fig. 3.42**, the distribution of turbulence intensity, $TI_v$, is shown in yellow bars divided into intervals with bin size of 5%. The left y-axis denotes the relative frequency of occurrence of $TI_v$ within different intervals. The annual mean turbulence intensity values for the entire measuring periods are 15% at 2008, 16% at 2009, and 14% at 2010. The maximum value of x-axes is taken to be 120 % for convenience.

The highest frequency of turbulence intensity is located in the range of 0-10% with majority of frequency measurements arranged as 29%, 27%, and 34% for the years 2008, 2009, and 2010 respectively. The cumulative frequency of turbulence is given on the right y-axis as a total number of elements.



**2008**                                                                                         **2009**



**2010**
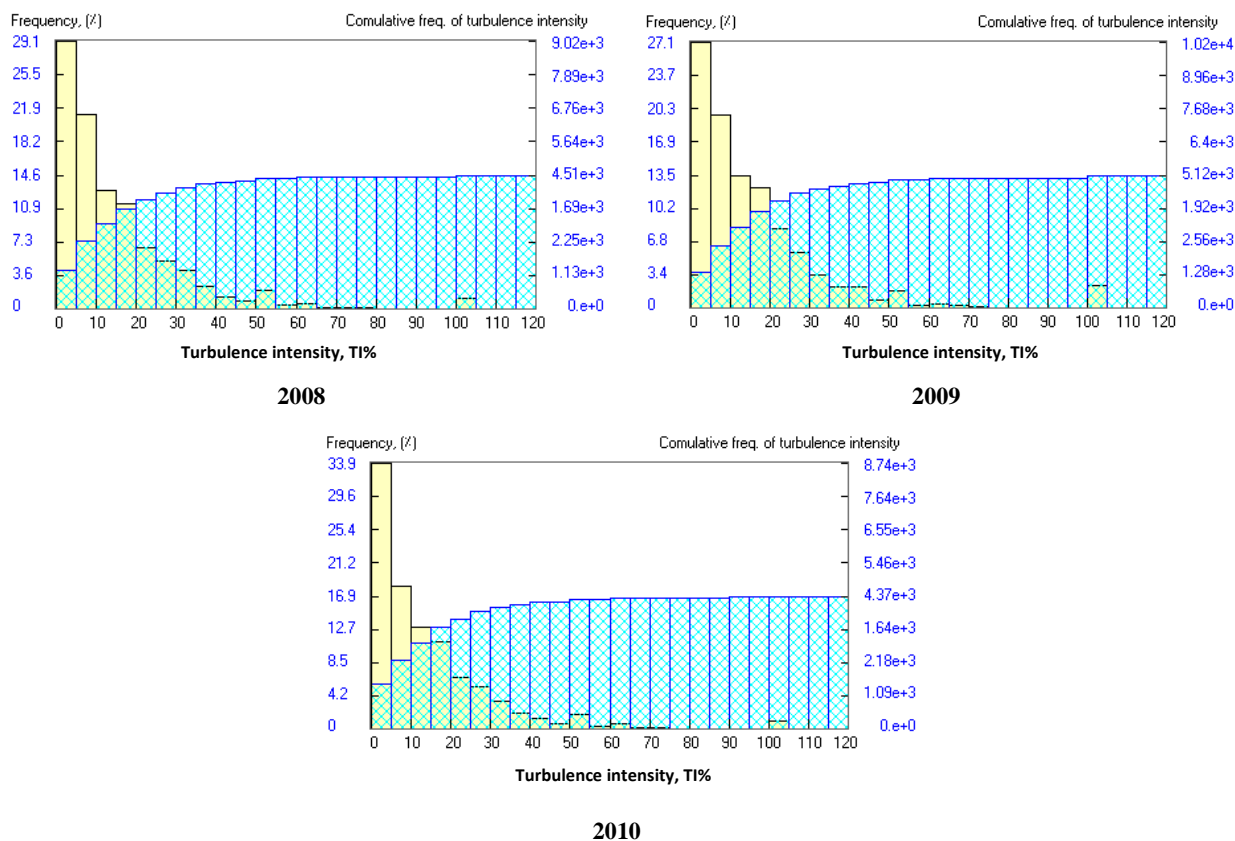
**Fig. 3.42 Frequency of *TI* and its cumulative as a function of *TI* which belongs to Nasiriya site.**

### 3.14.4 Distribution of *TI* versus wind speeds

The distributions (frequency) of $TI_v$ as a function of mean wind speed can be seen in **Fig. 3.43**, representing by green bars binned with intervals of 1m/s. The frequency of turbulence intensity is given on the y-axis as a total number of elements in each wind speed interval. The highest frequency of turbulence intensity occurs at wind speed interval 2-3m/s with value 22% for 2008 and 23% 2010, respectively. While in 2009, the highest frequency of turbulence intensity occurs at wind speed interval 1-2m/s with value 22%.

2008



2009



2010
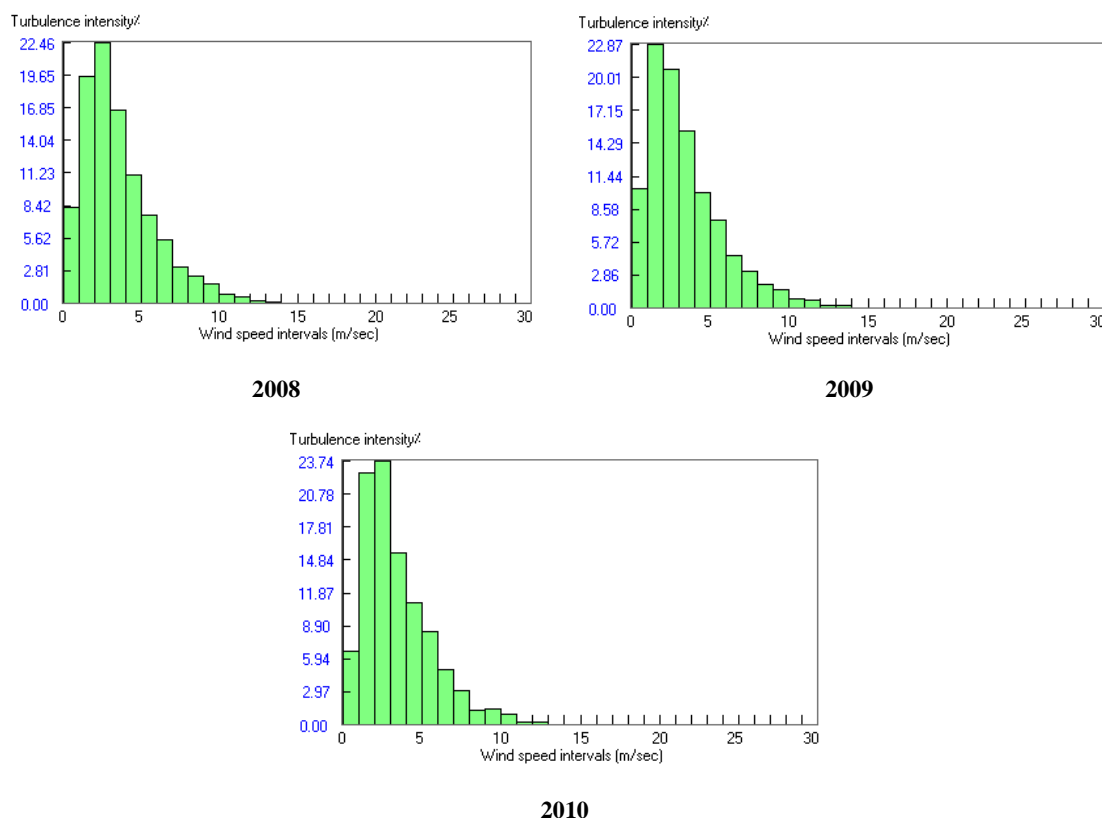
**Fig. 3.43 *TI* as a function of $\bar{v}$ which belongs to Nasiriya site.**

## 3.15 Turbulence in Kerbala

Turbulence in Kerbala will be studied based on data recorded every 10 minutes for the year 2012 from January to December. By adopting the same way that is applied in Nasiriya site, the turbulence for small and large wind turbine will also be compared with the NTM for 50th and 90th percentiles.

For the purpose of determining the appropriate wind turbine class in this region, a comparison with NTM must be done at speed 15m/sec. Sections below demonstrate this procedure.

## 3.15.1 Standard deviation of wind speed calculations

The standard deviation of wind speed is plotted as a function of mean wind speed ($\bar{v}$), in both **Figs. 3.44 and 3.45**. Now, all what we mentioned before about standard deviation calculation (**section 3.14.1**) is true here, but the following should be noted; **Fig. 3.44**, shows the standard deviation $\sigma_v$ of wind speed results for period January – December 2012. The results are plotted in red dots drawn under NTM that belongs to small wind turbine, while **Fig. 3.45** is drawn under NTM that belongs to large wind turbine. There is a large spreading

in the resultant values of $\sigma_v$ at this height and $\sigma_v$ takes both small and large values. For wind speeds lower than 10m/s there is a large amount of small scale standard deviations values concentrated on less than 1m/sec. This indicates that the flow at this height, is characterized by small scale eddies corresponding to situations with no, or only light, turbulence.

The majority of the $\sigma_v$ values lie underneath the NTM 50$^{th}$ percentile for small wind turbine as shown in **Figs. 3.44**. The most extreme value of $\sigma_v$ is started from 3m/s. The blue and cyan lines (left column and right column in these **Figs.**) are calculated from $\sigma_{50}$ and $\sigma_{90}$ (**Eqs. 2.120a** and **2.121a**) to make a comparison with the 50$^{th}$ and 90$^{th}$ percentiles of NTM respectively. A comparison between the linear regression and the NTM lines can be used as an indicator to the concentration position of $\sigma_v$, which gives a weight in the regression formula. This mean that a most of $\sigma_v$ have low values.
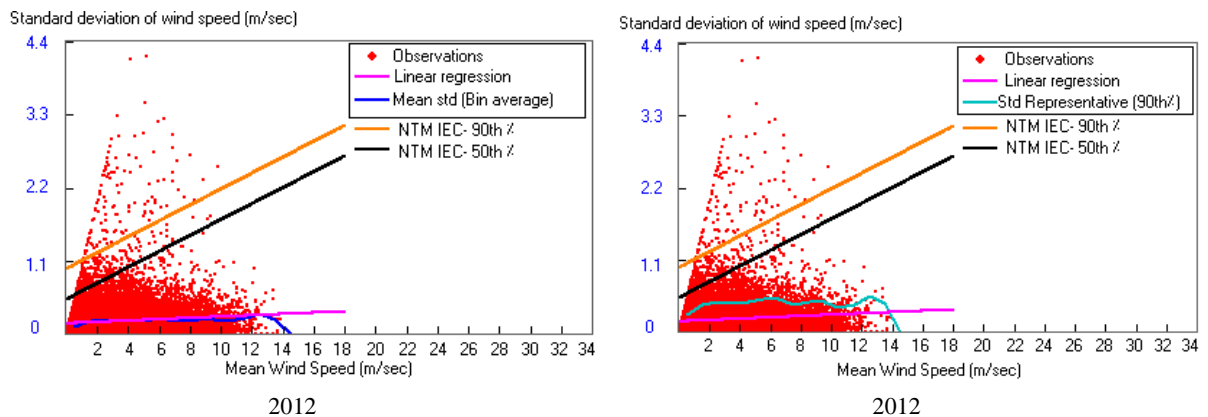


**Fig. 3.44 Standard deviation of wind speed as a function of $\overline{v}$ belongs to Kerbala site for SWT.**
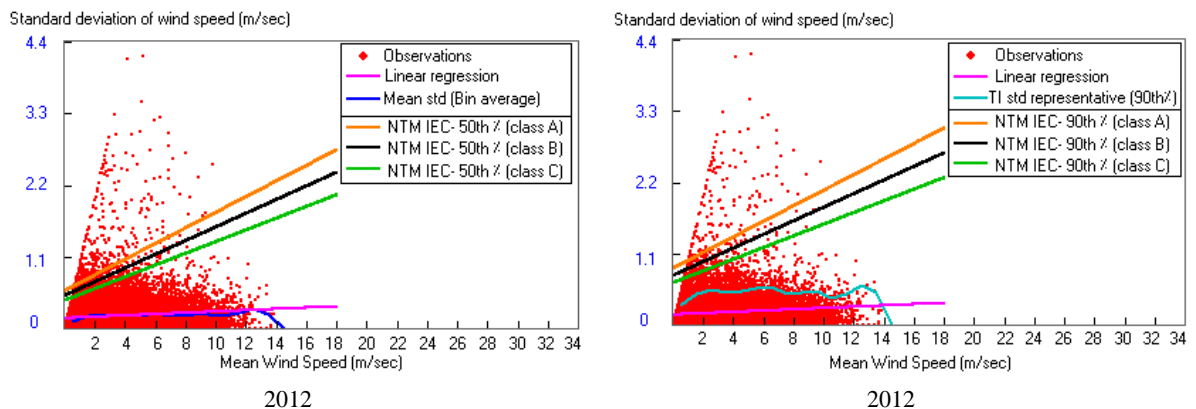


**Fig. 3.45 Standard deviation of wind speed as a function of $\overline{v}$ which belongs to Kerbala site for LWT.**

144

### 3.15.2 Turbulence intensity calculations

**Figs. 3.46** and **3.47** show the results of turbulence intensity $TI_v$ in the same way that we find in **section 3.14.2**. The y-axes of the graphs are cut at 0.6 for convenience. It can be seen from these **Figs**. that the large scale turbulence intensity occurs for lower wind speeds, and decreases continually, and most of the measured $TI_v$ clusters are under the NTM limits, except some points, where a few of the measurements contain larger values than that estimated by the NTM. In **Figs. 3.46** and **3.47**, the turbulence intensity is plotted for speed interval of 1m/s in blue line (left column in these **Figs**.). The cyan line represents the 90th percentile of the observed turbulence intensity. These lines (blue and cyan) are calculated from $TI_{50}$ and $TI_{90}$ (**Eqs. 2.120b** and **2.121b**), can then be compared to the 50th and 90th percentiles of NTM respectively. Turbulence has more scatter at low wind speeds. This is because deviation from neutral atmospheric stability is more pronounced at low wind speeds. A point of primary interest is the mean *TI* at 15m/s, is 0%. This indicates no turbulence and a category C is possible for both LWT and SWT.



**2010**                                                        **2010**
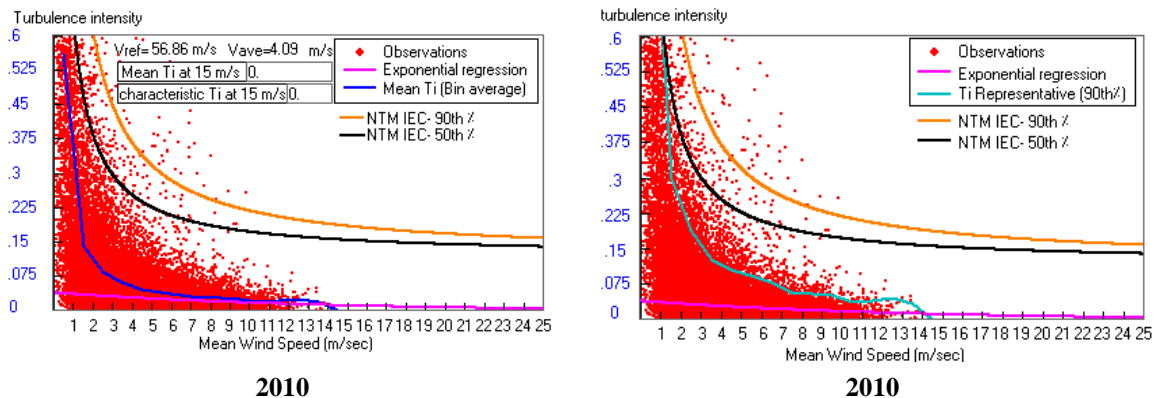
**Fig. 3.46.** *TI* as a function of $\bar{v}$ which belongs to Kerbala site for SWT.



**2012**                                                        **2012**
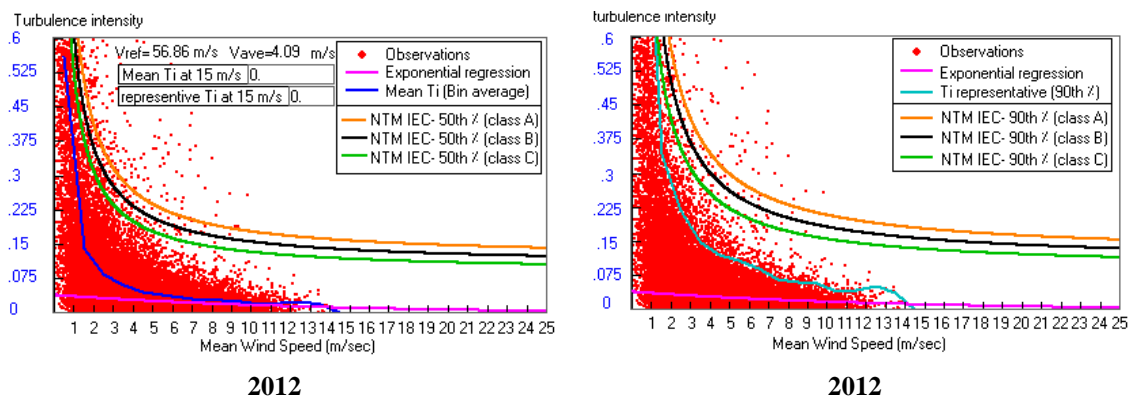
**Fig. 3.47.** *TI* as a function of $\bar{v}$ which belongs to Kerbala site for LWT.

145

### 3.15.3 Histogram of turbulence intensity

In **Fig. 3.48**, the distribution of turbulence intensity, $TI_v$, is shown as yellow bars divided into intervals with bin size 5%. The y-axis denotes the relative frequency of occurrence of $TI_v$, while the cumulative frequency of turbulence is given on the right y-axis to show total number of elements and how frequencies of turbulence intensity increase at each bin.

At altitude 10m height, the annual average value of $TI_v$ is 12%. The highest frequency of events has between 0-5% turbulence intensity with occurrence value 57.4%, on the other hand turbulence intensity in the range of 5-10% values reaches more than 14% from all measured data as seen in **Fig.** below. The distribution is skewed with a larger distribution of low $TI_v$. The maximum value of x-axes is taken to be $TI_v =120\%$ for convenience. The observations have a non Weibull distribution shape such as in Nasiriya site.
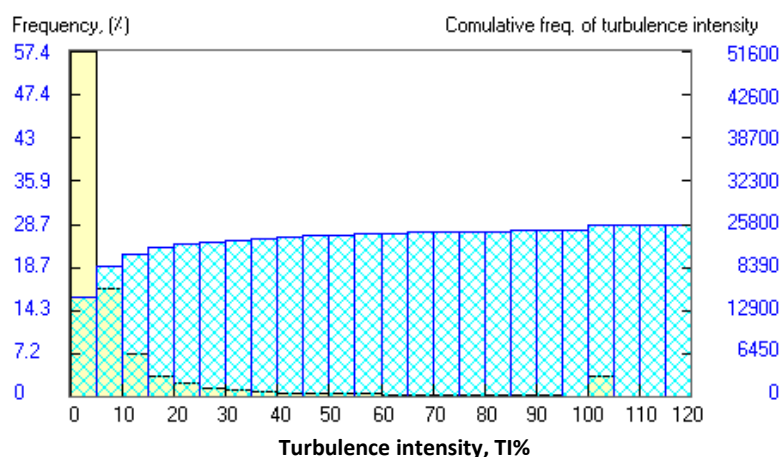


**Fig. 3.48 Frequency of *TI* and its cumulative as a function of $\bar{v}$ which belongs to Kerbala site.**

### 3.15.4 Distribution of *TI* versus wind speeds

The distributions of $TI_v$ as a function of mean wind speed can be seen in **Fig. 3.49**, represented by green bars binned with intervals of 1m/s. The frequency of turbulence intensity is given on the y-axis as a percentage of total number of elements. The highest frequency of turbulence intensity occurs at a wind speed ranging from 0-1m/sec with occurrence value 53%, besides that non wind speeds is higher than 10m/sec, see **Fig. 3.49**.
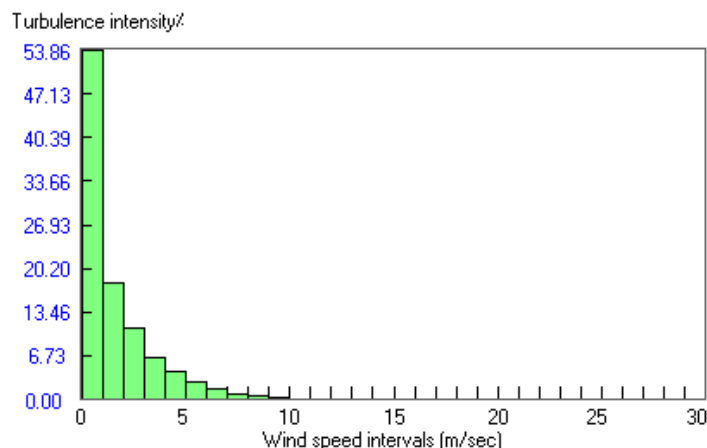
Fig. 3.49 *TI* as a function of $\bar{v}$ which belongs to Nasiriya site.

## 3.16 Representative *TI* Calculations for Directional Sectors

In this section, $90^{th}$ percentile representative turbulence intensity ($I_{rep}$) produced from different wind directions in Nasiriya and Kerbala sites will be produced. We use wind rose consisting of 8 sectors to provide some insight on the different turbulence intensity directions, and to have general thought about the reasons that might have produced them. First, the dominant wind direction must be calculated, and then distribute wind speeds according to their directions between rose's sectors. **Fig. 3.50** shows the wind roses for Nasiriya and Kerbala sites divided in 8 sectors, wind at these two locations blowing mostly from the western, northwestern, and northern directions specifically from sector 8, in addition to winds blowing from other directions.



| a- Nasiriya 2010 | b -Kerbala 2012 |
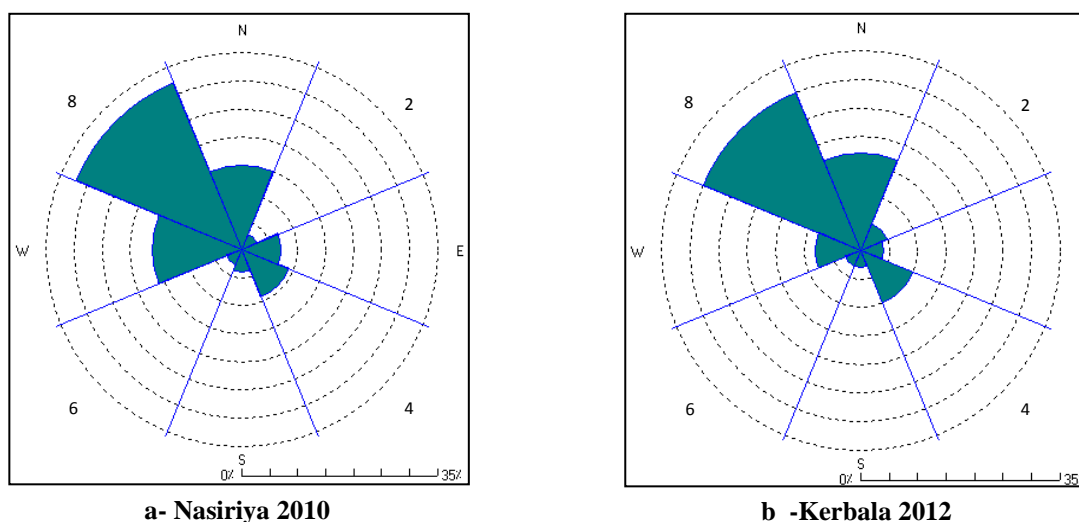
**Fig. 3.50 Wind roses for two locations.**

Now**,** it is possible to find *TI* at each sector, the plots of *TI* as a function of wind speed in 8 sectors for Nasiriya and Kerbala sites are shown in **Figs. 3.51** and **3.52**, respectively. The data were plotted following the procedure of IEC61400 edition 3 (red line) compared with NTM which represents 90th percentile of *TI*. The three curves of NTM give turbine category A, B, and C in green, yellow, and cyan respectively. It is obvious from these **Figs**. that there is no representative *TI* at wind speed 15m/sec for both sites. From Nasiriya area all sectors (directions) have *TI* values more than NTM at low wind speeds but the high *TI* is shown in sectors 5 and 6 (southern and southwestern directions). On the other hand, Kerbala site has moderate representative *TI* such that it has lower values than NTM; this is due to the effects of what exists in that direction around recorder station. Somehow there is a relationship between the occurrences of velocities in a sector with the severity of the *TI* in that sector, such that less turbulence in a sector where there is less wind frequency during that period, such as in sectors 2, 3, and 4 in both sites.

As mentioned before, the recommended turbine category for this site is C; **Figs**. below confirm this choice.

Sector 5

Sector 6

Sector 7

Sector 8

C     B     A     Irep
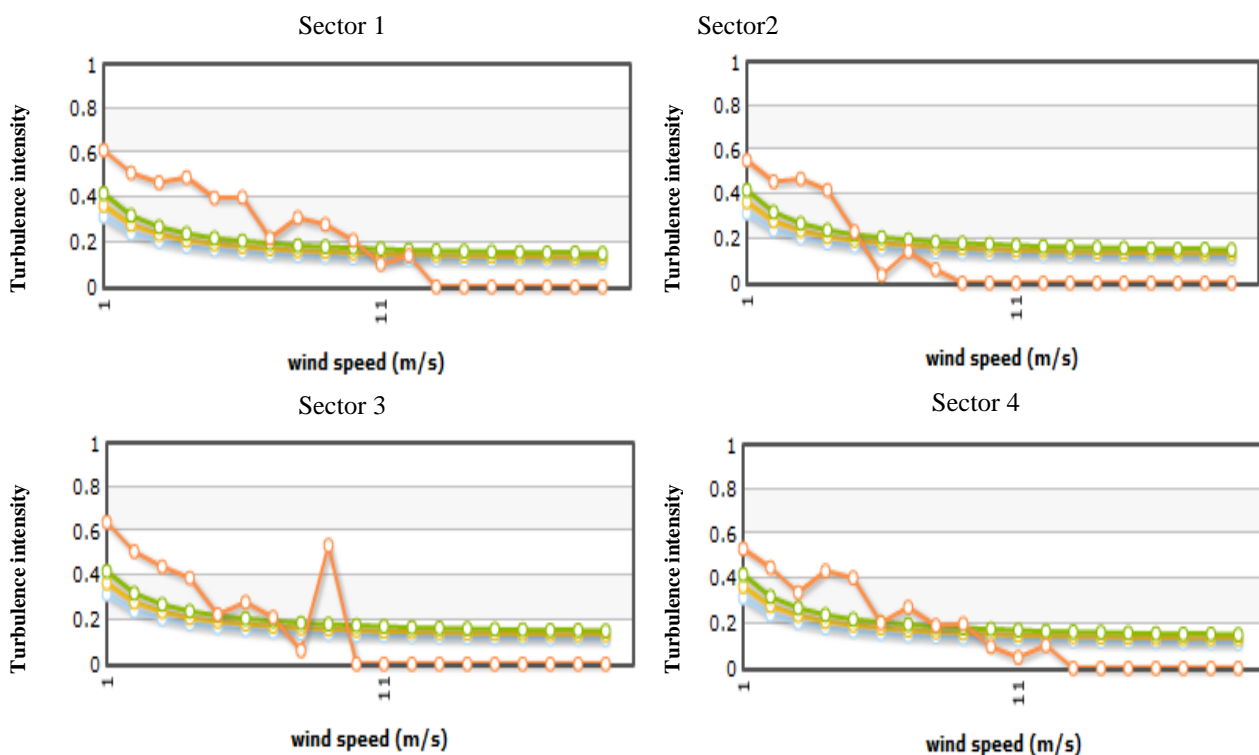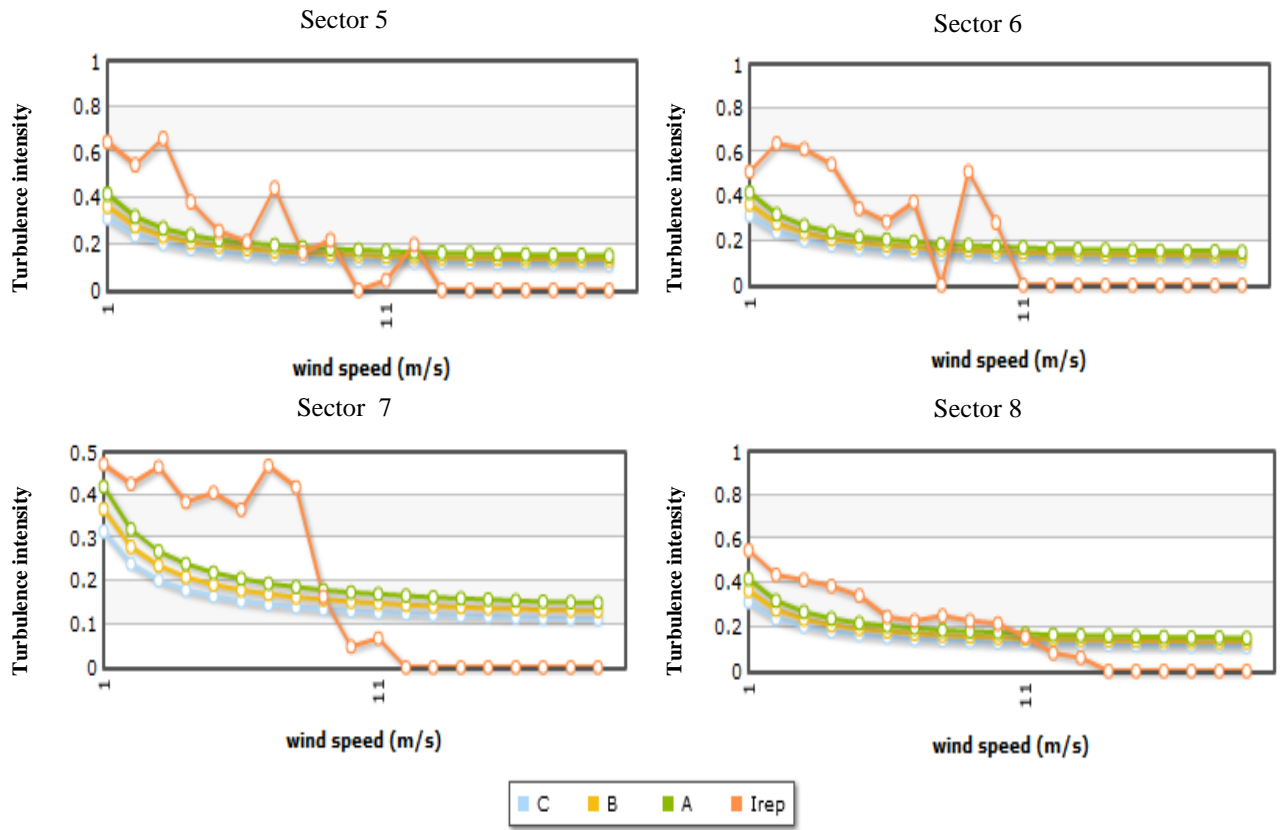
**Fig. 3.51 Representative turbulence intensity ($I_{rep}$) at different directions, Nasiriya-2010.**

Sector 1

Sector 2
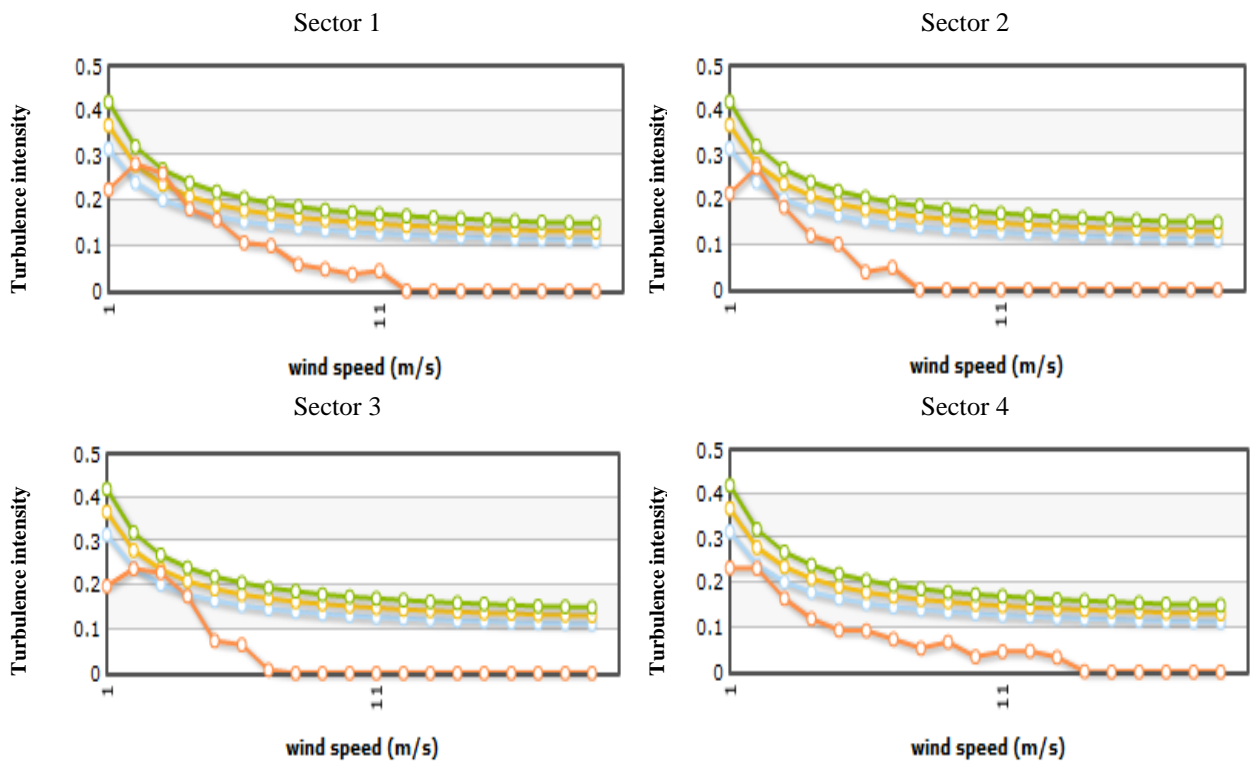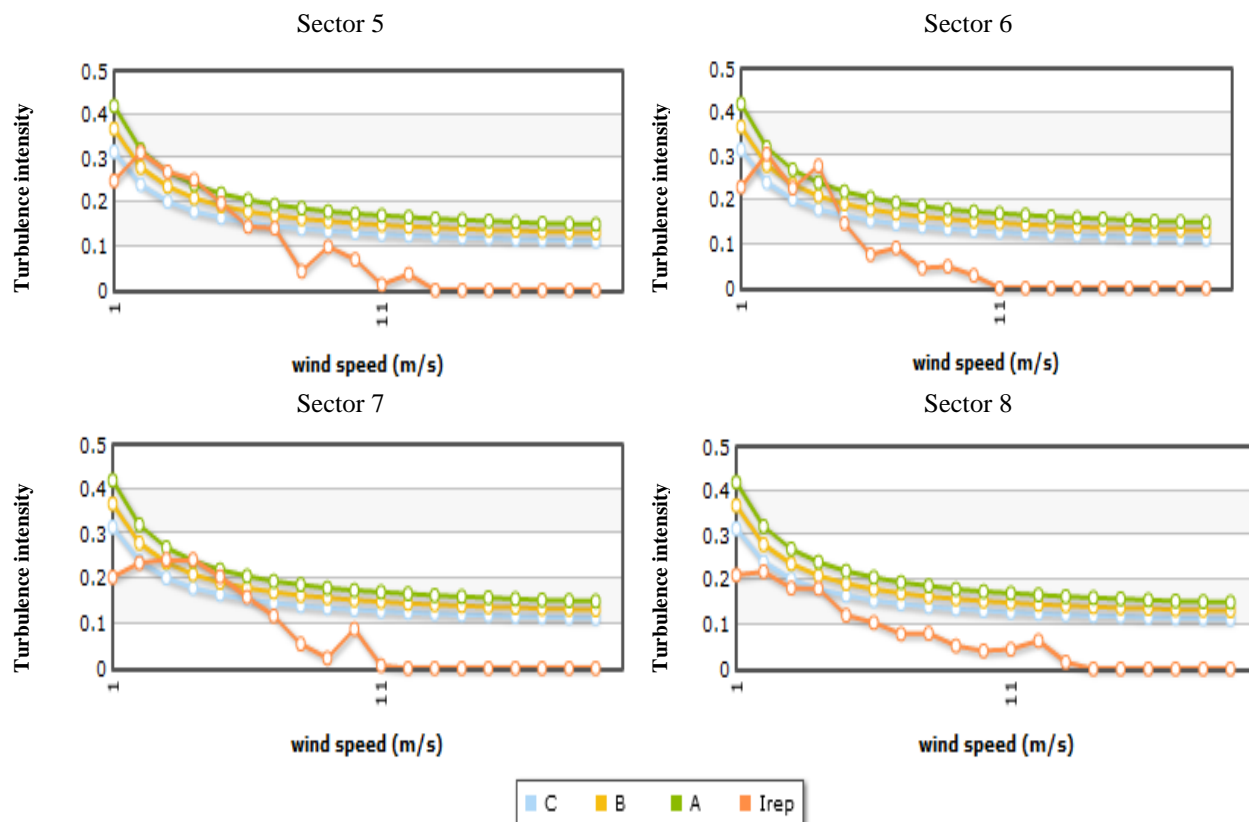
Sector 3

Sector 4

**Fig. 3.52 Representative turbulence intensity ($I_{rep}$) at different directions, Kerbala-2012.**

After computing $I_{rep\text{-}s}$ for each sector as shown in **Figs. 3.51** and **3.52**, now it could be possible to compute total $I_{rep}$ at wind speed 15m/sec for Nasiriya and Kerbala sites using **Eq. 2.126** only. As expected from proceeding calculations, the results show that $I_{rep}$ for both locations equal to zero, $I_{rep}= 0$ (see **Tables 3.24** and **3.25**)

**Table 3.24: $I_{rep\_s}$ and $I_{rep}$ for 8 sectors at wind speed 15m/sec for Nasiriya site.**

| Sector | 1 | 2 | 3 | 4 | 5 | 6 | 7 | 8 |
|---|---|---|---|---|---|---|---|---|
| **Center** | 0 | 45 | 90 | 135 | 180 | 225 | 270 | 315 |
| $I_{rep\_s}$% | 0.0 | 0.0 | 0.0 | 0.0 | 0.0 | 0.0 | 0.0 | 0.0 |
| $f_s$ % | 20.1 | 3.3 | 72 | 9.6 | 5.0 | 3.7 | 17.4 | 32.9 |
| **No. samples** | 1756 | 290 | 626 | 839 | 434 | 325 | 1524 | 2873 |
| $I_{rep}$ | 0 | | | | | | | |

**Table 3.25: $I_{\text{rep\_s}}$ and $I_{\text{rep}}$ for 8 sectors at wind speed 15m/sec for Kerbala site.**

| Sector | 1 | 2 | 3 | 4 | 5 | 6 | 7 | 8 |
|---|---|---|---|---|---|---|---|---|
| Angle (centered) | 0 | 45 | 90 | 135 | 180 | 225 | 270 | 315 |
| $I_{\text{rep\_s}}\%$ | 0.0 | 0.0 | 0.0 | 0.0 | 0.0 | 0.0 | 0.0 | 0.0 |
| $f_s$ % | 17.9 | 5.7 | 4.9 | 10.3 | 3.4 | 2.9 | 8.8 | 31.9 |
| No. samples | 9238 | 2964 | 2523 | 2325 | 1756 | 1504 | 4554 | 16484 |
| $I_{\text{rep}}$ | 0 | | | | | | | |

## 3.17 Effects of Turbulence on Power Curve

The power curve measurement at a test site must include a measure of the turbulence level to permit a possible correction to the power curve. The effects of turbulence on wind turbine power curves are estimated in **Fig. 3.53**. It is obvious that there is no change in the theoretical power curves of the two sites, because turbulence intensity at these sites is not high enough to make change in the theoretical power curves.
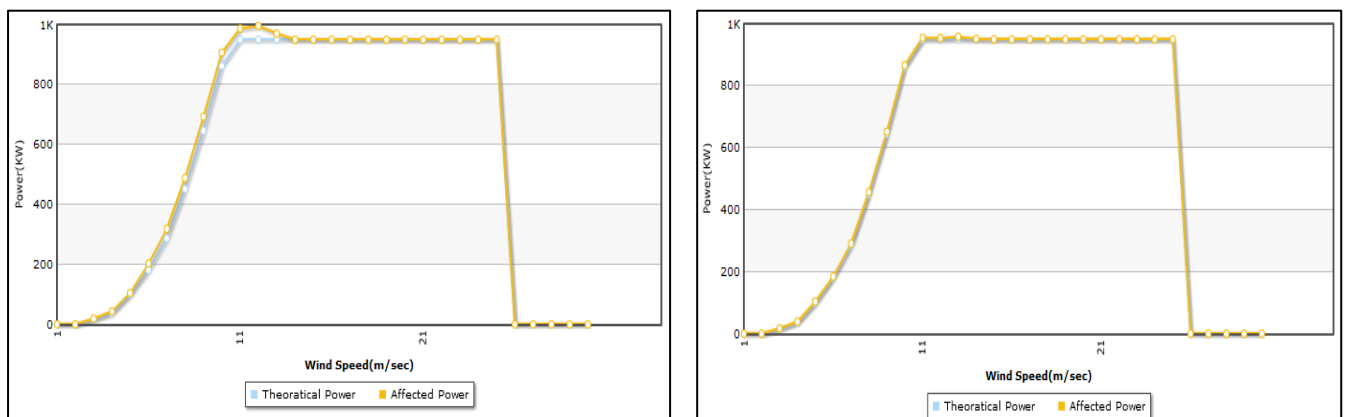


a- Nasiriya-2010                                    b- Kerbala-2012

**Fig. 3.53 Effect of turbulence intensity on power curve at two sites.**

## 3.18 Vertical Extrapolation of Turbulence Intensity

The data belonging to Nasiriya location were recorded from Weather Underground website. This site has mean wind speed (listed in **Table 3.23**) equals 4.17m/s. Since, the prediction of mean wind speed at different heights

(using power law) is possible, thus, it could extrapolate the turbulence intensity to new heights using **Eq. 2.128**. Since *TI* at wind speed 15m/sec and 10m height in Nasiriya site was equal to zero, thus all turbulence intensity values at new height will be equal to zero also. The same thing is true for Kerbala site (having mean wind speed 3.67m/s) and the new extrapolated turbulence intensity will equal zero also.  But for the purpose of studying the effect of altitude on the *TI*, it is convenient to take the annual average values of *TI* as 0.14 for Nasiriya and 0.12 for Kerbala (calculated before in **sections 3.14** and **3.15**), then the values are extrapolated from 10m height to new different height. The results are shown in table below.

**Table 3.26: Extrapolation of *TI* values to new different heights**

| Height | | | 20m | 30m | 40m | 50m | 60m | 70m | 80m |
|---|---|---|---|---|---|---|---|---|---|
| Nasiriya | $v_{meas}$ **4.17 m/s** | $v_{pred}$ **(m/sec)** | 4.59 | 4.86 | 5.06 | 5.22 | 5.35 | 5.47 | 5.57 |
| | $TI_{meas}$ **0.14** | $TI_{pred}$ | 0.127 | 0.120 | 0.115 | 0.111 | 0.109 | 0.106 | 0.104 |
| Kerbala | $v_{meas}$ **3.67 m/s** | $v_{pred}$ **(m/sec)** | 4.04 | 4.28 | 4.45 | 4.59 | 4.71 | 4.81 | 4.91 |
| | $TI_{meas}$ **0.12** | $TI_{pred}$ | 0.109 | 0.102 | 0.098 | 0.095 | 0.093 | 0.091 | 0.089 |

**Figs. 3.54** and **3.5**5 show how turbulence intensity decrease with height belonging to Nasiriya and Kerbala sites respectively. This can be explained by going back to **Eq. 2.128**, which shows that any increment in the predicted wind speed ($v_{pred}$) with height will decrease the second term in it, which in turn causes a decreasing of predicted turbulence intensity ($TI_{pred}$) value. Since the increment in wind speed with altitude is logarithmic, thus the decrease in $TI_{pred}$ is logarithmic also.
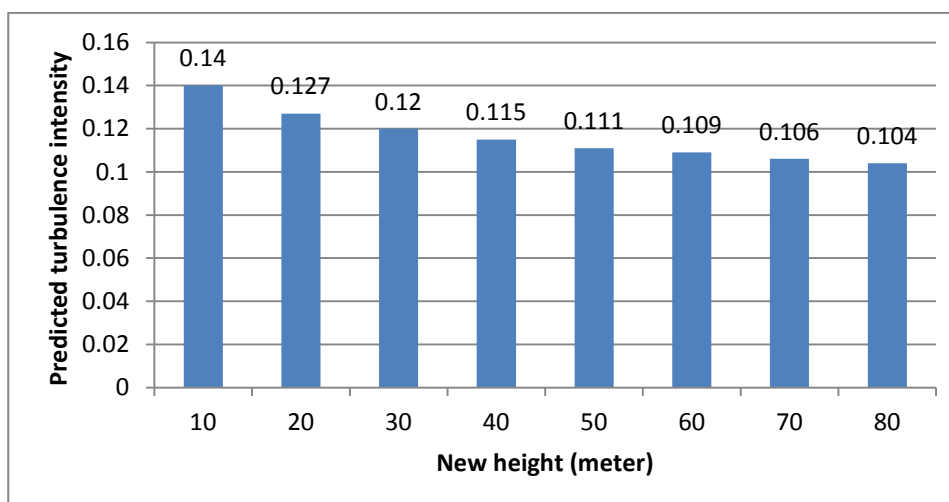
**Fig 3.54 *TI* extrapolation to new heights, Nasiriya-2010.**
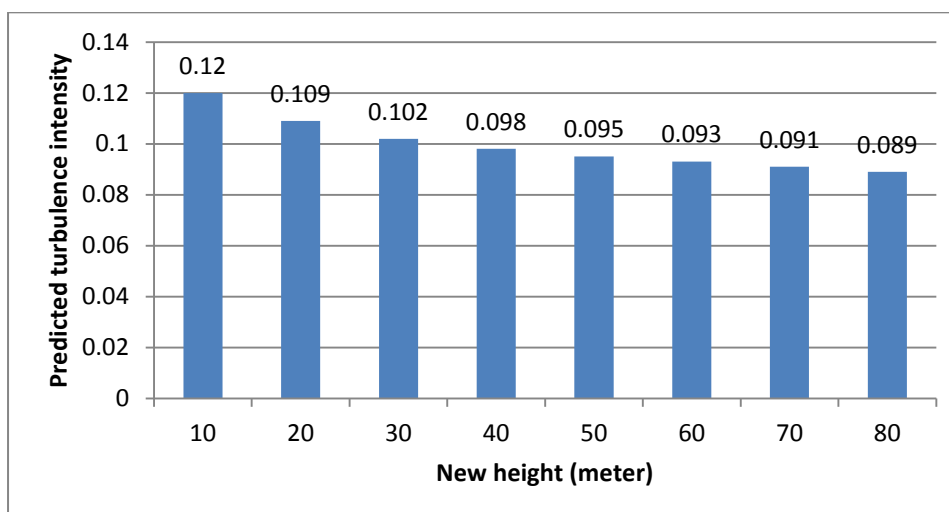


**Fig 3.55 *TI* extrapolation to new heights, Kerbala-2012.**
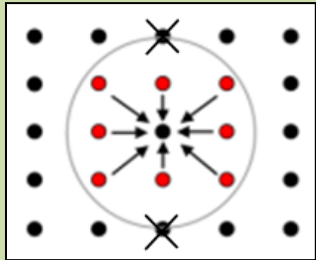
## 3.19 Wake Effect

Placing the turbine within a wind farm will cause a reduction in wind speed and increase in turbulence that occurs downstream of wind turbine, this effect could be measured by effective turbulence intensity $I_{\text{eff}}$.

In projects involving more than a handful of wind turbines, wake effects must be added to ambient turbulence intensity (previously estimated) to calculate $I_{\text{eff}}$. For the purpose of studying this factor, it is imposed a presence of a virtual wind farm located at Nasiriya area. In general, Frandsen model will be adopt, the wake effects in the form of the added turbulence have to be calculated using **Eq. 2.132**. The model takes into account some different parameters in addition to

structural fatigue materials used in blades. For our case, these parameters will be given in different values to study there effects on $I_{eff}$.

**Table 3.27: The values used for studying effective turbulence intensity $I_{eff}$.**

| Input | Values |
|---|---|
| Location | Nasiriya |
| Date | 2010 |
| Certificated | IEC61400-edition 3 |
| Model | Frandsen |
| No. of neighbours = 8 |  |
| Distance (ver. and hor.) | 4 D |
| Pdf | 0.06 |
| Wohler exponent | 10 class fibre |
| Diameter (meter) | 71m |
| Calm | 0.2 m/sec |

## 3.20 $I_{eff}$ for Nasiriya Site

The parameters and configurations that are used in this adopted model (Frandsen model) to calculate $I_{eff}$ for Nasiriya location are listed in **Table 3.27**, where eight wind turbines surrounded reference one (the interested one). The important parameters include the distance between turbines, probability density function taken for wake condition, the Wohler exponent of the considered material, and finally rotor diameter.

The $I_{eff}$ is represented by ambient turbulence intensity added to the effectiveness of neighbouring wind turbines. Effective turbulence intensity will generally decrease with increasing wind speed due to decreasing turbine thrust coefficient (**Eq. 2.134**). To reduce wake interference, turbines are generally spaced farther

apart along the predominant wind directions. Moreover, decreasing the number of surrounded wind turbines will contribute to reducing wake effect. These two effects will be studied at Nasiriya site in the cases below:

i.    *$I_{eff}$ for zero neighbouring turbines*

**Fig. 3.56** shows the $I_{eff}$ for $TI_{50}$ (red line) and $I_{eff}$ for $TI_{90}$ percentile (blue line) values at Nasiriya site (2010) compared to NTM. Here, the effects of the surrounding turbines are canceled because it is assumed that the reference turbine (under interest) stands alone, thus the turbine will be subject to only ambient turbulence intensity (previously estimated) without wake effect. Accordingly, $I_{eff}$ will equal $I_o$ in **Eq. 2.132** because $\dot{N}$ =0 (zero neighbouring turbines).
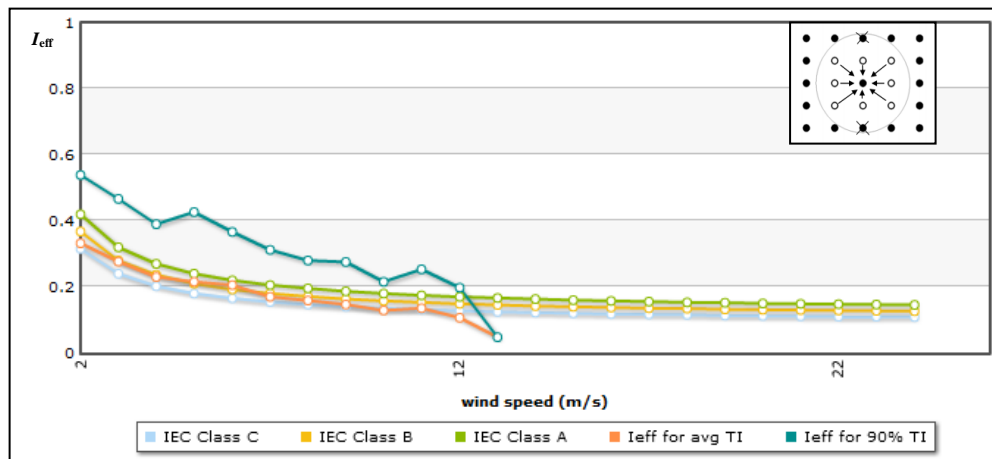


**Fig. 3.56 Effective turbulence intensity in case of zero neighbors at Nasiriya site 2010.**

ii.    *$I_{eff}$ for different numbers of neighbouring turbines*

The effect of different numbers of turbines on the reference one in virtual farm is shown in **Fig. 3.57**. The red line represents $I_{eff}$ (at $TI_{50}$), while blue line is the representative value of $I_{eff}$ (at $TI_{90}$). Any increasing in the no. neighbouring wind turbines will cause an increasing in the value of $I_{eff}$. For each graph in the **Fig.** bellow there is a plot (at upper right corner) demonstrate how the turbines distributed around the reference one, where the reference turbine drown as black dot inside a circle, while any turbine exist beside the central one will be represented by red dot. It is important to know that we will take the wake effect from only wind turbines that inside the circle and exclude the others which they

are outside the circle (represented by black dots). The distance between turbines located at horizontal and vertical array taken as 4 times reference turbine diameter (related to rotor diameter of the reference turbine), while the distance between the turbines located at the corner sides to the reference one is subject to Pythagoras law.

The $I_{eff}$ values for **Figs. 3.56** and **3.57**-**h** are listed in **Table 3.28**. It is obvious from this table that $I_{eff}$ has no values at wind speed 15m/sec, thus C category is appropriate for this turbine.


-a-


-b-


-c-


-d-


-e-


-f-

-g-                                                            -h-
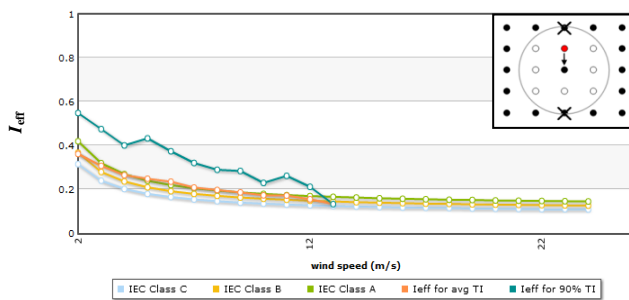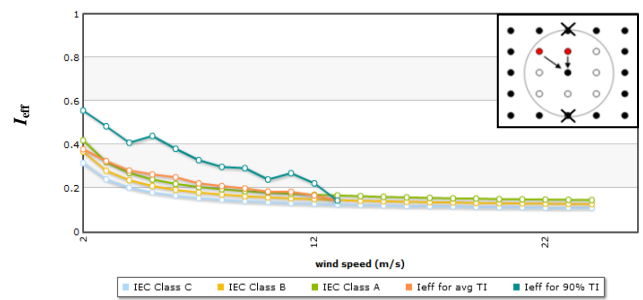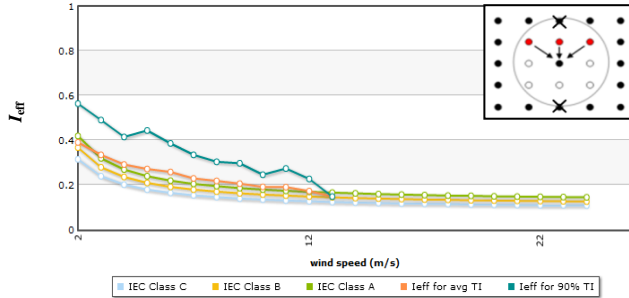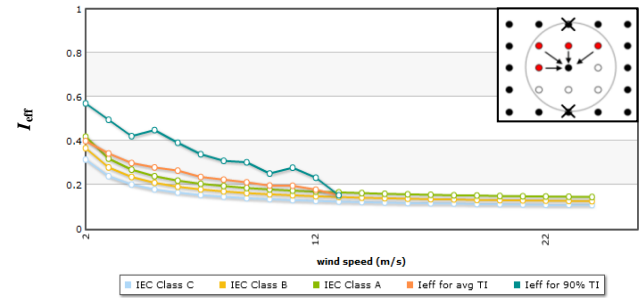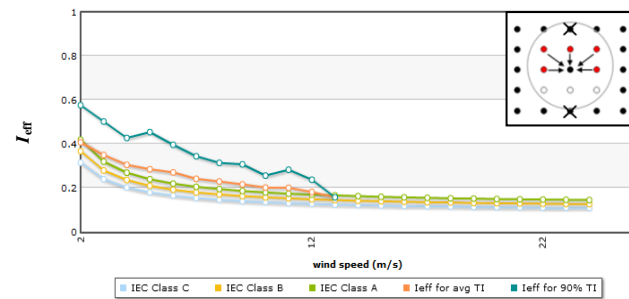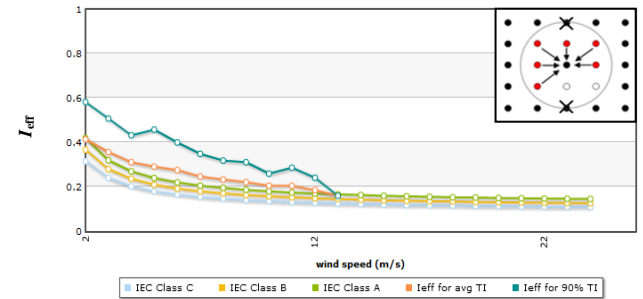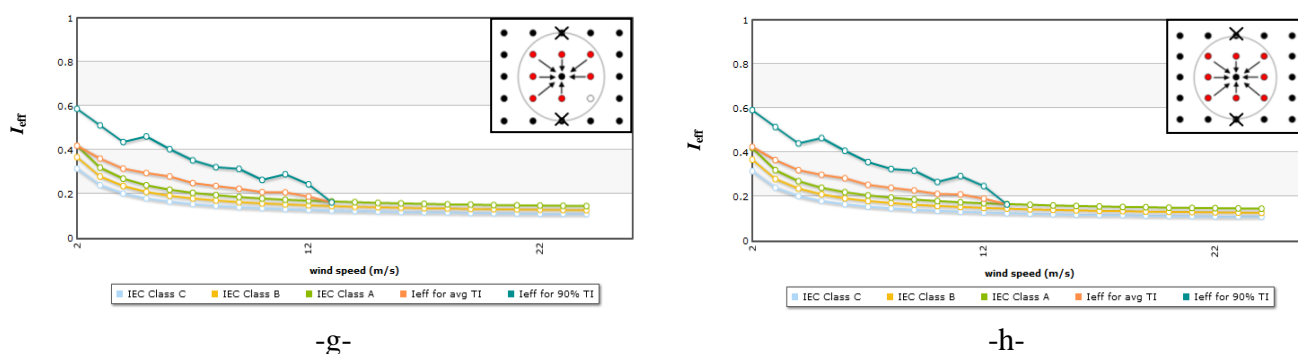
**Fig. 3.57 The effect of different numbers of neighbouring turbines on the $I_{\text{eff}}$ at Nasiriya site 2010, $\dot{m}$=10.**

**Table 3.28: The $I_{\text{eff}}$ at different wind speeds and number of neighbors.**

| $\bar{v}$ m/sec | 5 | 6 | 7 | 8 | 9 | 10 | 11 | 12 | 13 | 14 | 15 |
|---|---|---|---|---|---|---|---|---|---|---|---|
| **Case** | Zero neighbouring turbines | | | | | | | | | | |
| $I_{\text{eff}}$ at $TI_{50}$ | 0.22 | 0.21 | 0.17 | 0.16 | 0.15 | 0.13 | 0.14 | 0.11 | 0.05 | 0 | 0 |
| $I_{\text{eff}}$ at $TI_{90}$ | 0.43 | 0.37 | 0.31 | 0.28 | 0.28 | 0.21 | 0.25 | 0.20 | 0.05 | 0 | 0 |
| **Case** | 8 neighbouring turbines, 4 D | | | | | | | | | | |
| $I_{\text{eff}}$ at $TI_{50}$ | 0.30 | 0.28 | 0.25 | 0.24 | 0.23 | 0.21 | 0.21 | 0.19 | 0.16 | 0 | 0 |
| $I_{\text{eff}}$ at $TI_{90}$ | 0.46 | 0.41 | 0.36 | 0.33 | 0.32 | 0.27 | 0.29 | 0.25 | 0.16 | 0 | 0 |

iii.    *$I_{\text{eff}}$ for different distances to neighbouring turbines*

In this section, we will examine how $I_{\text{eff}}$ depends on the distance between reference turbine and neighbouring turbines. **Fig. 3.58** illustrates the fact that increasing in the distance between the reference turbine and the one located at the northern direction will be accompanied by decreasing in $I_{\text{eff}}$ values. The increment in distance is related to rotor diameter of reference turbine represented by D. When the distance becomes 10 times the rotor diameter, the wake effect will be canceled and the reference turbine will be affected by ambient turbulence intensity only (see **Fig. 3.58** c & d).

a- at 5D



c- at 10D



b- at 8D



d- at 15D
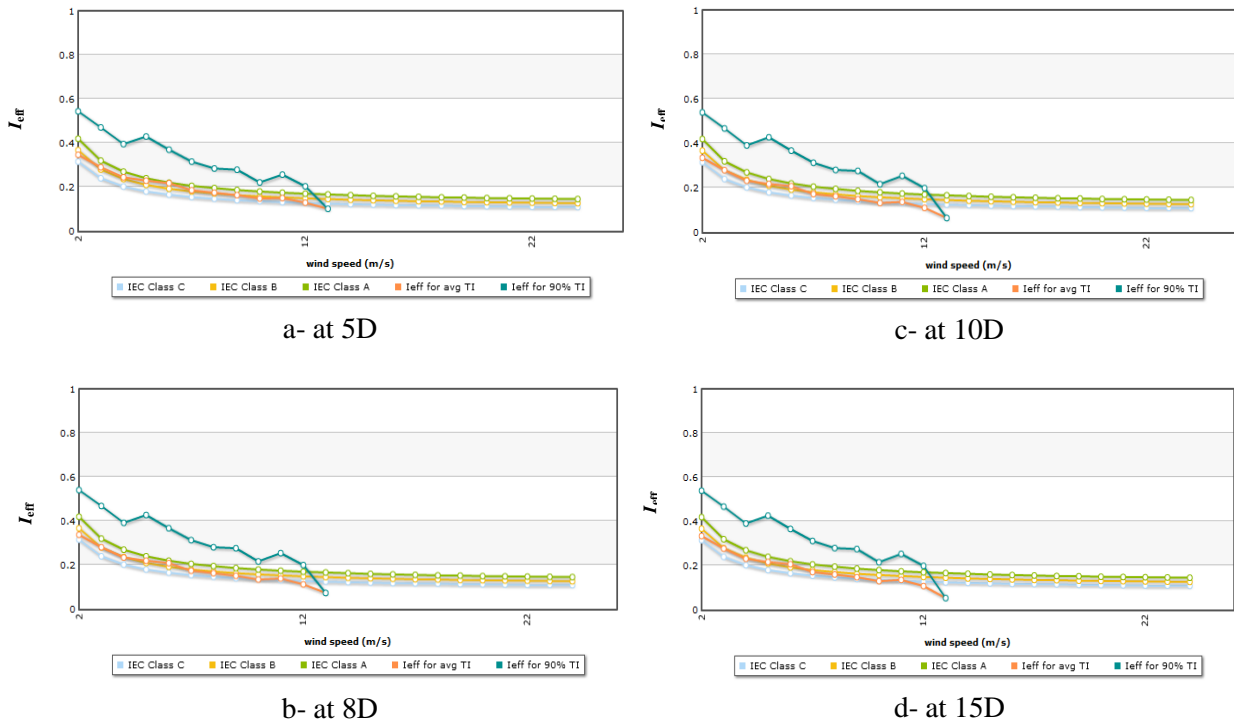
**Fig. 3.58 The effect of one neighbor turbine located at different distances from the reference turbine at Nasiriya site-2010, $\dot{m}$=10.**

Numerical $I_{\text{eff}}$ for $50^{\text{th}}$ and $90^{\text{th}}$ percentile values of *TI* drawn in **Fig. 3.58** (a, c, and d) is given in **Table 3.29** below. This table shows how $I_{\text{eff}}$ changes its values with increasing distance between reference and effective wind turbines, also its obvious that $I_{\text{eff}}$ has no change in its values when distance becomes more than 10 times rotor diameters.

**Table 3.29: The effective turbulence intensity at different wind speeds and neighbor distance from the reference turbine.**

| $\bar{v}$ m/sec | 5 | 6 | 7 | 8 | 9 | 10 | 11 | 12 | 13 | 14 | 15 |
|---|---|---|---|---|---|---|---|---|---|---|---|
| **Case** | 1 Turbine located at north site and 5 D distance from reference one | | | | | | | | | | |
| $I_{\text{eff}}$ at $TI_{50}$ | 0.23 | 0.22 | 0.19 | 0.17 | 0.16 | 0.15 | 0.15 | 0.13 | 0.10 | 0 | 0 |
| $I_{\text{eff}}$ at $TI_{90}$ | 0.43 | 0.37 | 0.32 | 0.28 | 0.28 | 0.22 | 0.26 | 0.20 | 0.10 | 0 | 0 |
| **Case** | 1 Turbine located at north site and 10 D distance from reference one | | | | | | | | | | |
| $I_{\text{eff}}$ at $TI_{50}$ | 0.22 | 0.21 | 0.17 | 0.16 | 0.15 | 0.13 | 0.14 | 0.11 | 0.05 | 0 | 0 |
| $I_{\text{eff}}$ at $TI_{90}$ | 0.43 | 0.37 | 0.31 | 0.28 | 0.28 | 0.22 | 0.25 | 0.20 | 0.05 | 0 | 0 |

| Case-c | 1 Turbine located at north site and 15 D distance from reference one | | | | | | | | | | |
|---|---|---|---|---|---|---|---|---|---|---|---|
| $I_{eff}$ at $TI_{50}$ | 0.22 | 0.21 | 0.17 | 0.16 | 0.15 | 0.13 | 0.14 | 0.11 | 0.05 | 0 | 0 |
| $I_{eff}$ at $TI_{90}$ | 0.43 | 0.37 | 0.31 | 0.28 | 0.28 | 0.22 | 0.25 | 0.20 | 0.05 | 0 | 0 |

### iv.    $I_{eff}$ *for different sectors for 8 neighbour turbine*

Finally, the representation of $I_{eff}$ for eight different sectors at Nasiriya site throughout the year 2010 is given in **Fig. 3.59**. The Wohler exponent is taken as $\dot{m}=10$, the distance from northern, eastern, southern, and western turbines to the reference one is taken as 4 times rotor diameter, while the distance from the reference one to those at corners is subject to Pythagoras law (i.e. 8 neighbouring turbines). **Table 3.30** shows the values of $I_{eff\_s}$ for each sector in **Fig. 3.59** beside total $I_{eff}$ at bin 9m/sec (founded by **Eq. 2.135)**.
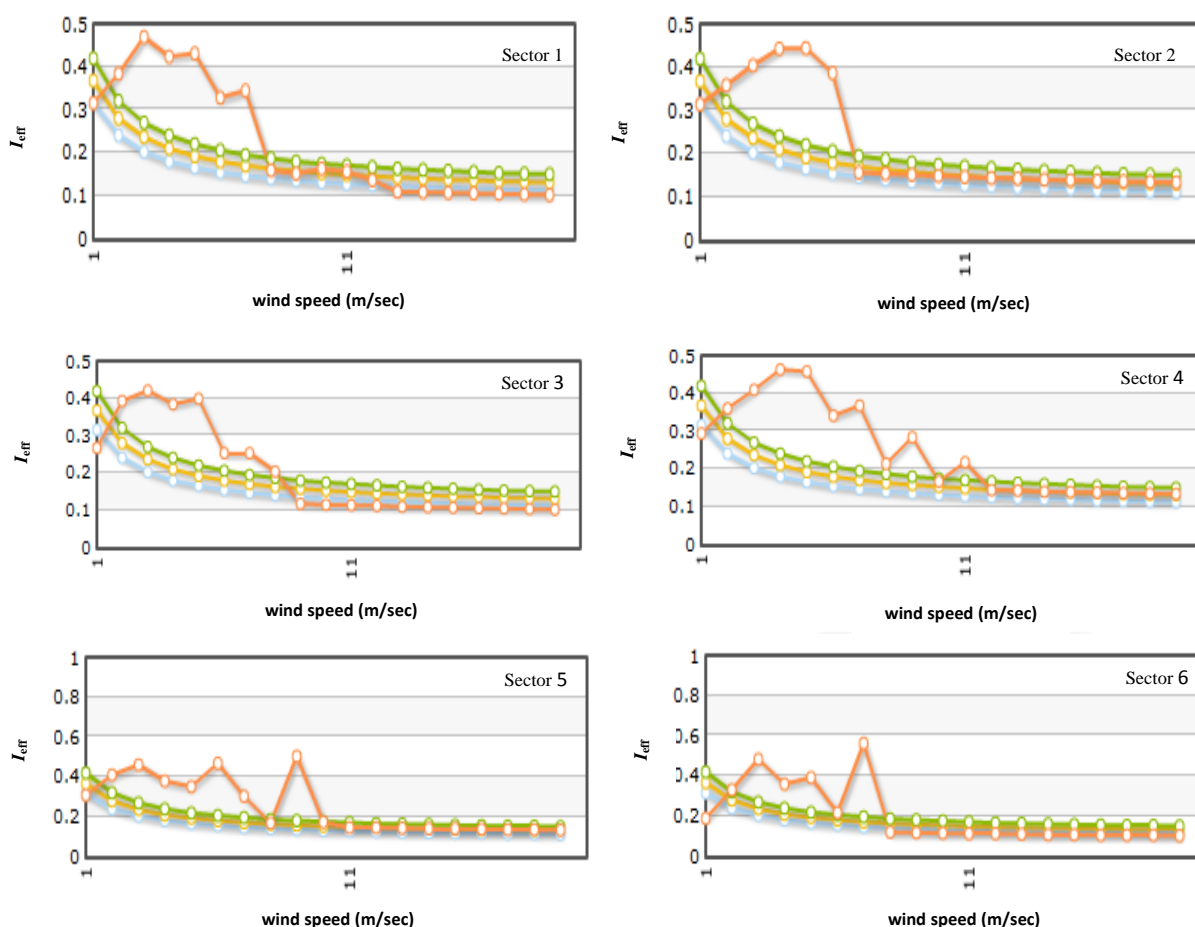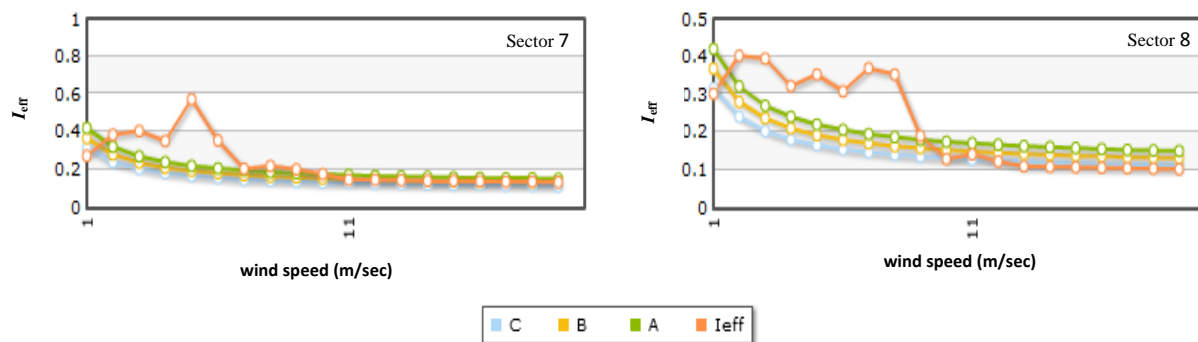
**Fig. 3.59 Effective turbulence intensity at different sectors.**

**Table 3.30: $I_{eff\_s}$ for 8 sectors and total $I_{eff}$ at bin 9m/s (where $\dot{m}$=10, D=71m, 8 turbines).**

| Sector | 1 | 2 | 3 | 4 | 5 | 6 | 7 | 8 |
|---|---|---|---|---|---|---|---|---|
| Angle (centered) | 0 | 45 | 90 | 135 | 180 | 225 | 270 | 315 |
| $I_{eff\_s}$% | 15.1 | 15.1 | 11.7 | 28.4 | 50.3 | 11.7 | 20.0 | 18.9 |
| $(I_{eff\_s})$^$\dot{m}$ | 6.3e-9 | 6.2e-9 | 4.9e-10 | 3.4e-6 | 1.0e-3 | 4.9e-10 | 1.0e-7 | 5.9e-8 |
| $f_{\_s}$% | 18.4 | 2.9 | 6.7 | 9.2 | 4.4 | 3.2 | 16.4 | 32.0 |
| No. samples | 1605 | 253 | 584 | 802 | 386 | 279 | 1431 | 2798 |
| $I_{eff\_total}$ | 0.58 | | | | | | | |

## 3.21 Economics

Economics are analyzed into three divisions, namely

### 3.21.1 Calculating the cost per kilowatt-hour

In general, the calculation is obtained simply from the total cost of installing and running the turbine divided by the number of kilowatt-hours generated over the turbine lifetime. In details, the needed inputs are represented by the cost of the turbine including installation costs and annual maintenance costs. The costs of electricity (Cents/kWh) generated by SUZLON S64-950 turbine in the preceding five areas are given in table below (**Table 3.31**), where the turbine cost is $1,200,000, maintenance cost as $12000 (1%), and installation cost as $60000 (5%). After entering the preceding costs into **Eq. 2.136**, the numerator is equal to $1,500,000 (where turbine and other costs =$1,260,000).

**Table 3.31: The cost per kilowatt hour for wind energy at specific sites.**

| At 57m height | Ali Al-karbee | Baghdad | Basrah | Nasiriya | Kerbala |
|---|---|---|---|---|---|
| Ann. Ene. (kWh) | 1534516 | 751988 | 3010194 | 3856869 | 2930388 |
| For 20 years (kWh) | 30690320 | 15039760 | 60203880 | 77137380 | 58607760 |
| Cent/kWh | 4.8 | 10 | 2.5 | 2 | 2.6 |

Because of the wide variety of economic analysis in different countries and states, it is impossible to include all of them in a single table. Thus, the economics of the electricity produced by a turbine could be represented by figures. All proceeding entries are used and the result is shown in **Fig. 3.60** for Ali Al-karbee. From this figure, it is obvious how the cost per kilowatt-hour is reduced from approximately \$4.8 at wind speed 5m/sec to \$1.4 at wind speed 10 m/sec.
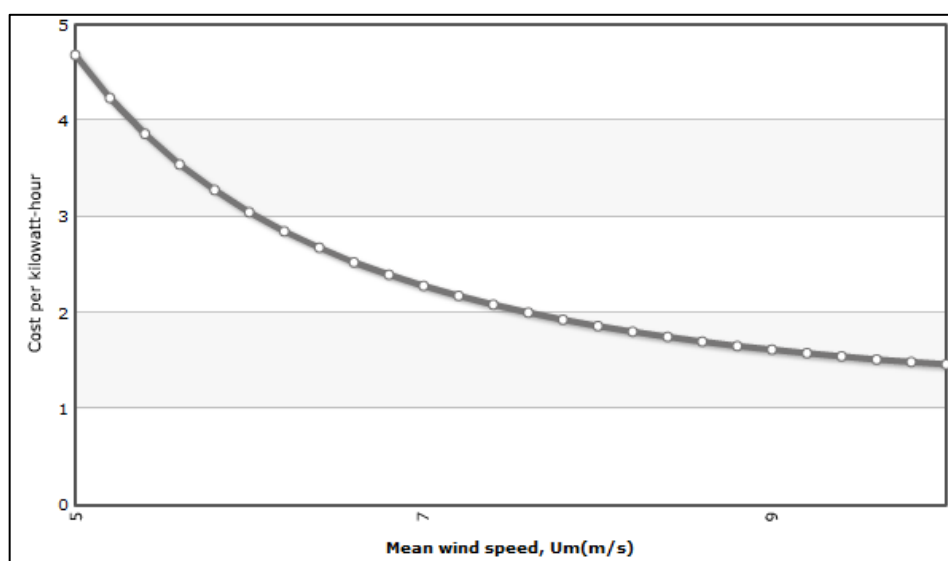


**Fig. 3.60 The coast per kilowatt-hour.**

### 3.21.2 Total returns to total cost ratio

Below in **Fig. 3.61** which is an example for SUZLON S64-950 turbine. The turbine cost, installation costs and annual maintenance costs is taken as above, but the reference price has been adjusted to 4.8Cent/kWh just like in Ali Al-karbee. After entering the preceding costs, the total return to the total cost ratio as a function of the mean wind speed is given in graphical form (**Fig.3.61**).

Any increase in wind speed is accompanied by an increase in output power, which in turn causes an increment in y-axis ratio according to **Eq. 2.137.**
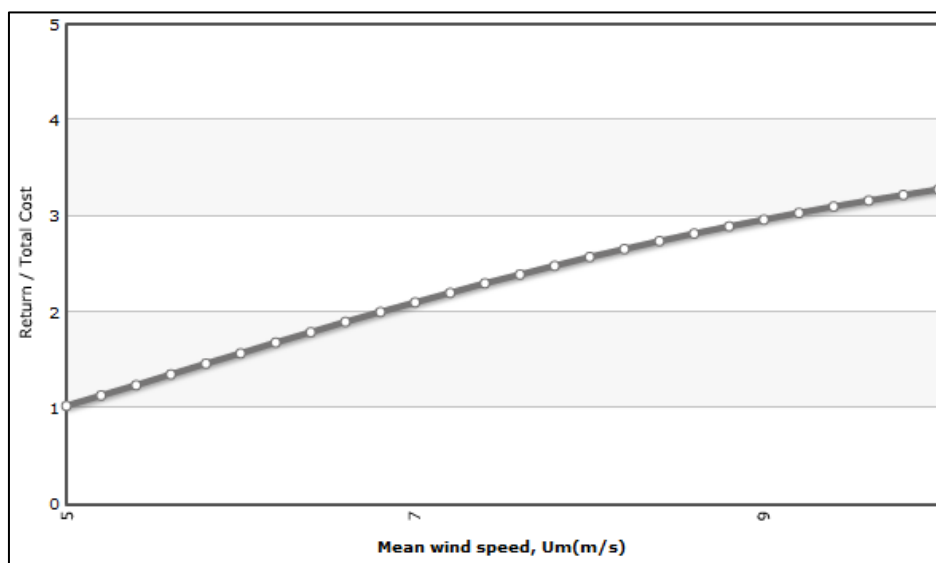


**Fig. 3.61 Total return to the total cost.**

### 3.21.3 Calculating the payback time

In order to estimate how long it will take to recover the cost of an investment in a wind turbine graphically, **Fig. 3.62** below demonstrates the payback period. Taking the same costs in above, **Fig. 3.62** shows the extent of the importance of increasing the mean wind speed, such that the recovering cost is reduced from approximately 9 years at wind speed 5 m/sec to 5 years at the wind speed of 10 m/sec for that type of turbine.
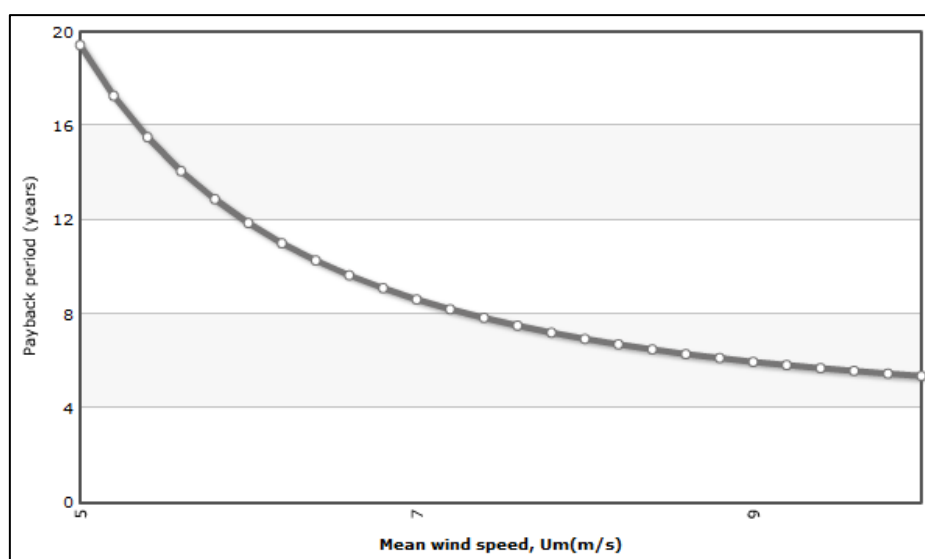


**Fig. 3.62 The payback period.**

# Chapter Four

# CHAPTER FOUR

## *Conclusions and Suggestions for Further Works*

### 4.1 Conclusion

From the calculated results and preceding studies, the following conclusions could be drawn:

1- The use of two parameter Weibull pdf to estimate wind potential energy at a given site, gives good results according to several studies, related softwars, the international standard IEC 61400-12, and other international recommendations.

2- The accuracy of wind speed distribution representation is very important condition due to the irregular nature of wind. Therefore nine techniques are tested in order to find the most suitable model for Weibull parameters estimation. The comparisons show that the EEM surpasses other techniques in power estimation.

3- Weibull shape parameter is important factor, because it is determining C.V. or $\sigma_v/\bar{v}$ values (**Eq. 3.1**), by which it is possible to calculate Weibull scale parameter directly through simple equation, and *k* estimates reference wind speed in order to determine wind turbine class at a site through **Tables 2.6, 2.7,** and **2.8** (**Appendix 4**).

4- Extrapolation of wind speed through power or logarithmic laws gives an adequate result for power estimation, while using Weibull parameters extrapolation equations give overestimate estimation.

5- Under studied circumstances, large wind turbines will suffer from larger amount of strain and loadings due to the frequent occurrence of rapid wind changes that is to be expected in turbulent environments, but the extreme loadings on the construction will be smaller due to the lower mean wind

speeds (because extreme load has direct proportionality to mean wind speed).

**6-** Turbulence intensity at 15m/s was calculated for Nasiriya and Kerbala sites and they equal to zero. Thus, turbine with category C is sufficient to cover turbulence at those sites.

**7-** There is a large amount of very low $\sigma_v$ at low wind speeds, corresponding to the presence of small amounts of turbulent eddies. Thus much of the mechanically produced turbulence near the surface has vanished instantly because the slow growth of $\sigma_v$ with increasing wind speed results in low turbulence intensities.

**8-** The observations from Nasiriya and Kerbala sites show that the flow and turbulence characteristics of terrain deviate slightly from what is estimated by the NTM, as it is defined for the standard LWT and SWT classes, and that is beyond the roughness of the site.

**9-** Turbulence increases the output power from a wind turbine, at the same time increases fatigue load and periodic maintenance, which reduces the turbine life and increases turbine total cost.

**10-** In this study, the wake interference effects on the performance characteristics of a wind turbine are investigated. Different number of turbines with similar model and the same rotor diameter were used. From the results it could be concluded that the power losses for a turbine operating in the wake of another depend on the distance between the turbines and their operating conditions. Compared with the unobstructed turbine, the thrust of the downstream turbine is significantly lower. The reduction in power and thrust coefficients for the downstream turbine is a result of the lower free stream speed than the upstream turbine and thus, less energy is available in the flow. However, by adjusting the turbines geometry and sizes in a farm the output power from the downstream turbine can be substantially increased.

11- The square layout wind farm is not recommended due to the drop in the extracted energy that could reach 35% due to the wake effect**, [Hus13]**. This means installing wind turbines inside the wind farm surrounded by other turbines should be avoided due to the higher effect of the wake on the performance of the wind farm.

12- Increasing mean wind speed at a site will increase the total returns ratio besides decreasing the payback time and cost unit of electricity.

13- From the feasibility study, it is possible to say that the turbine SUZLON S64-950 has low cost per kilowatt hour for each of Nasiriya, Basrah, and Kerbala. While each of karbee and Ali Al- Baghdad has medium and high cost of energy, respectively. This arrangement is beyond to power output and number of generation hours of each site.

## 4.2 Suggestions for Further Works

This section recommends some future research directions as follows:

1- The thesis uses wind speed data series recorded at Iraqi Meteorological Organization and Seismology in addition to Weather Underground website. For more accurate results, masts dedicated for wind energy applications must be setup.

2- Conventional probabilistic distributions of wind speed can not accurately represent all wind regimes observed in a region. Thus, several kinds of mixture probability functions could be applied to estimate wind energy potential, such as the bimodal Weibull function (WW) and mixture Gamma–Weibull function (GW).

3- Equipment failure or extreme weather events can result in incomplete data series which it is necessary for analysis and calculations. Thus, it is desirable to have complete wind speed time series for a period of time. Therefore, data estimation is necessary process to compensate missing data values.

**4-** The procedure of determining if a site is suitable for wind power production requires reliable long-term data. This can be achieved by measuring the wind speed for a short time period, e.g. a year, then, regenerate data using a Measure-Correlate-Predict (MCP) method.

**5-** Estimate environmental conditions such as extreme wind, flow inclination and vertical wind shear. These parameters are needed in order to select the optimal turbine for selected site.

**6-** Compare the turbulence intensity difference between two small wind turbines installed at two sites, the first one installed in a complex environment (urban site above a rooftop), second one in uniform area. The turbulence data is analyzed and the results are compared to the normal turbulence model (NTM) of standard SWT classes (IEC 61400-2 Design requirements for small wind turbines).

**7-** Frandsen model has been used in the wake study using Visual Basic program. Thus, wake effect could be extended using other models such as Jensen or Larsen models.

**8-** Studying the effect of atmospheric stability and the effect of hub height on power production are recommended for wake effect. Also, the study could be extended to include the effect of turbine yaw and material of blade.

**9-** The wake effects largely rely on the thrust coefficients of the turbines. These thrust coefficients can be given by the manufacturer or can be calculated with an adequate simulation software. But, if the thrust coefficient for the wind turbines is not known, a generic value $C_T = 7c/V_{hub}$, where c is a constant equal to 1m/s can be used. For future study, you could apply both the real turbine specific thrust coefficient and the generic thrust coefficient and compare the results.

# References

# References

[Sha12] Shaw S. D., "*Development and Validation of the Wind Energy Calculator (WEC) For Use As A Module in the Larger Complimentary Energy Decision Support Tool (CEDST) Project*", M.Sc. Thesis, University of Guelph, 2012.

[And07] Andrews J, and Jelley N., "*Wind Power. Energy Science, Principles, Technologies and Impacts*", New York (USA), Oxford University Press Inc., pages 99-130, 2007.

[Alk07] Al-Karaghouli A., "*Current status of renewable energies in the middle east-north african region*", Federal Ministry for the Environmental, Nature Conservation and Nuclear Safety, 2007.

[REN14] REN21 Community, "*Renewables 2014-Global Status Report*", Renewable Energy Policy Network for the 21st century, Paris, 2014.

[Sha13] Shaban A. H., "*Optimum Site Selection of Windmills-Turbine in Iraq Utilizing Remote Sensing and GIS Techniques*", Ph.D. Thesis, University of Baghdad, College of Science, Department of Physics, 2013.

[Jou14] Joudah H. G., "*The Variance of Wind Properties and Their Usability in Producing Electric Power South Latitude 33o in Iraq*", M.Sc. Thesis, Al-Mustansiriyah University, College of Education, Geography Department, 2014.

[Kaz12] Kazem H. A., Chaichan M. T., "*Status And Future Prospects of Renewable Energy in Iraq*", Renewable and Sustainable Energy Reviews, Vol.16, 6007–6012, 2012.

[Ahm10] Ahmed S. T., "*Review of Solar Energy and Alternative Energies Applications in Iraq*", the first conference between Iraqi and Germany universities DAAD, Arbil, Iraq, 2010.

[Cor78] Corotis R. B., Sigl A.B., Klein J., "*Probability Models of Wind Velocity Magnitude and Persistence*", Solar Energy, 20:483–93, 1978.

[Koe82] Koeppl G. W., "*Putnam's Power from the Wind*", 2rd ed., New York, Van Nostrand Reinhold, 1982.

[Oli97] Oliva R. B., "*Result After First Year of Automated Wind Measurements in Santa Cruz, Southern Patagonia*", Wind Engineering, 21:113–24, 1997.

[Cha01] Chadee J. C. and Sharma C., "*Wind Speed Distributions: A New Catalogue of Defined Models*", Wind Engineering, 25:319–37, 2001.

[Sin09] Sinan A. and Ebru K. A., "*Estimation of Wind Energy Potential Using Finite Mixture Distribution Models*", Energy Conversion and Management, 50:877–884, 2009.

[Cha11] Chang T.P., "*Estimation of Wind Energy Potential Using Different Probability Density Functions*", Applied Energy 88:1848–1856, 2011.

[Wuj13] Wu J., Jie W., Dezhong C., "*Wind Energy Potential Assessment for the Site of Inner Mongolia in China*", Renewable and Sustainable Energy Reviews, 21:215–228, 2013.

[Pel78] Pelka D.G., Robert T. P., Runbir S., "*Energy from the Wind*", American Journal of Physics, Vol. 46, Issue 5, pp. 495, May 1978.

[Ric93] Richardson, R.D. and McNerney G.M., "*Wind Energy Systems*", Proceedings of the IEEE, Vol. 81 , Issue 3, 1993.

[Ahm04] Ahmed M.A. and Ahmed F., "*Assessment of Wind Power Potential for Coastal Areas of Pakistan*", Turkish Journal of Physics, Vol.30, pp.127-135, 2006.

[Sov13] Sovacool B.K., "*The Avian Benefits of Wind Energy: A 2009 Update*", Renewable Energy, Vol. 49, pp.19-24, 2013.

[Scr71] Scruton C. and Rogers E.W., "*Wind Effect on Buildings and Other Structures*", Philosophical Transactions of the Royal Society of London, A.269, pages 353-383, 1971.

[Ell90] Elliot D. L. and Cadogan J. B., "*Effects of Wind Shear and Turbulence on Wind Turbine Power Curves*" European Community Wind Energy Conference and Exhibition. Madrid, Spain, September 10-14, 1990.

[Par06] Park M. and Park S., "*Effects of Topographical Slope Angle and Atmospheric Stratification on Surface Layer Turbulence*", Boundary Layer Meteorology, Springer, 118, pp.613-633, 2006.

[Rod10] Rodrigues C. V., Matos J. C., Paiva L. T., Palma J. M., "*Analysis of the Similarity in Turbulence Intensity and Wind Shear as Function of the Wind Velocity: Field Measurements and Numerical Results*", European Wind Energy Conference, Warsaw, Poland, pp 20–23, Apr. 2010.

[Ern12] Ernst B. and Seume J. R.," *Investigation of Site-Specific Wind Field Parameters and Their Effect on Loads of Offshore Wind Turbines*", Energies, Vol.5, pp.3835-3855; 2012.

[Ell91] Elliott D.L., "*Status of Wake and Array Loss Research*" Wind power Conference, Palm Springs, California, 24-27, Sep. 1991.

[Hua06] Huang H.S. and Chiang C.T., "*Reliability Worth Assessment of Distribution System with Large Wind Farm Considering Wake Effect*", Power India Conference, 2006.

[Yon10] Yongxing L. and Xinxin F., "*Wake Flow Theories and Model Development for Wind Turbines*", Power and Energy Engineering Conference (APPEEC), Asia, Mar. 28-31, 2010.

[Hus13] Husiena W., Wedad E., Dekam E., "*Effect of the Wake Behind Wind Rotor on Optimum Energy Output of Wind Farms*", Renewable Energy, Vol.49, pp.128-132, 2013.

[Ala86] Al-Azzawi S.I. and Zeki N.A., "*The Wind Power Potential in Iraq*", 1986, Cited by [Mod07]

[Rad87] Radwan A., "*Wind Energy in Saudi Arabia*", In Alternative Energy Sources, Vol. 3, 1987.

[Dar88] Darwish A. S. and Sayigh A. A., "*Wind Energy Potential in Iraq*", Journal of Wind Engineering and Industrial Aerodynamics, Vol.27, pp.179-189, 1988.

[Pal91] Pallabazzer R . and Gabow A., "*Wind Resources in Somalia*" Solar Energy, Vol. 46, Issues 5, pp.313-320, 1991.

[Hbb00] Abboud B. A., "*The Exploitation of Renewable Energies in the Planning of Remote Human Settlements*"; M.Sc. Thesis, University of Baghdad, Center for Urban and Regional Planning, 2000.

[Hir06] Hirat I. A., "*Disparity of Wind Directions and its Types in Iraq*", Ph.D. Thesis, Al-Mustansiriya University, College of Education, Department of Geography, 2006.

[Moh07] Mohammed G. K. and Aboelyazied M. K., "*Wind Turbines Power Curve Variability*", Renewable Energy, Vol.209, pp.230-237, 2007.

[Ali07] Ali E., Moubayed A., and Outbib N., "*Comparison Between Solar and Wind Energy in Lebanon*", Proc. of 9th Int. Conf. on Electrical Power Quality and Utilization, Barcelona, 2007.

[Aza10] Azad A. K., Alam M. M., and Rafiqul I. M., "*Statistical Analysis of Wind Gust at Coastal Sites of Bangladesh*" International Journal of Energy Machinery, Vol.3, No.1, pp.9-17, 2010.

[Ahr01] Ahrens C. D., "*Essentials of Meteorology - An Invitation to the Atmosphere*", 3rd edition, Brooks/Cole, 2001.

[Mat06] Mathew S., "*Wind Energy Fundamentals, Resource Analysis and Economics*", Springer-Verlag, Berlin Heidelberg 2006.

[Dan10] Dan C., "*Wind Power Basics*", Canada, Friesens, Apr. 2010.

[Lif] http://life-experimental.net/2013/11/24/continental-vs-oceanic-weather-patterns/

[Was] Wind Atlas Analysis and Application Program (WAsP) help facility, Version 10.

[Bro12] Brower M. C., "*Wind Resource Assessment*", A Practical Guide to Developing a Wind Project, John Wiley & Sons Inc., 2012.

[Man02] Manweel J. F., McGowan J. G., and Rogres A. L., "*Wind Energy Explained-Theory, Design and Application*", John Wiley & Sons, 2002.

[Gar06] Gary L. J., "*Wind Energy Systems*", Electronic Edition, October 2006.

[Pat06] Patel M. R., "*Wind and Solar Power Systems-Design, Analysis, and Operation*", 2nd edition, CRC Press Taylor & Francis Group, 2006.

[Wuj13] Wu J., Jianzhou W., and Dezhong C., "*Wind Energy Potential Assessment for the Site of Inner Mongolia in China*", Renewable and Sustainable Energy Reviews 21, pp. 215–228, 2013.

[Nan04] Nancy R. T., "*Seven Basic Quality Tools*", the Quality Toolbox Milwaukee, Wisconsin: American Society for Quality. p.15, Retrieved 2010-02-05, 2004.

[Qam09] Qamar Z. C., "*An Investigation on Wind Power Potential of Gharo-Sindh, Pakistan*", Pakistan Journal of Meteorology, Vol.6, Issue 11, July 2009.

[Tak] Takeshi Kamio, Makoto Iida, and Chuichi Arakawa, "*Influences of the Estimating Methods on Weibull Parameter for Wind Speed Distribution in Japan*", Italy, European Wind Energy Conference & Exhibition MIC – Milano Convention Centre, 7-10 May, 2007.

[Aza11] Azad, A. K., and Manabendra S., "*Weibull's Analysis of Wind Power Potential at Coastal Sites in Kuakata, Bangladesh*", International Journal of Energy Machinery, Vol.4, No.1, pp.36-45, 2011.

[Aza12]  Azad A. K., and Alam M. M., "*Analysis of Wind Power Potential in Sandwip Sea belt of Bangladesh*", Proceedings of IEEE, 2nd International Conference on the Developments in Renewable Energy Technology, Dhaka, Bangladesh, pp.143-146, 2012.

[Sun12] Sunday O. O., Adaramola M. S., and Paul S. S., "*Analysis of Wind Speed Data and Wind Energy Potential in Three Selected Locations in South-East Nigeria*", International Journal of Energy and Environmental Engineering, 3:7, 2012.

[Mod07] Mohammad A. I., "*Wind Energy Assessment in Iraq*", Ph.D. Thesis, Al-Mustansiriya University, College of Science, Department of Atmospheric Sciences, 2007.

[Ulg02] Ulgen K. and Hepbasli A., "*Determination of Weibull Parameters for Wind Energy Analysis of Izmir, Turkey*", International Journal of Energy Research, 2002.

[Bry06] Bryan D., "*The Weibull Analysis Handbook*", 2nd ed., ASQ American Society for Quality 2006.

[Lys83] Lysen E. H., "*Introduction to Wind Energy*", Development corporation information department, 2nd edition, 1983.

[Rei11] Reiszadeh M. and Motahar S., "*The Wind Energy Potential in The Coasts of Persian Gulf Used in Design and Analysis of A Horizontal Axis Wind Turbine*", World Renewable Energy Congress, Wind Energy Applications, Sweden, 8-13, May, pp.4059-4065, 2011

[Odo12] Odo F.C., and Akubue G.U., "*Comparative Assessment of Three Models for Estimating Weibull Parameters for Wind Energy Applications in a Nigerian Location*", International Journal of Energy Science (IJES) Vol.2, No.1, pp.22-25, 2012.

[Ayo12] Ayodele T.R., Jimoh A.A., Munda J.L., Agee J.T., "*Statistical analysis of wind speed and wind power potential of Port Elizabeth using Weibull parameters*" Journal of Energy in Southern Africa Vol.23, No.2, May 2012.

[Sal13] Salahaddin A. A., "*Comparative Study of Four Methods for Estimating Weibull Parameters for Halabja, Iraq*", International Journal of Physical Sciences Vol.8, No.5, pp.186-192, February 2013.

[Ibr13] Ibraheem A. A., "*Graphical and Energy Pattern Factor Methods for Determination of the Weibull Parameters for Ali Algharbi Station, South East of Iraq*", Eng. & Tech. Journal.Vol.31, No.1, 2013.

[Myu03] Myung I. J., "*Tutorial on Maximum Likelihood Estimation", Journal of Mathematical Psychology*", 47, pp.90–100, 2003.

[Par10] Paritosh B. and Rakhi B. B., "*A Study on Weibull Distribution for Estimating the Parameters*", Journal of applied quantitative methods, Vol.5 No.4, Shantiniketan, India, 2010.

[Vey05] Y. Veysel, ARAS H., H. E. ÇELİK, "*Statistical Analysis of Wind Speed Data*", Eng. & Arch. Fac. Eskişehir Osmangazi University, Vol. XVIII, No. 2, 2005.

[Ahm09] Ahmad S., Wan W. M. A., Bawadi M. A., and Sanusi M. S. A., "*Analysis of Wind Speed Variation and Estimation of Weibull Parameters for Wind Power Generation in Malaysia*", M.Sc. Thesis, School of Civil Engineering, University of Science Malaysia, 2009.

[Rin09] Rinne H., "*The Weibull Distribution*", Taylor & Francis Group, LLC Chapman & Hall/CRC, 2009.

[Sil05] Silva G., Pereira A., Faro D., Feitosa E., "*On the Accuracy of the Weibull Parameters Estimators*", Brazilian Wind Energy Centre, Federal University of Pernambuco, Coletânea de Artigos-Energia Solar e Eólica, Vol.2, 2005.

[Lao12] laofe Z. O., Folly K. A., Zaccheus O. O., "*Statistical Analysis of the Wind Resources at Darling for Energy Production*", International Journal of Renewable Energy Research, Vol.2, No.2, 2012.

[Alb06] Al-Buhairi M. H., "*A Statistical Analysis of wind Speed Data and An Assessment of Wind Energy Potential in Taiz-Yemen*", Assiut University Bulletin For Environmental Researches, Vol.9, No.2, October 2006.

[Kol12] Kollu R., Rayapudi S. R., Narasimham S.V., and Krishna M. P., "*Mixture Probability Distribution Functions to Model Wind Speed Distributions*", International Journal of Energy and Environmental Engineering 3:27, 2012.

[Hos11] Hossain M. S., "*Investigating Whether the Turbulence Model from Existing Small Wind Turbine Standards is Valid for Rooftop Sites*", M.Sc. Thesis, School of Engineering and Energy, Murdoch University, Feb. 2011.

[Car11] Carpman N., "*Turbulence Intensity in Complex Environments and its Influence on Small Wind Turbines*", M.Sc. Thesis, Department of Earth Sciences, Uppsala University, Department of Earth Sciences, Sweden, 2011.

[Yan06] Yanlian Z., Xiaomin S., Zhilin Z., Renhua Z., Jing T., Yunfen L., Dexin G., and Guofu Y., "*Surface Roughness Length Dynamic Over Several Different Surfaces And Its Effects On Modeling Fluxes*", Science in china Series, Earth Sciences Vol.49, pp.262-272, 2006.

[Gas12] Gasch R., and Twele J., "*Wind Power Plants-Fundamentals, Design, Construction and Operation*", 2$^{nd}$ edition, Springer, 2012.

[Ern12] Ernst B., and Seume J. R., "*Investigation of Site-Specific Wind Field Parameters and Their Effect on Loads of Offshore Wind Turbines*", Vol.5, pp.3835-3855, 2012.

[Rag12] Ragheb M., "*Wind Shear, Roughness Classes and Turbine Energy production*", Available at: https://netfiles.uiuc.edu/mragheb (Accessed: 14 August 2012).

[Sil06] Silva J., Ribeiro C., Guedes R., "*Roughness Length Classification of Corine Land Cover Classes*", Megajoule Company publications – for renewable energy consultancy, 2007.

[Ros98] Rosen K. "*An Assessment of Potential for Utility Scale Wind Power Generation in Eritrea*", M.Sc. Thesis, San Jose State University, 1998.

[Dav12] Davis C. J., "*Computational Modeling of Wind Turbine Wake Interactions*", M.Sc. Thesis, Department of Civil and Environmental Engineering, Colorado State University, 2012.

[IEC05] IEC61400-1, "*Wind Turbines – Design Requirements*", 3$^{rd}$ ed., International Standard, 2005.

[Cir13] Circe (research center for energy resources and consumption), "*Characterization of Wind Resources*", Zaragoza. Apr**.** 2013.

[Gip04] Gipe P., "*Wind Power: Renewable Energy for Home, Farm, and Business*", Chelsea Green Publishing, 2004.

[Jus78] Justus C.G., Hargraves W.R., Mikhail A. and Graber D., "*Methods for Estimating Wind Speed Frequency Distributions*", Journal of Applied Meterology,Vol.17, pp.350-353, Mar.1978.

[Dor78] Doran J. C. and Verholek M. G., "*A Note on Vertical Extrapolation for Weibull Velocity Distribution Parameters*", Journal of Applied Meteorology, Vol.17, Iss.3**,** pp.410-412, 1978.

[Ola12] Olayinka S. O. and Olaolu O. A., "*Assessment of Wind Energy Potential and the Economics of Wind Power Generation in Jos, Plateau State, Nigeria*", Energy for Sustainable Development, Vol.16, pp.78–83, 2012.

[Tem12] Temitope R. A., Adisa A. J., Josiah L. M., John T. A., "*Statistical Analysis of Wind Speed and Wind Power Potential of Port Elizabeth Using Weibull Parameters*", Journal of Energy in Southern Africa, Vol.23, No.2, May 2012.

[Enc] http://www.daviddarling.info/encyclopedia/S/AE_small_wind_electric_system_resource_evaluation.html, Encyclopedia of Alternative Energy.

[Par95] Parsa M.J. Mapdi M., "*Wind power statistics and evaluation of wind power density*", Renewable Energy, Vol.6, 5/6, pp.623-628, 1995.

[Min09] Minina A., "*Technical Wind Energy Potential in Russia*", M.Sc. Thesis, Appeenranta University of Technology, Faculty Of Technology, Bioenergy Technology, 2009.

[Par09] Paraschivoiu I., "*Wind Turbine Design – With Emphasis on Darrieus Concept*", Presses internationals Polytechnique, 2009.

[Ton10] Tong W., "*Wind Power Generation and Wind Turbine Design*", Witpress, Kollmorgen Corp., USA, 2010.

[Pow] http://www.wind-power-program.com.

[Doe05] DOE National Laboratory, "*Small Wind Electric Systems*", Consumer's Guide, Produced for the U.S. Department of Energy by the National Renewable Energy Laboratory, Mar. 2005.

[Fro10] Frohboese P., and Schmuck C., "*Thrust Coefficients Used for Estimation of Wake Effects for Fatigue Load Calculation*", European Wind Energy Conference, Warsaw, Poland, 2010.

[Nem11] Nemes C. and Munteanu F., "*The Wind Energy System Performance Overview: Capacity Factor vs. Technical Efficiency*", International Journal of Mathematical Models and Methods in Applied Sciences, Vol.5, pp.159-166, 2011.

[Win08] Windpower program Guide, "*Basic Concepts*", PelaFlow Consulting, 2008.

[Ewe09] European Wind Energy Association EWEA, "*Wind Energy - The Facts, a Guide to the Technology, Economics and Future of Wind Power*", London, Sterling, VA : Earthscan, 2009.

[Hug] Hughes T., "*Determining Wind Power Density and Wind Power Classes from Wind Speed Information*", Windpower Tutorial, Environmental Verification and Analysis Center, University of Oklahoma.

[Eri12] Erick B. A., João B. V., Humberto A. C., Lutero C. L. and Gerson P. A., "*Evaluation of the Wind Energy Potential of a Mountainous Region in the Ceará State, Brazil*", International Transaction Journal of Engineering, Management, & Applied Sciences & Technologies, Vol.3, No.1, 2012.

[Ahm12] Ahmed S. A., Mahammed H. O., "*A Statistical Analysis of Wind Power Density Based on the Weibull and Ralyeigh models of Penjwen Region Sulaimani/ Iraq*", Jordan Journal of Mechanical and Industrial Engineering, Vol.6, No.2, pp.135 – 140, Apr. 2012.

[Yan13] Yaniktepe B., Koroglu T., Savrun M.M., "*Investigation of Wind Characteristics and Wind Energy Potential in Osmaniye, Turkey*", Renewable and Sustainable Energy Reviews, 21, pp. 703–711, 2013.

[Sad12] Sadeghi M., Gholizadeh B., Gilanipour J. and khaliliaqdam N., "*Economic analysis using Wind energy, Case study Baladeh city, North of Iran*" International Journal of Agriculture and Crop Sciences, Vol.4, No.11, pp.666-673, 2012.

[Far12] Farh H. M., Eltamaly A. M., and Mohamed A. A., "*Wind Energy Assessment for Five Locations in Saudi Arabia*", International Conference on Future Environment and Energy, Vol.28, Singapoore, 2012.

[Elm09] Elmabrouk A. M., "*Estimation of Wind Energy and Wind in Some Areas (Second Zone) In Libya*", Department of Aeronautical Engineering, Al-Fateh University, Faculty of Engineering. Tripoli / Libya, Ecologic Vehicles Renewable Energy, Monaco, Mar. 26-29, 2009.

[Nie09] Nielsen M., Jørgensen H. E. and Frandsen S. T., "*Wind and Wake Models for IEC 61400-1 Site Assessment*", Risø DTU, National Laboratory of Sustainable Energy, Wind Energy Division, Denmark, 2009.

[Fra07] Frandsen S. T., "*Turbulence and Turbulence Generated Structural Loading in Wind Turbine Clusters*", Risø-R-1188(EN), by, Risø National Laboratory, Roskilde, Denmark, January 2007.

[IEC06] IEC, "*Wind turbines — Part 2: Design Requirements for Small Wind Turbines*", British Standard BS EN 61400-2, 2006,

[Bur01] Burton T., Sharpe D., Jenkins N., and Bossanyi E., "*Wind Energy Handbook*", John Wiley & Sons, Ltd, 2001.

[Nel09] Nelson V., "*Wind Energy Renewable Energy and the Environment*", Taylor & Francis Group, 2009.

[Pet98] Petersen E. L., Mortensen N. G., Landberg L., Hùjstrup J., and Frank H. P., "*Wind Power Meteorology Part I: Climate and Turbulence*", by; Department of Wind Energy and Atmospheric Physics, Riso National Laboratory, Denmark Wind Energy, Vol.1, pp.2-22, 1998.

[Mah11] Mahbub A. Z., Rehman S., Meyer J., and Al-Hadhrami L. M., "*Wind Speed and Power Characteristics at Different Heights for A Wind Data Collection Tower In Saudi Arabia*", World Renewable Energy Congress, Sweden, 8-13, pp. 4082-4089, May 2011.

[Mad08] Madsen P. H., "*Introduction to the IEC 61400-1 Standared*", Risø DTU, National Laboratory for Sustainable Energy, Aug. 2008.

[Mor11] Morten N., "*Presentation of Windfarm Assessment Tool*", Risø DTU, Dec. 2011.

[Ves11] Vestas, "*Wind Project Planning: Wind Turbine Classes*", Accessed Oct. 2011.

[Moh14] Mohammed A. Saleh, Ayad A. Ani, Firas A. Hadi "Ambient Turbulence Intensity Calculation for Al-Nasiriyah Province in Iraq", Iraqi Journal of Science, Vol.55, No.2A, pp.561-571, 2014.

[Rob12] Robichaud R., Fields J., and Owen R. J., "*Naval Station Newport Wind Resource Assessment*", NREL, Feb., 2012.

[DTU11] DTU - Denmark Technical University, "Turbulence Modeling : the IEC61400-1 Turbulence Model 2011", http://130.226.56.171/products/WAT/wathelp/WATmodelling.htm.

[Tan] Tanigaki S., Kogaki T., Matsumiya H., and Imamura H. "*Japanese Wind Turbulence Characteristics in Relation to Turbulence Model in IEC61400-1ed.3*", Warsaw Poland, European Wind Energy Conference & Exhibition, Tuesday 20 Friday 23 April 2010.

[Gia08] Giannì M., "*Turbulence Analysis using WindSim: Experiences in $I_{ref}$ Calculation*", User Guide, Tønsberg, pp.16-17, Jun. 2008.

[Lan11] Langreder W., Pedersen H. S., "*Vertical Extrapolation of Turbulence in Forests*", EWEA Brussels Belgium, Europe's Premier Wind Energy Event, 2011.

[Gau] Gaumond M., R´ethor´e P. E., Bechmann A., S Ott, G C Larsen, A Pe˜na and K S Hansen "*Benchmarking of Wind Turbine Wake Models in Large Offshore Wind Farms*", Denmark, DTU Wind Energy, Technical report.

[Mus13]  Musial W., Elliott D., Fields J., Parker Z., Scott G., and Draxl C., "*Assessment of Offshore Wind Energy Leasing Areas for the BOEM New Jersey Wind Energy Area*", NREL, Oct. 2013.

[Lon13] Longatt F. G., Wall P., Terzija V., "*Wake effect in Wind Farm Performance: Steady-State and Dynamic Behavior*", Renewable Energy Elsevier, 39, pp.329-338, 2012.

[Ren07] Renkema D. J., "*Validation of Wind Turbine Wake Models*", M.Sc. Thesis, Faculty of Aerospace Engineering, Delft University of Technology, Jun. 2007.

[Ver02] Veritas D. N., "*Guidelines for Design of Wind Turbines* ", 2$^{nd}$ ed., A publication from DNV/Risø, Wind Energy Department, Risø National Laboratory, 2002.

[Wpr] http://www.wind-power-program.com/turbine_economics.htm

[Bla09] Blanco M. I., "*The Economics of Wind Energy*", Renewable and Sustainable Energy Reviews, Department of Economics, University of Alcala, Madrid, Spain, Vol.13, pp.1372–1382, 2009.

[Wan09] Wang L., Yeh T., Lee W., and Chen Z., "*Benefit Evaluation of Wind Turbine Generators in Wind Farms Using Capacity-Factor Analysis and Economic-Cost Methods*", IEEE Transactions On Power Systems, Vol. 24, No.2, May 2009.

[Sey09] Seyit, A. A. and Ali D., "*A New Method to Estimate Weibull Parameters for Wind Energy Applications*", Energy Conversion Management, 50, 1761, 2009.

[Hoj80] Hojstrup J., "*Velocity Spectra in the Unstable Planetary Boundary Layer*", American Meteorological Society, Vol. 39, pp.2239-2248, Oct. 1980.

# Appendices

# Appendix A

## Declaration:

Form this research work; it has been extracted two papers. The first one is

## Ambient Turbulence Intensity Calculation for Al-Nasiriyah Province in Iraq

Mohammed A. Saleh[1], Ayad A. Ani[2], Firas A. Hadi[*3]

[1]Ministry of Electricity, Planning Study Office, Baghdad, Iraq
[2]Department of Physics, College of Science, Al-Nahrain University, Baghdad, Iraq
[3]Ministry of Science and Technology, Baghdad, Iraq

**Abstract**

Before setting a turbine in a wind farms allocated for power generation, it must be know the appropriate turbine class for that site depending on the turbulence intensity of the winds in the studied area and the IEC-61400 standard. The importance of identifying a class of wind turbine is due to the complex environmental conditions that produce turbulent air which, in turn, may cause damage to the turbine blades and weakness in the performance. Therefore, the ambient turbulence intensity is a very important factor in determining the performance and productivity of the wind turbines.

In this research we calculate Turbulence Intensity "TI" in the province of Nasiriyah, south of Iraq (Lat. 31.052049 , Lon. 46.261021) for the years 2008, 2009, and 2010, in addition to determine the wind turbine class that appropriate for the site after comparison with the Normal Turbulence Model "NTM" belongs to IEC 61400-1, edition2 and IEC 61400-1, edition3.

**Keywords:** wind energy, IEC 61400-1, turbulence intensity, normal turbulence model.

حساب شدة اضطراب الرياح لمحافظة الناصرية في العراق

محمد احمد صالح[1] ، اياد عبد العزيز عباس[2] ، فراس عبد الرزاق هادي[*3]

[1] وزارة الكهرباء، دائرة التخطيط، بغداد، العراق

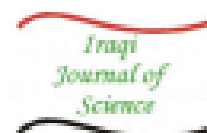[2] قسم الفيزياء، كلية العلوم، جامعة النهرين، بغداد، العراق

[3] وزارة العلوم والتكنولوجيا، دائرة بحوث الطاقات المتجددة، بغداد، العراق

الخلاصة

أن سرعة صنف توربين الرياح الملائم لموقع معين قبل نصبه في مزارع توليد الطاقة الكهربائية يحدد بالاساس على شدة اضطراب الرياح هناك وعلى المعيار IEC-61400. والسبب في حتمية تحديد صنف التوربين يعود الى تعرضه بعد النصب الى ظروف بيئية معقدة تسبب اضطراب شديد في الرياح مما يؤدي الى تلف عجلات التوربينات وضعف في الاداء ، لذا فأن شدة الاضطراب هو عامل مهم جدا في تحديد أداء توربينات الرياح وأنتاجيتها.

في هذا البحث تم حساب شدة اضطراب الرياح في محافظة الناصرية (Nasiriyah) الواقعة جنوب العراق (خط عرض 31.052049 وطول 46.261021) وللسنوات 2008 و 2009 و 2010، اضافة الى تحديد صنف توربين الرياح الملائم للنصب في ذلك الموقع بعد المقارنه مع نموذج الاضطراب الطبيعي القياسي (NTM) الذي يقع ضمن كلا من IEC 61400-1,edition2 و IEC 61400-1,edition3.

The second one is

تقدير معاملات ويبل وقدرة الرياح لثلاث مواقع في العراق

اياد عبد العزيز عباس[1]، محمد احمد صالح[2]، فراس عبد الرزاق هادي[2]*، رونق عادل عبد الوهاب[3]

[1] قسم الفيزياء ، ، كلية العلوم ، جامعة النهرين ، بغداد ، العراق.
[2] وزارة الكهرباء ، دائرة التخطيط ، بغداد ، العراق.
[3] وزارة العلوم والتكنولوجيا ، دائرة بحوث الطاقات المتجددة ، بغداد ، العراق.

الخلاصة

في هذا البحث تم تقدير معاملات توزيع ويبل وقدرة الرياح لثلاث مواقع متفرقة من العراق وهي: بغداد، البصرة وذي قار، وذلك بعد جمع وتنضيد البيانات المتوفرة من الموقع الالكتروني Weather Under Ground ولكل محطة من محطات الدراسة وللسنوات 2009–2010. وبارض اجزاء التطبيقات الإحصائية والعمليات الرياضية وتقدير طاقة الرياح تم بناء برمجيات خاصة لحساب معاملات ويبل (كونه التوزيع الأمثل لاحصائيات سرع الرياح) وهي معلمة الشكل (k) Shape Parameter ومعلمة القياس Scale Parameter (c) باستخدام طريقة الإمكان الأعظم (MLE) وطريقة المربعات الصغرى (Least squares method)، كذلك تم حساب التكرار السنوي لسرع الرياح مع ملاحظة السرعة الأكثر توافرا خلال العامين المذكورين باستخدام نفس البرنامج، بعدها تم رسم توزيع دالة ويبل (دالة كثافة الاحتمالية) بالاضافة الى حساب الكميات الإحصائية المهمة لبيانات الرياح كمعدل سرع الرياح والانحراف المعياري للقيم وأعلى قيمة وأقل قيمة كانت خلال فترة الدراسة .

# Weibull Parameters and Wind Power Assessment for Three Locations in Iraq

Ayad A. Ani[1] , Mohammed A. Saleh[2] , Firas A. Hadi[2]* , Rawnak A. Abdulwahab[3]

[1]Department of Physics, College of Science, Al-Nahrain University, Jadreia, Baghdad, Iraq.
[2]Ministry of Electricity, Planning Study Office.
[3]Ministry of Science and Technology, Jadreia, Baghdad, Iraq.

**Abstract**

In this research, we built a program to assess Weibull parameters and wind power of three separate locations in Iraq: Baghdad, Basrah and Dhi-qar for two years 2009 and 2010, after collecting and setting the data available from the website "Weather Under Ground" for each of the stations Baghdad, Basrah and Dhi-qar. Weibull parameters (shape parameter and scale parameter) were estimated using maximum likelihood estimation method (MLE) and least squares method (LSM). Also, the annual wind speed frequencies were calculated noting speed most readily available through the above two years. Then, we plotted Weibull distribution function and calculate the most significant quantities represented by mean wind speed, standard deviation of the values, the highest value and the lowest value during those years.

Keywords: Weibull parameter estimation, Statistical analysis of the wind resources.

---

* Email: firasmost1@yahoo.com

# Appendix B

## Correlation Coefficient, R

- The quantity R, called the linear correlation coefficient, measures the strength and the direction of a linear relationship between two variables. The linear correlation coefficient is sometimes referred to as the Pearson product moment correlation coefficient in honor of its developer Karl Pearson.
- The value of R is such that $-1 < R < +1$. The $+$ and $-$ signs are used for positive linear correlations and negative linear correlations, respectively.
- Positive correlation:  If x and y have a strong positive linear correlation, R is close to $+1$.  An R value of exactly $+1$ indicates a perfect positive fit. Positive values indicate a relationship between x and y variables such that as values for x increases, values for y also increase.
- Negative correlation:  If x and y have a strong negative linear correlation, R is close to $-1$.  An R value of exactly $-1$ indicates a perfect negative fit. Negative values indicate a relationship between x and y such that as values for x increase, values for y decrease.
- No correlation: If there is no linear correlation or a weak linear correlation, R is close to 0.  A value near zero means that there is a random, nonlinear relationship between the two variables
- Note that R is a dimensionless quantity; that is, it does not depend on the units employed.
- A perfect correlation of $\pm 1$ occurs only when the data points all lie exactly on a straight line. If $R = +1$, the slope of this line is positive.  If $R = -1$, the slope of this line is negative.
- A correlation greater than 0.8 is generally described as strong, whereas a correlation less than 0.5 is generally described as weak. These values can vary based upon the "type" of data being examined.  A study utilizing scientific data may require a stronger.

# Coefficient of Determination, $R^2$ :

- The coefficient of determination, r 2, is useful because it gives the proportion of the variance (fluctuation) of one variable that is predictable from the other variable.It is a measure that allows us to determine how certain one can be in making predictions from a certain model/graph.
- The coefficient of determination is the ratio of the explained variation to the total variation.
  The coefficient of determination is such that $0 < r\,2 < 1,$ and denotes the strength of the linear association between x and y.
- The coefficient of determination represents the percent of the data that is the closest to the line of best fit.  For example, if r = 0.922, then r 2 = 0.850, which means that 85% of the total variation in y can be explained by the linear relationship between x and y (as described by the regression equation).  The other 15% of the total variation in y remains unexplained.
- The coefficient of determination is a measure of how well the regression line represents the data.  If the regression line passes exactly through every point on the scatter plot, it would be able to explain all of the variation. The further the line is away from the points, the less it is able to explain.

# Appendix C

The power curve for a wind turbine provides somewhat realistic calculations for expected energy yield according to the wind conditions at the respective site. The SUZLON S64-950 wind turbine data are displayed both in tabular and graphical form.

In the graphical presentation, the mean power results are shown along with the turbine data from the power curve table in a steady wind
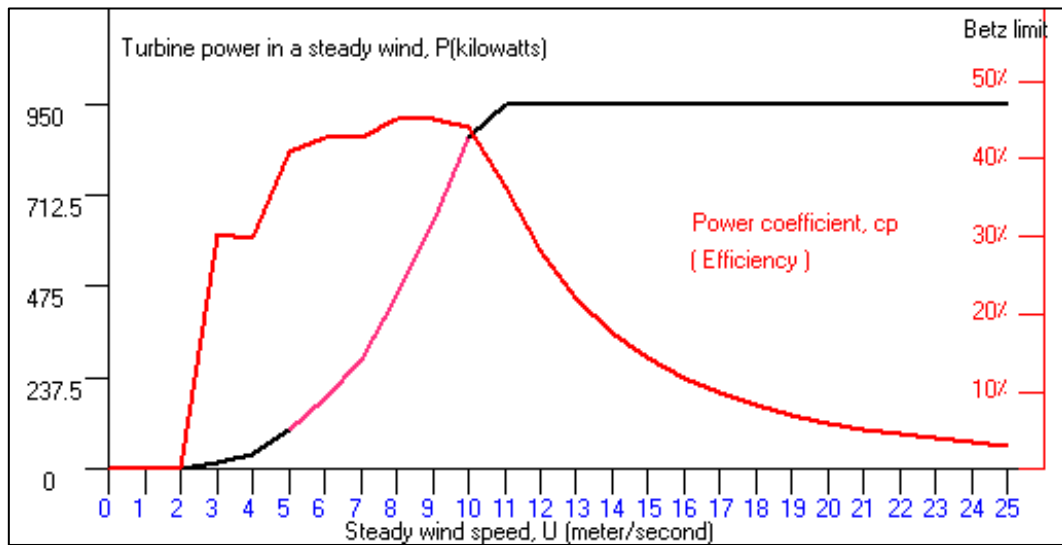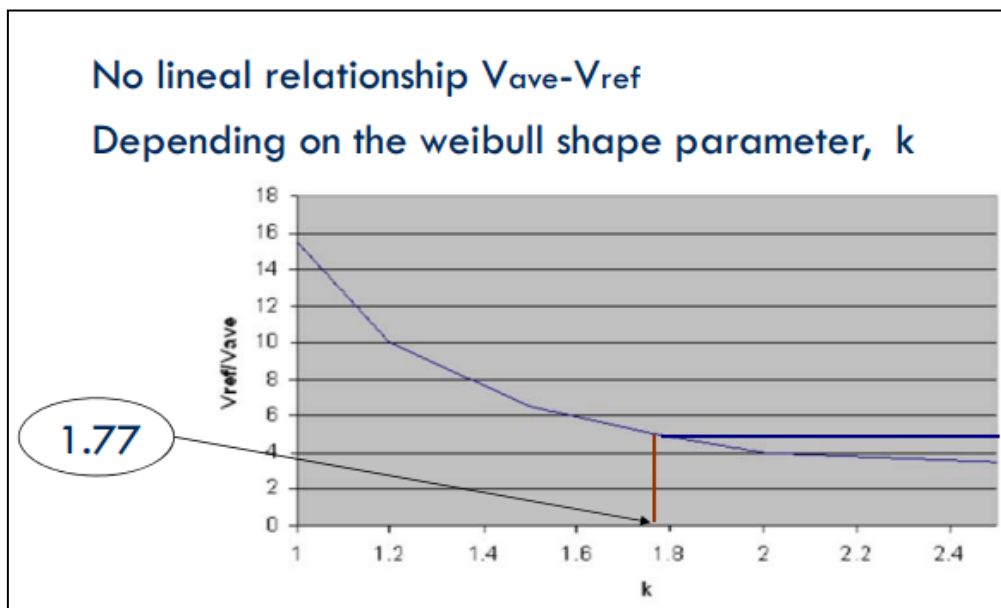


**Turbine power curve and power coefficient**

# The turbine power curve and power coefficient

| Wind speed (m/sec) | Power (KW) | Power coefficient Cp (-) |
|---|---|---|
| 1 | 0 | 0 |
| 2 | 0 | 0 |
| 3 | 16 | 30.1 |
| 4 | 37.17 | 29.5 |
| 5 | 99.95 | 40.6 |
| 6 | 180.98 | 42.5 |
| 7 | 287.09 | 42.5 |
| 8 | 451.62 | 44.8 |
| 9 | 645.49 | 44.9 |
| 10 | 861.49 | 43.7 |
| 11 | 950 | 36.2 |
| 12 | 950 | 27.9 |
| 13 | 950 | 21.9 |
| 14 | 950 | 17.6 |
| 15 | 950 | 14.3 |
| 16 | 950 | 11.8 |
| 17 | 950 | 9.8 |
| 18 | 950 | 8.3 |
| 19 | 950 | 7.0 |
| 20 | 950 | 6.0 |
| 21 | 950 | 5.2 |
| 22 | 950 | 4.5 |
| 23 | 950 | 4.0 |
| 24 | 950 | 3.5 |
| 25 | 950 | 3.1 |

# Appendix D

## The relation between k and $v_{ref}/v_{ave}$



No lineal relationship Vave-Vref
Depending on the weibull shape parameter, k

1.77

# الملخص

في السنوات القليلة الماضية، شهد العالم اندفاعا نحو استخدام مصادر الطاقة النظيفة والمتجددة من أجل التقليل من التلوث البيئي وتكلفة الطاقة واستهلاك الوقود. لذلك انصب هذا العمل نحو قطاع مهم من قطاعات الطاقة المتجددة وهو طاقة الرياح، حيث تم تقسيم العمل الى اربعة محاور وهي:-

- احصائيات الرياح wind statistics:

ويعرض هذا البند التحليل الإحصائي لبيانات الرياح موزعة على خمس مواقع في العراق (علي الغربي، بغداد، البصرة، الناصرية، كربلاء) وعلى فترة زمنية سنوية وشهرية. حيث اجريت التحليلات باستخدام دالة توزيع ويبل، لهذا اجريت مقارنة بين تسع طرق احصائية لغرض تقدير معلمات هذا التوزيع. اظهرت النتائج أن الطريقة الجديدة EEM تعطي أفضل تقدير لكثافة الطاقة. تم اختيار توربين افتراضي من نوع -SUZLON S64 950 وعامل القدرة هو المعيار المستخدم لبيان مدى ملائمته مع مواقع الدراسة، ايضا اظهرت النتائج ان عامل القدرة يساوي0.12، 0.03، 0.05، 0.08، 0.09 لكل من علي الغربي، بغداد، البصرة، الناصرية، كربلاء على التوالي.

- شدة الاضطراب ($TI$):

أن حساب شدة الاضطراب هو عامل مهم جدا في تحديد الأداء والإنتاجية في توربينات الرياح. وهذا يوجب علينا معرفة صنف التوربين المناسب قبل نصبه في حقل توربينات الرياح. في هذا البند تم حساب معدل شدة الاضطراب يعني $TI$ ($50^{th}$ quantile) وممثل شدة الاضطراب ($90^{th}$ quantile) $TI$ في محافظتي الناصرية وكربلاء، بالإضافة إلى تحديد فئة توربين الرياح بعد المقارنة مع NTM العائد للمعيار IEC. واشارت النتائج أن فئة التوربين C هي الفئة المناسبة لتركيبها في المواقع المختارة.

- عامل الاثر Wake effect:

درست تأثيرات توربينات الرياح المنبع على أداء توربينات الرياح المصب (المرجع) من خلال عامل $I_{eff}$ لمحافظة الناصرية. حيث شملت الدراسة تأثير كل من عدد التوربينات المحيطة بالتوربين المرجع بالاضافة الى اثر المسافة الفاصلة بين التوربينات على عامل $I_{eff}$. أيضا تم تقدير $I_{eff}$ لثمان قطاعات في الموقع المختار، كما وتبين هذه الدراسة كيف ان قيمة $I_{eff}$ تزداد بزيادة عدد التوربينات المحيطة، وكيف يمكن خفض هذه القيمة عن طريق تركيب توربينات المنبع على مسافة بعيدة عن المرجع.

- التحليل المالي Economic analysis:

وقد استخدمت ثلاثة أساليب للتحليل الاقتصادي وهي:-

■ تكلفة الطاقة التي تعتمد على الكيلوواط ساعة.

■ نسبة مجموع العائدات من الكهرباء التي تنتجها توربينات الرياح الى مجموع تكاليف التوربين.

■ فترة الاسترداد.

# بناء نموذج رياضي احصائي لطاقة الرياح في العراق باستخدام دوال مختلفة لتوزيع ويبل

أطروحة

مقدمـة إلى كليـــة العلـــوم / جامعة النهرين

كجزء من متطلبات نيل درجة دكتوراه فلسفة في علوم الفيزيـــاء

من قبل

**فراس عبد الرزاق هادي**

بكالوريوس علوم (فيزياء) – جامعة بغداد – كلية العلوم 1998

ماجستير علوم (فلك) – جامعة بغداد – كلية العلوم 2001

إشراف

| الاستاذ الدكتور | رئيس باحثين الدكتور |
|---|---|
| اياد عبد العزيز العاني | محمد احمد صالح |